Imperial College London

Department of Metabolism, Digestion and Reproduction

Clinical and cellular characterisation of HNF1A transcription factor variants in people with young-onset diabetes

PhD candidate Ines Cherkaoui, MSc

September 2023

A thesis submitted for the degree of Doctor of Philosophy

Declaration

I declare that this thesis is my own work and has not been submitted for any degree or other purposes. I have acknowledged all sources of information and assistance used in the preparation of this thesis.

Ines Cherkaoui

Copyright declaration

Abstract

HNF1A-MODY, is a common form of monogenic diabetes. *HNF1A* variants of unknown significance can be a challenge to pathogenic, and in turn may prevent a diagnosis of HNF1A-MODY. This means individuals with HNF1A-MODY who could benefit from sulfonylurea treatment, may not receive it. This thesis focuses on two *HNF1A* variants of unknown significance: the homozygous p.A251T (the world's first observed homozygous potentially pathogenic variant) and heterozygous p.S19L. The overarching objective of this thesis was to assess the impact of these variants on the function of the HNF1A protein, β-cell insulin secretion, and the fundamental mechanisms driving the MODY phenotype. These investigations employed a comprehensive multimodal strategy, integrating a clinical study with *in vitro* functional assays utilising diverse cell lines, including immortalised and patient-derived β-cell-like cells. The clinical study underscores the difficulty in ascertaining the pathogenicity of an *HNF1A* variant of unknown significance exclusively through clinical characteristics and predictive biomarkers. *In silico* and *in vitro* assessments revealed that the homozygous p.A251T variant exerts a moderate impact on the HNF1A protein function, leading to a mild reduction in transactivation activity compared to wildtype *HNF1A.* In contrast, the heterozygous p.S19L variant exhibited a notable reduction in HNF1A protein function when compared to the wild-type, resulting in diminished transactivation activity and altered the subcellular localisation of the HNF1A protein. Due to the limitations of basic *in vitro* methodologies in elucidating the mechanism underlying the p.A251T variant's impact, β-cell-like cells were generated carrying the *HNF1A* p.A251T. The A251T β-like cells displayed impaired insulin secretion in response to glucose and a decreased relative expression of insulin, as well as disrupted Ca^{2+} entry oscillation compared to iPSC β-cell-like cells derived from healthy donor. This study emphasises the significance of a comprehensive multimodal approach, combining clinical data, *in silico* analyses, and *in vitro* assessments, to accurately classify *HNF1A* variant pathogenicity.

Acknowledgments

First and foremost, I would like to express my heartfelt gratitude to my supervisors, Prof. Guy Rutter and Dr. Shivani Misra, for the opportunity of working in this very exciting project and their mentoring, support and guidance throughout this scientific and personal journey.

Words do not suffice to describe how grateful I am to my colleagues Pauline, Liliane, Elina, Steve, Ming, and all the Cell Biology lab. Your support and help have been truly invaluable; I feel indebted to you all. Thanks to Shazi for all the shared and for reminding me that even the smallest things can mean everything.

To *Las mujeres de Camden*, whom I shared with both the happiest and the saddest moments of this adventure, thank you! You have been my daily source of smiles and laughter, reminding me that I can overcome any obstacle. Andy, Candice, you are dear to my heart.

To my friends Caroline, Jeff, Anne Laure, Charis, and Jem, you have coloured my life in London with laughter, inspiration, and endless energy. Each of you holds a special place in my heart. To the wonderful improvisers of la FBI, thank you for making every Tuesday a time of joy and creativity. To Thomas, Floriane, Cindy, Anne, Lou, Sihame, Raphael, Ilyas and all my dear friends in Paris, and Nantes without all your support and encouragement, I would have not been able to make this life-changing achievement.

To my brother, who understands the challenges of being a doctoral student, you have provided unwavering support. From your passion and dedication, I draw my strength, and your wisdom has been a guiding light. To my sister, you have often reminded me of the true value of life, and with you, I cherish every shared moment. Writing this thesis is just a chapter, but you will forever be a part of every chapter in my life.

Last, but not least, to the most important pillars of my life, my parents. You have cemented in me the values of hard work, perseverance, and resilience. Merci beaucoup Maman et Baba pour votre soutien constant, votre dévouement et la force que vous avez insufflée en moi.

شكراً جزيلاً

Ines Cherkaoui,
London, August 2023

Contents

List of Figures

List of Tables

Selected abbreviations

AAs: Amino Acids

ABCC8: ATP-binding cassette transporter subfamily C member 8

ABEs: Adenosine Base Editors

ACE: Angiotensin-converting enzyme

ALP: Alkaline Phosphatase

ALT: Alanine Aminotransferase

AP: Alkaline Phosphatase

APH: Aphidicolin

APPL1: Adaptor protein phosphotyrosine interacting with PH domain and leucine zipper 1

BMI: Body Mass Index

BLK: B-lymphocyte kinase

CBE: Cytosine Base Editors

CRISPR: Clustered Regularly Interspaced Short Palindromic Repeat

DCoH: Dimerization Cofactor of HNF1

DKA: Diabetic Ketoacidosis

DM: Diabetes Mellitus

DPP-4: Dipeptidyl Peptidase-4

Dx: Diagnosis

FHx: Family History

GAD-65: Glutamic Acid Decarboxylase-65

GADA: Glutamic Acid Decarboxylase Autoantibodies

GCK: Glucokinase

GLP-1: Glucagon-Like Peptide-1

GLUT1: Glucose Transporter 1

GLUT2: Glucose Transporter 2

GSIS: Glucose-Stimulated Insulin Secretion

HbA1c: Hemoglobin A1c

HDL: High-Density Lipoprotein

HLA: Human Leukocyte Antigen

HNF1A: Hepatocyte Nuclear Factor 1 Alpha
HNF1B: Hepatocyte Nuclear Factor 1 B
HNF4A: Hepatocyte Nuclear Factor 4 Alpha
hESCs: Human Embryonic Stem Cells
hiPSCs: Human Induced Pluripotent Stem Cells
Hs CRP: High-Sensitivity C-Reactive Protein
HTFR: Hemoglobin A1c Test Reliability
IA-2: Insulinoma-associated protein-2
IAA: Insulin Autoantibodies
IGF-1: Insulin-like Growth Factor 1
INS: Insulin
KCNJ11: Potassium Inwardly Rectifying Channel Subfamily J Member 11
KLF11: Kruppel-Like Factor 11
LDL: Low-Density Lipoprotein
MHC: Major Histocompatibility Complex
MODY: Maturity-Onset Diabetes of the Young
NAFLD: Non-Alcoholic Fatty Liver Disease
NEUROD1: Neurogenic Differentiation 1
NKX6.1: Nirenberg and Kim Homeobox 6.1 or NK6 Homeobox 1
OCT-4: Octamer-Binding Transcription Factor 4
OGTT: Oral Glucose Tolerance Test
PDX1: Pancreatic and Duodenal Homeobox 1
SDM: Site-Directed Mutagenesis
T1D: Type 1 Diabetes
T2D: Type 2 Diabetes
TCA cycle: Tricarboxylic Acid Cycle
Trigs: Triglycerides
UGIs: Uracil Glycosylase Inhibitors
VDCCs: Voltage Dependent Ca2+ Channels
VUSs: Variants of Unknown Significance
WT: Wild-Type
WHR: Waist-Hip Ratio

1 Chapter 1: Introduction

1.1 The Endocrine Pancreas: The Regulator of Glucose Homeostasis

The pancreas carries out an exocrine and an endocrine function, each performed by distinct cell types. The exocrine pancreas consists of acinar cells responsible for the manufacturing, packing and regulated secretion of digestive enzymes, and a ductal system which collects, and flushes these secretions to the duodenum where they digest the macromolecules in our food (Grapin-Botton, 2005; Furuya *et al.*, 2013). The endocrine pancreas comprises the islets of Langerhans, which consist of five different cell types that collectively regulate glucose homeostasis (Alfa *et al.*, 2015). The main cell types within the islets include β-cells, responsible for insulin secretion; α-cells, involved in glucagon production; and δ-cells, which secrete somatostatin (Arnes *et al.*, 2012; Shih, Wang and Sander, 2013; Bastidas-Ponce *et al.*, 2017; Larsen and Grapin-Botton, 2017; Bakhti, Böttcher and Lickert, 2019). In addition, there are less common cells such as pancreatic polypeptide (PP) cells, responsible for the secretion of pancreatic polypeptide, and ε-cells, which are involved in the production of ghrelin and gastrin secretion, especially in developing pancreas, but decrease in abundance as the process of pancreatic development advances (Arnes *et al.*, 2012; Suissa *et al.*, 2013).

1.1.1 β-Cell Identity: NKX6.1 and PDX1 Markers

The β-cell identity is defined by the expression of specific genes that are essential for their development and function. The most commonly used β-cell markers are *PDX1* (pancreatic and duodenal homeobox 1) and *NKX6.1*,(NK6 Homeobox 1), which are transcription factors that regulate the expression of genes involved in β-cell biology (Offield *et al.*, 1996; Sander *et al.*, 2000; Schaffer *et al.*, 2013). These genes act as key regulators of β-cell identity, maturation, stability, and function, particularly as insulin-producing and secreting cells (Fujimoto and Polonsky, 2009, 2009; Taylor, Liu and Sander, 2013; Gao *et al.*, 2014; Petersen *et al.*, 2017). They serve as early

markers and play a crucial role in the differentiation of β-cell during pancreatic development.

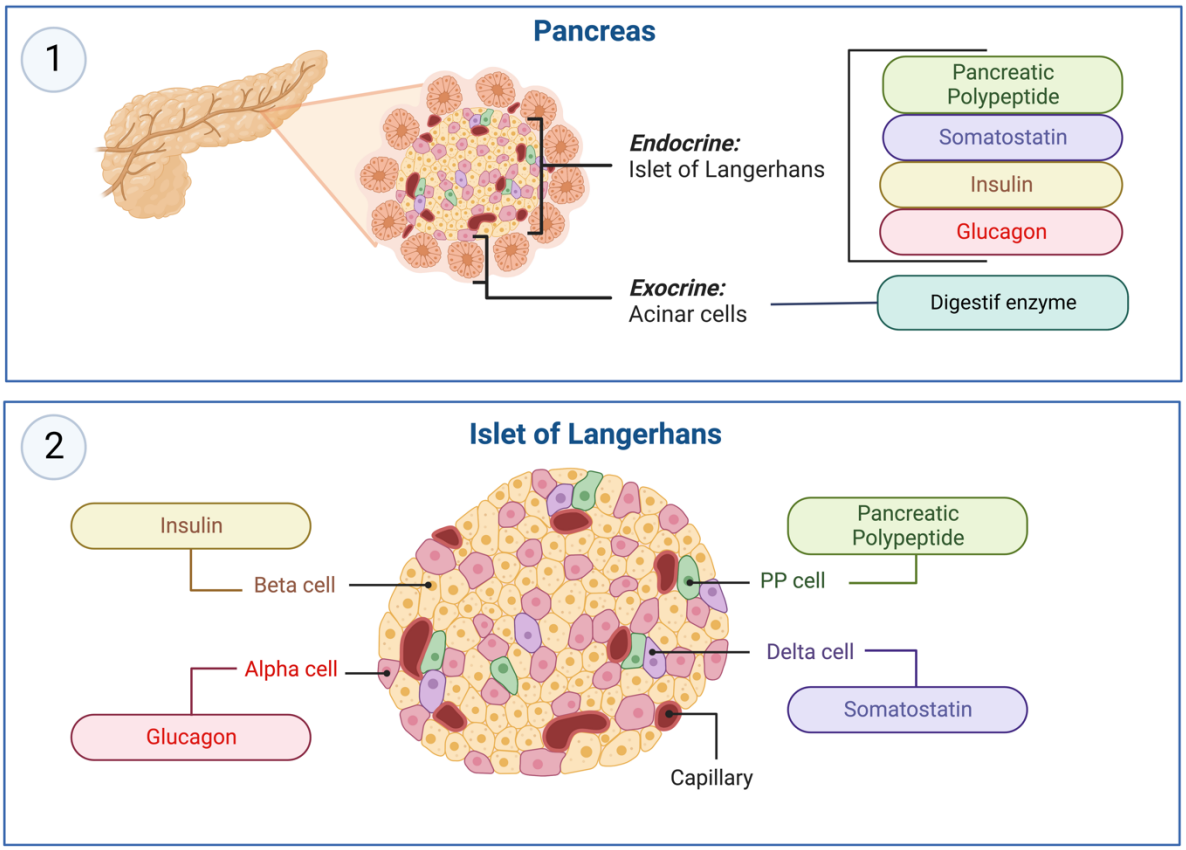

Figure 1.1 : **Schematic Representation of the Human Pancreas, with Emphasis on the Cell Types and Hormones of the of islets of Langerhans.**

The figure illustrates the dual function of the pancreas, highlighting its exocrine and endocrine roles through distinct cell types. Panel 1 depicts the exocrine pancreas, comprising acinar cells for digestive enzyme secretion and the endocrine pancreas secreting (PP) pancreatic polypeptide, somatostatin, insulin, and glucagon that collectively regulate glucose homeostasis. Panel 2 showcases the human adult endocrine pancreas, consisting of islets of Langerhans with different cell types regulating glucose homeostasis: β-cells for insulin secretion, α-cells for glucagon production, δ-cells secreting somatostatin, and less common PP cells secreting pancreatic polypeptide. The figure was drawn using Biorender.

1.1.2 β-Cells: Insulin Secretion and Glucose Metabolism

This study explores the functional aspects of β-cells, which constitute the main cell type (approximately 60%) of the islet of Langerhans (Cabrera *et al.*, 2006; Dolenšek, Rupnik and Stožer, 2015). β-cells secrete insulin firstly in response to elevated glycaemia. This involves the release of stored insulin from secretory granules (Rorsman and Renström, 2003). Insulin secretion can also be stimulated by nutrients that induce incretin release from the gut after a meal or by neurotransmitters (Irwin and Flatt, 2013).

Insulin secretion in β-cells is dependent on the concentration of glucose entering the cell, with secretion starting at a baseline glucose concentration of 3 mM and reaching its peak at 20 mM (Srivastava and Goren, 2003). The secretion of insulin begins with the transport of glucose into β-cells. Glucose transporters such as GLUT1 and GLUT2 are essential for glucose uptake in pancreatic β-cells (Heimberg *et al.*, 1995). Once in the β-cells, glucose undergoes glycolysis, starting with the phosphorylation of glucose by the enzyme glucokinase (*GCK*) to form glucose-6 phosphate (Bonner *et al.*, 2015). Subsequent metabolic steps lead to the generation of pyruvate in the mitochondria, which is further oxidised to Acetyl-CoA and enters the tricarboxylic acid cycle (TCA cycle), also known as the Krebs cycle. During the TCA cycle, ATP is produced, generating 2 ATP molecules per glucose molecule (Maechler, Carobbio and Rubi, 2006). Elevated ATP levels inhibit ATP-sensitive potassium channels (K_{ATP} channels), causing membrane depolarisation and subsequent opening of voltage-dependent Ca^{2+} channels (Cook *et al.*, 1988). This Ca^{2+} influx triggers the exocytosis of insulin from secretory granules into the bloodstream (Rorsman and Renström, 2003).

The Figure 1.2 illustrates the simplified mechanism by which insulin is secreted in response to glucose uptake by β-cells.

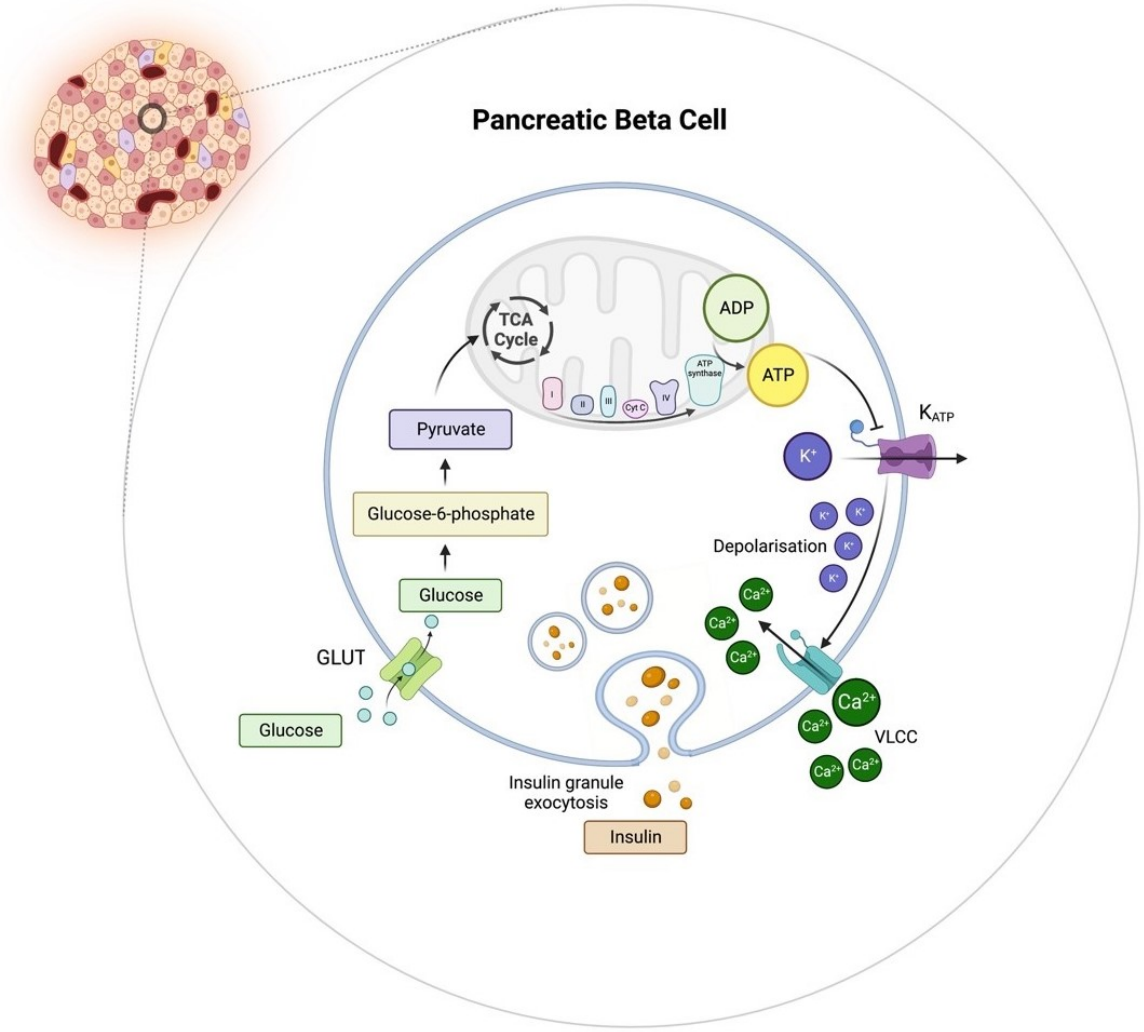

Figure 1.2: **Pancreatic β-cell Function: Metabolism of Glucose.**

The figure illustrates the mechanism by which pancreatic β-cells secrete insulin in response to glucose uptake. Glucose enters the cell through GLUT (GLUT1/2) transporters via diffusion mechanism. Inside the β-cell, glucose is phosphorylated into glucose-6-phosphate by the enzyme glucokinase. Glycolysis converts glucose-6-phosphate into pyruvate, which can be further oxidised in the mitochondria through the Tricarboxylic Acid Cycle, known as Krebs cycle, generating energy in the form of ATP (2 ATP for 1 glucose molecule). Elevated ATP levels inhibit the ATP-sensitive potassium (K_{ATP}) channels, leading to the accumulation of intracellular K^+ cation and subsequent depolarisation of the β-cell membrane. The membrane depolarisation triggers the influx of Ca^{2+} cytosolic through voltage dependent Ca^{2+} channels (VDCCs), resulting in the exocytosis of insulin secretory granules into the bloodstream. The release of insulin triggers a series of cellular events that promote the uptake and storage of glucose in various cell types, including adipose tissue, muscles, and the liver. The figure was drawn using Biorender.

1.1.3 Pancreatic β-cell Insulin Secretion and Calcium Signalling

Ca^{2+} plays a key role in insulin secretion, as its entry into the cells causes membrane depolarisation (as illustrated in the Figure 1.2) (Klec *et al.*, 2019). In β-cells, the influx of Ca^{2+} ions trigger the release of insulin-containing secretory granules. This process is marked by synchronised oscillations that correspond to changes in the electrical activity of the cell membrane. These oscillations are facilitated by paracrine signalling mediated through gap junctions (Grapengiesser, Gylfe and Hellman, 1988; Santos *et al.*, 1991).

Recent studies have shown that there is heterogeneity in the Ca^{2+} response among β-cells, with individual β-cells playing distinct roles to coordinate Ca^{2+} oscillations in response to glucose uptake (Chabosseau *et al.*, 2023). In a single islet, coordinated Ca^{2+} responses to elevated glucose concentrations stimulus are facilitated by specialised cells known as "hubs". These hubs act as pacemakers, responding earlier and more robustly to changes in glucose concentration than other β-cells (Valdeolmillos *et al.*, 1993; Lei *et al.*, 2018). When these hub cells are inhibited, it disrupts the coordination of Ca^{2+} oscillations within the islet, impairing the collective responsiveness of β-cells to glucose and compromising insulin secretion (Lei *et al.*, 2018).

Ca^{2+} influx in response to glucose are oscillations, either slow oscillations driven by changes in cytosolic Na^{+} levels or fast oscillations triggered by the activation of Ca^{2+} channels VDCCs mediated by an increase in ATP levels and K^{+} cytosolic accumulation (Nunemaker *et al.*, 2006; Fridlyand, Tamarina and Philipson, 2010). Ca^{2+} oscillations drive pulses of insulin secretion, which, in turn, safeguard β-cells from losing their responsiveness to glucose by preventing insulin receptor desensitisation (Goodner, Sweet and Harrison, 1988; Jones, Persaud and Howell, 1992).

Diabetes can occasionally be triggered by a prolonged elevation of cytosolic Ca^{2+} levels in β-cells in response to high glucose. This can lead to the loss of pulsatile insulin secretion and initiate β-cell death, which ultimately contribute to the

development of diabetes (O'Rahilly, Turner and Matthews, 1988; Bingley *et al.*, 1992; Hellman *et al.*, 1994).

1.1.4 Pancreatic Development

Pancreas development is a complex and meticulously orchestrated process that depends on precise cell signalling and the expression of specific transcription factors and morphogens at specific time points and locations during embryonic development (Shih, Wang and Sander, 2013; Pan and Brissova, 2014). These factors play an essential role in determining the fate of pancreatic progenitor cells and the differentiation of numerous cell types.

The pancreas develops from the endoderm, a primary germ layer that forms during early embryogenesis at approximately 26 days of gestation. This developmental process is marked by the formation of epithelial buds on opposing sides of the foregut endoderm. The dorsal bud is formed at approximately 30 days of gestation, followed by the subsequent development of two ventral buds. Eventually, due to gut rotation, the ventral buds fuse together. As a result, the final anatomical arrangement of the pancreas is established. Specifically, the pancreas's head arises from both the dorsal and ventral pancreas, while the body and tail of the pancreas originate exclusively from the dorsal pancreas (Pan and Brissova, 2014; Henry *et al.*, 2019; Ehrhardt and Gomez, 2023).

The development of the pancreas is regulated by several signalling pathways, the main including the Sonic Hedgehog (*Shh*) and Notch signalling (Kim and MacDonald, 2002). The notochord suppresses Shh protein signals from the endoderm in the region where the pancreas develops (Hebrok, 2003). During the initial stages of development, the primitive gut tube is divided into three regions the foregut, midgut, and hindgut, which are delineated by the notochord, aorta, and two vitelline veins. The foregut undergoes a process of specification towards a pancreatic endoderm fate. In the early stages of human pancreatic bud formation, specific transcription factors expression of *PDX1* and Nirenberg and Kim homeobox 6.1 (*NKX6.1*) indicate the maturation of the buds into pancreas (Sherwood, Chen and Melton, 2009; Jennings *et al.*, 2013; Pan

and Brissova, 2014). Notch signalling, on the other hand, suppresses the differentiation of endocrine cells while promoting exocrine cell differentiation (Li, Zhai and Teng, 2015). These signalling pathways contribute to the complex and coordinated process of pancreas development.

1.2 Diabetes Mellitus

1.2.1 Overview Diabetes (Definition, Epidemiology, Treatment, and Symptoms)

Diabetes mellitus (DM) is a chronic metabolic disorder that results from the body's inability to properly regulate glycaemia. This can be caused by either insufficient insulin production or impaired insulin function, or a combination of both (American Diabetes Association, 2011; Petersmann *et al.*, 2019). Persistent hyperglycaemia can result in complications that impact both small (microvascular) and large (macrovascular) blood vessels. Microvascular complications, such as retinopathy, nephropathy, and neuropathy, are caused by damage to small blood vessels. On the other hand, macrovascular complications, including cardiovascular complications, which represent the primary cause of mortality in individuals with diabetes, and peripheral vascular disease, caused by the accumulation of lipid deposits in arteries (American Diabetes Association, 2011; Petersmann *et al.*, 2019).

The diagnosis of diabetes relies on specific clinical criteria, encompassing the fasting plasma glucose (FPG) value (≥126 mg/dL, 7 mmol/L) or the measurement of haemoglobin A1c (HbA1c) levels (≥6.5%, 48 mmol/mol). Additionally, oral glucose tolerance tests (OGTT) play a crucial role, involving a measurement of the plasma glucose value during a 75-g oral glucose tolerance test (ElSayed, *et al.*, 2023).

DM can be classified into distinct types, with the most common forms being Type 1 Diabetes (T1D), Type 2 Diabetes (T2D), and gestational diabetes (Petersmann *et al.*, 2019). T1D is characterised by an autoimmune response, leading to the destruction of pancreatic β-cells, and causing a near-complete deficiency of insulin. However, the extent of β-cells loss can vary depending on the age at diagnosis, with a more complete loss observed when diagnosed at a younger age (less than 12 years) and

less loss in older individuals (Katsarou *et al.*, 2017; Leete *et al.*, 2018; Thompson *et al.*, 2023). T2D usually develops due to a combination of insulin resistance (where target cells become less responsive to insulin) and β-cell dysfunction (a decline in insulin production) (DeFronzo *et al.*, 2015). Thus, endocrine pancreatic failure is a *sine qua non* for frank diabetes (Kahn *et al.*, 2009), and ultimately determines disease progress (Cook *et al.*, 1993).

Gestational diabetes, which manifests during pregnancy, is associated with hormonal changes occurring in this period. Notably, placental lactogen, among other hormones, can impede the effectiveness of insulin, consequently leading to insulin resistance (Buchanan and Xiang, 2005).

Other types of diabetes have distinct underlying causes that contribute to the onset of the condition (e.g. genetic, infections, the use of steroids, etc.) (Petersmann *et al.*, 2019). Monogenic diabetes refers to specific subtypes of diabetes caused by genetic factors. The two predominant forms of monogenic diabetes are Maturity-Onset Diabetes of the Young (MODY), which has recently been redefined solely as monogenic diabetes, and neonatal diabetes (Hattersley and Patel, 2017).

According to data from the International Diabetes Federation Diabetes Atlas, the current worldwide prevalence of diabetes in adults aged 20-79 is estimated to be 537 million individuals. Projections suggest that this prevalence will rise to approximately 643 million by the year 2030 and further increase to an estimated 783 million by 2045 (Kumar *et al.*, 2023).

Early detection and appropriate treatment are crucial in preventing complications associated with diabetes. The management of hyperglycaemia varies based on the type of diabetes. For individuals with T1D, characterised by low to undetectable insulin levels, insulin is essential for managing the condition. Insulin can be administered through injections, given once or twice daily, or through an insulin pump, which delivers a continuous supply of insulin (Holt *et al.*, 2021).

People with T2D may need to use insulin or oral medications, also known as tablets. These tablets come in different types, each with its own effect. Metformin (1,1-

dimethylbiguanide) is a widely prescribed medication known for its capacity to decrease hepatic glucose production and improve insulin sensitivity. This is achieved through the elevation of insulin receptor tyrosine kinase activity, enhanced insulin receptor expression, and promotion of glycogen synthesis. Additionally, metformin elevates plasma levels of Glucagon-Like Peptide-1 (GLP-1) and induces gene expression of incretin receptors in islet cells. These mechanisms collectively contribute to the treatment T2D by reducing insulin resistance and subsequently lowering fasting plasma insulin levels (Viollet *et al.*, 2012).

Sulfonylureas and meglitinides are commonly employed in the treatment of T2D, by stimulating insulin secretion within the β-cells. These drugs function by binding to the SUR1 subunit of K_{ATP} channels, resulting to their closure. This K_{ATP} channels inhibition induces the depolarisation of the β-cell membrane, subsequently opening VDCCs and allowing the extracellular Ca^{2+} influx, stimulating insulin secretion (Del Prato and Pulizzi, 2006; Sola *et al.*, 2015).

Dipeptidyl Peptidase-4 (DPP-4) inhibitors and GLP-1 receptor agonists enhance glucose-dependent insulin secretion, while also effectively inhibiting glucagon release and delaying gastric emptying. DPP-4 inhibitors exert their action by preventing the degradation of active GLP-1, resulting in an increase in the levels of circulating total GLP-1. GLP-1, upon binding to its receptors, enhances insulin gene expression and synthesis within β-cells, effectively restoring glucose sensitivity and responsiveness to glucose challenges (Richter *et al.*, 2008; Meier, 2012; Nauck *et al.*, 2021).

Sodium-glucose cotransporter-2 (SGLT2) inhibitors function by inhibiting glucose reabsorption in the kidneys, leading to increased urinary glucose excretion and, consequently, reduced glycaemia (Rosenstock *et al.*, 2012).

To further enhance glycaemic control effectively, additional interventions can be employed in conjunction with treatment. These may include lifestyle modifications such as a nutritious balance diet and regular exercise (in individuals with the physical capacity to implement such measures) (Petersmann *et al.*, 2019; ElSayed, Aleppo,

Aroda, Bannuru, Brown, Bruemmer, Collins, Hilliard, Isaacs, Johnson, Kahan, Khunti, Leon, Lyons, Perry, Prahalad, Pratley, Seley, Stanton, Gabbay, *et al.*, 2023).

1.2.2 Polygenic Forms of Diabetes

1.2.2.1 Type 1 Diabetes

Type 1 Diabetes (T1D) is an autoimmune disorder characterised by the destruction of β-cells in the pancreas (Katsarou *et al.*, 2017). The destruction of insulin-producing cells occurs because of an autoimmune response. This response leads to a deficiency in insulin production, which in turn causes hyperglycaemia. Prolonged hyperglycaemia can lead to diabetic ketoacidosis (DKA) characterised by acidic blood pH due to the increased production and utilisation of ketones (Katsarou *et al.*, 2017).

T1D primarily manifests during childhood or adolescence and accounts for approximately 10% of all diabetes cases. In 2021, the estimated global prevalence of T1D was approximately 8.4 million individuals. Out of this population, around 18% were younger than 20 years, 64% fell between the ages of 20 and 59 years, and 19% were aged 60 years or older (Gregory *et al.*, 2022). The prevalence were estimated from cross-sectional prevalence study and further calculated estimates using a model based on cross-sectional prevalence study data (Gregory *et al.*, 2022).

Research has shown that autoantibodies against specific β-cell antigens can be detected prior to the onset of hyperglycaemia. These autoantibodies target proteins that are essential for the function of β-cells. The specific β-cell antigens that autoantibodies target include GAD-65 (glutamic acid decarboxylase-65), IA-2 (insulinoma-associated protein-2), and ZnT8 (zinc transporter 8) (Krischer *et al.*, 2015; Katsarou *et al.*, 2017). The detection of autoantibodies against β-cell antigens can be used to diagnose diabetes in its early stages, however, over time, the detection of autoantibodies can become negative (Yu, Zhao and Steck, 2017).

The cause for the autoimmune response in T1D is still uncertain due to the complex nature of the disease and the involvement of multiple factors. T1D is considered a

polygenic disease, which means there is a genetic predisposition due to the combined effects of multiple genes rather than a single gene.

In T1D, certain alleles of the major histocompatibility complex (MHC) genes, also known as the human leukocyte antigen (HLA) complex, are associated with an increased predisposition to developing the disease. Specifically, the *HLA-DQB1* and *HLA-DRB1* genes are the most strongly associated with T1D. These genes code for proteins that are involved in presenting antigens to the immune system. When these proteins are altered, they can trigger the immune system to attack the β-cells in the pancreas (Nejentsev *et al.*, 2007; Todd *et al.*, 2007; Tumer, Simpson and Roberts, 2023).

While genetic factors play a significant role in the development of the disease, they are not the only cause T1D. There are multiple environmental factors, such as viral infections, early life exposures, and pollution, that can also contribute to the onset of T1D. These environmental factors interact with genetic predisposition, collectively influencing the disease's development and progression (Chapman *et al.*, 2012).

Effective management of T1D necessitates regular insulin administration, as the destruction of β-cells leads to near-complete to complete insulin deficiency. Insulin can be administered via one or multiple daily injections, or alternatively, an insulin pump may be employed for this purpose.

Closed-loop systems utilise insulin pumps to integrate continuous glucose monitoring with automated insulin delivery, thereby enabling real-time management of glycaemia. To achieve this, a subcutaneous sensor is employed to collect real-time data. Subsequently, the system employs algorithm-driven calculations to precisely determine the insulin dosage required to maintain glycaemic control within a predefined target range. Following these calculations, the closed-loop system administers insulin through an infusion pump. This technological advancement not only enhances the quality of life for patients but also alleviates the constant burden of insulin management (Elleri, Dunger and Hovorka, 2011; McCall and Farhy, 2013; Berget, Messer and Forlenza, 2019).

Managing T1D involves additional components alongside insulin therapy, including diet management (e.g. carbohydrate counting to match insulin doses), physical activity, and weight management (Katsarou *et al.*, 2017).

Islet transplantation and pancreas is also a therapeutic approach for T1D, involving the transplantation of insulin-producing islet cells from a donor pancreas into the recipient's liver (Shapiro, Pokrywczynska and Ricordi, 2017). This intervention has the potential to achieve insulin independence and enhance metabolic control significantly. However, the islet transplantation presents a risk of immune rejection and strategies such as glucocorticoid-free immunosuppression are used to improve the chances of successful graft survival and long-term efficacy by reducing the risk of rejection (Shapiro *et al.*, 2000; Rother and Harlan, 2004). Researchers have been investigating new treatments for T1D, including immunotherapies that preserve β-cell function and prevent further destruction by the immune system (Bluestone, Buckner and Herold, 2021). Eventually, regenerative cell therapy is another promising approach, and this study will present an overview of the current state of research in this area (Aguayo-Mazzucato and Bonner-Weir, 2010; Aly, 2020).

1.2.2.2 Type 2 Diabetes

Type 2 Diabetes (T2D) is the most common form of diabetes accounting for approximately 98% of diagnosed diabetes cases, according to the International Diabetes Federation, although the exact proportion may vary between countries (Saeedi *et al.*, 2019). In T2D, the body develops insulin resistance, which impairs its ability to effectively use insulin, leading to elevated glycaemia (DeFronzo *et al.*, 2015). The β-cells compensate by producing more insulin to maintain normal glycaemia. Over time, this compensatory mechanism is also impaired, resulting in decreased insulin production, inadequate glycaemic control, and persistent hyperglycaemia.

T2D is multifactorial, caused by a combination of genetic and environmental factors. The main risk factors for developing T2D includes obesity, a family history of diabetes, physical activity, and diet (Fletcher, Gulanick and Lamendola, 2002; DeFronzo *et al.*, 2015).

The proportion of genetic involvement in T2D is estimated to range from 20% to 80% (Poulsen *et al.*, 1999; Ali, 2013). T2D is polygenic, implying that it results from the collective influence of two or more genes variants to induce the T2D phenotype. Genome-Wide Association Studies (GWAS) have been conducted to explore the genetic component of T2D, revealing the involvement of over 400 genes associated with T2D, involved in metabolic β-cell function, insulin signalling pathways, and glucose homeostasis (Fuchsberger *et al.*, 2016). The two most common genes that have been associated with T2D are: Transcription factor-7–like 2 (*TCF7L2*) and calpain 10 (*CAPN10*). Additionally, several other genes have been identified but further exploration is required to uncover their roles in T2D development. These genes include peroxisome proliferator-activated receptor gamma (*PPARG*), insulin receptor substrate 1 and -2 (*IRS1* and *2*), potassium inwardly-rectifying channel, subfamily J, member 11 (*KCNJ11*), hepatocyte nuclear factor 1 alpha (*HNF1A*), 4 alpha (*HNF4A*) and *HNF1B* (Cauchi and Froguel, 2008; Ali, 2013; Läll *et al.*, 2017).

The management of T2D focuses on controlling hyperglycaemia, blood pressure, and cholesterol levels, while also preventing complications. Lifestyle modifications are indispensable in the treatment of individuals who are overweight and have T2D including a healthy diet, and regular exercise (DeFronzo *et al.*, 2015). Hyperglycaemia in T2D is managed through the administration of medications like metformin, sulfonylureas, meglitinides, DPP-4 inhibitors, GLP-1 receptor agonists, and SGLT2 inhibitors. These pharmacological agents function to regulate insulin secretion and glucose reabsorption by the kidney, thereby effectively controlling glycaemic levels (Kahn, Cooper and Del Prato, 2014).

Hypertension and dyslipidaemia are prevalent in T2D contribute significantly to the development of cardiovascular disease, leading to increased mortality rates (Rawshani, Rawshani and Gudbjörnsdottir, 2017). Angiotensin-converting enzyme (ACE) inhibitors, angiotensin II receptor blockers (ARBs), diuretics, and statins are commonly used to lower blood pressure and cholesterol to prevent cardiovascular disease which is a leading cause of death in people with T2D (Kahn, Cooper and Del Prato, 2014).

1.2.2.3 Monogenic Diabetes Mellitus

Monogenic diabetes is a rare form of diabetes (1%-5% of all diabetes cases) caused by a single-gene mutation that is inherited in an autosomal dominant manner (Hattersley and Patel, 2017). There are two main types of monogenic diabetes: Maturity-Onset Diabetes of the Young (MODY) and neonatal diabetes mellitus (Hattersley and Patel, 2017).

1.2.2.4 Neonatal Diabetes Mellitus

Neonatal diabetes mellitus is a form of diabetes that is diagnosed in the first few weeks or months of an infant's life usually before 6 months of age (Aguilar-Bryan and Bryan, 2008). It is caused by dominant mutations in specific genes that affect the development or function of insulin-producing cells in the pancreas. These mutations result in impaired insulin production, leading to hyperglycaemia (Polak and Cavé, 2007; Aguilar-Bryan and Bryan, 2008). The occurrence of neonatal diabetes mellitus is relatively rare, with a minimum incidence of 1 in 100,000 live births. This incidence may vary among different ethnic groups, but no ethnic group has been found to be predominantly affected (Polak and Cavé, 2007; Iafusco *et al.*, 2012).

Neonatal diabetes mellitus can be divided into two main subtypes: transient neonatal diabetes mellitus and permanent neonatal diabetes mellitus. Transient neonatal diabetes mellitus is a rare form of diabetes that typically resolves spontaneously during the first few months or years of life. The cause of transient neonatal diabetes mellitus is unknown, but it is thought to be caused by a combination of genetic and environmental factors (Naylor *et al.*, 2011; Lemelman, Letourneau and Greeley, 2018). Persistent neonatal diabetes mellitus is caused by genetic mutations, predominantly affecting the *KCNJ11* and *ABCC8* genes, which account for over 50% of all cases of neonatal diabetes mellitus (Polak and Cavé, 2007; Iafusco *et al.*, 2012). The treatment for neonatal diabetes includes insulin therapy, as well as early intervention with sulfonylureas for individuals with neonatal diabetes that are responsive to this medication (von Mühlendahl and Herkenhoff, 1995; Polak and Cavé, 2007; Aguilar-Bryan and Bryan, 2008; Lemelman, Letourneau and Greeley, 2018).

1.2.2.5 Maturity-Onset Diabetes of the Young

Monogenic diabetes, formerly known as Maturity-Onset Diabetes of the Young (MODY), comprises approximately 1-5% of all documented diabetes cases (Urakami, 2019). MODY manifests with early-onset diabetes and affected individuals do not necessarily require insulin for managing their glycaemia. The age at which diabetes develops is typically before 35 years (B. M. Shields *et al.*, 2010; Gardner and Tai, 2012), however, certain MODY subtypes may exhibit atypical clinical features with a variable age of onset, making the diagnosis more challenging. In addition, T1D and T2D can both have an early onset, occurring in people under the age of 30 further complicating the diagnosis of MODY. Due to its rarity (compared to T1D and T2D) and the diverse clinical presentations, MODY is frequently misdiagnosed as T1D (Tosur and Philipson, 2022). Clinicians may not consider MODY, leading to delays in treatment and incorrect disease management (B. M. Shields *et al.*, 2010).

1.2.3 MODY: A Rare Form of Diabetes

The precise prevalence of MODY remains uncertain, primarily due to disparities influenced by factors including ethnic diversity and variations in genetic testing across different populations. The actual prevalence of MODY may likely be underestimated, and variations in prevalence exist among each individual subtype (Kavvoura and Owen, 2012; Urakami, 2019).

In European populations, the United Kingdom has undertaken comprehensive studies into MODY prevalence, thereby contributing valuable insights to the assessment of its occurrence within the population. MODY is estimated to underlay approximately 2% to 5% of non-insulin dependent diabetes cases (Fajans, Bell and Polonsky, 2001). The prevalence of MODY is estimated to be approximately 1 in 23,000 in children and 1 in 10,000 in adults based on European cohorts (Nkonge, Nkonge and Nkonge, 2020). In the UK, the estimated prevalence of MODY, is 2.5%, with a minimum of 68 to 108 cases per 1,000,000 individuals (B. M. Shields *et al.*, 2010).

Studies on the prevalence of MODY in regions outside of Europe are limited (Nkonge, Nkonge and Nkonge, 2020). Within the United States, it is approximated that MODY

constitutes 1.2% of all cases of paediatric diabetes mellitus (Pihoker *et al.*, 2013). In addition, the minimum number of cases of monogenic diabetes diagnosed in individuals under the age of 20 is 21 per 1,000,000. (Pihoker *et al.*, 2013).

A study in Western Australia found that the prevalence of MODY individuals diagnosed with diabetes before the age of 35 years is 0.24%. This corresponds to an estimated minimum prevalence of 89 cases per 1,000,000 for the entire Australian population (Davis *et al.*, 2017, 2019, p. 2). The prevalence of MODY in African, Asian, South American, and Middle Eastern populations is not well-established. This lack of non-European populations where the prevalence of MODY have been examined, contributes to the overall underestimation of the global prevalence of the pathology (Nkonge, Nkonge and Nkonge, 2020).

1.2.3.1 Genetics of MODY

Monogenic diabetes, formerly known as MODY is a genetic disorder with 11 identified subtypes, each characterised by a specific mutated gene. These genes are glucokinase (*GCK*) (Froguel *et al.*, 1992; Chakera *et al.*, 2015), hepatocyte nuclear factor 1 alpha (*HNF1A*) (Ellard and Colclough, 2006), hepatocyte nuclear factor 4 alpha (*HNF4A*) (Ellard and Colclough, 2006), hepatocyte nuclear factor 1 β (*HNF1B*) (Horikawa *et al.*, 1997), ATP-binding cassette transporter subfamily C member 8 (*ABCC8*) (Bowman *et al.*, 2012), potassium inwardly rectifying channel subfamily J member 1 (*KCNJ1*) (Bonnefond *et al.*, 2012), insulin (*INS*) (Molven *et al.*, 2008), pancreas-duodenum homeobox protein 1 (*PDX1*) (Staffers *et al.*, 1997), neurogenic differentiation 1 (*NEUROD1*) (Fajans, Bell and Polonsky, 2001), carboxyl-ester lipase (*CEL*) (Raeder *et al.*, 2006), and adaptor protein phosphotyrosine interacting with PH domain and leucine zipper 1 (*APPL1*) (Prudente *et al.*, 2015).

GCK and HNF1A-MODY represent the predominant subtypes within the MODY spectrum, followed by HNF4A and HNF1B, with the remaining MODY subtypes being rare (Urakami, 2019).

Each subtype, their gene locus, former name, and specific clinical features associated are summarise in Table 1. The subsequent sections of the introduction will centre on HNF1A-MODY.

Table 1-1: **MODY Subtypes, Former Names, Proportions, Clinical Characteristics, and Treatments.**

This table presents the genes identified as causing MODY, including *HNF4A, GCK, HNF1A, PDX1, HNF1B, NEUROD1, KLF11, CEL, INS, ABCC8, KCNJ11,* and *APPL1*. The clinical presentation and possible treatments for each gene are presented. For some rare cases, comprising less than 1% of the total MODY, limited clinical data are available, resulting in a few described clinical features not as accurate as the most common MODY subtypes. The most observed genes causing MODY are *GCK*, *HNF1A*, *HNF4A*, and *HNF1B*. Treatment options include oral antidiabetic medication (OAD), specified sulfonylurea when applicable, as well as insulin and diet intervention.

Causative Gene Name	% of all MODY	Clinical features	Possible Treatment	Refs
HNF4A (MODY 1)	5-10	Congenital hyperinsulinism, hypoglycaemia during infancy, low triglycerides, neonatal diabetes	Sulfonylurea	(Fajans, Bell and Polonsky, 2001; Ellard *et al.*, 2008; Anık *et al.*, 2015)
GCK (MODY 2)	30-50	Stable mild fasting hyperglycaemia at birth	No medication, diet	(Froguel *et al.*, 1993; Naylor, Knight Johnson and del Gaudio, 1993)
HNF1A (MODY 3)	30-65	Glycosuria, progressive defect insulin secretion	Sulfonylurea	(Naylor, Knight Johnson and del Gaudio, 1993; Valkovicova *et al.*, 2019a)
PDX1 (MODY 4)	<1	Permanent neonatal diabetes	OAD, insulin, diet	(Naylor, Knight Johnson and del Gaudio, 1993; Wright *et al.*, 1993; Stoffers *et al.*, 1997)
HNF1B (MODY 5)	5	Renal anomalies, urogenital tract anomalies, pancreatic hypoplasia	Insulin	(Bellanné-Chantelot *et al.*, 2004; Ulinski *et al.*, 2006)
NEUROD1 (MODY 6)	<1	Neurological abnormalities, permanent neonatal diabetes	OAD, insulin	(Kristinsson *et al.*, 2001)
KLF11 (MODY 7)	<1	Like early onset type 2 diabetes	OAD, insulin	(Neve *et al.*, 2005; Fernandez-Zapico *et al.*, 2009)
CEL (MODY 8)	<1	Exocrine insufficiency, lipomatosis	OAD, insulin	(Raeder *et al.*, 2006; Johansson *et al.*, 2011)

INS (MODY 10)	<1	Neonatal diabetes, child, or adult-onset diabetes	OAD, insulin	(Edghill *et al.*, 2008; Meur *et al.*, 2010)
ABCC8 (MODY 12)	<1	Permanent neonatal diabetes	OAD, sulfonylureas	(Bowman *et al.*, 2012)
KCNJ11 (MODY 13)	<1	Neonatal diabetes	OAD, insulin	(Bonnefond *et al.*, 2012; Liu *et al.*, 2013)
APPL1 (MODY 14)	<1	Child or adult-onset diabetes	OAD, insulin, diet	(Prudente *et al.*, 2015)

1.2.4 The Importance of Genetic Variant Pathogenicity in MODY Attribution

HNF1A-MODY is caused by autosomal dominant mutations in specific genes, but diagnosis can be complicated by the presence of genetic variants whose impact on disease development is uncertain. These genetic variants of unknown significance (VUSs) play a pivotal role in challenging the understanding of HNF1A- MODY genetic basis and clinical manifestation, prompting the need for comprehensive investigations to elucidate their functional and pathological implications.

Assessing the pathogenic nature of VUS necessitates a comprehensive approach involving clinical study, *in vitro* and computational assessments (Althari *et al.*, 2020). However, obtaining these multi-modal assessments can be challenging. Despite conducting *in vitro* analyses to understand the impact of VUSs on protein function, the precise clinical relevance, and the translation of findings to the clinical and physiological context of specific MODY-associated gene variants remain unclear. This uncertainty gives rise to limitations in making precise HNF1A-MODY prognoses and develop precise therapeutic strategies (Colclough *et al.*, 2014).

Genetic variants in genes associated with HNF1A-MODY can appear "*de novo*," meaning they arise spontaneously in the affected individual making further difficult to determine whether the variant is pathogenic or benign (B. M. Shields *et al.*, 2010; Flannick *et al.*, 2013; Althari and Gloyn, 2015).

1.2.5 HNF1A/HNF4A-MODY: An Example of Precision Medicine in Diabetes

The use of precision-targeted therapeutic interventions has the potential to provide personalised treatment for individuals with MODY. Specifically, sulfonylureas have demonstrated efficacy in treating MODY caused by mutations in *HNF1A* or *HNF4A*, and optimise long-term management of glycaemia for individuals who are correctly diagnosed with these MODY subtypes (Pearson *et al.*, 2003, 2006; Shepherd *et al.*, 2009). This therapy has the potential to eliminate or reduce the need for insulin injections, which can improve quality of life by avoiding the side effects of insulin therapy, such as weight gain and hypoglycaemia. Additionally, this therapy addresses the challenges associated with insulin administration via injections or pumps by

enabling the use of less invasive treatments, sulfonylureas oral medications, which may only require once-daily administration (Russell-Jones and Khan, 2007; Hattersley and Patel, 2017; Delvecchio, Pastore and Giordano, 2020).

Accurate diagnosis of HNF1A/HNF4A-MODY through DNA sequencing and comprehensive interpretation of VUSs pathogenicity is essential for ensuring that individuals receive the most appropriate treatment and prevent diabetes-related complications (e.g. cardiovascular disease, kidney failure, neuropathy, and retinopathy, etc.) (Pearson *et al.*, 2003; Shepherd *et al.*, 2009).

1.2.6 Clinical Diagnosis of HNF1A-MODY

Clinical criteria play a crucial role in accurately identifying patients with MODY and differentiating it from other forms of diabetes. To confirm MODY and determine the specific gene associated with the observed phenotypes, DNA sequencing remains essential. Over time, clinicians have developed guidelines and methodologies to identify individuals who should undergo sequencing, building upon a better understanding of HNF1A-MODY subtypes and diagnostic methodologies (Ellard *et al.*, 2008; Shields *et al.*, 2012; Juszczak *et al.*, 2016; Peixoto-Barbosa, Reis and Giuffrida, 2020). HNF1A-MODY can be identified based on several clinical characteristics including an early age of diagnosis typically before 35 years, as well as a diabetes history spanning two generations within the family. Individuals with HNF1A-MODY typically exhibit a non-obese phenotype and may not necessarily rely on insulin therapy. Mild hyperglycaemia is often observed at the time of diagnosis (Shields *et al.*, 2012; Juszczak *et al.*, 2016; Urakami, 2019; Nkonge, Nkonge and Nkonge, 2020).

The clinical presentations of HNF1A/HNF4A-MODY, T1D, and T2D can overlap, especially when diagnosed at an early onset. This can make it difficult to confidently diagnose the disease. Not only does the age of onset overlap, but also the family history, as all three types of diabetes have potential genetic inheritance. For example, in T1D, certain genes in the HLA region are associated with the disease (Noble and Valdes, 2011). In T2D, meta-analyses of genome-wide association studies (GWAS) have identified hundreds of genes that are associated with the risk of developing the

disease (Xue *et al.*, 2018), and in MODY, 11 genes have been identified that are responsible for causing the condition (see Introduction section: Genetics of MODY) (Urakami, 2019).

A cumulative trial that administers sulfonylurea to individuals suspected of having MODY with the intention of diagnosing *HNF1A* or *HNF4A* mutations is impractical from a cost-effectiveness standpoint. Additionally, sulfonylurea is employed in the treatment of both T2D and various monogenic diabetes (e.g. neonatal diabetes caused by *KCNJ11* and *ABCC8* genes mutations (Lemelman, Letourneau and Greeley, 2018), rendering it incapable of furnishing discerning insights into the precise genetic aetiology underlying the patient's diabetic condition. Hence, biomarkers and distinguishable clinical criteria need to be employed, and suspicion of MODY should be confirmed with DNA sequencing.

One key distinction between MODY and T1D, is the preservation of β-cell function in HNF1A-MODY patients. Unlike T1D, characterised by autoimmune-mediated β-cell destruction resulting in diminished or negligible insulin levels, individuals afflicted with MODY exhibit a prolonged preservation of β-cell function, coupled with the absence of autoantibodies. Fasting C-peptide levels in HNF1A-MODY patients are generally higher compared to T1D and can still be lower than those observed in individuals with insulin resistance, helping to distinguish MODY from T2D (American Diabetes Association, 2009; Juszczak *et al.*, 2016; Urakami, 2019). In accordance with the UK guidelines for genetic testing in MODY, the diagnosis of MODY should be considered if the random non-fasting C-peptide value is equal to or greater than 200 pmol/L, particularly in the context of the recent update specific to HNF1A-MODY diagnosis, which also includes a threshold of glucose levels exceeding 8 mmol/l (140 mg/dL) (Peixoto-Barbosa, Reis and Giuffrida, 2020).

When individuals with T1D have detectable C-peptide for an extended period, it poses a challenge in using this clinical characteristic alone to diagnose HNF1A/HNF4A-MODY. This highlights the need to consider additional clinical criteria to confidently diagnose the specific subtype. Instead, the absence of autoantibodies (e.g., islet cell antibodies (ICA), antibodies to glutamic acid decarboxylase (GAD-65), insulin

autoantibodies (IAA), and IA-2A to protein tyrosine phosphatase) may serve as an initial test to differentiate between HNF1A/HNF4A-MODY and T1D. Nonetheless, the autoantibody test results may become negative over time, thus leading to an overlap with MODY (Wenzlau and Hutton, 2013; Yu, Zhao and Steck, 2017). The absence of ketoacidosis without insulin dependence serves as a valuable clinical criterion indicating the possibility of an HNF1A-MODY diagnosis, differentiating it from T1D (Peixoto-Barbosa, Reis and Giuffrida, 2020).

As outlined in the UK guidelines for genetic testing in MODY, Body Mass Index (BMI) serves as a discriminative parameter between T2D and HNF1A/HNF4A-MODY. Notably, BMI exhibits elevated levels in T2D cases (Ling and Rönn, 2019). In the case of individuals from White ethnic backgrounds, a BMI below 30kg/m² for adults is taken into consideration for MODY testing. Meanwhile, for those belonging to ethnic groups with a high prevalence of T2D, a BMI below 27kg/m² is regarded as significant (Guidelines for Genetic Testing in MODY R141).

An ongoing area of research involves studying the lipid profile of individuals with HNF1A-MODY. Notably, individuals with HNF1A -MODY exhibit higher levels of HDL cholesterol (high-density lipoprotein) and lower levels of LDL (low-density lipoprotein). This lipid profile presents a promising candidate for clinical criteria, although further research is needed to ascertain its reliability (Fendler *et al.*, 2011; McDonald *et al.*, 2012; Ma *et al.*, 2020).

One notable biomarker associated with HNF1A-MODY is high-sensitivity C-reactive protein (hs-CRP). This biomarker has shown distinctive patterns in individuals with HNF1A-MODY compared to other forms of diabetes. Hs-CRP, an inflammation marker, has demonstrated lower levels in individuals with HNF1A-MODY when contrasted with individuals affected by different diabetes types. This divergence in hs-CRP levels provides valuable insights into the potential utility of hs-CRP as a diagnostic biomarker for HNF1A-MODY (Juszczak *et al.*, 2018; Peixoto-Barbosa, Reis and Giuffrida, 2020)

For diagnosing HNF1A/HNF4A-MODY and selectively perform genomic DNA sequencing for individuals suspected to have MODY, the combination of multiple

clinical features that fit with either type seems ideal. This approach includes considering family history, age at diagnosis, low BMI, detectable C-Peptide but not insulin resistance, and low hs-CRP among others. Through the strategic utilisation of this integrated clinical criteria approach, genetic sequencing becomes a more efficient allocation of resources in terms of both cost and time. This approach enables the targeted selection of patients for sequencing, bypassing the need to sequence all individuals with early-onset diabetes. Instead, the emphasis is placed on identifying individuals who meet a set of distinct criteria. This methodology is essential for cost-effectiveness, ensuring that only those likely to have MODY undergo sequencing (Kleinberger and Pollin, 2015).

	Type 1 diabetes	Type 2 diabetes	HNF1A-MODY
Clinical features	FHx of Diabetes Insulin-dependent diabetes Young-onset <40 DKA	FHx of Diabetes Usually >40, but also young-onset Ab (-) Overweight or obesity Conditions associated with insulin resistance (acanthosis nigricans, hypertension, dyslipidaemia)	FHx of Diabetes Young-onset <40 Ab (-) Lean BMI Sulfonylurea sensitivity No insulin resistance
Biomarker	Ab (+) C-Peptide low	Insulin resistance (OGTT) High fasting insulin Dyslipidaemia	hs-CRP low C-Peptide normal range

Figure 1.3 : **Distinctive Clinical Features and Biomarkers in T1D, T2D, and HNF1A-MODY.**
This figure provides a comprehensive overview of distinct clinical features and biomarkers related to three discrete diabetes subtypes: T1D, T2D, and HNF1A-MODY. The clinical presentations distinctive to each diabetes subtype are detailed as follows: T1D: Typically, onset in childhood or adolescence, often presenting with diabetic ketoacidosis. Presence of two or more islet-directed autoantibodies characterises this subtype. T2D: Characterised by the absence of antibodies, alongside manifestations of dyslipidaemia and insulin resistance. Frequently observed in individuals with elevated BMI, indicative of obesity. HNF1A-MODY: Frequently diagnosed at a young age (<40), often associated with non-insulin-dependent diabetes, and typically without ketoacidosis. Abbreviations used in the legend are Ab for Islet Islet Autoantibodies, FHx for Family History, OGTT for Oral Glucose Tolerance Test, hsCRP forHigh-sensitivity C-reactive protein, BMI for Body Mass Index, T1D, T2D for Type 1 and Type 2 Diabetes, MODY for Maturity Onset Diabetes of the Young.

1.2.7 Molecular Diagnosis of MODY

DNA sequencing is the recommended diagnostic approach for MODY, as it is essential for identifying MODY-causing mutations and diagnosing specific MODY subtypes. This is recommended for individuals who are diagnosed with diabetes before the age of 25, have a family history of diabetes spanning at least two consecutive generations, and exhibit evidence of endogenous insulin secretion (Ellard *et al.*, 2008; Shepherd *et al.*, 2009).

Genetic testing for MODY involves the sequencing of an individual's genomic DNA to identify genetic changes or variants in the known MODY genes (Murphy, Ellard and Hattersley, 2008). Common techniques include sanger sequencing and next-generation sequencing (NGS) (Pareek, Smoczynski and Tretyn, 2011; Slatko, Gardner and Ausubel, 2018). Two additional DNA screening methods for identifying MODY mutations include Multiplex ligation-dependent probe amplification (MLPA), which detects copy number variations in MODY genes, and Polymerase chain reaction (PCR)-based analysis, which amplifies specific DNA regions associated with MODY mutations (Milbury, Li and Makrigiorgos, 2009; Stuppia *et al.*, 2012).

These methods offer options for identifying genetic changes, such as deletions, duplications, or point mutations, that contribute to MODY, and the choice of method depends on the specific genetic alterations being investigated and available resources. It is recommended that genomic sequencing be performed on at least two generations of family members of MODY patients. The main limitation is the cost of genetic testing which may contribute to the underdiagnosis of MODY (Johansson *et al.*, 2017). As a result, genetic testing is typically reserved for cases where there is a strong suspicion of MODY. To date, many individuals who meet these criteria do not undergo genetic testing, and approximately 50% of confirmed MODY cases do not fulfil the established diagnostic criteria (Urakami, 2019).

1.2.8 Challenges in Assessing Variant Pathogenicity

The pathogenicity of a genetic variant causing MODY can be graded using a five-point scale based on its impact on protein function: 1, benign; 2, probably benign; 3, variant

of unknown significance; 4, probably pathogenic; and 5, pathogenic (Riggs *et al.*, 2020). If a variant is pathogenic, it is referred to as a "mutation" and is believed to cause protein damage that results in the disease phenotype. In contrast, variants that do not cause disease are called "polymorphisms". Previously published variants are compared with new ones using mutation databases, such as the Human Gene Mutation Database (HGMD) (Cooper, Stenson and Chuzhanova, 2006; Richards *et al.*, 2015).

In the context of clinical studies, there is a need for a cost-effective method to determine the pathogenicity of genetic variants. *In silico* approaches have become the standard methods for this purpose, as they are relatively inexpensive and can be performed quickly. *In silico* characterisation of a variant can be used initially to assess its potential to be pathogenic. If the variant is found to be potentially pathogenic, it can then be further characterised using *in vitro* assays to assess its effect on protein function (Flannick *et al.*, 2013; Althari and Gloyn, 2015; Richards *et al.*, 2015).

In silico methods use bioinformatic tools to predict the sequence conservation, protein structure, physicochemical properties, and splicing. Several commonly used bioinformatics prediction tools for genetic variant analysis include MutationTaster-2 (MT2) (Schwarz *et al.*, 2014), Sorting Tolerant from Intolerant (SIFT) (Ng and Henikoff, 2003), PolyPhen-2 (HumVar model) (Adzhubei *et al.*, 2010), Combined Annotation Dependent Depletion (CADD) (Kircher *et al.*, 2014), and Align Grantham Variation and Grantham Deviation (GVGD) (Tavtigian *et al.*, 2006).

In silico tests are cost-effective and time-efficient, but they have limited accuracy in predicting the pathogenicity of a variant. Therefore, these methods should be used in combination to improve precision. The results of *in silico* methods should only be used to decrease or increase the likelihood of a variant being pathogenic, and the confidence level of *in silico* predictions should not be solely relied upon for pathogenicity prediction when dealing with VUSs (Garcia, de Andrade and Palmero, 2022).

1.2.9 Developing an *In Vitro* Model for Studying MODY

Investigating VUS pathogenicity in *HNF1A* and *HNF4A* poses challenges as it depends on *in silico* approaches, which have limited reliability. Therefore, *in vitro* assays become essential for demonstrating the functional impact of a variant. There are established assays for the functional characterisation of gene changes in the MODY genes *HNF1A* and *GCK*. For *HNF1A*, which encodes a transcription factor, assessing the transcriptional and DNA-binding activity of the proteins comparing wild-type and variant proteins is crucial. Transactivation experiments involved overexpressing *HNF1A* in immortalised cell lines, followed by a luciferase activity assay. This assay measured the relative expression of luciferase, which is controlled by a promoter interacting with the HNF1A protein. Expression levels of HNF1A are usually examined through Western blot analysis or by isolating mRNA, followed by reverse transcription and quantitative PCR. Additionally, the subcellular localisation of HNF1A transcription factor can be investigated using immunofluorescence assays. The DNA-binding ability of HNF1A is assessed through Electrophoretic Mobility Shift Assays (EMSA), or alternatively specific assays employing indirect colorimetric tests using antibodies specific to HNF1A (Valkovicova *et al.*, 2019b; Althari *et al.*, 2020).

For *GCK*, which encodes for a kinase enzyme, kinetic analyses can help understand the variant's impact on protein function and stability. This enzyme kinetic analysis typically relies on spectrophotometry (Flannick *et al.*, 2013; Althari and Gloyn, 2015).

To assess the impact of genetic variants on protein function, cell types such as HeLa (derived from cervical cancer cells) and INS-1 cells (derived from a rat insulinoma cell line) are commonly used in functional assays *in vitro* (Asfari *et al.*, 1992). By introducing the gene of interest, including the variant of interest or a control gene, through transfection techniques, these cell models offer convenient and rapid approaches to gain insights into the fundamental impact of genetic variants (Chong, Yeap and Ho, 2021).

Modelling the complex development of MODY in depth is challenging. Initial *in vitro* functional assays conducted on commonly used immortalised cell lines may not

faithfully replicate the disease phenotype and are limited in their ability to predict the physiological impact of genetic variants. This is because these cell lines may not be derived from human β-cells expressing the genes of interest endogenously.

Despite these complexities, gaining a comprehensive understanding of human β-cells is essential. MODY-causing genes are primarily expressed in these cells, and their function may differ in β-cells from their expression in rodents or other established immortalised cell lines. It is crucial to understand how genes in MODY influence β-cells function.

Immortalised human β-cell lines, such as Endoc-BH1, Endoc-BH2, and Endoc-βH3, offer a valuable tool for studying MODY and addressing the limitations associated with primary β-cells and cell lines derived from other species than human. Although there are currently no immortalised β-cell lines derived from MODY patients, gene editing techniques can introduce MODY-causing mutations into these lines. Challenges exist in generating mutant cell lines with specific gene mutations due to the limited clonal efficiency of Endoc-BH1, Endoc-BH2, and Endoc-βH3. While these cell lines are useful for studying MODY pathophysiology, their suitability for investigating pancreas development related MODY genes may be limited (Benazra *et al.*, 2015).

The Endoc-βH5 cell line, the latest in immortalised human β-cells, closely replicates the physiological and functional traits of native human pancreatic β-cells to a greater extent than its predecessor Endoc-βH1,-βH2 and -βH3, exhibiting improved glucose responsiveness and insulin secretion levels (Blanchi *et al.*, 2023).

1.3 Human Pluripotent Stem Cells

Human pluripotent stem cells (hPSCs) encompass two types: human embryonic stem cells (hESCs) and human induced pluripotent stem cells (iPSCs). iPSCs and hESCs are both pluripotent, meaning they can self-renew indefinitely and differentiate into any cell type of the three germ layers: ectoderm, mesoderm, and endoderm (Martin, 1981; Thomson *et al.*, 1998; Takahashi and Yamanaka, 2006; Kolios and Moodley, 2013).

1.3.1 Human Embryonic Stem Cell

In 1998, Thomson et al. achieved a significant milestone by successfully deriving hESCs (Thomson *et al.*, 1998). Since then, hPSCs have played a crucial role in numerous studies, particularly in the investigation of disease development, regenerative therapies, and disease modelling. In the context of diabetes and the need for a deeper understanding of its pathogenicity, hPSCs offer a unique source for studying β-cells *in vitro* (Kroon *et al.*, 2008; Rezania *et al.*, 2012; Nostro *et al.*, 2015). By overcoming the limited availability of islet from donors, hPSCs provide an unlimited source of pancreatic β-cells.

hESCs are derived from the inner cell mass of blastocysts, initially consisting of five lines: H1, H13, and H14 for XY male genotype, and H7 and H9 for XX female genotype (Thomson *et al.*, 1998). Nowadays, there is a wide range of hESC lines available, offering flexibility for specific studies on directed differentiation and cell lineage. To investigate the development of pancreatic cells, researchers have developed hESC reporter lines that assist in characterising insulin-producing (INS+) cells generated *in vitro*. INS GFP/w hESCs are a commonly used reporter line, which includes the HES3 and MEL1 lines (Micallef *et al.*, 2012). These reporter lines involve the integration of a vector into the INS locus, for the insulin gene, enabling the identification of multiple clones once differentiated into insulin-producing β-cells (Rezania *et al.*, 2012; Pagliuca *et al.*, 2014).

Genetic modifications using techniques like CRISPR/Cas9 can be applied to introduce genetic variant into hESCs for the purpose of investigating mutations associated with monogenic diabetes. The utilisation of hESCs presents a distinct advantage due to their capacity to differentiate into cells resembling β-cells (Jiang *et al.*, 2007; Pagliuca *et al.*, 2014; Nostro *et al.*, 2015). This characteristic enables a meaningful comparison between genetically modified cells and healthy cells that originate from an identical initial stem cell lineage.

The differentiated β-cell-like cells obtained from hPSCs hold significant value for applications such as drug screening and the creation of disease models,

encompassing conditions like MODY, T1D or T2D among others (see Figure 1.4). There is also the potential for the transplantation of either healthy β-cell-like cells originating from iPSCs or hESCs. Such transplantation holds promise for the *in vivo* production of insulin and the potential reversal of diabetes (Nir, Melton and Dor, 2007; Aguayo-Mazzucato and Bonner-Weir, 2010).

1.3.2 Induced Pluripotent Stem Cells

iPSCs are a type of pluripotent stem cell that can be derived from adult somatic cells (Takahashi and Yamanaka, 2006). These cells, which can be derived from any individuals including monogenic diabetes probands, retain the identical genomic DNA and have the capacity for self-renewal, allowing for their maintenance *in vitro*.

In 2006, Takahashi K, Yamanaka S et al. published a study demonstrating the successful generation of iPSCs from mouse foetal fibroblasts (Takahashi and Yamanaka, 2006). This study demonstrated that cells could be reprogrammed from a mature differentiated state to an induced pluripotent one. Once de-differentiated, iPSCs exhibit the same potential as other human pluripotent stem cells to differentiate into various cell types.

Since then, researchers have used these findings to direct the differentiation of iPSCs into a wide range of cell types, including cardiomyocytes, hematopoietic cells, hepatocytes, intestinal organoids, pancreatic endocrine cells, neurons, just to name a few (Rowe and Daley, 2019; Sharma *et al.*, 2020). These advancements helped the study of genetic diseases including MODY, as iPSCs provide a valuable tool to study disease development, offering important insights into the pathogenesis of various disorders (Braverman-Gross and Benvenisty, 2021).

The reprogramming of iPSCs was achieved through genome sequencing and analysis of hESC profiles. OKSM vectors including *Nanog*, octamer-binding transcription factor 3 and 4 (*OCT3/4*), Krueppel-like factor 4 (*KLF4*), sex-determining region Y-box 2 (*SOX2*), and MYC proto-oncogene (*MYC*) were identified, and their overexpression induces pluripotency.

The reprogramming process involves three phases: initiation, maturation, and stabilisation (Buganim, Faddah and Jaenisch, 2013). The initiation stage of somatic cell reprogramming triggers morphological changes in the cells as they transition to a de-differentiated state. For example, fibroblasts that are reprogrammed with OKSM vectors transition from a mesenchymal to an epithelial state (Yoo *et al.*, 2014). In this stage, the OKSM factors act to suppress somatic gene expression while activating gene expression associated with pluripotency (Takahashi and Yamanaka, 2016).

As the maturation phase progresses, a small number of iPSC colonies emerge. The stabilisation phase follows and leads to the formation of iPSC colonies with the OKSM reprogramming factors silenced. These colonies display characteristics similar to those of human pluripotent stem cells, accompanied by the expression of genes associated with pluripotency (Buganim, Faddah and Jaenisch, 2013).

The main limitation is that the process is inefficient, approximately 0.1% from blood cells and 1% from fibroblasts, and the reasons behind this inefficiency remain unclear (Takahashi and Yamanaka, 2006; Hasegawa *et al.*, 2010; Malik and Rao, 2013).

1.4 Genome Editing in Human Pluripotent Stem Cells

MODY genes play a crucial role in β-cells function and pancreatic development. To better understand the impact of MODY-associated gene mutations on pancreatic development and identify the stages that are affected, researchers can differentiate hPSCs carrying specific mutations or variant found in MODY genes to understand their pathogenicity.

By utilising advanced molecular biology techniques, genetic variations can be introduced into existing hPSCs to generate β-cell-like cells with specific MODY-related gene variants. These engineered β-cell lines closely resemble cells derived from patients, making them valuable tools for studying monogenic diabetes. Through this approach, researchers can investigate the impact of MODY mutations on pancreatic development and gain insights into the underlying mechanisms of the disease (Vethe *et al.*, 2017; Li *et al.*, 2020).

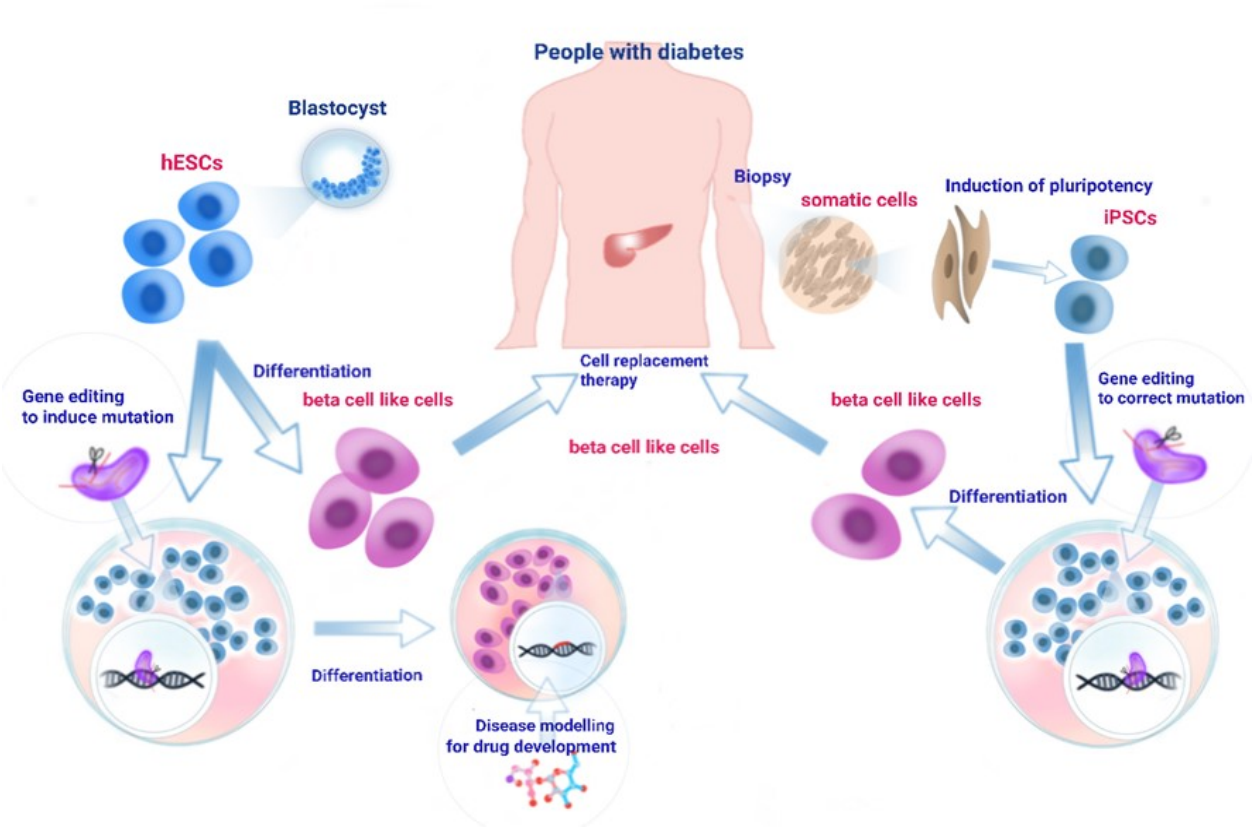

Figure 1.4: **Diabetic patient-derived iPSCs and hESCs-derived genetically modified cells generation, differentiation, and transplantation.**

iPSCs can be derived from skin fibroblasts, cord blood or peripheral blood cells after diabetic donor's biopsy. Somatic cells are reprogrammed by inducing overexpression of OKSM factors (*OCT3/4*, *SOX2*, *KLF4*, and *MYC*). After which, iPSCs can either be differentiated into β-cell-like cells by exposing iPSCs to specific β-cell growth factors and signalling proteins described in the development process of the pancreas. Alternatively, hESCs can undergo direct differentiation into β-cell-like cells using the same method as iPSCs. Mutations involved in diabetes can be studied by introducing precise gene modifications in hESCs (e.g., CRISPR/cas9). Differentiated hESCs/iPSCs into β-cell-like cells are used for drug screening and to model pathophysiology of disease (e.g., MODY, T1D, T2D, etc.). Eventually, healthy β-cell-like cells (T1D donors) or corrected β-cell-like cells can potentially be transplanted to express insulin *in vivo* and reverse diabetes.

1.4.1 CRISPR-Cas9 Tools for Editing and Introducing Genetic DNA Variants

CRISPR (Clustered Regularly Interspaced Short Palindromic Repeat) is a molecular biology technology that has impacted significantly the field of genetic research and genome editing (Doudna and Charpentier, 2014). It involves two crucial components: a single-stranded guide RNA (gRNA or sgRNA) and a CRISPR-associated endonuclease (Cas) (Al-Attar *et al.*, 2011; Doudna and Charpentier, 2014).

The gRNA serves as a DNA targeting molecule, binding to the Cas protein. Together, they recognise and bind to the specific genomic region targeted for modification. Near the target region is a protospacer adjacent motif (PAM), a short DNA sequence necessary for the Cas protein to cleave the DNA double strand at the desired DNA location (Haurwitz *et al.*, 2010; Wiedenheft, Sternberg and Doudna, 2012).

Upon introducing a DNA double-strand break (DSB) using CRISPR/Cas9, the cell initiates repair mechanisms to restore the integrity of the genome. The repair process involves two main pathways: non-homologous end-joining (NHEJ) and homology-directed repair (HDR) (Sung and Klein, 2006; Chang *et al.*, 2017). HDR is particularly useful for precise genetic engineering applications, allowing specific DNA sequences to be inserted or substituted at targeted genomic sites (Sung and Klein, 2006).

In the context of monogenic diabetes study of VUSs pathogenicity, HDR can be employed to introduce disease-associated variants into various cell types, enabling the study of disease mechanisms and the creation of *in vitro* disease models. However, HDR-mediated genome editing has a few limitations, including its inefficiency, mainly due to reliance on cellular repair mechanisms, in addition to its inaccurate editing associated with CRISPR technology (both on-target and off-target) (Guo *et al.*, 2018).

1.4.2 Novel Precise Base Editing Technologies

Base editing is a precise technique for modifying individual nucleotides in the genome without causing DNA breaks. It involves combining a modified Cas9 enzyme (dCas9) with deaminase enzymes that can convert one nucleotide into another. Cytosine base

editors (CBE) are a type of base editor that utilise dCas9 and APOBEC deaminase. The CBE can convert cytosine (C) to uracil (U), resulting in the formation of a U-G base pair. Cellular repair mechanisms then convert the U-G base pair to a U-A base pair, which is further converted to a T-A base pair. The efficiency and accuracy of base editing can be enhanced by incorporating uracil glycosylase inhibitors (UGIs) and other enzymes. Second-generation base editors, such as BE2, have been developed to ensure error-free repair and improve processing efficiency. Activation-induced cytidine deaminase (AID) and other deaminases have also been used in combination with engineered Cas9 to induce single point mutations. Different versions of base editors, like BE3 and BE4, have their limitations and strengths in terms of base editing efficiency and potential for indel formation. Besides cytidine deaminases, other deaminases and CRISPR endonucleases, such as Cpf1, can also be fused for base editing purposes.

Other types of base editors besides the cytosine base editor include adenosine base editors (ABEs) and prime editors. ABEs enable the conversion of A-T base pairs to G-C base pairs in genomic DNA. Prime editors utilise a prime editing guide RNA (pegRNA) to guide RNA to the target site and achieve more precise and efficient correction of specific nucleotides (Gaudelli *et al.*, 2017; Anzalone *et al.*, 2019). Together, these alternative techniques can modify any nucleotide into any other nucleotide, also known as single nucleotide variant (SNV), the substitution of a single nucleotide for another (McDaniel, Komor and Goren, 2022).

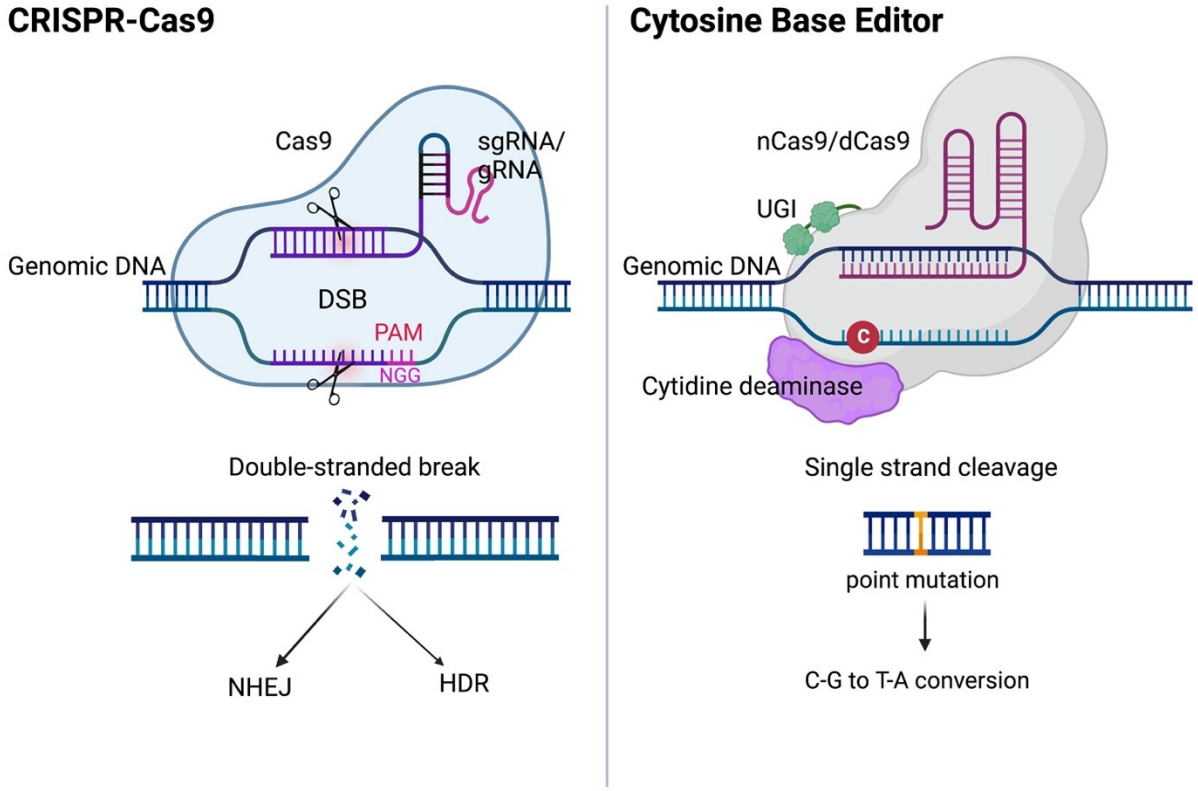

Figure 1.5: **Genome editing: CRISPR-Cas9 and Cytosine Base editor.**
Cas9 is directed to the target site within the genomic DNA through a chimeric single-guide RNA (sgRNA). The CRISPR/Cas9 system enables precise editing of genes by creating intentional breaks in the DNA, which are then repaired by DNA repair mechanisms like non-homologous end joining (NHEJ) and homology-directed repair (HDR). Cytosine base editors (CBEs) utilise a cytidine deaminase and an inactive dCas9 to facilitate a change from C to T (or G to A on the opposite strand). By incorporating an inhibitor of uracil DNA glycosylase (UGI) into dCas9, the process of base excision repair, which would reverse the mutation, is inhibited, ensuring the stability of the C to T change.

1.5 Generation of Pancreatic β-Cells

Recent advancements in hPSC culture and differentiation protocols have improved the efficiency and reproducibility of generating pancreatic β-cells. The process of differentiating into β-cells involves the use of specific cytokines and small molecules that mimic the signalling events occurring during pancreatic development. Precisely timed and staged addition of these molecules induces the expression of essential genes, facilitating a sequential and accurate differentiation process to generate functional β-cells secreting insulin.

First, hPSCs are differentiated into definitive endoderm (DE) by activating the Nodal pathway. Activin A, a member of the transforming growth factor-β (TGF-β) family, is essential for initiating the differentiation of hPSCs cells into endoderm and mesoderm through Nodal signalling (Zorn and Wells, 2007; Pauklin and Vallier, 2015). The Activin A is crucial for achieving efficient endoderm differentiation (Wang *et al.*, 2015). The definitive endoderm stage undergoes differentiation into the primitive gut tube/foregut. The initiation of the primitive gut tube stage of differentiation is induced *in vitro* removing activin A (D'Amour *et al.*, 2006). Following this, the initiation of pancreatic precursor cell differentiation is initiated by fibroblast growth factor (FGF) signaling, with FGF10 playing a significant role in stimulating the proliferation of pancreatic progenitors (Bhushan *et al.*, 2001).

KGF (keratinocyte growth factor) facilitates ductal cell proliferation, while activation of PKC (protein kinase C) promotes β-cell proliferation (Kroon *et al.*, 2008). The pancreatic precursor or progenitor cells then differentiate into pancreatic endocrine cells. During this differentiation process, the inhibition of Notch signalling in progenitor cells plays a critical role in determining their fate as either endocrine or exocrine cells. Specifically, the presence of Neurogenin-3 (Ngn3)-positive cells indicates their role as endocrine progenitors (Jiang *et al.*, 2007; Jang and Kim, 2010).

The use of retinoic acid treatment (RA), a derivative of vitamin A1, is essential for effectively differentiation from definitive endoderm cells into foregut endoderm cells expressing *PDX1* (Johannesson *et al.*, 2009). Activin A enhances *NGN3* expression,

and pro-endocrine gene expression is promoted by thyroid hormones and T3. Research findings suggest that cells expressing *NGN3* differentiate into endocrine progenitor cells as they demonstrate the ability to proliferate and generate cells that express specific transcription factors associated with islets, including *NKX6.1* (Jensen *et al.*, 2000).

Blocking liver differentiation and BMP signalling is necessary, requiring ALK4/5/7 inhibitor and Noggin to enhance endocrine lineage differentiation (Velazco-Cruz *et al.*, 2019). The last stage involves the differentiation process that leads to the specification and functionality of β-cells. Factors such as nicotinamide, GLP-1 (glucagon-like peptide 1), exendin 4, thyroid hormone, and VEGF (vascular endothelial growth factor) enhance β-cell development and function (191–193).

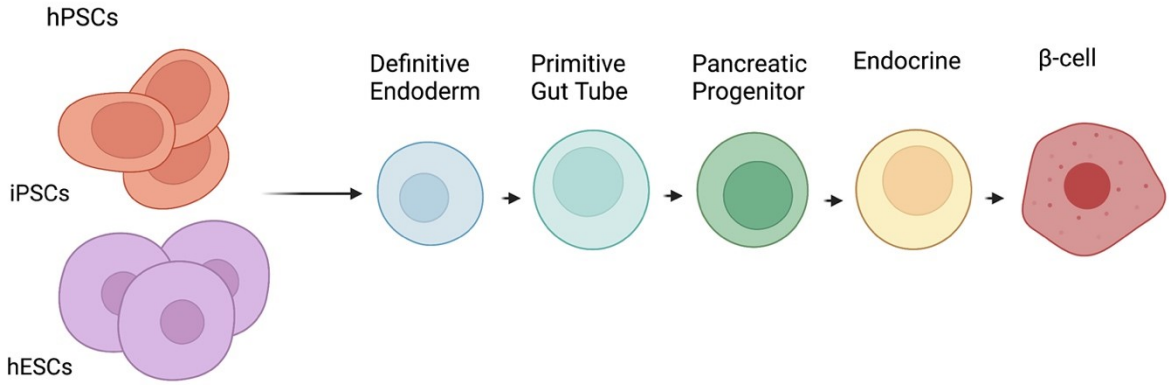

Figure 1.6 : **Generating β-Cells: A Schematic Overview**.
This figure illustrates the step-by-step process of generating β-cells from human pluripotent stem cells, both iPSCs and hESCs. The differentiation pathway involves the sequential development of hPSCs into definitive endoderm, primitive gut tube, and ultimately β-cells. This directed differentiation is carefully coordinated through the activation and inhibition of specific transcription factors at precise time points, enabling the maturation of stem cells into fully functional β-cells.

1.5.1 Differentiation of β-Like Cells and Native Human β-Cells: Distinctive Characteristics

The differentiation of hPSCs into β-cell-like cells results in cells that resemble native β-cells, but with some notable functional and developmental differences. β-cell-like cells derived from directed differentiation do not respond to glucose in the same way as native β-cells and secrete less insulin in response to glucose stimulation (Karimova, Gvazava and Vorotelyak, 2022). Additionally, a closer analysis of these β cell-like cells reveals that they are more closely aligned with immature β-cells in terms of their gene expression profile (Diane *et al.*, 2022).

Functionally, β-like cells derived from hPSCs display impaired glucose stimulated insulin secretion and this phenomenon has been attributed to metabolic failure, characterised by reduced phosphoenolpyruvate production, and decreased activity of glycolytic enzymes glyceraldehyde-3-phosphate dehydrogenase (GAPDH) and phosphoglycerate kinase (PKG). This reduced functionality poses challenges for direct comparisons, as stem cell-derived β-like cells exhibit lower responses compared to native human islets (Davis *et al.*, 2020).

β-cell directed differentiation protocols produce a mixture of cells resembling the native human islets of Langerhans, including α-like cells expressing glucagon and β-like cells expressing insulin (Riedel *et al.*, 2012). At the late stage of differentiation, some cells co-express both insulin and glucagon, resembling more immature α-precursor cells than β-like cells (Riedel *et al.*, 2012). These polyhormonal cells, transiently mis-expressing insulin, pose a limitation in β-cell differentiation protocols.

Efforts have been made to reduce their number and resemble *in vivo* native islet more closely including late-stage islet-like clusters, mice transplantation and the deaggregation-reaggregation protocol (Hilderink *et al.*, 2015; Nair *et al.*, 2019; Veres *et al.*, 2019). Recently, the utilisation of aphidicolin (APH) treatment has been employed to enhance the population of mono-hormonal β-cells. APH treatment exerts its effects by restraining cellular growth, which can be selectively controlled during the latter stages of differentiation through transient interference with DNA replication. This

approach has demonstrated the ability to elevate the expression of genes associated with metabolic signalling and insulin processing and release, specifically those co-expressing c-peptide and the *NKX6.1* β-cell marker (Sui *et al.*, 2021).

1.6 *HNF1A*: HNF Family, Gene Expression, Protein Expression, and Regulatory Targets

1.6.1 The Transcriptional Network of the HNF Family

Hepatocyte nuclear factor (HNF) constitutes a transcriptional functional network comprised of multiple genes belonging to the HNF family, including *HNF1A*, *HNF1B*, *HNF4A*, *HNF6*, and *HNF3*. (Lau *et al.*, 2018). The HNF transcription factor bind to a specific promoter or enhancer DNA sequence which regulates the expression of tissue-specific genes (Lau *et al.*, 2018). Each HNF has a specific spatial and temporal expression. Each HNF family member has isoforms which make its expression network complex (Boj *et al.*, 2001; Shih *et al.*, 2001).

Furthermore, this network of expression is an autoregulatory network, meaning that the expression of a particular HNF member can regulate the expression of others within the network (Kritis *et al.*, 1993). For instance, when *HNF1A* is knocked out (KO) in mice, it leads to a reduction in the gene expression of *HNF4A*, *HNF4γ*, and *HNF3* genes (Boj *et al.*, 2001; Shih *et al.*, 2001). It has been established as well that in the pancreas and liver, HNF1A transcription factor regulates HNF4A and its downstream transcriptional cascades (Kuo *et al.*, 1992; Eeckhoute, Formstecher and Laine, 2004).

1.6.2 *HNF1A* Gene

The *HNF1A* gene, located on chromosome 12 at 12q24.2, plays a key role in the development and function of several organs, including the pancreas, liver, gut, and kidney (Szpirer *et al.*, 1994; Geer *et al.*, 2010). It consists of 10 exons and acts as a transcription factor (Bellanné-Chantelot *et al.*, 2008). HNF1A transcription factor regulates genes associated with glucose metabolism, controlling crucial processes such as gluconeogenesis, glycogen synthesis, and glucose transport (Pontoglio *et al.*, 2000; Shih *et al.*, 2001; D'Angelo *et al.*, 2010). Three transcriptional isoforms of

HNF1A, namely *HNF1A-A*, *HNF1A-B*, and *HNF1A-C*, are generated through alternative splicing. These isoforms exhibit tissue-specific expression patterns, primarily due to their distinct N-terminal regions (98,99). *HNF1A-A* is predominantly involved in regulating insulin secretion and glucose homeostasis in the pancreas. *HNF1A-B* shows expression in the gut and liver, while *HNF1A-C* is mainly expressed in the kidney (98,99).

1.6.3 HNF1A Protein

The HNF1A protein consists of three distinct domains: an N-terminal dimerization domain (amino acids 1-32), a DNA-binding domain (amino acids 98-280), and a C-terminal transactivation domain (amino acids 281-628) (Baumhueter *et al.*, 1990; Rose *et al.*, 2000; Ryffel, 2001; Chi *et al.*, 2002). The protein structure and domain are presented in the Figure 3.1. As a transcription factor, it forms a homodimer and specifically binds to the inverted palindrome 5'-GTTAATNATTAAC-3' in the target genes (209). The DNA-binding domain of HNF1A comprises two sub-domains: POUs (amino acids 82-172) for protein stability and POUH (amino acids 198-281) for DNA binding initiation (Chi *et al.*, 2002).

To effectively interact with its target genes, HNF1A translocate into the nucleus, facilitated by specific amino acid sequences called nuclear localisation sequences (NLS) (amino acids 158-171, 197-205, and 271-282) (Chi *et al.*, 2002). The C-terminal transactivation domain consists of two subdomains: the serine-rich activation domain (amino acids 546-628) and the proline-rich domain (amino acids 281-318) (Chi *et al.*, 2002; Harries *et al.*, 2006). The structural characteristics of HNF1A protein collectively contribute to its functionality and regulatory mechanisms in gene regulation and cellular signalling.

1.6.4 Regulatory Targets of the HNF1A Protein

HNF1A has a wide range of functions in various organs. In the adult liver, it interacts with 222 target genes, while in the adult pancreatic islets, it interacts with 106 target genes (Odom *et al.*, 2004). In addition to its role in glucose metabolism and insulin

secretion, studies have demonstrated its involvement in the development of intestinal epithelial cell growth and differentiation (D'Angelo *et al.*, 2010; Yu *et al.*, 2019).

HNF1A regulates mitochondrial metabolism by modulating the transcriptional activity of angiotensin-converting enzyme 2 (ACE2) and exercises control over its activity in pancreatic islet cells. Even slight alterations in ACE2 activity in the pancreas can significantly impact glucose homeostasis (Chhabra *et al.*, 2013; Pedersen *et al.*, 2013; Shi *et al.*, 2018). In the intestine and kidneys, it is implicated in the regulation of HDL metabolism through the control of bile acid transporters (Shih *et al.*, 2001). HNF1A enhances the expression of organic cation transporters in the liver, which are important for medication uptake, including metformin (Shu *et al.*, 2007). Moreover, HNF1A is essential for the renal tubular reabsorption of glucose by regulating the expression of the low affinity/high-capacity glucose cotransporter SGLT2 (sodium glucose co-transporter 2) (Pontoglio *et al.*, 2000).

1.6.5 *HNF1A* Genetic Variants and Their Pathogenicity

The diagnosis of HNF1A-MODY requires DNA sequencing, and the classification of genetic variants a numerical scale ranging from 1 to 5, with 1 being benign and 5 being pathogenic (Riggs *et al.*, 2020). For variants of unknown significance, combining *in silico* predictions with *in vitro* functional protein analyses is recommended. Functional protein analyses, including transactivation assays, protein expression, DNA binding, and nuclear localisation, can be conducted as HNF1A is a transcription factor (Flannick *et al.*, 2013; Althari and Gloyn, 2015).

Pathogenic variants causing HNF1A-MODY can occur throughout the *HNF1A* gene and its promoter, without a specific hotspot identified (Colclough *et al.*, 2013). Mutations in the promoter can disrupt binding sites for other transcription factors in the liver and pancreas (Lau *et al.*, 2018). The dimerization domain of *HNF1A* frequently presents new variants, and mutations in this region impair the transactivation of specific target genes by disrupting the Dimerization complex with DCoH or PCBD1 (Simaite *et al.*, 2014). Mutations in the DNA-binding domain, particularly in the homeodomain (POUS and POUH), are associated with various human diseases,

including MODY, and can lead to a relative decrease in transactivation activity (Chi *et al.*, 2002; Harries *et al.*, 2006; Bellanné-Chantelot *et al.*, 2008; Colclough *et al.*, 2013). The transactivation domain has the lowest mutation rate, but functional assessment varies depending on the cell lines used to test the HNF1A activity *in vitro* (Colclough *et al.*, 2013). Mutations in the nuclear localisation regions of the DNA-binding and transactivation domains can result in incorrect subcellular localisation (Bjørkhaug *et al.*, 2003).

HNF1A-MODY variants impact β-cell function in various ways, including impaired glucose sensing, reduced proliferation, abnormal islet structure, and decreased insulin secretion. Decreased *HNF1A* gene expression is linked to reduced glycolysis and mitochondrial metabolism, exacerbating β-cell dysfunction (Dukes *et al.*, 1998; Pontoglio *et al.*, 1998). The effects of HNF1A mutations on β-cell function vary depending on their specific location within the protein. *In vitro* assays can assess the functional consequences of these variants (Althari and Gloyn, 2015). HNF1A-MODY variants exhibit a wide range of effects on β-cell function, which depend on the specific mutations and their location within the HNF1A protein. Understanding the pathogenicity of each variant is crucial for unravelling the role of HNF1A and its specific domains.

1.6.6 Association of *HNF1A* Variant with Type 2 Diabetes Risk

Certain mutations in the *HNF1A* gene have been associated with an elevated risk of T2D in recent studies (Gaulton, Ferreira, Lee, Raimondo, Mägi, Hreidarsson, *et al.*, 2015; Najmi *et al.*, 2017). For example, the E508K variant is a risk factor for T2D in the Mexican population, while the G319S variant is linked to T2D in the Canadian Oji-Cree population (Hegele *et al.*, 1999; Moreno-Estrada *et al.*, 2014). Certain variants, such as I27L and A98V, are risk factors of T2D by influencing levels of LDL-cholesterol and C-reactive protein (Chiu *et al.*, 2000; Locke *et al.*, 2018). Gaining a clear understanding of the pathogenicity of *HNF1A* variants is crucial for effectively managing diabetes, as it helps determine their association with the risk of T2D or MODY. Additional research is required to fully understand the impact of *HNF1A* variants on metabolic pathways and their role in the development of diabetes mellitus.

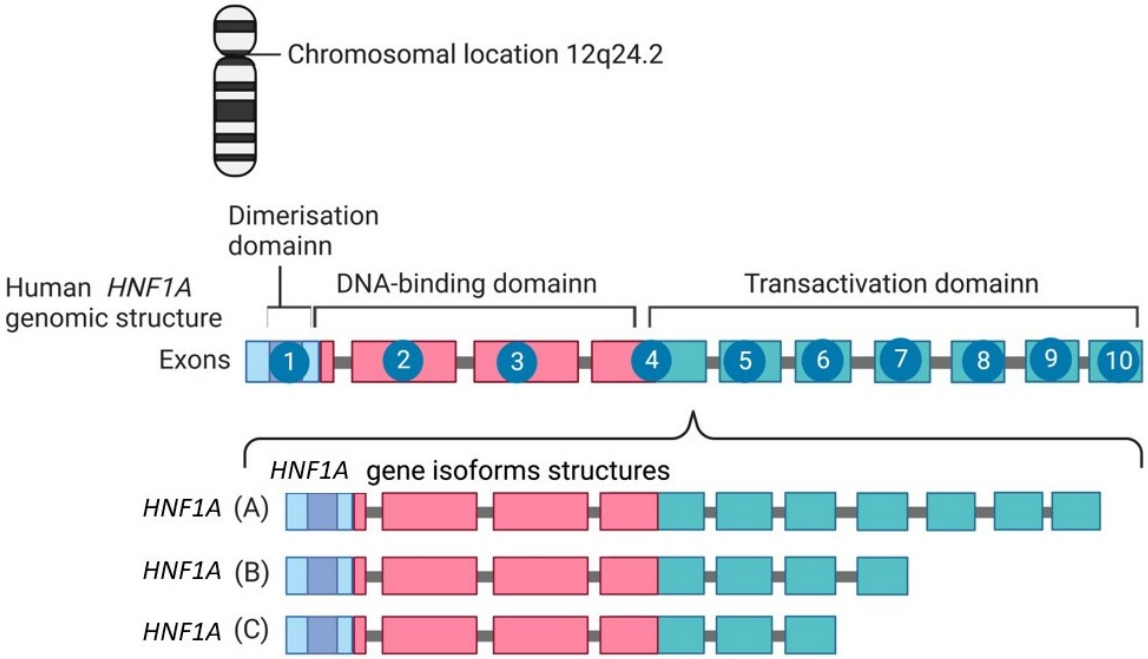

Figure 1.7: ***HNF1A* Schematic Representation of the Gene and Protein Domains.**

The human *HNF1A* gene is located on chromosome 12 (NC_000012.12) in the 12q24.2 region. It generates three transcriptional isoforms (isoform A, B, and C) through alternative splicing and different polyadenylation from the same promoter. The isoforms vary in length, with *HNF1A* A being the longest (10 exons), *HNF1A* B being shorter (7 exons), and *HNF1A* C being the shortest (6 exons). The HNF1A protein consists of three domains: a dimerization domain, a DNA-binding domain (DBD), and a transactivation domain.

1.7 Presentation of the Two *HNF1A* Variants of Unknown Significance Studied

This study focuses on investigating the pathogenicity of two variants of unknown significance in the *HNF1A* gene. These variants, p. A251T and p. S19L, were identified in probands participating in the 'MY DIABETES' study, where individuals from different ethnic groups and an early-onset diabetes diagnosis were recruited. The first variant, p.A251T, is a homozygous missense variant that has shown a modest reduction in transactivation potential based on *in vitro* functional assessment (Misra *et al.*, 2020). However, its exact impact on insulin secretion and β-cell function remains unclear and requires further investigation. The second variant, p.S19L, is a heterozygous variant with unknown significance but is predicted to have a deleterious effect on protein function according to *in silico* studies. Comprehensive characterisations, both *in silico* and *in vitro*, are necessary to determine the pathogenicity of this variant.

1.8 Aims and Objectives

The hypothesis is that the p.S19L and p.A251T variants alter the function of the HNF1A protein, affecting β-cell function.

Overall Aim: To undertake a multimodal investigation, integrating *in vitro* functional assays across various cell lines (including immortalised cell lines, stem cell genome-edited β-cell-like cells, and patient-derived β-cell-like cells) with clinical studies in order to ascertain the functional impacts and pathogenicity of *HNF1A* variants of unknown significance.

Aim of Study 1: To compare clinical and biochemical data of patients with established pathogenic *HNF1A* mutations and those with variants of unknown significance from the Imperial NHS Trust MODY service. This comparison is made to determine whether clinical data could help differentiate disease-causing variants from benign ones.

Aim of Study 2: To utilise previously established functional assays to assess transactivation potential, subcellular localisation, DNA-binding activity, and protein

expression of *HNF1A* p.S19L and p.A251T variants in immortalised cell lines. Comparisons will be made with Wild-Type (WT) *HNF1A* and previously identified MODY-causing variants.

Aim of Study 3: To generate the p.S19L variant in hESCs through genome editing. Additionally, generate iPSCs from p.A251T patient-fibroblasts and differentiate them into β-like cells using a directed differentiation protocol.

Aim of Study 4: To conduct innovative functional assays to thoroughly characterise the function of iPSC-derived β-like cells carrying variants of unknown significance to acquire a clearer understanding of the impact of these variants on β-cell function.

2 Chapter 2: Clinical study Distinguishing MODY Subtypes and Assessing Pathogenicity of VUS

2.1 Introduction

2.1.1 Challenges in Distinguishing Early Onset Diabetes

Before the fourth decade of life, distinguishing between T1D, MODY, and early onset type 2 diabetes (EOT2D) can present significant clinical challenges, based on the clinical presentation of these different diabetes subtypes (Thanabalasingham *et al.*, 2012; Hattersley *et al.*, 2018; American Diabetes Association, 2020). While T2D is typically diagnosed in adults over the age of 40 years, EOT2D affects individuals at an early age, usually with a family history of diabetes (Thanabalasingham *et al.*, 2012; American Diabetes Association, 2020; Magliano *et al.*, 2020). EOT2D therefore often shares common features with MODY, including age of onset and family history of diabetes (B. M. Shields *et al.*, 2010; Fajans and Bell, 2011; Magliano *et al.*, 2020).

While obesity and a high Body Mass Index (BMI) are often linked to T2D, recent studies have revealed that these factors may not consistently indicate a T2D diagnosis, especially in cases of early-onset diabetes. Similarly, it is important to acknowledge that individuals with MODY can also exhibit a BMI within the overweight or obese range (22), highlighting the intricate nature of using BMI alone as a diagnostic criterion.

Several cross-sectional studies, focusing specifically on the prevalence of dyslipidaemia (McDonald *et al.*, 2012; Fu *et al.*, 2019; Ma *et al.*, 2020), have provided valuable insights into distinguishing between T2D and MODY. Lipid profile combining high-density lipoprotein cholesterol (HDL), triglyceride, and low-density lipoprotein (LDL) levels, have been investigated as potential biomarkers for specific subtypes of MODY, such as HNF1A and HNF4A-MODY (McDonald *et al.*, 2012; Fu *et al.*, 2019; Ma *et al.*, 2020). Notably, individuals diagnosed with HNF1A-MODY tend to exhibit a more favourable lipid profile with high levels of HDL cholesterol, low levels of LDL cholesterol, compared to those with T2D (McDonald *et al.*, 2012).These findings

suggest that lipid markers could serve as valuable indicators to differentiate between HNF1A-MODY and T2D

MODY and T1D can have similar presentations, including a family history of diabetes. However, MODY is inherited in an autosomal dominant pattern, while T1D is not. In T1D, a family history of autoimmune diseases or T1D itself may be present, indicating a genetic predisposition to the condition. Additionally, both diabetes types manifest typically before the age of 40 (Thanabalasingham and Owen, 2011; Atkinson, Eisenbarth and Michels, 2014, p. 1).

Patients with T1D are distinguished from other forms of diabetes using C-peptide measurement as they typically exhibit low or undetectable levels of C-peptide (B. M. Shields *et al.*, 2010; Atkinson, Eisenbarth and Michels, 2014). It has been estimated that approximately 35% to 80% of individuals with T1D maintain persistent β-cell function and sustained endogenous insulin secretion for over 5 years (Coune and Paquot, 2022; Taylor *et al.*, 2022). Individuals with T1D who exhibit detectable levels of insulin (or C-peptide) at the time of diagnosis, make it difficult to distinguish between T1D and MODY based solely on this parameter (Pearson *et al.*, 2003; Atkinson, Eisenbarth and Michels, 2014, p. 1; Kuhtreiber *et al.*, 2015).

Additional tests, such as evaluating the presence of specific autoantibodies (Islet cell cytoplasmic autoantibodies (ICA), Glutamic acid decarboxylase autoantibodies (GADA), Insulinoma-associated-2 autoantibodies (IA-2A), Zinc Transporter 8 (ZnT8) Antibody and Insulin autoantibodies (IAA)) are required to distinguish T1D and MODY with precision (T. J. McDonald *et al.*, 2011). However, this approach is not always reliable, as antibodies may become undetectable over time. As a result, negative antibodies can be observed in both MODY and long-duration T1D (Yu, Zhao and Steck, 2017; Fritzler *et al.*, 2018).

Diabetic Ketoacidosis (DKA) stands as a clinical marker serving as pivotal in distinguishing between MODY and T1D. DKA is a severe life-threatening complication resulting from prolonged hyperglycaemia, marked by a distinctive clinical presentation that includes symptoms of acidosis (Fazeli Farsani *et al.*, 2017). The residual insulin

production observed in individuals with HNF4A/HNF1A-MODY induce a diminished susceptibility to DKA as the presence of residual insulin helps mitigate the accumulation of ketones in the bloodstream (Stride *et al.*, 2002).

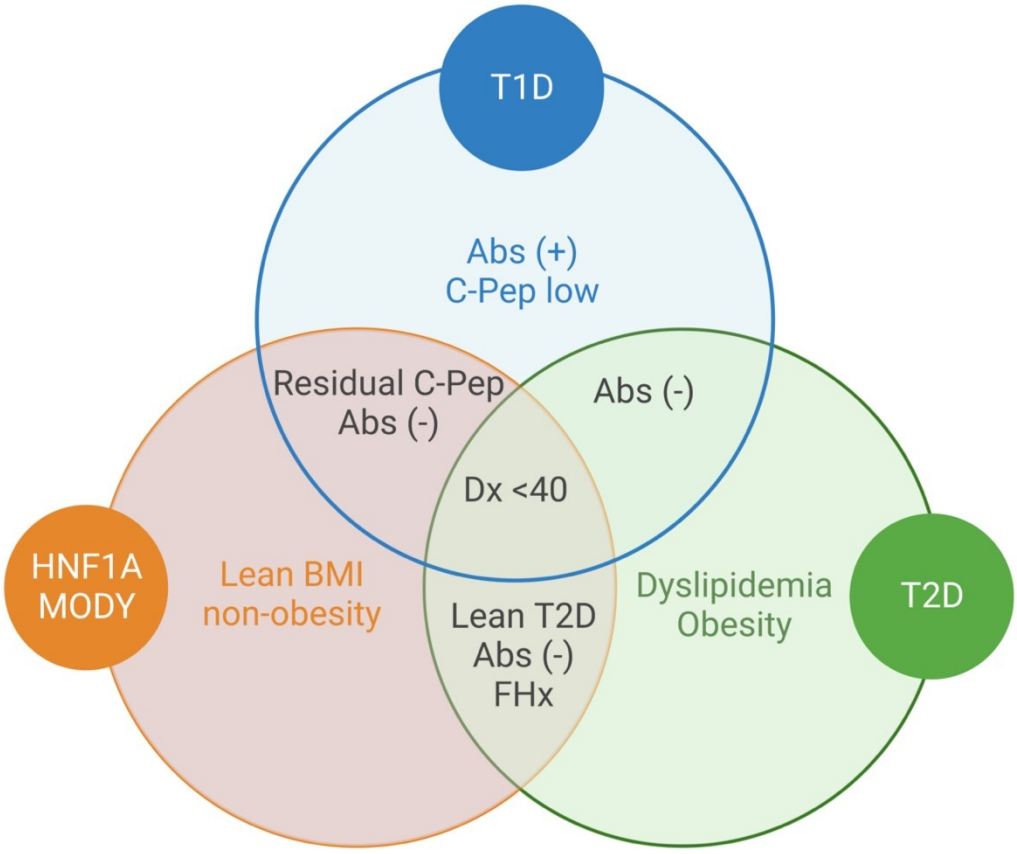

Figure 2.1: **Venn Diagram Depicting Clinical Features and Biomarker Overlap Among Different Diabetes Subtypes: HNF1A-MODY, T1D, and T2D.**

The intersecting areas delineate concordant attributes. The blue circle (uppermost): Corresponds to T1D. T1D's clinical features include low to non-detectable C-Peptide levels and the autoantibody detection (ICA, GADA, IA-2A, IAA, and ZnT8A). The green circle (to the right): Corresponds to T2D, characterised by insulin resistance, along with dyslipidaemia and elevated BMI, typically being overweight or obese (BMI~30kg/m^2 or beyond). The orange circle (to the left): Represents HNF1A-MODY, marked by lean BMI (<30 kg/m^2). The Blue-Orange Intersection: Signifies overlapping clinical features prevalent in both T1D and HNF1A-MODY, including residual C-peptide levels, with absence of autoantibody detection noted Abs (-). The Orange-Green Intersection: Showcases Abs (-) and a familial history of diabetes (FX), inclusive

of instances of lean T2D with a BMI below 30 kg/m^2, prevalent in both HNF1A-MODY and T2D. The Shared Green-Blue Region: Designates T1D/T2D, inclusive Ab (-). The Orange-Green-Blue Intersection: Includes diagnosis under the age of 40 years (Dx <40), applicable to all three subtypes.

2.1.2 Clinical Criteria and Biomarkers for Accurate Diagnosis of MODY

Accurate diagnosis of MODY subtypes and their distinction from T1D and T2D is essential to ensure appropriate treatment for patients (Pearson *et al.*, 2000, 2003, 2006; Jang, 2020). Specifically, the precise identification of HNF1A-MODY and HNF4A-MODY holds the potential to enhance diabetes management, given that individuals with these MODY variants frequently exhibit sensitivity to sulfonylureas (Pearson *et al.*, 2006)

Clinically diagnosing MODY presents a challenge due to the absence of a single universal set of criteria applicable to all MODY subtypes (Hattersley and Patel, 2017). A combination of clinical criteria and biomarkers must be employed, including features such as early onset typically before the age of 35, a familial history of diabetes (preferably involving one parent and extending across two generations), absence of obesity, non-insulin dependence, negative autoantibody test results and fasting C-peptide levels (as detailed in the Introduction section 1.2.6) (J. D. Shields *et al.*, 2010; Hattersley and Patel, 2017). These tools should be at the very least utilised to aid in identifying individuals who warrant genetic testing for MODY. However, it is important to note, as mentioned in the section, that each of these criteria individually possesses limitations that render the exclusive reliance on clinical characteristics a challenging approach for diagnosis.

Utilising genetic sequencing as a method for MODY diagnosing is not cost-effective, primarily due to the current high cost associated with sequencing procedures. Moreover, even in the event of potential cost reductions in genome sequencing, it remains imperative to strategically allocate resources towards individuals presenting a higher probability to suffer from a MODY diabetes, including those with familial

predisposition or exhibiting clinical indicators suggestive of the condition (Naylor *et al.*, 2014).

2.1.3 Genome Sequencing and the Challenge of Variants of Uncertain Significance

Genetic sequencing is essential for the accurate diagnosis of MODY by identifying specific genetic variants that are responsible for the disease. The main challenge remains in interpreting the sequencing results when a variant of unknown significance (VUS) or a novel variant is detected in genes associated with MODY.

Numerous guidelines have been established to standardised protocol for evaluating the pathogenic nature of variants (as presented in the introduction's section 1.2.8) (Ellard *et al.*, 2008; Althari and Gloyn, 2015; Richards *et al.*, 2015; Juszczak *et al.*, 2016). This approach involves a combination of *in silico* computational predictions and *in vitro* assessment of gene function and corresponding proteins. The pathogenicity of variants is categorised on a grading scale ranging from 1 to 5. A grade of 1 indicates a benign variant, 2 implies a likely benign variant, 3 designates a VUS, 4 suggests a likely pathogenic variant, and 5 signifies a pathogenic variant (Wallis *et al.*, 2013; Althari and Gloyn, 2015; Richards *et al.*, 2015).

Limitations persist concerning the interpretation of genetic data by clinicians, particularly when dealing with VUSs. This difficulty becomes more pronounced in situations where access to *in vitro* functional studies is limited. Furthermore, although *in vitro* studies provide valuable insights into the pathogenicity of variants, they often come with considerable costs and necessitate specialised expertise. The lack of functional assessment data makes it further challenging for clinicians to determine the clinical significance VUSs, which further complicate the diagnosis and management of MODY cases (Peixoto-Barbosa, Reis and Giuffrida, 2020).

2.1.4 Contribution of the MY DIABETES Study in Characterising Young-Onset Diabetes

To address challenges in diabetes classification the MY DIABETES study (Principal investigator Dr. Shivani Misra), was set up and aimed to characterise young-onset diabetes in various ethnic groups within the UK by incorporating molecular genetic testing into a systematic diagnostic approach. Data from this cross-sectional study offers a valuable opportunity to assess the efficacy of clinical features and biomarkers in determining the pathogenicity of VUS in causing disease.

This study was conducted using a non-interventional, cross-sectional study design, which aimed to compare the phenotype of early-onset diabetes in participants from white European, African/Caribbean, and South Asian ancestry in the UK. Participants were diagnosed with diabetes before the age of 30 years. The study employed clinical, biochemical, and genetic evaluations to ascertain the prevalence of MODY and to establish comparisons among individuals of different ethnicities.

This clinical study will use data from three cohorts of the MY DIABETES study: the HNF1A and HNF4A-MODY cohort, the T2D cohort, and the HNF1A and HNF4A VUSs cohort. The study will conduct an in-depth analysis of clinical features to evaluate how clinical characteristics can assist in determining the pathogenicity of VUS and assess the usefulness of these characteristics, acknowledging their limitations.

2.1.5 Aims of the Clinical Study

The aims of this clinical study are:

Aim of Study 1: To evaluate the difference in clinical phenotype between the T2D and HNF1A/HNF4A-MODY cohorts by undertaking a descriptive analysis with statistical testing.

Aim of Study 2: To identify clinical features most predictive of HNF1A/HNF4A -MODY using multivariable regression models.

Aim of Study 3: To compare the clinical features of participants with *HNF1A* or *HNF4A* VUS to participants with T2D and *bona fide* MODY.

2.2 Methods

2.2.1 Study Participants: Methodology, Cohort Characteristics, Recorded Clinical Data, and Recruitment Approach

The study participant and respective clinical data used in this chapter were obtained from the "MY DIABETES" study, which received ethical approval from the Imperial College Joint Research Office (CRO 13SM0659) on 11/04/2013, with LREC approval number 13/LO/0944. This study was conducted from 2014 to 2021.

To be included in the MY DIABETES study, individuals had to meet specific criteria. They were required to have received a diabetes diagnosis before the age of 30 years, regardless of the type of diabetes, based on fasting glucose, oral glucose tolerance test, or HbA1c measurements following the guidelines established by the World Health Organization. Additionally, participants were required to self-report their ethnicity as one of the following: white European, South Asian, or African-Caribbean. Those who self-reported as Asian, European, or African-Caribbean were required to have at least two grandparents from the corresponding region.

Individuals with established secondary causes of diabetes, including recurrent pancreatitis, pancreatectomy, new-onset diabetes following transplantation, Cushing's syndrome, acromegaly, or steroid-induced diabetes, were excluded from the study. Participants who were currently enrolled in a clinical trial involving an investigational medicinal product that could potentially impact the study results, as determined by the research team, were also excluded.

2.2.2 Statistical Analysis

The following clinical features were assessed for comparisons between HNF1A- and HNF4-MODY and T2D cohorts of MY DIABETES study: gender, age at diagnosis, family history, current insulin treatment, high-sensitivity C-reactive protein (hs-CRP), capillary glucose, HbA1c, fasting c-peptide, liver function tests including ALT and ALP, triglycerides, LDL and HDL cholesterol, waist-to-hip ratio (WHR), and BMI.

To test the hypothesis that each continuous biomarkers and clinical characteristics follow a Gaussian distribution, we perform the Kolmogorov-Smirnov test. The results indicated that all continuous data: age at diagnosis, capillary glucose, WHR, HbA1c, BMI, hs-CRP, fasting c-peptide, ALT, ALP, triglycerides, LDL and HDL; did not follow a normal distribution ($p<0.05$).

To compare these variables, a non-parametric Mann-Whitney U test was employed, and the data were reported as median (interquartile range); $p<0.05$ was considered statistically significant and were not corrected for multiple comparisons due to *a priori* hypotheses regarding the variables selected.

To examine the interaction between categorical variables such as family history, gender, and current treatment with MODY, data were reported per distribution in a contingency table. Contingency tables were statistically analysed using Fisher's exact test as the sample size for the HNF1A and HNF4A-MODY cohort was small ($n<50$).

To evaluate the likelihood of each variable (either clinical criteria or biomarkers) for predicting HNF1A and HNF4A-MODY cohort, univariate logistic regression was employed. Individuals were recorded for binary values 0 for ‘T2D’ or 1 for ‘HNF1A and HNF4A-MODY’. Univariate logistic regression was used to assess continuous and categorical variables variable in predicting HNF1A and HNF4A-MODY. All variables with $p<0.05$ was considered statistically significant and were selected for further analysis for model prediction for of HNF1A and HNF4A-MODY.

The probability of developing HNF1A and HNF4A-MODY was evaluated using multiple sets of variables, but only the most relevant variables were included in the final analysis: non-insulin treatment, HDL level, and age at diagnosis. The p-value and odds ratio for each variable was calculated, a significant level of $p<0.05$ was considered statistically significant. The goodness of fit of the model for probability of HNF1A and HNF4A-MODY assessing multivariable was test using the Hosmer-Lemeshow.

GraphPad Prism 9 was used for all the data analysis and to create graphs. This statistical methodology followed established best practices to compare cohorts. For all test only a significant level of $p<0.05$ was considered statistically significant.

2.3 Results Analysis of Clinical Characteristics, Biomarkers, and Pathogenicity of VUSs

2.3.1 Study 1 Descriptive Analysis of Clinical Parameters from MY DIABETES Study: HNF1/4A-MODY, Type 2 Diabetes and *HNF1A* or *HNF4A* Variants of Uncertain Significance

This analysis was initiated through a thorough selection of clinical features from the VUS, pathogenic HNF1A/HNF4A MODY cohort, and T2D cohorts. These parameters were chosen based on previous studies that have demonstrated their ability to characterise T2D and classify VUS as potential risk factors for T2D or indicators of clinical characteristics and biomarkers for HNF1A/HNF4A-MODY (). The chosen clinical features include the gender, age at diagnosis, family history of diabetes, BMI, WHR, capillary glucose levels, HbA1c, fasting C-peptide levels, inflammatory markers like hs-CRP, liver function indicators including ALT and ALP enzymes, and a lipid profile featuring levels of triglycerides, HDL, and LDL. These criteria underwent first comparative analysis across the two cohort MODY HNF1A/HNF4A, and T2D, to ascertain their effectiveness in differentiating between these two types of diabetes.

Table 2-1: **Summary Table of Clinical Criteria for Three Cohorts: T2D, HNF1A/HNF4A MODY, and HNF1A/HNF4A VUS Cohorts.**

Clinical criteria	
Physical measurements	BMI, Waist-to-Hip Ratio (WHR)
Diabetes indicators	Capillary blood glucose levels, glycated hemoglobin (HbA1c), fasting C-peptide, age at diagnosis
Inflammation test	High Sensitivity C-reactive protein (hs-CRP)
Lipid profile	Triglycerides, HDL cholesterol, and LDL cholesterol
Liver profile markers	Alanine aminotransferase (ALT) and Alkaline phosphatase (ALP) enzymes

2.3.2.1 Characterisation of Study Cohorts HNF1A/4A VUS, T2D and HNF1A and HNF4A-MODY.

Three distinct cohorts were studied: HNF1A/4A VUS (n=6), T2D (n=385), and HNF1A and HNF4A-MODY (n=15). The clinical features of all three cohorts are presented in Table 2-2

All individuals across the three cohorts were diagnosed with diabetes before the age of 30, resulting in a similar age range among the cohorts. The HNF1A/4A VUS cohort had a median age at diagnosis of 22 years (interquartile range (IQR) 18-27.25, n = 6), the T2D cohort had a median age at diagnosis of 22 years (IQR 17-27, n = 385), and the HNF1A and HNF4A-MODY cohort had a median age at diagnosis of 18 years (IQR 14-19, n = 15).

The gender distribution exhibited an equal distribution between males and females within the HNF1A/4A VUS cohort (50% male/female, n=6). Similarly, the T2D cohort (n=385), females comprised 57.92%, while males constituted 42.08%. In contrast, the HNF1A and HNF4A-MODY cohort (n=15) demonstrated a notable gender disparity, with males accounting for 73.33% and females for 26.67%, signifying a higher proportion of males within this cohort.

Across all three cohorts, a large number of individuals had a familial history of diabetes. Specifically, 100% of individuals in the HNF1A/4A VUS cohort had a familial history of diabetes, 72.21% of individuals in the T2D cohort had a familial history of diabetes and 93.33% of the participants in the HNF1A/4A-MODY cohort had a familial history of diabetes.

The physical examination revealed elevated BMIs across all three cohorts (HNF1A/4A VUS: median BMI 28.0 kg/m², IQR 26.7-30.4; T2D: median BMI 29.0 kg/m², IQR 24.7-34.1, HNF1A/4A MODY cohort: median BMI 25.1 kg/m², IQR 22.0-29.0). The waist-to-hip ratio (WHR) assessments were in the upper range according to WHO healthy WHR values of 0.9 or less for men and 0.85 or less for women (Moosaie *et al.*, 2021).However, these thresholds were not met in any of the cohorts. Specifically, the HNF1A/4A VUS cohort exhibited a median WHR of 0.91 (IQR 0.88-0.95), the T2D

cohort showed a median WHR of 0.92 (IQR 0.87-0.96), and the HNF1A/4A-MODY cohort had a median WHR of 0.86 (IQR 0.80-0.95). The analysis of glycaemic index values reveals that the HNF1A/4A-MODY cohort show lower capillary glucose levels in comparison to the T2D cohort HNF1A/4A-MODY cohort median of 7.55 mmol/L, IQR 6.15-8.95; T2D median of 8.60 mmol/L, 6.77-11.53). Conversely, both the HNF1A/4A VUS cohort and the T2D cohort exhibit similar glycaemic index profiles (with a median capillary glucose level of 8.55 mmol/L for HNF1A/4A VUS, 7.67-11.98, and a T2D median of 8.60 mmol/L, 6.77-11.53).

The fasting C-peptide levels, giving endogenous insulin secretion, the T2D cohort exhibited the highest median fasting C-peptide level of 512.0 pmol/L (IQR 233.0-888.5), possibly attributed to the characteristic insulin resistance seen in T2D. The HNF1A/4A VUS cohort showed a lower median level of 433.5 pmol/L (IQR 189.8-814.3), which closely resembled the HNF1A and HNF4A-MODY cohort, with a median of 480.0 pmol/L (IQR 349.0, 713.0).

The data shows that individuals in the HNF1A/4A VUS cohort and HNF1A/4A MODY cohort exhibit lower hs-CRP levels (median 2.5 mg/L, 0.5-3.0, and median 2.0 mg/L, 0.5-3.0, respectively) when compared to the T2D cohort (median 5.0 mg/L, with a range of 2.3-10.4 mg/L).

The three cohorts exhibit distinct liver profiles, with the ALT and ALP measurements of the VUS cohort closely resembling those of the HNF1A/4A-MODY cohort. The median ALT level for the VUS cohort was 18 U/L (IQR 16-33), and the median ALT level for the HNF1A/4A-MODY cohort was 19 U/L (IQR 16-28). The median ALP level for the VUS cohort was 74 U/L (IQR 59-103), and the median ALP level for the HNF1A/4A-MODY cohort was 79 U/L (IQR 60-92). In contrast to the VUS and HNF1A/4A-MODY cohorts, the T2D cohort showed higher levels of both enzymes. The median ALT level for the T2D cohort was 23 U/L (IQR 15-35), and the median ALP level was 81 U/L (IQR 65-100).

The lipid profile of the HNF1A/4A pathogenic cohort was more favourable than the other two cohorts, with lower LDL and triglyceride levels. The pathogenic cohort had

a median LDL-cholesterol level of 1.7 mmol/L (0.9-2.2), which was lower than the median levels of 2.4 mmol/L (1.6-2.9) in the VUS cohort and 2.4 mmol/L (1.8-3.1) in the T2D cohort. The T2D cohort also had a higher median triglyceride level of 1.4 mmol/L (1.0-2.1) than the VUS cohort (median 0.9 mmol/L, 0.6-1.6) and the HNF1A/4A pathogenic cohort (median 1.0 mmol/L, 0.8-1.9).

Table 2-2: **Summary of clinical parameters of diabetic probable T2D cohort.**

Hepatocyte nuclear factor-1 alpha (HNF1A) and Hepatocyte nuclear factor-4 alpha (HNF4A) pathogenic cohort and HNF1A/4A variant of unknown significance (abbreviated VUS) cohort and their comparison of clinical parameters among HNF1A/HNF4A-MODY including VUS and Type 2 Diabetes (T2D) Cohorts. The data are presented as median (interquartile range) unless categorical (%, n). For continuous non-normal clinical characteristics and biomarkers, the Mann-Whitney test was used to compare between groups. Categorical values were analysed using contingency tables, and Fisher's exact test was performed. TGs stands for triglycerides, and FHx for family history of diabetes. Statistical significance was considered at *p < 0.05, **p < 0.01, and ***p < 0.001 and were not corrected for multiple comparisons due to a priori hypotheses regarding the variables selected.

Characteristics	HNF1A/4A VUS cohort (n=6)	Probable T2D cohort (n=385)	HNF1A/4A pathogenic cohort (n=15)	P-value comparison T2D and HNF1A/4A pathogenic
Males/Females	50%/50%(n=6)	42 %/58% (n=385)	73%/27% (n=15)	0.29
Age at diagnosis (yr)	22 (18,27.25)	22 (17,27)	18 (14,19)	**0.001
FHx	100% (n=6)	72 % (n=277)	93 % (n=14)	0.13
% Currently on insulin	83% (n=5)	69% (n=265)	33% (n=5)	**0.008
BMI (kg/m²)	28.0 (26.7,30.4)	29.0 (24.7,34.1)	25.1 (22.0,29.0)	*0.02
Waist-to-Hip Ratio	0.91 (0.88,0.95)	0.92 (0.87,0.96)	0.86 (0.80,0.95)	*0.01
Capillary Glucose (mmol/L)	8.55 (7.67,11.98)	8.60 (6.77,11.53)	7.55 (6.15,8.95)	0.15
HbA1c (mmol/mol)	63 (54,75)	67 (52,83)	55 (50,64)	0.12
fasting C-peptide (pmol/L)	433.5 (189.8,814.3)	512.0 (233.0,888.5)	480.0 (349.0,713.0)	0.89
hs-CRP (mg/L)	2.5 (0.5,3.0)	5.0 (2.3,10.4)	2.0 (0.6,3.0)	**0.004
ALT	18 (16,33)	23 (15,35)	19 (16,28)	0.24
ALP	74 (59,103)	81 (65,100)	79 (60,92)	0.40
TGs (mmol/L)	0.9 (0.6,1.6)	1.4 (1.0,2.1)	1.0 (0.8,1.9)	0.27
HDL-cholesterol (mmol/L)	1.0 (0.8,1.4)	1.2 (1.0,1.4)	1.3 (1.0,1.9)	0.07
LDL-cholesterol (mmol/L)	2.4 (1.6,2.9)	2.4 (1.8,3.1)	1.7 (0.9,2.2)	***0.0001

2.3.2.2 Statistical Comparison between Pathogenic HNF1A and HNF4A-MODY and T2D Cohorts

Various characteristics were selected for comparison to investigate potential differences between the HNF1A/HNF4A-MODY cohort and the T2D cohort. These characteristics (presented in section 2 of this Chapter 2–73) include age at diagnosis, family history, gender, current insulin treatment, HbA1c level, BMI, lipid profile (LDL cholesterol, HDL cholesterol, and triglycerides), biomarker of inflammation (hs- C-reactive protein), and liver function tests (ALT and ALP). Since all the continuous variables of biomarkers and clinical characteristics exhibit a non-normal distribution, non-parametric analysis was conducted.

Individuals in the T2D cohort exhibited significantly higher age at diagnosis compared to the HNF1A/HNF4A-MODY cohort (p-value = 0.001). Specifically, the median age at diagnosis for T2D was 22 (17-27), while for the HNF1A/HNF4A-MODY cohort, it was 18 (14-19). This finding suggests that lower age could be considered a clinical characteristic associated with individuals diagnosed with HNF1A/HNF4A-MODY as compared to the T2D cohort. In terms of physical features, the T2D cohort exhibited significantly higher BMI values (median 29.0 kg/m², 24.7-34.1) compared to the HNF1A/HNF4A pathogenic cohort, which had a median BMI of 25.1 kg/m² (22.0-29.0, *p-value=0.02). Moreover, the WHR was significantly higher in the T2D cohort (median 0.92, 0.87-0.96) compared to the HNF1A/HNF4A pathogenic cohort (median 0.86, 0.80-0.95), with a *p-value=0.01.

Regarding lipid profiles, a borderline significant difference (p-value = 0.07) was observed in HDL-cholesterol levels between the T2D cohort (median 1.2 mmol/L, 1.0-1.4) and the HNF1A/HNF4A pathogenic cohort (median 1.3 mmol/L, 1.0-1.9 mmol/L. Additionally, the T2D cohort also had a significantly higher median LDL-cholesterol level of 2.4 mmol/L (1.8-3.1) compared to the HNF1A/HNF4A-MODY cohort with a median LDL-cholesterol level of 1.7 mmol/L (0.9-2.2); with a ***p-value < 0.0001.

Eventually, the T2D cohort had significantly higher median hs-CRP levels of 5.0 mg/L (2.3-10.4) compared to the HNF1A/4A MODY pathogenic cohort with median hs-CRP levels of 2.0 mg/L (0.6-3.0), **p-value = 0.004.

2.3.3 Study 2: Logistic Regression Analysis of Predictive Clinical Characteristics for HNF1A and HNF4A-MODY

The objective of this second study is to evaluate the clinical characteristics that hold the predictive potential for HNF1A/HNF4A-MODY by using univariate and multivariable logistic regression. An initial step involved performing univariate logistic regression analysis to assess the predictive efficacy of various clinical features and biomarkers in distinguishing between HNF1A and HNF4A MODY and T2D. Variables displaying a p-value below 0.05 were deemed statistically significant and subsequently selected for further analysis.

To determine the significance of each variable in predicting MODY, the logarithm of the odds ratio (Log OR (β)) and its corresponding standard error (SE (β)) was assessed (reported in Table 2-3). Additionally, the z-value were calculated by dividing the log odds ratio by its standard error as reported in Table 2-3. The exponential value of the log odds ratio (OR (exp[β])) and its 95% confidence interval (95% CI OR) are also reported, representing the odds ratio and its range of uncertainty, respectively (reported in Table 2-3).

The results obtained through univariate logistic regression indicate that various clinical characteristics do not appear to significantly contribute to the predictive value for MODY. However, due to the limited sample size within the HNF1A/HNF4A MODY cohort, it is essential to recognize that there are limitations stemming from reduced statistical power. Consequently, the robustness and reliability of the findings may have been affected, potentially yielding false negative results. These clinical characteristics include factors such as gender (coded as male=1/female=0), family history (coded as "False"=1 for no family history), metabolic measurements comprising capillary glucose, HbA1c, and fasting C-peptide, as well as physical features like BMI and

WHR. Additionally, markers of liver function did not demonstrate a statistically significant association ($p > 0.05$) with HNF1A and HNF4A-MODY (see in Table 2-3).

On the other hand, age at diagnosis emerged as a predictor for HNF1A and HNF4A MODY with significant correlation ($*p < 0.05$, Table 2-3) leading to its inclusion in subsequent multivariable logistic regression analysis. A younger age at diagnosis exhibited a robust relation with an enhanced probability of HNF1A and HNF4A MODY occurrence. Moreover, the inflammation biomarker hs-CRP was identified as a significant predictor ($*p < 0.05$) for HNF1A and HNF4A MODY. Lower hs-CRP levels were associated with an increased likelihood of both HNF1A and HNF4A MODY.

Regarding the lipid profile, while triglyceride and LDL cholesterol levels did not exhibit statistical significance in predicting HNF1A and HNF4A-MODY, there was a tendency for lower values to be linked with a greater likelihood of HNF1A and HNF4A-MODY. Conversely, elevated levels of HDL cholesterol were found to be associated with an increased probability of HNF1A and HNF4A-MODY occurrence ($*p < 0.05$).

Lastly, the absence of insulin dependency was established as statistically significant ($*p < 0.05$) in predicting HNF1A and HNF4A-MODY.

In summary, these findings indicate that factors such as a younger age at diagnosis, low levels of hs-CRP, high HDL cholesterol, and non-insulin dependence are significantly associated with an increased likelihood of HNF1A and HNF4A-MODY. These variables hold the potential to serve as effective indicators for predicting the occurrence of HNF1A and HNF4A-MODY in individuals.

To gain a more comprehensive understanding of the predictive potential of these variables for HNF1A and HNF4A-MODY, age at diagnosis, hs-CRP, HDL level, and non-insulin dependence were further analyses using multivariate regression and present in the following section. This method allows for the simultaneous consideration of these multiple variables, providing a more thorough assessment of their predictive relevance and testing how well the model can predict the occurrence of HNF1A/HNF4A MODY in individuals who meet the clinical criteria cited.

Table 2-3: **Clinical Differentiators between T2D and HNF1A/HNF4A MODY.**

The table presents results of univariate logistic regression for clinical criteria and biomarkers in predicting MODY vs. T2D. It includes the Log OR(β), representing logistic regression β coefficients; SE(β), indicating the standard error for the β coefficient; z, the standardized effect size; OR the odds ratio for a one-unit increases in the explanatory variable; and 95% CI OR, which stands for the 95% confidence interval for the odds ratio. Clinical features abbreviations: Body Mass Index (BMI), Waist-to-Hip Ratio (WHR), ALT (Alanine Aminotransferase), ALP (Alkaline Phosphatase), hs-CRP (high-sensitivity C-reactive protein), and C-pep representing C-peptide levels. Statistical significance was evaluated at *p < 0.05, **p < 0.01, and ***p < 0.001.

Clinical features	Log OR (β)	SE (β)	z	*p* value	OR (exp[β])	95% CI OR
Age at diagnosis (years)	-1.15	0.72	2.75	0.005**	0.32	0.07 to 1.21
BMI	-1.66	0.87	1.78	0.07	0.19	0.03 to 0.91
WHR	-1.08	1.46	1.45	0.21	0.34	0.008 to 4.70
Glucose (mmol/L)	-2.05	0.90	1.39	0.11	0.13	0.02 to 0.81
HbA1c (mmol/mol)	-1.97	0.90	1.57	0.12	0.14	0.02 to 0.78
Fasting C-pep (pmol/L)	-2.969	0.40	0.82	0.41	0.05	0.02 to 0.10
hs-CRP (mg/L)	-2.58	0.42	0.73	0.46	0.08	0.03 to 0.17
ALT	-2.43	0.56	1.44	0.15	0.09	0.03 to 0.27
ALP	-2.36	0.81	1.08	0.28	0.09	0.02 to 0.49
Trigs (mmol/L)	-2.75	0.61	1.11	0.27	0.06	0.02 to 0.22
HDL (mmol/L)	0.89	0.40	2.22	0.03*	2.43	1.00 to 5.15
LDL (mmol/L)	-2.20	0.88	1.37	0.17	0.11	0.018 to 0.56
Gender (Male)	-0.60	0.60	1.00	0.32	0.55	0.15 to 1.67
Insulin Tx (False)	-1.5	0.56	2.71	0.007*	0.22	0.07 to 0.63
Family History (False)	-1.4	1.05	1.38	0.17	0.23	0.01 to 1.2

2.3.3.1 Multivariable Logistic Regression Analysis of Biomarkers and Clinical Characteristics in Predicting HNF1A and HNF4A-MODY

A multivariable logistic regression model was used to test the association of various variables with the likelihood of having HNF1A and HNF4A-MODY. The variables included in the model were age at diagnosis, hs-CRP, HDL cholesterol, LDL cholesterol, and non-insulin-dependent individuals. The results of the multivariable logistic regression model are presented in the Table 2-4.

The findings present a statistically significant positive relation between non-insulin dependence and the likelihood of HNF1A and HNF4A-MODY occurrence. The coefficient for non-insulin treatment stands at 1.8 (β1, Table 2-4), indicating that individuals not relying on insulin treatment have 1.8 times higher log odds of developing HNF1A and HNF4A-MODY compared to those who necessitate insulin for treatment (**$p < 0.01$).

Likewise, the age at diagnosis also establishes a statistically significant positive relation with the likelihood of HNF1A and HNF4A-MODY. The coefficient for age at diagnosis is -0.1 (β2, Table 2-4), signifying that with each unit increase in age at diagnosis, the log odds of having HNF1A and HNF4A-MODY decrease by a factor of -0.1 (**$p < 0.01$).

Moreover, the HDL level demonstrates a statistically significant and favorable relationship with the likelihood of HNF1A and HNF4A-MODY occurrence. The coefficient for HDL level is 1.0 (β3, Table 2-4), suggesting that for every unit increase in HDL level, the log odds of experiencing HNF1A and HNF4A-MODY elevate by a factor of 1.0 (*$p < 0.05$).

In summary, these findings provide evidence that non-insulin treatment, a younger age at diagnosis, and higher HDL levels are associated with an elevated probability of having HNF1A and HNF4A-MODY.

The model's effectiveness in predicting HNF1A and HNF4A MODY was evaluated using the Hosmer-Lemeshow test. The analysis yielded a Hosmer-Lemeshow statistic

of 3.0, and the non-significant p-value (p-value=0.9) further emphasizes the strong agreement between the model's predictions and the actual data. This observation highlights the model's capacity for accurately predicting the occurrence of HNF1A and HNF4A-MODY.

Table 2-4 : **Results of Multivariable Logistic Regression.**

The table presents the multivariable regression models aimed at identifying predictive clinical features for HNF1A/HNF4A-MODY, compared with T2D cohort clinical features, specifically non-insulin dependency, age at diagnosis, and HDL levels. The table presents the β coefficients (log odds ratio for a one-unit increase in the explanatory variable), SE(β) (standard error for the β coefficient), and Z (standardized effect size). Statistical significance was determined at *p < 0.05, **p < 0.01, and ***p < 0.001.

Dependent variable MODY	Coefficient	Z stat |Z|	*p* value
T2D vs HNF1A/4A pathogenic cohort			
Intercept	-3.22	-2.93	0.003**
No insulin treatment (relative to being on insulin)	1.81	2.73	0.006**
Age of diagnosis (years)	-0.12	-2.59	0.01**
HDL levels	0.99	2.22	0.03*
Multivariable model *p* value=0.93			

2.3.4 Study 3: Comparative Analysis of Clinical Data Among Cohorts: HNF1A and HNF4A-MODY Confirmed Mutations, T2D, and Variant of Unknown Significance Cohort

2.3.4.1 Genetic Testing for *HNF1A* and *HNF4A* Gene Variants: Pathogenic, Likely Pathogenic, and VUSs in Patients

The cohort of VUS in our study consisted of six variants, including five in the *HNF1A* gene: heterozygous p.Pro379Ser, p.Arg321His, p.Lys23Glu, and p.Ala239Val and homozygous p.Ala251Thr. The remaining variant was identified in the *HNF4A* gene: heterozygous p.Arg114Gln. These variants have not been previously classified as pathogenic or benign, and their clinical significance in the context of monogenic diabetes of the young remains unclear.

The cohort of probands with pathogenic and likely pathogenic variants in the *HNF1A* and *HNF4A* genes comprised nine reported variants. These variants are confirmed to be pathogenic and include 1501+1G>A, (788G>A) p.Arg263His, p.Leu144Pro, p.Gly292fs,(686G>A) p.Arg229Pro, (608G>A) Arg203His, p.Pro112Leu, and (347C>T) Ala116Val, and are all in a heterozygous state.

2.3.4.2 Description of Individuals with VUS: Clinical Characteristics and Biomarker Values

This chapter section is dedicated to a comprehensive exploration of the VUSs cohort based on outcomes from multivariable regression analysis. Due to their closely overlapping clinical presentation, challenges arise in categorising participants into distinct groups—T2D, *HNF1A*/*HNF4A* pathogenic variant cohorts. For instance, across all three cohorts, individuals typically present with diabetes before the age of 30. While family history often corresponds with *HNF1A* and *HNF4A* MODY-causing variants, it may also indicate variations related to risk factors for T2D (as discussed in Introduction 2.1.2).

Employing descriptive analysis of the clinical features of each individual within the HNF1A/HNF4A VUS cohort, this study endeavours to establish whether specific

clinical criteria can effectively discern if each HNF1A/HNF4A VUS individual aligns more closely with the T2D cohort as early-onset type 2 diabetics or if they demonstrate a propensity for harbouring pathogenic *HNF1A* or *HNF4A* variants. This descriptive analysis will centre around identifying clinical criteria likely indicative of HNF1A/HNF4A-MODY. Specifically, the relevance of parameters such as hs-CRP, lipid profile (HDL cholesterol, LDL cholesterol), and the presence of non-insulin-dependent individuals in predicting the likelihood of HNF1A and HNF4A-MODY will be investigated. Table 2-5 provides comprehensive details about the entire VUS cohort, while Table 2-2 outlines the median and interquartile ranges.

Participant MD-EH-008

In the case of MD-EH-008, despite being on insulin treatment, which might raise doubts about HNF1A/HNF4A MODY association, MD-EH-008 exhibited physical attributes akin to the HNF1A/HNF4A MODY cohort. With a BMI of 26.8 kg/m² and a WHR of 0.85, her BMI stands lower than the median BMI of the T2D cohort 29.0 kg/m² (24.7,34.1, Table 2-2), displaying a resemblance to the median BMI of the HNF1A/4A pathogenic cohort 25.1 kg/m² (22.0,29.0, Table 2-2). Notably, her WHR of 0.85 closely corresponds with the median WHR of the HNF1A/4A pathogenic cohort 0.86 (0.80, 0.95, Table 2-2), indicating a potential alignment with HNF1A/4A-MODY.

However, her hs-CRP level is recorded as 3 mg/L (Table 2-5), falling within the range of (IQR) 2.3 - 10.4 mg/L calculated for the T2D probable cohort. While elucidating the lipid profile could provide further insights, regrettably, specific measurements for triglycerides, HDL, and LDL are not provided. The clinical data of participant MD-EH-008 are inconclusive about whether the VUS is associated with T2D or the HNF1A-HNF4A MODY pathogenic cohort. This makes it difficult to confidently assign the VUS pathogenicity.

Participant MD-WH-138

Participant MD-WH-138's clinical presentation and laboratory findings are more suggestive of T2D than HNF1A/HNF4A MODY due to his BMI of 28.9 kg/m2 (T2D median 29.0 kg/m², 24.7-34.1, Table 2-2Table 2-5), his WHR of 0.90 (T2D median =

0.92, 0.87-0.96, Table 2-2), and his triglyceride level of 1.2 mmol/L (T2D median = 1.4 mmol/L, IQR = 1.0-2.1, Table 2-2). Additionally, his HDL level of 0.9 mmol/L is lower than the median HDL levels of both cohorts (T2D median = 1.2 mmol/L, 1.0-1.4; HNF1A/HNF4A pathogenic cohort = 1.3 mmol/L, 1.0-1.9, Table 2-2). His LDL level of 2.6 mmol/L is the highest among all individuals with a VUS, and it is higher than the median LDL levels of both cohorts (T2D = 2.4 mmol/L, 1.8-3.1; HNF1A/HNF4A pathogenic cohort = 1.7 mmol/L, 0.9-2.2, Table 2-2).

However, participant MD-WH-138 is not currently on insulin treatment, which would better fit the HNF1A and HNF4A pathogenic cohort. Additionally, his hs-CRP levels (<3.0 mg/L) remain close to the HNF1A and HNF4A pathogenic cohort (0.6 - 3.0 mg/L, Table 2-2).

Overall, further testing is needed to confirm the diagnosis as participant MD-WH-138's clinical presentation and laboratory findings are more suggestive of T2D than MODY, but his hs-CRP levels and lack of insulin treatment are more suggestive of HNF1A/HNF4A MODY.

Participant MD-GH-036

Participant MD-GH-036 is currently receiving insulin treatment, which is more consistent with T2D than HNF1A/HNF4A - MODY. Similarly, her BMI of 28.3 kg/m2 (T2D median = 29.0 kg/m², 24.7-34.1, Table 2-2) and WHR of 0.98 (T2D median = 0.92, 0.87-0.96Table 2-2) are both closer to the T2D cohort than the HNF1A/ HNF4A-MODY cohort. However, her hs-CRP level of 2 mg/L (HNF1A/ HNF4A-MODY median = 2.0 mg/L, 0.6-3.0, Table 2-2) is equal to the median for the HNF1A/HNF4A-MODY cohort and lower than the median for the T2D cohort. The participant MD-GH-036 did not provide measurements for triglycerides, HDL, or LDL, so her lipid profile was not included in the analysis.

The outcome of these findings makes it challenging to determine whether she is more inclined towards T2D or HNF1A/HNF4A-MODY. Overall, the participant MD-GH-036's clinical manifestation and laboratory results better align with T2D characteristics rather than MODY. Nonetheless, the uncertainty arising from her hs-CRP level and the

absence of lipid profile data poses difficulty in arriving at a conclusive determination of her condition.

Participant MD-SG-012

Participant MD-SG-012 exhibits several clinical features that are consistent with the T2D cohort. She is currently undergoing insulin treatment, her BMI of 26.3 kg/m² is lower than the T2D cohort's median (29.0 kg/m²), and her WHR of 0.95 surpasses the median WHR of both cohorts. These physical traits resemble those observed in the T2D cohort.

However, her lipid profile bears a resemblance to those associated with HNF1A/HNF4A-MODY. Specifically, her triglyceride level of 0.68 mmol/L is significantly lower than the levels observed in both cohorts (1.4 mmol/L in the T2D cohort and 1.0 mmol/L in the HNF1A/HNF4A pathogenic cohort, Table 2-2). Additionally, her HDL-cholesterol level of 1.43 mmol/L surpasses the median levels of both cohorts (1.2 mmol/L in the T2D cohort and 1.3 mmol/L in the HNF1A/HNF4A pathogenic cohort, Table 2-2). Her LDL-cholesterol level of 1.4 mmol/L is lower than the T2D cohort's median of 2.4 mmol/L, but it is more near to the HNF1A/HNF4A pathogenic cohort's median of 1.7 mmol/L.

MD-SG-012's hs-CRP level is recorded at 3.2 mg/L, aligning with the hs-CRP range of 2.3 - 10.4 mg/L calculated for the T2D probable cohort.

Taking her lipid profile into consideration, the potential inclusion of MD-SG-012 within the HNF1A/HNF4A cohort appears more likely, as this profile aligns with the cohort's characteristic of having lower LDL and triglyceride levels, coupled with higher HDL levels. However, the situation is nuanced: despite her insulin treatment categorising her within the T2D cohort and her hs-CRP value being closer to that of T2D, the intricate findings reveal clinical features that could align with both cohorts. This complexity introduces challenges in determining whether MD-SG-012 should be classified as having T2D or HNF1A/HNF4A-MODY.

Participant MD-IC-112

Participant MD-IC-112 is currently receiving insulin treatment, which suggests that he may have T2D. His BMI of 34.9 kg/m² surpasses the median BMI of both cohorts (29.0 kg/m² for T2D and 25.1 kg/m² for HNF1A/HNF4A-MODY, Table 2-2), which also supports the T2D diagnosis. Additionally, MD-IC-112's lipid profile resembles that of the T2D cohort, with higher LDL levels and lower HDL levels. Specifically, his HDL level of 0.84 mmol/L is lower than the median HDL levels of both cohorts (1.2 mmol/L for T2D and 1.3 mmol/L for HNF1A/HNF4A-MODY, Table 2-2) and a LDL level of 2.30 mmol/L higher than the median values of both cohorts and closer to the median of the T2D cohort (2.4 mmol/L, Table 2-2). However, one specific parameter sets apart MD-IC-112 from typical T2D cases, as evidenced by a lower hs-CRP level of 0.6 mg/L. Notably, this value falls within the established range of 0.6 - 3.0 mg/L calculated for HNF1A HNF4A-MODY.

In summary, the clinical profile exhibited by participant MD-IC-112 suggests a greater likelihood of having T2D rather than HNF1A/HNF4A-MODY. However, it is important to acknowledge a contradictory aspect in this assessment, with the presence of a lower hs-CRP level that resembles the HNF1A HNF4A-MODY cohort.

Participant MD-IC-004

Participant MD-IC-004 is currently undergoing insulin treatment, which suggests that he may have T2D. However, his WHR of 0.92 surpasses the median WHR of the HNF1A/HNF4A pathogenic cohort (0.86) and aligns with the median WHR of the probable T2D cohort (0.92, Table 2-2), suggesting T2D. His BMI of 27.8 kg/m^2 falls slightly below the median BMI of the T2D cohort (29.0 kg/m^2, Table 2-2), yet closely resembles the value of the HNF1A/HNF4A pathogenic cohort, indicating a partial alignment. MD-IC-004's lipid profile shows a LDL level measures 3.02 mmol/L, which is the highest among individuals with VUS and more closely resembles the median of the T2D cohort (2.4 mmol/L, Table 2-2), his triglyceride level of 1.74 mmol/L surpasses the median values of the T2D cohort (1.4 mmol/L, Table 2-2) and his HDL level of 1.19 mmol/L is lower than the median values of both the probable T2D cohort (1.2 mmol/L,

Table 2-2) and the HNF1A/HNF4A pathogenic cohort (1.3 mmol/L, Table 2-2). This indicates an unfavourable lipid profile, reflecting higher triglyceride levels and lower HDL levels akin to the dyslipidaemia pattern observed in T2D.

Conversely, MD-IC-004's hs-CRP level is below 0.2 mg/L, which aligns with the range (0.6 - 3.0 mg/L, Table 2-2) established for the HNF1A and HNF4A pathogenic cohort.

In summary, MD-IC-004's clinical features, including BMI, WHR, lipid profile, and insulin treatment, predominantly suggest a predisposition towards T2D. However, the low hs-CRP level contradicts the typical T2D pattern observed in this study's T2D cohort. Despite the indications toward T2D (physical features and lipid profile), the distinctive hs-CRP level introduces complexities in definitively classifying MD-IC-004 within the T2D or HNF1A/4A pathogenic cohort.

Table 2-5 : **Clinical Characteristics of Individuals with Variants of Unknown Significance in HNF1A or HNF4A**

The table provides an overview of the clinical characteristics of the six individuals within the Variant of Uncertain Significance (VUS) cohort. The clinical traits selected for analysis and comparison include Age at Diagnosis (Age Dx), Insulin Treatment (Insulin Tx), Family History (FHx), Body Mass Index (BMI), Waist-to-Hip Ratio (WHR), Triglycerides (TG) level in millimoles per litter (mmol/L), High-Density Lipoprotein (HDL) cholesterol level in mmol/L, Low-Density Lipoprotein (LDL) cholesterol level in mmol/L, and high-sensitivity C-reactive protein (hsCRP) level (mg/L). These traits are evaluated in the context of comparison with the cohort of pathogenic variants of HNF1A/HNF4A- MODY and the T2D cohort.

Study ID	Age Dx	Insulin Tx	FHx	BMI	WHR	TG (mmol/L)	HDL (mmol/L	LDL (mmol/L)	hsCRP (mg/L)
MD-EH-008	27	Yes	Yes	26.8	0.85	NP	NP	NP	3
MD-WH-138	26	No	Yes	28.9	0.90	1.2	0.9	2.6	<3
MD-GH-036	18	Yes	Yes	28.3	0.98	NP	NP	NP	2
MD-SG-012	28	Yes	Yes	26.3	0.95	0.68	1.43	1.4	3.2
MD-IC-112	18	Yes	Yes	34.9	0.89	0.54	0.84	2.30	0.6
MD-IC-004	18	Yes	Yes	27.8	0.92	1.74	1.19	3.02	<0.2

2.4 Discussion

The thorough analysis undertaken in this clinical study underscores the challenges associated with assigning pathogenicity to VUS based solely on clinical presentation.

While some clinical features, such as family history of diabetes, glycaemic index, and liver profile, did not exhibit significant differences across all groups, the study revealed that certain physical features including BMI and WHR, age at diabetes diagnosis, insulin dependence, the inflammatory marker hs-CRP, and lipid profile including LDL cholesterol displayed significant difference between the two cohorts.

However, none of these clinical features could definitively determine pathogenicity for the VUS group. Notably, individuals with HNF1A/HNF4A VUS could exhibit characteristics attributable to both cohorts. For instance, individual MD-WH-138 demonstrated elevated BMI and dyslipidaemia resembling T2D yet had low hs-CRP and lacked current insulin treatment, aligning more with MODY. This underscores the variability in clinical presentation among individuals and the limitations of relying solely on predictive factors that initially differentiate between the T2D and HNF1A/HNF4A-MODY cohorts, as these features may not consistently align with pathogenicity assignment.

The logistic regression analysis demonstrated that age at diagnosis, the inflammation biomarker hs-CRP, non-insulin dependence, and lipid profile were significant predictors for distinguishing HNF1A and HNF4A-MODY from T2D. A younger age of onset, lower levels of hs-CRP, lower triglyceride and LDL cholesterol levels, and higher levels of HDL cholesterol are associated with HNF1A and HNF4A-MODY.

These findings offer valuable insights into potential clinical characteristics and biomarkers contributing to the prognostication of HNF1A and HNF4A-MODY within clinical settings. The examination of a combination of clinical features, including insulin dependency, lipid profile, and the inflammation biomarker hs-CRP, may be relevant when assessing HNF1A/HNF4A MODY pathogenicity. However, it's important to acknowledge the inherent limitations of these factors, as they may not consistently align with individual cases. A pertinent example supporting this notion comes from a

study by Tim J. McDonald et al. in Diabetes Care (2011), which observed lower hs-CRP levels in individuals with HNF1A-MODY compared to other forms of diabetes. It's worth noting that the study also emphasises that some individuals with T2D exhibited low levels of hs-CRP and did not consistently display higher inflammatory marker levels (Tim J. McDonald *et al.*, 2011).In conclusion, the findings of this study reaffirm the intricate nature of establishing VUS pathogenicity. While certain clinical features help in diagnosis, a more comprehensive investigative approach, combining both *in vitro* and *in silico* analyses, is imperative to overcome the limitations of relying solely on clinical evaluation (Althari and Gloyn, 2015). The subsequent chapter will centre on *in silico* and *in vitro* assessment, aiming to assign VUS pathogenicity.

3 Chapter 3: Investigation into the Pathogenicity of *HNF1A* Variants, p.A251T and p.S19L Associated with Young Onset Diabetes.

Summary

Chapter 2 investigated the potential pathogenicity of VUS within the *HNF1A* and *HNF4A* genes. This clinical study involved a statistical analysis and a comparative examination of clinical features of three cohorts: individuals with HNF1A/HNF4A-MODY, those with T2D, and those with *HNF1A* and *HNF4A* VUSs. The objective was to evaluate the ability of clinical characteristics and biomarker measurements alone to determine the pathogenicity of VUS. However, the clinical study was inconclusive in establishing whether the identified VUS served as risk factors for T2D, disease-causing mutations in HNF1A/HNF4A-MODY, or benign variants. Since clinical criteria appear insufficient to assess the impact of these variants, further investigations are required using computational (*in silico*) and laboratory (*in vitro*) methods. This chapter focuses on two VUSs, i.e., p.A251T and p.S19L, and investigates whether these affect the function of the HNF1A protein. We conclude that the homozygous *HNF1A* p.A251T variant exhibits relatively mild impacts on protein function compared to wildtype *HNF1A* whilst the heterozygous p.S19L variant showed a significant decrease in HNF1A function compared to WT. Specifically, p.A251T moderately reduced transactivation activity, whereas p.S19L significantly diminishes transactivation activity and alters the subcellular localisation of the HNF1A protein, compared to WT respectively.

3.1 Introduction

3.1.1 HNF1A-MODY

HNF1A-MODY is caused by a mutation in the HNF1A transcription factor, typically resulting in heterozygous mutations that lead to haploinsufficiency of the HNF1A protein. For an accurate diagnosis of HNF1A-MODY, it is essential to identify the specific mutation through genomic DNA sequencing methods such as Sanger sequencing or next-generation sequencing (3,4, 3.1.4 Functional Analysis of *HNF1A* Variants: *In Silico* and *In Vitro* Investigations).

3.1.2 HNF1A Protein Function and Structure

The HNF1A protein, a transcription factor, comprises three domains: a dimerization domain (residues 1–32) (5,6,Figure 3.1), a DNA-binding domain (DBD), which consists of two POU sub-domains: POUs (82–172) and POUH (198–281) (7,8, Figure 3.1), and a transactivation domain (residues 282–631) (9,10, Figure 3.1). The DBD domain POUs contributes to protein stability, while POUH plays a crucial role in facilitating protein-DNA interaction (Baumhueter *et al.*, 1990; Chi *et al.*, 2002). The specific nuclear localisation signal (NLS) and location, that facilitates the transportation of HNF1A into the nucleus, remains not fully defined (Fareed *et al.*, 2021). HNF1A functions as a homodimer and regulates genes by binding to the inverted palindrome sequence 5'-GTTAATNATTAAC-3' through its DNA-binding motif known as the helix-turn-helix (Rose *et al.*, 2000).

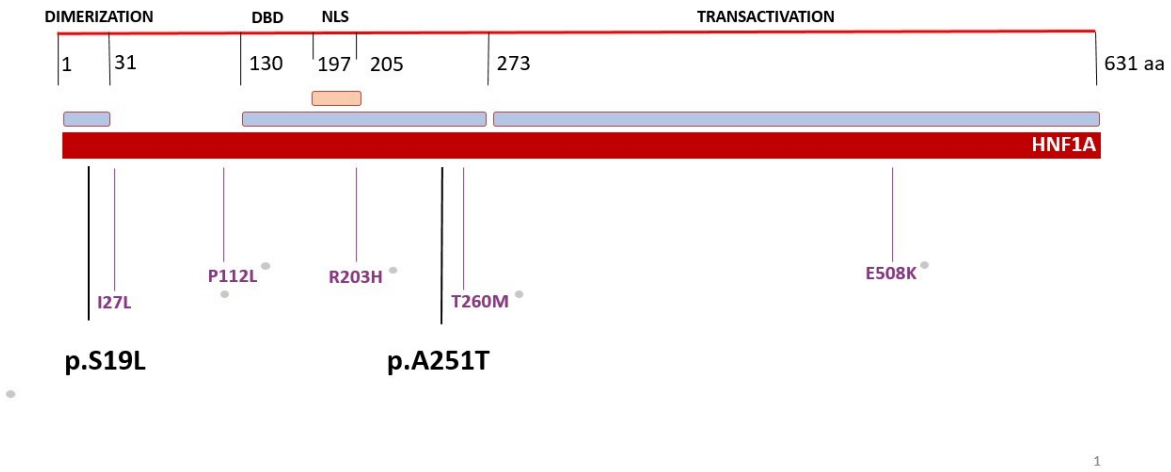

Figure 3.1: **Schematic Representation of the HNF1A Protein domains.**
The HNF1A protein has three domains: the dimerization domain, the DNA-binding domain (DBD) with the nuclear localisation signals (NLS), and the transactivation domain. The *HNF1A* p.A25T and p.S19L variants of interest are depicted in bold black and are located within the transactivation domain and the dimerization domain, respectively. The functional assays *in vitro* employed positive control variants (purple) in plasmid constructs (grey dots), which were provided by the Oxford Centre for Diabetes Endocrinology and Metabolism.

3.1.3 *HNF1A* Variant Pathogenicity

HNF1A pathogenic variants exert a wide range of impacts on protein function. Among these variants, missense mutations are the most common, impacting the dimerization or DNA-binding domains, while truncating mutations are commonly observed in the transactivation domain (Horikawa *et al.*, 1997; Ellard and Colclough, 2006; Colclough *et al.*, 2013).

Mutations in the dimerization site can potentially disrupt the complex formation with HNF1A coactivator DCoH, leading to reduced binding of HNF1A to DNA targets and a decrease in transactivation activity (Rose *et al.*, 2004). Mutations in the DNA-binding homeodomain, particularly in the POUS and POUH subdomains, are common and associated with MODY (Chi *et al.*, 2002; Chi, 2005). The transactivation domain of

HNF1A has a low mutation rate, but it may affect transactivation activity (Colclough *et al.*, 2013).

Accurately assessing the impact of *HNF1A* variants is crucial for effective management of HNF1A-MODY symptoms, as it guides clinicians to select appropriate treatment, considering that individuals with HNF1A-MODY are sensitive to sulfonylurea and may transition completely from insulin therapy (Pearson *et al.*, 2003; Shepherd *et al.*, 2009). However, not all variants are currently classified as pathogenic or benign. VUS pose challenges in understanding their implications on HNF1A function and require further investigation to enable accurate treatment.

3.1.4 Functional Analysis of *HNF1A* Variants: *In Silico* and *In Vitro* Investigations

The current recommended approach for assessing the pathogenicity of variants in *HNF1A* involves conducting functional investigations using both computational study *(in silico*) or laboratory-based (*in vitro*) methods (Althari and Gloyn, 2015; Najmi *et al.*, 2017). The access to functional study results is limited for most clinicians, which poses a challenge in understanding the impact of *HNF1A* variant pathogenicity on protein function.

To characterise functionally variants in HNF1A-MODY patients, well-established, multi-tiered, and reproducible assays have been developed (Althari and Gloyn, 2015; Althari *et al.*, 2020). The first step involves *in silico* studies, which are necessary to classify variants bioinformatically and predict their pathogenic potential. These tools provide scores from 1 to 5 indicating the likelihood of a variant being pathogenic. A variant is classified as pathogenic when it receives a score ranging from 4 to 5 in the tests conducted for its classification. The main limitation of *in silico* studies is their reliance on experimental data collected from previous *in vitro* studies from nearby mutations. Ideally, the combination of *in silico* predictions with laboratory-based protein analyses can provide a more reliable assessment of the functional impact associated with *HNF1A* VUSs.

Given that HNF1A is a transcription factor which binds to DNA to regulate the activity of target genes, *in vitro* protein function analysis has been tailored to examine these specific functions (Bjørkhaug *et al.*, 2003; Galán *et al.*, 2011; Najmi *et al.*, 2017; Althari *et al.*, 2020). These experiments include transactivation assays to measure variant impact in regulating reporter gene expression, and DNA binding activity assays to evaluate the transcription factor's ability to bind to specific DNA regions. Nuclear (versus cytosolic) localisation assays can be used to determine the extent of its presence in the cell nucleus, where it regulates target genes. The descriptions of each of these methods can be found in the methodology section of this chapter (3.2 Methods).

3.1.5 Presentation of Two *HNF1A* Variants to be Studied

This study aims at exploring the pathogenicity of two newly identified *HNF1A* variants of unknown significance. These variants were discovered in probands participating in the MY DIABETES study and in the Imperial NHS Trust MODY service, London.

The first variant to be described is a homozygous *HNF1A* missense variant, p.A251T (c.751G>A) and was identified from an insulin-treated individual. A metabolic characterisation has been performed in both heterozygous carriers of the p.A251T variant and individuals homozygous for the p.A251T variant. The identification of this homozygous variant in MODY-HNF1A patients is of interest as it was previously believed that homozygous mutations in *HNF1A* were embryonically lethal (Harries, Brown and Gloyn, 2009). Primary *in silico* and *in vitro* functional studies have been assessed which show evidence that the p.A251T variant is likely to be pathogenic and disease causing (Misra *et al.*, 2020). The development of MODY and the underlying mechanism of protein dysfunction associated with the homozygous *HNF1A* p.A251T variant are still unclear. Hence, additional investigations are necessary to elucidate the pathogenicity of this variant and its specific cellular and molecular effects.

The genome analysis of the proband in the Imperial NHS Trust MODY service uncovered a novel variant, *HNF1A* p. S19L (c.56C>T), which has not been previously studied for its functional consequences *in vitro* and is classified as a variant of

unknown significance. To determine its pathogenicity and gain a comprehensive understanding of its functional implications, this study includes additional investigation involving *in silico* and *in vitro* analyses combined.

3.1.6 Aim of the *In Silico* and *In Vitro* Functional Study

The hypothesis is that the recently identified *HNF1A* variants, p.A251T and p.S19L, have an impact on the HNF1A protein function.

Aim: To develop a molecular and cellular approach using established functional assays to determine the effects of *HNF1A* variants on transactivation potential, nuclear localisation, DNA binding, and protein expression, comparing them to human Wild Type (WT) *HNF1A,* known MODY-causing variants *HNF1A* or risk factors for T2D, in immortalised cell lines (INS-1, HeLa and Endoc-βH3).

3.2 Methods

All details regarding the medium composition, supplier brand, catalogue numbers, primary and secondary antibodies, their respective references, and dilutions, forward and revers primer primers sequences are presented in the Table 6-1.

The investigation of variant pathogenicity follows the methodology developed by the Gloyn laboratory at Stanford University's Division of Endocrinology (Althari and Gloyn, 2015).

3.2.1 Plasmid Design

A vector containing human pancreatic *HNF1A* cDNA in a pcDNA3.1 backbone was utilised for all functional studies, provided by the Oxford Centre for Diabetes Endocrinology and Metabolism (Althari *et al.*, 2020). This vector serves as HNF1A Wild-Type (WT) control, allowing for comparison with the *HNF1A* constructs containing variants. Additionally, the pcDNA3.1 backbone plasmid was employed as a control for “empty” vector, without genetic material or for value correction in DNA-binding activity assays. The variants used as positives controls for HNF1A impaired protein function included the MODY-causing mutations p.P112L (Bjørkhaug *et al.*, 2003), p.R203H (Colclough *et al.*, 2013), and p.T260M (Glucksmann *et al.*, 1997; Pavić *et al.*, 2018), and the p.E508K variant associated with an increased risk of T2D (Martagón *et al.*, 2018), offered by the Oxford Centre for diabetes Endocrinology and Metabolism, Churchill Hospital.

3.2.2 Site-Directed Mutagenesis

To generate the *HNF1A* variants of interest p.S19L, p.A251T, and the common variant p.I27L as control of impaired HNF1A function for the dimerization domain, site-directed mutagenesis was performed on the *HNF1A* cDNA in the pcDNA3.1 vector using the Q5 Site-Directed Mutagenesis Kit (New England BioLabs, Figure 3.6). Site-directed mutagenesis was performed using PCR amplification with Q5 Hot Start High-Fidelity 2X Master Mix, Forward Primer, Reverse Primer, and Template *HNF1A* cDNA. The PCR amplification process used Q5 Hot Start High-Fidelity (New England Biolabs)

with its specific cycling conditions consisting of an initial denaturation step at 98°C for 30 seconds, followed by 25 cycles of denaturation at 98°C for 10 seconds, annealing at a temperature range of 50-72°C for 30 seconds, and extension at 72°C for 30 seconds per kilobase of DNA. Next, PCR product were incubated with a KLD (provided with Q5 Site-Directed Mutagenesis Kit), a combination of enzymes including Kinase, Ligase, and DpnI restriction enzyme, at room temperature. The KLD mix product was transformed into NEB 5-alpha Competent E. coli cells. This was achieved by placing the KLD mix/Competent cells mixture on ice for 30 minutes, followed by a brief heat shock at 42°C for 30 seconds, and then returning it to ice. To promote cell recovery, the mixture was supplemented with SOC medium (provided with Q5 Site-Directed Mutagenesis Kit) and incubated at 37°C with shaking at 250 rpm for 1 hour. Finally, the transformed cells were spread onto an ampicillin selection plate and incubated overnight at 37°C.

3.2.3 Plasmid Isolation

Plasmids were extracted from competent *E. coli* cells using the QIAprep Spin Miniprep Kit (Qiagen), following the provided instructions. The principle of the plasmid DNA purification is to use spin columns with a silica membrane, which can retain plasmid DNA in the presence of a high concentration of chaotropic salt. After washes and elution, the DNA was quantified using a Nanodrop 2000 spectrophotometer (ThermoScientific).

The sequence of all constructs was validated using Sanger sequencing (Primer sequence for sequencing: 5'-CCGAGCCATGGTTTCTAAACTG-3'). Reporter gene in pGL3 vector, contained HNF1A transcription factor recognition sequence next to a *Firefly* luciferase reporter gene and either the Rat Albumin promoter, pGL3-RA, or HNF4A P2 promoter, pGL3-P2, both constructs were offered by the Oxford Centre for diabetes Endocrinology and Metabolism. A reporter pRL-SV40 (Promega) containing *Renilla reniformis* luciferase gene, was used as a transfection control for all the experiments.

3.2.4 Cell Culture and Transfection

HeLa cells were cultured at 5% CO_2, at 37 °C, in T-75 cell culture flasks (Sarstedt), in DMEM (Gibco,) supplemented with 1% penicillin-streptomycin (ThermoFisher) and 10% Foetal Bovine Serum (FBS, Gibco). HeLa cells were passaged at ≥ 70% confluency.

The INS1 832/3 cells were maintained at 5% CO_2, at 37 °C, in T75 cell culture flasks, in RPMI-1640 medium (ThermoFisher) supplemented with 10% FBS, 2 mM L-glutamine brand (Sigma), 1 mM sodium pyruvate (ThermoFisher), 10 mM HEPES (Sigma), and 0.05 mM β-mercaptoethanol (Sigma). INS1 832/3 were passaged every 4 days at ≥ 70% confluency.

Both cell lines were passaged using Trypsin-EDTA Solution 1X (Sigma) at 37°C for 5 minutes to detach the cells from the culture flasks. To neutralize the trypsinization process, a serum-containing medium was added, depending on the cell line. Prior to plating the Endoc-βH3 cells, T-25 flasks (Sarstedt) were coated with ECM Gel (Sigma) diluted two-fold with cold DMEM 1h at room temperature.

Endoc-βH3 cells were cultured at 5% CO_2, at 37 °C, in T25 ECM-coated flasks in DMEM medium supplemented with 1% penicillin-streptomycin and specific components, including 5.6 mM glucose (Sigma), 2% BSA fraction V (Sigma), 50 µM β-mercaptoethanol, 10 mM nicotinamide (Sigma), 5.5 µg/ml human transferrin (Sigma) and 6.7 ng/ml sodium selenite (Sigma) and medium was filtered with corning bottle-top vacuum filter system (SLS). The Endoc-βH3 cells were passaged ¼ dilution once a week using Accutase Cell dissociation (ThermoFisher) incubation at room temperature for 5-8 minutes to allow complete detachment without damaging the cells.

3.2.5 Transfection

Transfection was performed using 3 µl Lipofectamine 2000 (Thermo Fisher). Transfection Reagent and a total of 2 µg of DNA including: 0.25 µg pcDNA3.1 containing WT *HNF1A* or 0.25 µg pcDNA3.1 variants *HNF1A* or pcDNA3.1 empty

vector, 0.50 µg of the reporter gene pGL3-RA, and 0.010 µg pRL-SV40 in a total volume of 500µl of specific medium depending on the cell line.

3.2.6 Transactivation Assay

The HeLa, INS1 832/3, or Endoc-βH3 cells were cultured in a p24-culture plate until they reached over 90% confluence. The cells were transiently transfected (48h). The cells were transfected with either *HNF1A* WT or variant plasmids, along with the reporter plasmids pGL3-RA/pGL3-P2 and pRL-SV40 (Plasmid Design). Following a 48-hour period of transfection, the cells were washed multiple times with Phosphate-buffered saline (Sigma). Then, the cells were lysed using the lysis buffer provided with the Dual-Luciferase Reporter Assay (Promega Corp). A portion of the lysate was immediately used for the luciferase assay, while the remaining portion was stored at -80°C for further analysis of expression levels.

The luciferase assay was performed following the manufacturer's instructions. This involves the sequential addition of fast reaction substrates to the lysate (Figure 3.1). These substrates were specifically designed to react with the expressed luciferase types and produce chemiluminescence, enabling the measurement of luciferase activity.

The luminometer (Berthold Tube Luminometer) was programmed to perform two measurements with delays in capturing, first the luminescence signals of *Firefly* Luciferase (using LAR II solution provided with the kit) and second, the *Renilla* Luciferase (using Stop & Glo Reagent). In summary, cell lysate was added to a luminometer tube containing LAR II (100µl), and luminescence was measured. Then, Stop & Glo Reagent (100µl) was added to the tube, and the luminescence signal is subsequently read (Figure 3.1).

The normalised ratio in activity was calculated for each variant “Experimental Reporter Activity/Control Reporter Activity” and then averaged for all replicates’ readings. Luciferase measurements were given in percentage activity compared to WT.

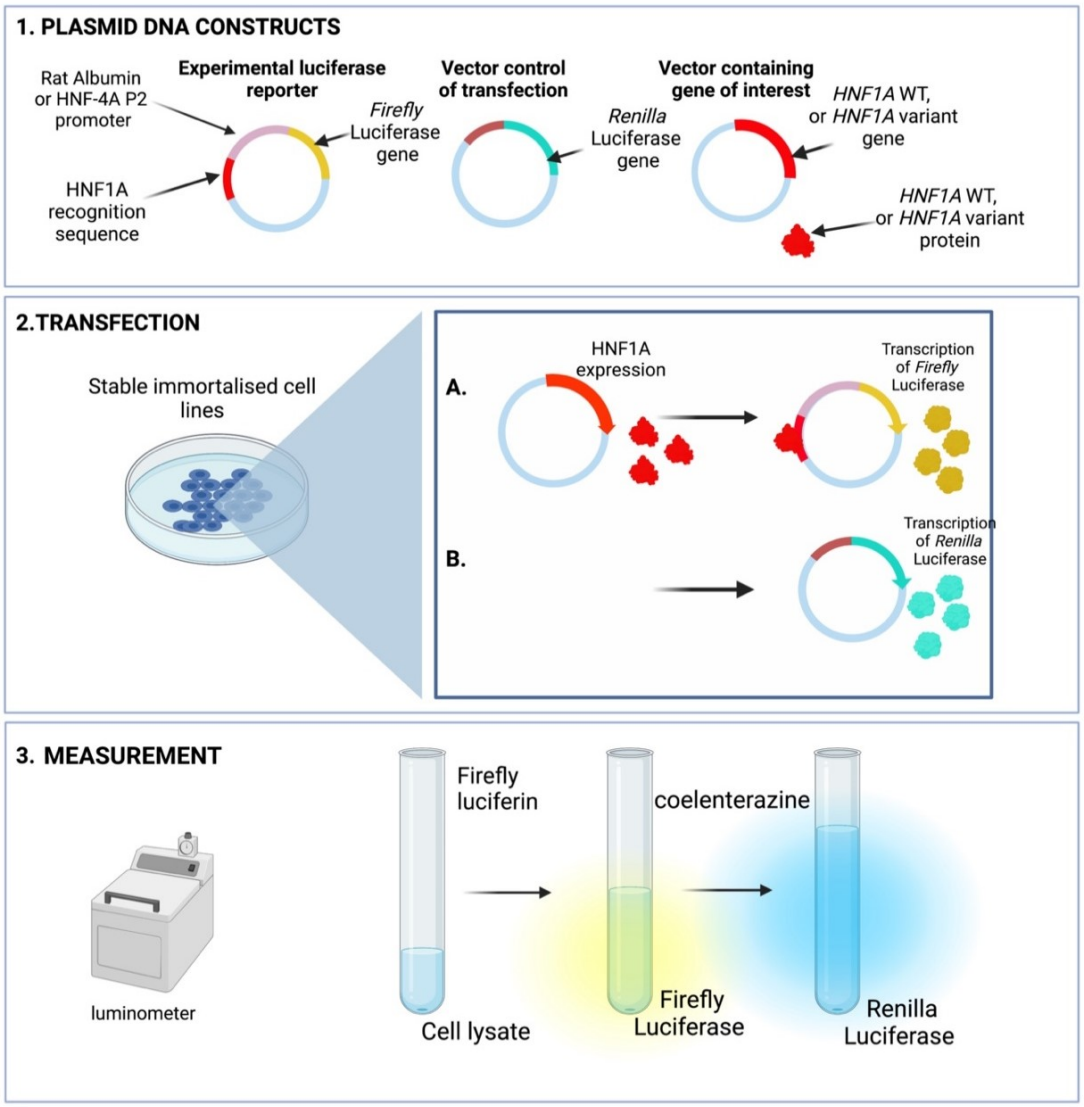

Figure 3.2 : **Method Transactivation Activity Assessment using the Dual-Luciferase Reporter Assay.**

Panel 1 illustrates the plasmid constructs used in the transactivation activity experiments conducted in various immortalised cell lines (HeLa, INS-1 832/3, and Endoc-βh3 cells). Either wild-type HNF1A plasmids (WT) or variant HNF1A plasmids, in conjunction with reporter plasmids with *Firefly* Luciferase gene and a promoter with HNF1A recognition sequence inside (pGL3-RA) and Vector control of transfection with a *Renilla* Luciferase gene (pRL-SV40), were transiently transfected into each cell type. In panel 2, after transfection the cell expressed either the WT or variant HNF1A protein. This protein then bound to its recognition sequence leading to the transcription of *Firefly* Luciferase. The transactivation activity of HNF1A was measured by assessing the expression of reporter *Firefly* Luciferase. Panel 3 displays the transactivation assay measurement. The bioluminescence signals of *Renilla* Luciferase serve as a transfection efficiency control, and the bioluminescence signals of *Firefly* Luciferase indicate transactivation activity.

3.2.7 DNA-Binding Assay

HeLa cells were transiently transfected (24h), with WT or variant HNF1A plasmids (Figure 3.3). Nuclear protein extract was obtained using the nuclear extraction kit (Abcam). The nuclear extract was then incubated with a biotin-labelled oligonucleotide containing the target HNF1A DNA binding sequence. DNA-binding of HNF1A was determined using DNA-Protein Binding Assay Kit (Colorimetric) (Abcam) according to the manufacturer's guidelines. The resulting oligo-protein complex was captured on the assay microwell and detected using a HNF1A primary antibody (Santa Cruz) and Horseradish Peroxidase (HRP) secondary antibodies (GE Healthcare). Quantitative measurements of the colorimetric reactions were performed using Microplate Reader (BMG reader).

The analysis involved calculating the binding activity using the formula: "Binding Activity = (Sample OD – Blank OD) x sample dilution."

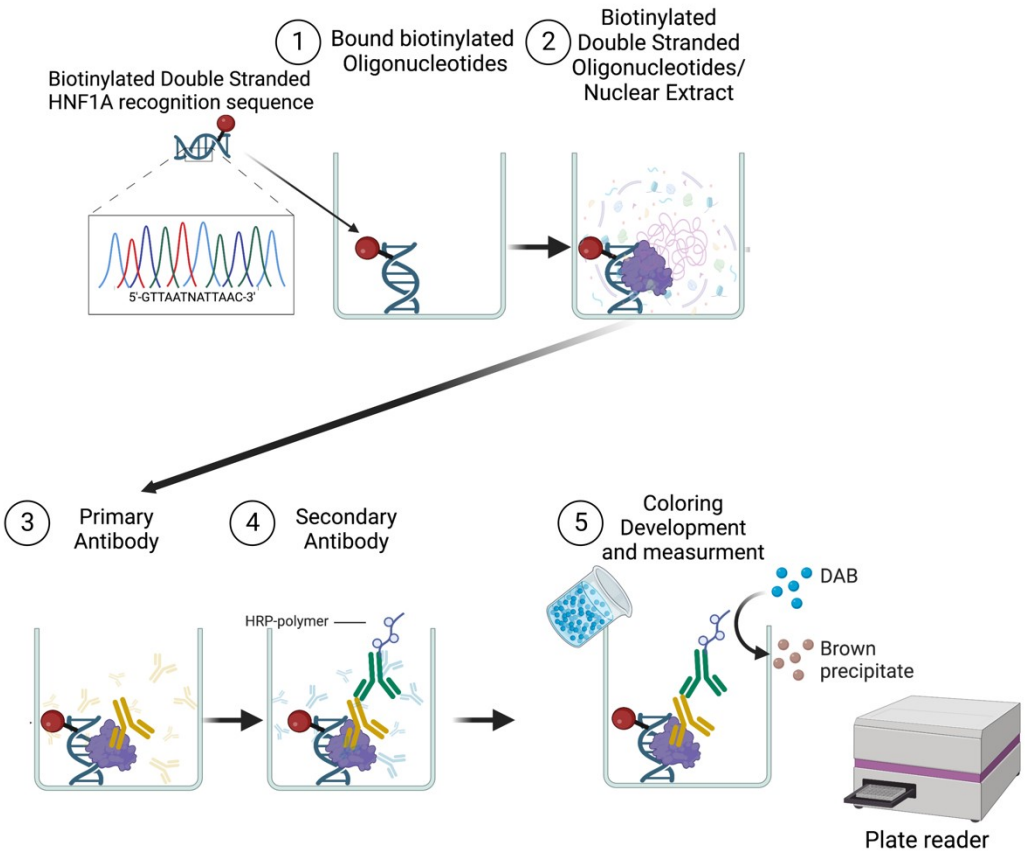

Figure 3.3: **DNA-Binding Colorimetric Assay.**

The figure depicts a colorimetric assay designed to measure DNA-binding activity. In this assay, the HNF1A protein binds to a specific biotinylated double-stranded recognition sequence, resulting in its immobilisation onto a microwell plate. Next, the protein is detected using a primary and secondary antibody. The measurement is performed using a colorimetric assay, utilising a colour-development reaction system involving a detection secondary antibody. The secondary antibody is linked to horseradish peroxidase (HRP), an enzyme that catalyses the reaction of DAB (3,3′-Diaminobenzidine). This reaction results in the oxidation of hydrogen peroxide and the formation of a brown precipitate at the location of HRP. The absorbance measured from this assay is directly proportional to the concentration of HNF1A protein bound to its recognition site in the microwell.

3.2.8 Western Blotting

Lysate extracted from DNA-binding assay, for WT or variant *HNF1A* was mixed with 2X Laemmli loading buffer and denatured at 95 °C for 5 minutes. The samples were then separated by 10% SDS-PAGE (Sigma) and transferred onto polyvinylidene difluoride membranes for subsequent immunoblotting. The membranes were blocked using a 5% BSA blocking solution and then incubated at 4°C overnight with a primary antibody, mouse monoclonal HNF1A antibody (Santa Cruz) at a dilution of 1:1000 in 1X TBS buffer with 0.1% Tween-20 and 5% BSA. Membranes were washed 3-5 times and the secondary antibody, Mouse HRP-conjugated antibody (GE Healthcare), was incubated at a dilution of 1:1000. The membranes were subsequently subjected to a stripping process to remove antibodies, followed by re-probing with Lamin B1 to assess the endogenous expression of nuclear lamina (Abcam). The quantification of protein bands on Western blots was performed using Fiji software. The expression of the *HNF1A* WT or variant was quantified relative to the expression of Lamin B1.

3.2.9 Subcellular Localisation

INS1 832/3 cells (Asfari *et al.*, 1992) were transiently transfected (24h), with WT or variant HNF1A plasmids. The HNF1A subcellular localisation of WT and *HNF1A* variants was assessed using a primary 6x-His Tag Monoclonal Antibody (ThermoFisher) followed by a secondary antibody, Alexa Fluor 488 (ThermoFisher). The slides were mounted using ProLong Diamond Antifade Mounting solution with DAPI (Invitrogen) and examined using the Eclipse T-I Microscope with a spinning disc confocal system (Nikon), x40, oil immersion. A minimum of 30 cells were analysed to determine the presence of staining in the nucleus only and in both the nucleus and cytoplasm, 3 experiments were performed using 3 biological replicates for each variant and WT.

3.2.10 Statistical Analysis

The Shapiro test (Shapiro and Wilk, 1965) was used to assess the normality of the data. Mean ± SEM was reported for normally distributed data, while median with interquartile range (IQR) was reported for data that did not follow a normal distribution.

Unpaired Student's two-tailed t-test was used for comparing two groups when the data met parametric assumptions. In cases where the data did not meet parametric assumptions, the Mann-Whitney U test was employed for two-group comparisons. For parametric comparisons involving multiple groups, One-Way ANOVA was used, and for non-parametric comparisons, the Kruskal-Wallis test was utilised. Statistical analysis was performed using GraphPad Prism 9 software. A p-value less than 0.05 was considered statistically significant.

3.3 Results Functional Assessment Study of *HNF1A* VUSs

3.3.1 Baseline Clinical Assessment: Establishing the Initial Patient Profile

The clinical findings discussed in this chapter were obtained from the MY DIABETES (MODY in Young-Onset Diabetes in Different Ethnicities) study, which was led by Dr. Shivani Misra, Professor Des Johnston, Professor Andrew Hattersley and Dr Nick Oliver. The clinical research findings related to the *HNF1A* variant p.A251T were published in the journal Diabetes Care in 2020 (Misra *et al.*, 2020). Anonymised participant data for the *HNF1A* variant p.S19L were ascertained from the Familial Genetics of Diabetes study (REC 16/LO/1595).

3.3.2 *HNF1A* Variant p.A251T

A homozygous *HNF1A* variant (p.A251T) has been sequenced in several members of a family with young-onset diabetes (Misra *et al.*, 2020). Clinical features were investigated in the insulin-treated family members which were diagnosed with diabetes before the age of 20. Probands were all diagnosed with T1D as teenagers and were treated with insulin. In addition, the father of the insulin-treated family members shows criteria for prediabetes and the mother developed gestational diabetes (Misra *et al.*, 2020).

Clinical studies were performed, assessing firstly C-reactive Protein in the probands as biomarkers of HNF1A-MODY. Levels of hs-CRP were low (≤0.2–0.8 mg/L) for all members of the proband's family except the father who showed a higher value (1.4 mg/L) (Misra *et al.*, 2020). Remarkably, all subjects with homozygous *HNF1A* variant in the study demonstrated sensitivity to sulfonylureas treatment, facilitating a transition from insulin therapy to a low dosage of sulfonylurea treatment (Misra *et al.*, 2020).

Table 3-1: ***HNF1A* p.A251T Clinical Presentation.**

Baseline clinical presentation of p.Ala251Thr from MY DIABETES study (Misra *et al.*, 2020).

Characteristics	Value
HNF1A Variant	NM_000545 c.751G>A; p. Ala251Thr Homozygous missense variant
Family history	Both parents of the proband heterozygous carriers of the p.A251T *HNF1A* variant. The father fulfilled the criteria for prediabetes, while the mother developed gestational diabetes during her pregnancy which persisted postpartum
Age at diagnosis (years)	18
Diagnosis	Proband, identical twin, and sister presented with T1D as teenagers
HbA1c (%, mmol/mol)	6.9%, 52
GAD, IA-2 and ZnT8 antibodies	Negative for all three probands
Fasting C-peptide/glucose pmol/L	Low (≤0.2–0.8 mg/L) in homozygous and heterozygous individuals, higher (1.4 mg/L) in heterozygous father
Current treatment	Proband transition from insulin therapy to sulfonylurea therapy: once-daily dose of 1.25 mg glibenclamide, which was then increased twice-daily
Mixed Meal Tolerance Test Results	Blood glucose plateaued at 12.5 mmol/L with a rise in C-peptide

3.3.3 *HNF1A* Variant p.S19L

The 34-year-old proband was diagnosed with gestational diabetes age 23 years and in subsequent years had borderline glucose levels with eventual commencement of metformin and a label of ‘type 2 diabetes’. She remained on metformin monotherapy, had a BMI of 22.6 kg/m2 and an HbA1c of 7.6% (59 mmol/mol). There was no family history of diabetes. Next generation sequencing of known MODY-causing genes revealed a novel variant c.56C>T (p. Ser19Leu) missense variant. The proband tested negative for GAD, IA-2 antibodies and ZnT8 antibodies. Fasting C-peptide was 387 pmol/L with paired glucose 10 mmol/L. Neither parent had diabetes (normal HbA1c), and neither were carriers for the p.S19L variant. Mixed meal tolerance tests on and off a 40mg gliclazide dose showed more rapid normalisation of glucose levels with higher peak C-peptide levels on gliclazide than off (Table 3-2).

Table 3-2: ***HNF1A* p.S19L Clinical Presentation.**

Baseline clinical presentation of p. Ser19Leu proband.

Characteristics	Value
HNF1A Variant	NM_000545 c.56C>T; *HNF1A* p.Ser19Leu Heterozygous missense variant
Family history	No parental history of diabetes
Age at diagnosis (years)	23
Diagnosis	Gestational diabetes at 24 years, later labeled as type 2 diabetes
BMI (kg/m^2)	22.6
HbA1c (%, mmol/mol)	7.6, 59
GAD, IA-2 and ZnT8 antibodies	Negative
Fasting C-peptide/glucose pmol/L	387
Current treatment	Metformin monotherapy
Mixed Meal Tolerance Test Results	Higher peak C-peptide levels and faster normalisation of glucose levels with gliclazide compared to without medication (40mg dose)

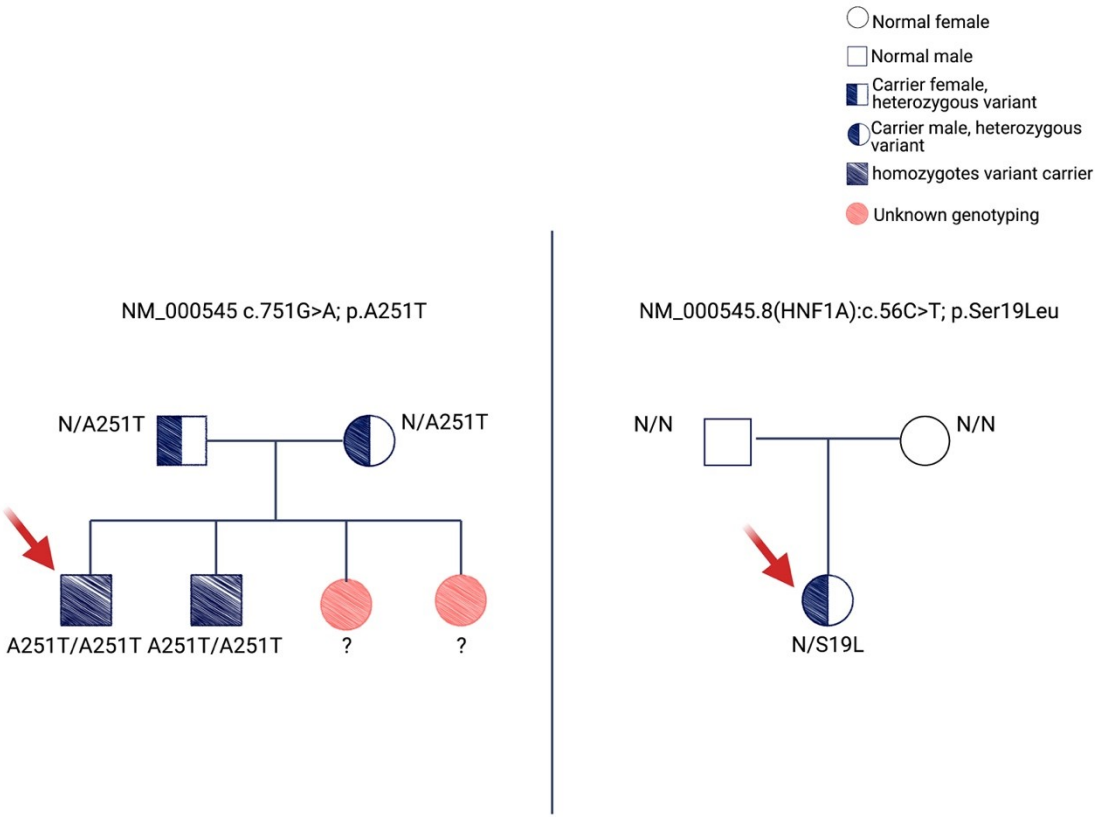

Figure 3.4: **Pedigree Analysis of Probands Carrying the *HNF1A* p.A251T and p.S19L Variants.** The figure shows the pedigrees of two probands, one carrying the p.A251T variant and the other carrying the p.S19L variant. Family members are shaded in blue when they are homozygous variant carriers, half blue when they are heterozygous variant carriers, and pink when the genotyping is unknown. Squares represent female carriers, while circles represent male carriers. N denotes the normal allele, A251T represents the variant allele for p.A251T, and S19L represents the variant allele for p. S19L.

3.3.4 *In silico* Predictions

3.3.4.1 *HNF1A* Variant p.A251T

Some investigations of the *HNF1A* p.A251T variant have been described previously (Misra *et al.*, 2020). Well-established *in silico* tools were assessed in line with the American College of Medical Genetics classification (Richards *et al.*, 2015) and compared with previously described *in silico* data for MODY-causing mutations surrounding p.A251T (Juszczak *et al.*, 2018). The HNF1A structure was studied *in silico* using FoldX (Schymkowitz *et al.*, 2005) using data from a nearby MODY-causing mutation, p.V246 L (Table 3-3, 14). These investigations showed that *HNF1A* p.A251T is in a highly conserved area of the DNA-binding domain of HNF1A which is known as the POUs homeodomain. This region is divided into two subdomains, POUs and POUH (P *et al.*, 2017), while POUs subdomain helps in maintaining the stability of the protein, the POUh subdomains help initiating the transcription factor DNA-binding (Chi, 2005). The *HNF1A* p.A251T variant is located at the interface of the two subdomains, and the *in silico* investigations showed that p.A251T is likely to form a novel hydrogen bond which might affect HNF1A protein functions (Misra *et al.*, 2020). All the *in silico* data classified the *HNF1A* p.A251T variant as uncertain significance (Table 3-3).

Dr. Richard B. Sessions conducted a structural analysis using CHIMERA software to validate these findings. The analysis revealed that the HNF1A protein has a tightly packed interface between the two POUs/POUh subdomains, which maintain the relative orientation of the DNA-binding helices. Additionally, the findings revealed that the *HNF1A* p.A251T variant resides in a loop region within the POUh domain, precisely at the interface between POUs and POUh. Residue 251 plays a specific role in facilitating the interaction between these subdomains by positioning its sidechain within the interface. The potential disruption of this interaction is expected to influence HNF1A's DNA binding ability, although the degree of significance in this regard remains uncertain. This outcome depends on the extent to which the interface is disrupted or modified, as well as the positioning of the binding helices (P *et al.*, 2017).

Table 3-3: **Summary of *In Silico* Testing Results for Predicting Pathogenicity of the *HNF1A* p.A251T Variant.**

Database of MY DIABETES study, listed in Supplementary Data Table 2, Shivani Misra, 2020 (Misra *et al.*, 2020). GnomAD, genome aggregation database; dbSNP, single nucleotide polymorphism database; SIFT, sorting intolerant from tolerant; PolyPhen2, polymorphism phenotyping version 2, Align-GVGD: Grantham variation (GV) and Grantham deviation (GD); POUH/S, pituitary-octamer-unc DNA-binding (H) homeodomain and (S) specific, sub-domains.

Parameter	Description of finding
Mutation Database searches	Three homozygous individuals' sequence with *HNF1A* p.A251T variant (proband, his identical twin, and a sister), presented with T1D
Sequence Variant Database	Not listed in GnomAD, dbSNP, Exome Variant Server or 1000 genomes
Amino Acid Change	Alanine (non-polar) to Threonine (uncharged polar)
Protein Domain Location	DNA-Binding
Species conservation	Conserved in 16 out of 17 orthologues, including 10 mammalian orthologues
In silico prediction	Likely pathogenic: SIFT, PolyPhen2 & Align-GVGD Uncertain: Grantham Distance is 58 (>50 pathogenic)
Cryptic Splice Site	Not predicted to create splice site
Protein structural modelling	Mild alteration of POUH/ POUS interface of the HNF1A DNA-binding domain, but not as deleterious as confirmed mutations in the same area

3.3.4.2 *HNF1A* Variant p.S19L

In the study, a novel missense change was identified in a patient diagnosed with diabetes at the age of 23, at the HNF1A amino acid residue 19, serine to leucine (Table 3-4). The identified variant *HNF1A* p.S19L is located within the dimerization domain of HNF1A and is conserved across 19 species with a high conservation score. Multiple *in silico* prediction tools, including SIFT, PolyPhen 2, and AlignGVGD, suggest that the variant is likely to have a deleterious impact on the function of HNF1A (Table 3-4).

The structure of HNF1A consists of a homodimer composed of alpha-helical hairpins, which collectively form a 4-helix bundle (Figure 3.5, Panel A) (Rose *et al.*, 2000). The HNF1A homodimers form associations through the identical interface and can bind to the HNF1A co-activator DCoH (dimerization cofactor of HNF1) (Figure 3.5, Panel B). The complex HNF1A-DcoH regulates binding to different HNF1A effectors (Rose *et al.*, 2004).The residue S19 occurs at the end of helix 1 and acts as a C-terminal cap by donating a hydrogen bond from its sidechain OH to the backbone carbonyl of residue L16 (Figure 3.5, Panel C). This initiates the tight turn between helices 1 and 2 that allows the dimer to form.

Leucine, by contrast, is a good helix-former and its substitution at 19 (S19L) will not favour the helices 1 and 2 formation, resulting in the disruption of dimer formation. In addition, S19 stabilises the dimer via the sidechain OH of S19 accepting a hydrogen bond from the sidechain NH2 of Q9 on the opposite chain. The strength of both hydrogen bonds arises from their nearly optimal N-H...O hydrogen bond lengths and angles. The S19L substitution is likely to impact the DCoH binding site because it is located at the interface HNF-1/DCoH. In the S19L variant the sidechain L19 is juxtaposed with the sidechain of L45 in DCoH (Figure 3.5, Panel C). Structural analysis of p.S19L suggests a less probable scenario where the disruption caused by the p.S19L mutation fails to destabilise the HNF1A homodimer. In this case, it is conceivable that the HNF1A-DCoH complex's affinity is increased by maintaining the native dimeric conformation of HNF1A (Figure 3.5).

Table 3-4: **Summary of Findings from *In Silico* Testing to Predict Pathogenicity of the p.S19L *HNF1A* Variant.**

GnomAD, genome aggregation database; dbSNP, single nucleotide polymorphism database; SIFT, sorting intolerant from tolerant; PolyPhen2, polymorphism phenotyping version 2; AlignGVGD: Align Grantham variation (GV) and Grantham deviation (GD).

Parameter	Description of finding
Mutation Database searches	Heterozygous p.S19L novel missense variant identified in a Caucasian lady diagnosed with T2D aged 23-year-old
Sequence Variant Database	Not listed in GnomAD, dbSNP, Exome Variant Server or 1000 genomes
Amino Acid Change	Serine (polar) to Leucine (nonpolar)
Protein Domain	Dimerization domain
Species conservation	Conserved across 19 species with a high conservation score
In silico prediction	SIFT, PolyPhen 2, AlignGVGD: suggest that the variant is likely to have a deleterious impact on the function of HNF1A
Protein structural modelling	Unlikely to be "silent" - highly probable that the p.S19L variant destabilises the folded dimeric state of the N-terminal 30 residues inducing a decrease in transcriptional activation

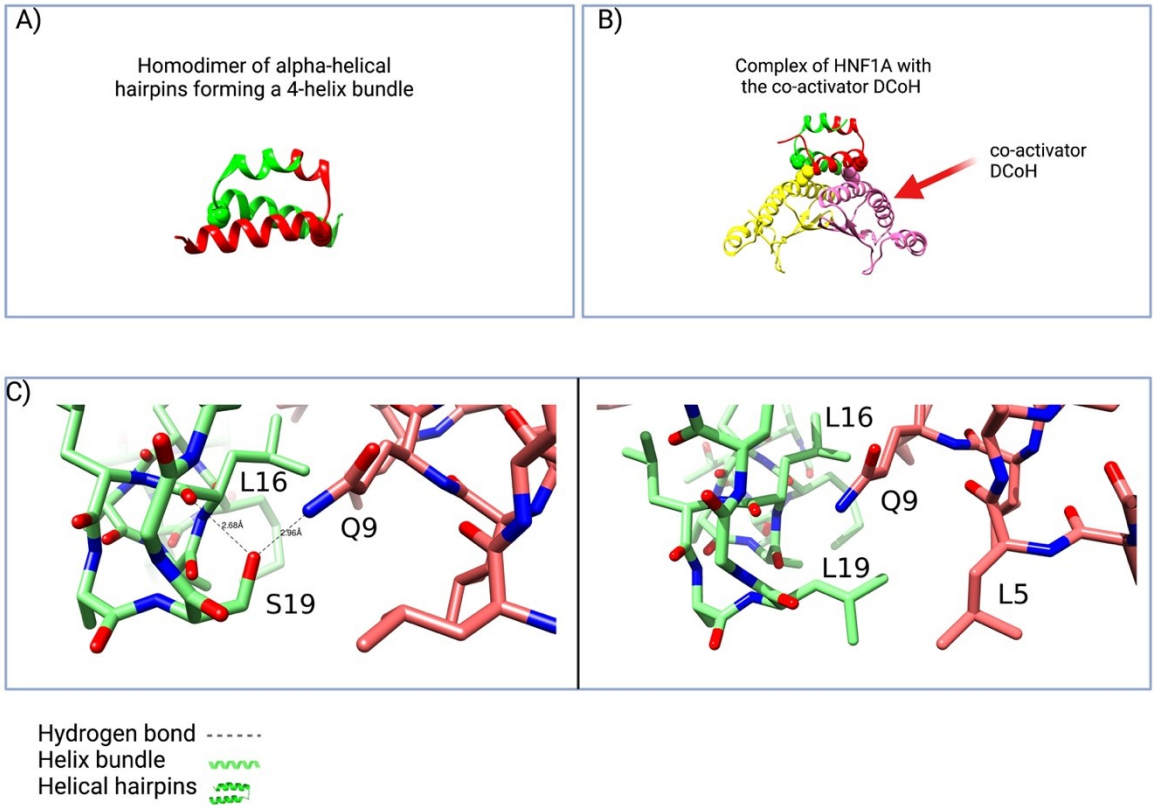

Figure 3.5: **Modelling HNF1A Protein Structural Effect of S19L Variant.**
Panel A: The HNF1A dimer (residues 1-32) interacts with its DNA-binding motif, forming a helix-turn-helix structure. Panel B: The HNF1A dimer is bound to a DCoH (dimerization cofactor of HNF1) dimer. Panel C: Examination of the HNF1A-DCoH interface reveals the role of specific amino acids. On the left, the wild-type side chains of S19 in HNF1A and L5 in DCoH are depicted. S19, located at the end of helix 1 of HNF1A, acts as a C-terminal capping residue by forming a hydrogen bond with the backbone carbonyl of residue L16. It also contributes to dimer stabilisation by accepting a hydrogen bond from the side chain NH2 of Q9 on the opposite DCoH chain. On the right, the S19L substitution affects the DCoH binding site. The S19L variant demonstrates that the L19 side chain is positioned next to the L5 side chain in DCoH, predicted to impact dimerization and binding to DCoH co-activator.

In summary, the findings of p.A251T variants of *HNF1A* indicate that the p.A251T variant is located at the interface of the POUs/POUh domains, which is a critical region sensitive to substitutions. Structural modelling suggests that the p.A251T variant is likely to have mild effects.

On the other hand, the *HNF1A* p.S19L change is expected to have a detrimental impact on protein function by destabilising the folded dimeric state of the N-terminal 30 residues. This disruption would consequently lead to a reduction in transcriptional activation. Alternatively, although less likely, the p.S19L variant might preserve the HNF1A homodimer conformation, potentially leading to an increased affinity for DCoH binding.

3.3.5 *In Vitro* Functional Assessments

3.3.5.1 Overview of Plasmid Constructs Generated by Site-Directed Mutagenesis

Constructs carrying the *HNF1A* p.S19L, p.A251T and p.I27L variants for transactivation assays were generated using site-directed mutagenesis of human pancreatic *HNF1A* cDNA in vector pcDNA3.1A. The sequence of all constructs was validated using sanger sequencing (Figure 3.1). The sequencing analysis confirmed a corresponding change in the coding sequence mutation within the gene. Specifically, the mutation in the coding region is referred to as p.S19L, caused by a single nucleotide change of c.56C>T. This alteration leads to an amino acid substitution from serine (Ser) to leucine (Leu) at position 19. Additionally, the substitution of c.79A>C, resulting in an amino acid change of p.I27L. This substitution is classified as a missense variant at position 27, where the amino acid is changed from isoleucine (Ile) to leucine (Leu). Lastly, the mutation c.751G>A; p.Ala251Thr corresponds to the amino acid change p.A251T, involving an alanine (Ala) being replaced by threonine (Thr) at position 251.

All functional assay results were compared with WT HNF1A transactivation activity, and positive controls using variants previously shown to cause HNF1A haploinsufficiency, which were provided by the Oxford Centre for Diabetes Endocrinology and Metabolism. As the *HNF1A* p.A251T variant is located in the DNA-binding domain, functional results for this variant were compared to known *HNF1A* mutations within the DNA-binding (Table 3-5: *HNF1A* p.R503H (Colclough *et al.*, 2013); *HNF1A* p.P112L (Bjørkhaug *et al.*, 2003); *HNF1A* p.T260M (Glucksmann *et al.*, 1997; Pavić *et al.*, 2018); *HNF1A* p.E508H (Martagón *et al.*, 2018) and *HNF1A* p.A251T (Misra *et al.*, 2020). Some previously described variant used as positive controls were known to be MODY-causing variants, including p.T260M (Glucksmann *et al.*, 1997; Pavić *et al.*, 2018) and p.P112L (Bjørkhaug *et al.*, 2003) or known to cause T2D, such as p.E508K (Martagón *et al.*, 2018). As *HNF1A* p.S19L variant is localised in the dimerization domain, functional assay results for this variant were compared

with previously studied results of common variant *HNF1A* p.I27L, located in the same protein domain (Bjørkhaug *et al.*, 2003; Holmkvist *et al.*, 2006; Locke *et al.*, 2018).

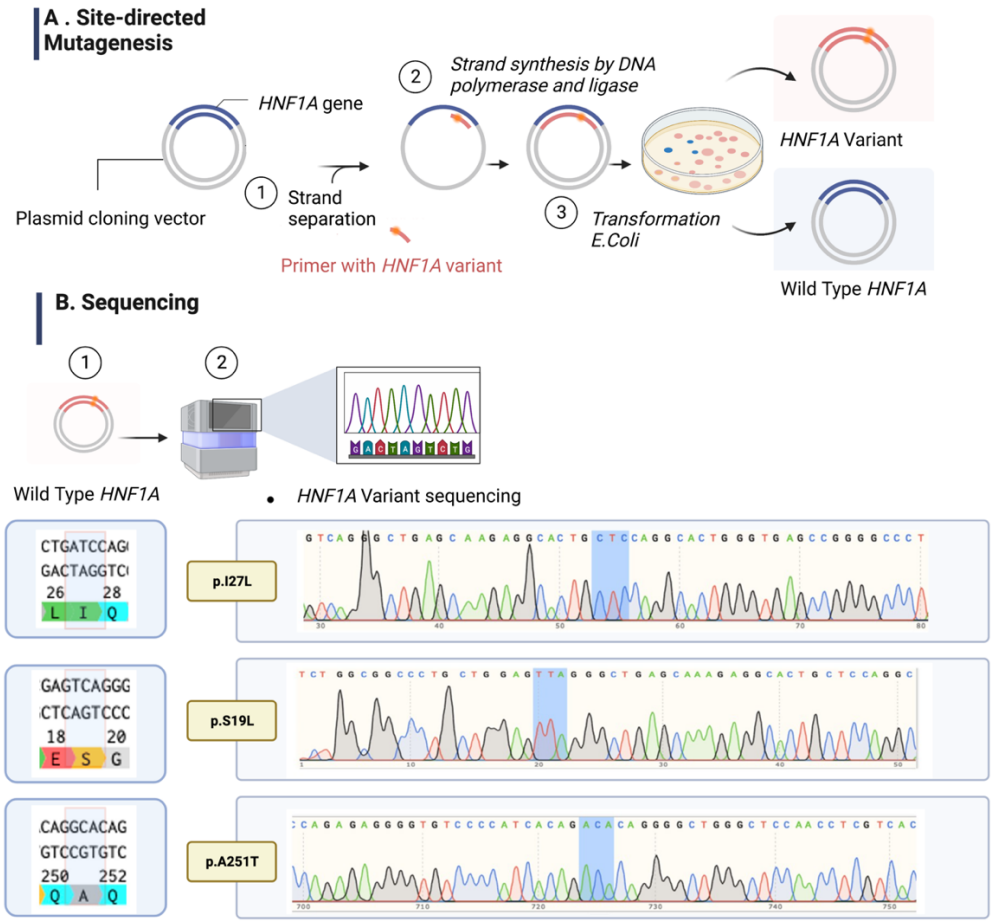

Figure 3.6: **Site Directed Mutagenesis.**

Panel A: Site-Directed Mutagenesis (SDM) method. The SDM consists of three main steps: 1) PCR amplification is performed using specific oligonucleotide primers that contain mismatched nucleotides in the centre, allowing the introduction of the desired *HNF1A* variant. 2) PCR product is incubated with a combination of three enzymes: a kinase, a ligase, and DpnI restriction enzyme. This enzymatic combination facilitates the insertion of the PCR product into a plasmid, while removing the template DNA. 3) The circularized product is transformed into competent cells (bacterial strand *E.Coli*), and the resulting colonies are sequenced to select the one which has incorporate the desired variant. Panel B: Results of SDM conducted as part of this study. Three bacterial colonies were selected, each containing a different variant of interest: *HNF1A* p.S19L, *HNF1A* p.A251T; and a common variant within the dimerization site *HNF1A* p.I27L, used as positive control for reduced function of HNF1A in this specific protein domain. The WT *HNF1A* sequence is shown (left), along with the sequence results obtained after the selection of colonies through SDM (right).

3.3.5.2 Transcriptional Activity Assay *HNF1A* p.A251T and p.S19L VUSs

The initial functional assay for *HNF1A* p.A251T and p.S19L variants involved evaluating their transactivation activity. This was accomplished by employing well-established *in vitro* protocols using luciferase reporter constructs (Transactivation Assay, Figure 3.2 :). The assays were conducted in three different cell lines: common immortalised human HeLa cells (Culliton, 1974; Lucey, Nelson-Rees and Hutchins, 2009), INS-1 rat insulinoma cell line (Asfari *et al.*, 1992) and Endoc-βH3 immortalised β-cell line (Benazra *et al.*, 2015).

The p.A251T and p.S19L variants lie within two important domains of HNF1A protein (Figure 3.1), the transactivation domain, and the dimerization domain, respectively. The transactivation potential of each variant was compared to human over-expressed *HNF1A* WT construct and positive control *HNF1A* variant for defect in transactivation construct (Method: in Figure 3.2 :, Results: Figure 3.7, Figure 3.8). To assess the transcriptional activity of *HNF1A* variants p.A251T and p.S19L, a luciferase reporter constructs was employed driven by the HNF1A protein binding to Rat Albumin promoter in HeLa cells and the HNF4A P2 promoter in INS1 832/3 cells and Endoc-βH3, following established protocols from previous published studies (Figure 3.2 :, 19,20,26,43). This approach allowed us to investigate the impact of the p.A251T and p.S19L variants on HNF1A's transcriptional activity, comparing them to well-characterised *HNF1A* variant causing young onset diabetes. Across all tested promoters and cell types, the *HNF1A* p.S19L variant induce a reduction in transcriptional activity compared to the WT, with 70% of WT HNF1A transactivation activity in HeLa cells (***p=0.0003), a 57% of WT HNF1A transactivation activity in INS-1 cells (**p=0.005) and 86% of WT HNF1A transactivation activity in Endoc-βH3 cells (ns, Figure 3.8).

To compare with a variant in the dimerization domain, the common HNF1A variant p.I27L, associated with an increased risk of developing T2D, showed approximately 80% of WT transactivation activity in HeLa cells (Holmkvist *et al.*, 2006; Gaulton, Ferreira, Lee, Raimondo, Mägi, DIAbetes Genetics Replication And Meta-analysis (DIAGRAM) Consortium, *et al.*, 2015) (Figure 3.7). The p.I27L variant was

approximately 80% of the WT transactivation activity. These results are consistent with a previous study that reported a maximum reduction of 30% for this variant in HeLa cells (Bjørkhaug *et al.*, 2003; Locke *et al.*, 2018). In comparison, the HNF1A p.S19L exhibited a more substantial reduction of the WT transactivation activity.

Compared to well-known *HNF1A* variants located in the DNA-binding domain that reduce transactivation activity, such as *HNF1A* p.P112L (Bjørkhaug *et al.*, 2003) and p.T260M (Glucksmann *et al.*, 1997; Pavić *et al.*, 2018), the variant *HNF1A* p.A251T has minimal impact on transcriptional activity. This effect was observed only in HeLa cells, where no endogenous *HNF1A* was expressed. In HeLa cells, HNF1A p.P112L exhibited 30% of WT activity (Figure 3.7, **p = 0.005), and HNF1A p.T260M showed 34% of WT activity (Figure 3.7, *p = 0.01), while the HNF1A p.A251T had no significant effect in HeLa cells, with 89.62% of WT activity (ns).

In INS-1 832/3 cells, the effects of previously-identified mutations *HNF1A* p.P112L and p.T260M were less severe, suggesting a compensating effect of endogenous HNF1A. HNF1A p.T260M displayed 41% of WT activity (Figure 3.7, *p-value = 0.05), and HNF1A p.P112L showed 32% of WT activity (Figure 3.7, *p-value = 0.03). In contrast, HNF1A p.A251T showed similar activity to WT, with 101% of WT activity (ns) in INS-1 832/3 cells. In human in Endoc-BH3 cells, the transcriptional activity was similar to WT (106% activity, ns).

The results for the variant *HNF1A* p.A251T are consistent with previously described results showing a slight tendency toward reduction in transactivation activity (Table 3-5) (Misra *et al.*, 2020).

Table 3-5: **Summary of Transactivation Potential of HNF1A: *In Vitro* Findings from Previous Studies.**

All variants' results were compared with WT HNF1A transactivation activity, (*p < 0.05, **p < 0.005). Are described below: *HNF1A* p.R503H variant, using rat albumin reporter construct in HeLa cells and using HNF4A P2 promoter in INS-1 cells, from the Oxford dataset (Najmi *et al.*, 2017; Althari *et al.*, 2020); *HNF1A* p.I27L using GLUT2 promoter from the Bergen dataset (Bjørkhaug *et al.*, 2003); *HNF1A* p.P112l (Bjørkhaug *et al.*, 2003) using rat albumin promoter and INS-1 cell line using HNF4AP2 promoter; *HNF1A* p.T260M using rat albumin promoter and INS-1 cell line using HNF4AP2 promoter (Glucksmann *et al.*, 1997; Pavić *et al.*, 2018); *HNF1A* p.E508H using rat albumin promoter in HeLa cells and HNF4AP2 promoter (32). INS-1 cells (Martagón *et al.*, 2018) and *HNF1A* p.A251t using rat albumin promoter in HeLa cells and using HNF4AP2 promoter in INS-1 cells (Misra *et al.*, 2020).

Variant construct in pcDNA3.1 vector	Transactivation in HeLa in % WT activity	Transactivation in INS-1 assays in % WT activity
p.R203H *	~40 and ~60%	~50% and ~100%
p.P112L **	~15–30%	~50%
p.I27L	~70%	~90%
p.T260M **	~20%	~40%
p.E508K *	~70%	~80%
p.A251T	~160%	~80%

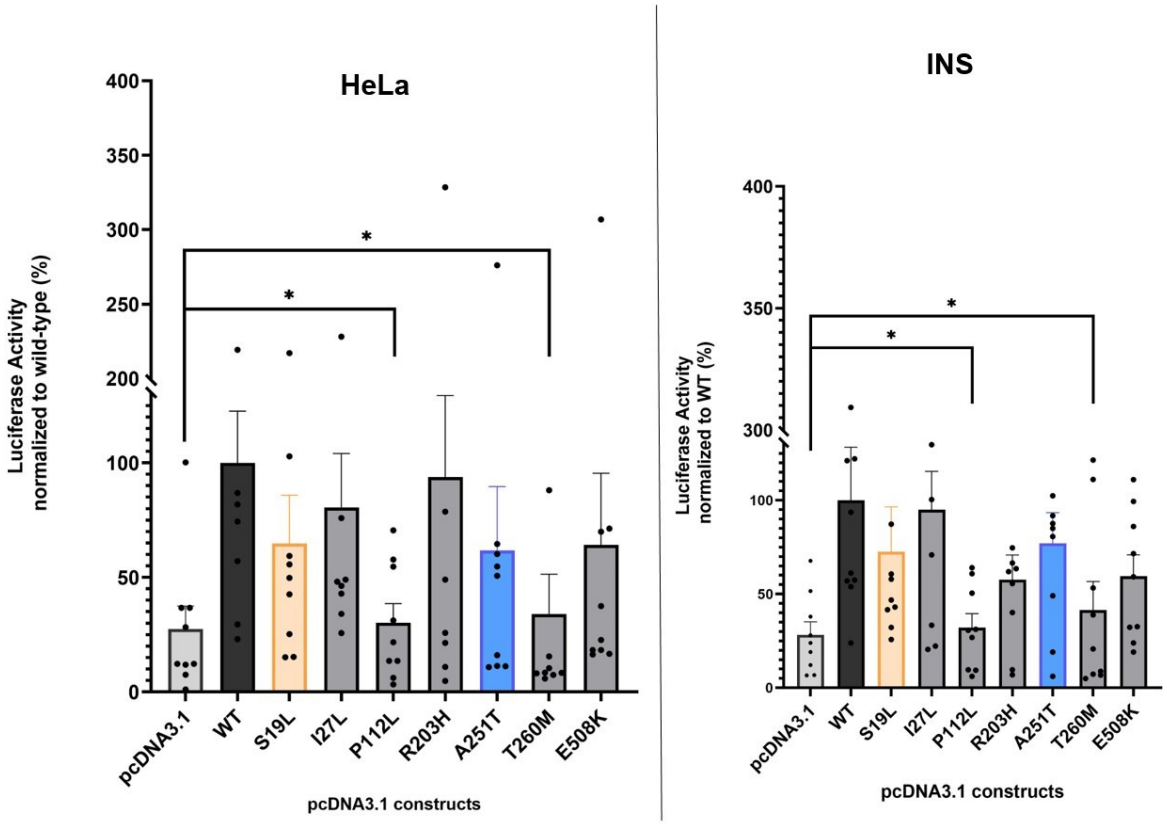

Figure 3.7: **Assessment of *HNF1A* Variant Transcriptional Activity via Luciferase Reporter Assay in HeLa and INS1 832/3 Cells.**

Cells were transiently transfected with wild type (WT) *HNF1A*, or variant *HNF1A*, or empty pcDNA3.1 vector plasmid, together with reporter plasmids pGL3-RA (Rat Albumin promoter containing HNF1A recognition sequence) and pRL-SV40 (control of transfection, *Renilla Luciferase* construct). Luciferase measurements are given in percentage activity compared with WT HNF1A activity. Each point represents the mean of nine readings. 3 experiments were performed using 3 biological replicates for each variant, WT, and empty plasmids (*$p < 0.05$, **$p < 0.005$). Transactivation activity of HNF1A common variant and mutations in each HNF1A protein domain were used as positive control for impaired WT HNF1A function: P112L (Bjørkhaug *et al.*, 2003), T260M (Glucksmann *et al.*, 1997; Pavić *et al.*, 2018), R203H (Colclough *et al.*, 2013), E508K (32), I27L (Najmi *et al.*, 2017; Althari *et al.*, 2020) (published functional assay data described in Table 3-5).

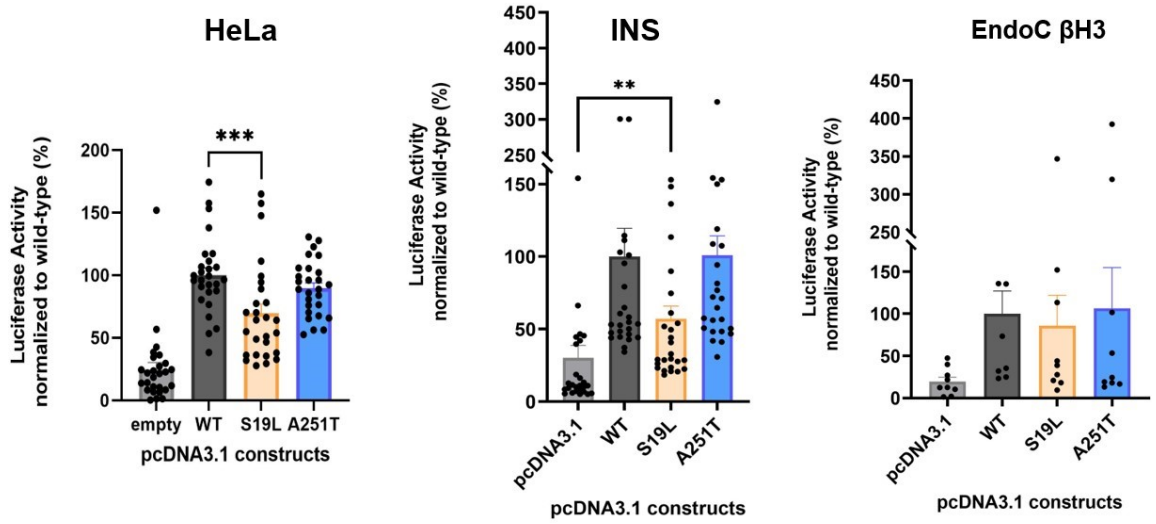

Figure 3.8: **Assessment of Transcriptional Activity of *HNF1A* Variants via Luciferase Reporter Assay in HeLa, INS1 832/3 Cells, and Endoc-BH3**.

Cells were transiently transfected with WT *HNF1A*, or variant *HNF1A*, or empty pcDNA3.1 vector plasmid, together with reporter plasmids pGL3-RA and pRL-SV40. Luciferase measurements are given in percentage activity compared with WT. Each point represents the mean of 27 readings for HeLa and INS1 832/3 cells, 9 reading for Endoc-BH3 (*$p < 0.05$, **$p < 0.005$, *** $p < 0.0005$)

3.3.5.3 DNA-Binding *HNF1A* p.S19L and p.A251T Variants

To investigate the impact of *HNF1A* variants of interest p.S19L and p.A251T on the functionality of the HNF1A protein, DNA-binding activity was examined.

The *HNF1A* DNA-binding sequence has been labelled with biotin to quantify HNF1A DNA-binding activity, in nuclear extracts. The *HNF1A* p.S19L variant is located in the dimerization domain, which is not known to play a role in HNF1A DNA-binding activity or its regulation (Valkovicova *et al.*, 2019b). In the present study, it was observed that the *HNF1A* p.S19L variant induce a non-significant 18% reduction in HNF1A DNA-binding activity compared to the WT, as indicated by Figure 3.10 (p-value = 0.9). This suggests that the *HNF1A* p.S19L variant exerts minimal to no influence on DNA-binding. These results were consistent with another common variant in the dimerization domain, p.I27L, which showed a 25% decrease in DNA-binding activity compared to WT HNF1A protein, similarly, not statistically significant (Figure 3.10, p-value = 0.8). These findings suggest that variants at the dimerization site have a minimal effect on HNF1A DNA-binding. In addition, they suggest that if reduced transactivation activity is observed, it is not induced simply by a defect in DNA-binding.

Three known pathogenic variants of *HNF1A* associated with young onset diabetes were investigated as positive controls for reduced DNA-binding activity: p.P112L (Bjørkhaug *et al.*, 2003), p.R203H (Colclough *et al.*, 2013), and p.T260M (Glucksmann *et al.*, 1997; Pavić *et al.*, 2018). The findings revealed significant decreases in DNA binding activity for all three variants. Specifically, the HNF1A p.P112L variant exhibited a substantial decrease of 76% in DNA binding (Figure 3.10, Dunnett's 1-way ANOVA, *p-value = 0.01), while the p.R203H variant displayed a reduction of 65% (Figure 3.10, Dunnett's 1-way ANOVA, *p-value = 0.04). The HNF1A p.T260M variant demonstrated a significant decrease of 75% in DNA binding activity compared to the WT HNF1A protein (Figure 3.10, Dunnett's 1-way ANOVA, p-value = 0.0132). These findings validate the functional consequences of these pathogenic variants and serve as positive controls for comparing their effects on DNA-binding activity with the variant of interest in this study, *HNF1A* p.A251T, also located within the DNA-binding domains.

The HNF1A p.A251T exhibited a tendency to decrease WT HNF1A protein DNA-binding activity by 52%, although this reduction was not statistically significant (Figure 3.10, Dunnett's 1-way ANOVA, ns, p-value = 0.1221). This suggests that the *HNF1A* p.A251T variant has a smaller effect on DNA-binding compared to the established pathogenic mutations within the same domain.

Since the DNA-protein binding colorimetric assay was used to study DNA-binding activity, it was not possible to correct the DNA-binding calculated values based on protein expression. This is because a western blot experiment is typically used to quantify protein signals, while the colorimetric assay provides relative levels of HNF1A DNA-binding by measuring absorbance. However, the expression levels of both the WT HNF1A protein and its variants were examined by western blot analysis, and no significant differences were observed between variant and WT HNF1A protein level (see Figure 3.9). This indicates that the expression level of both the HNF1A protein and its variants does not have an impact on the DNA-binding results.

In summary, our findings indicate that both variants, HNF1A p.S19L and p.A251T, exhibit a non-significant reduction in DNA-binding ability. The HNF1A p.S19L variant, located in the dimerization site, demonstrated a modest impact, with non-significant decrease of less than 20% in DNA-binding ability. This modest reduction is comparable to the effect observed with the common variant p.I27L in the same protein domain.

On the other hand, the HNF1A p.A251T variant, located in the DNA binding site, at the interface of the POUh and POUs subdomains, displayed a tendency to decrease DNA-binding activity. However, this reduction was not statistically significant and was less severe than the positive control variants, HNF1A p.R203H, p.P112L, and p.T260M, which have previously been shown to significantly impair DNA binding. These results suggest that the p.A251T variant may have a milder impact on the function of HNF1A protein compared to the pathogenic variants within this domain.

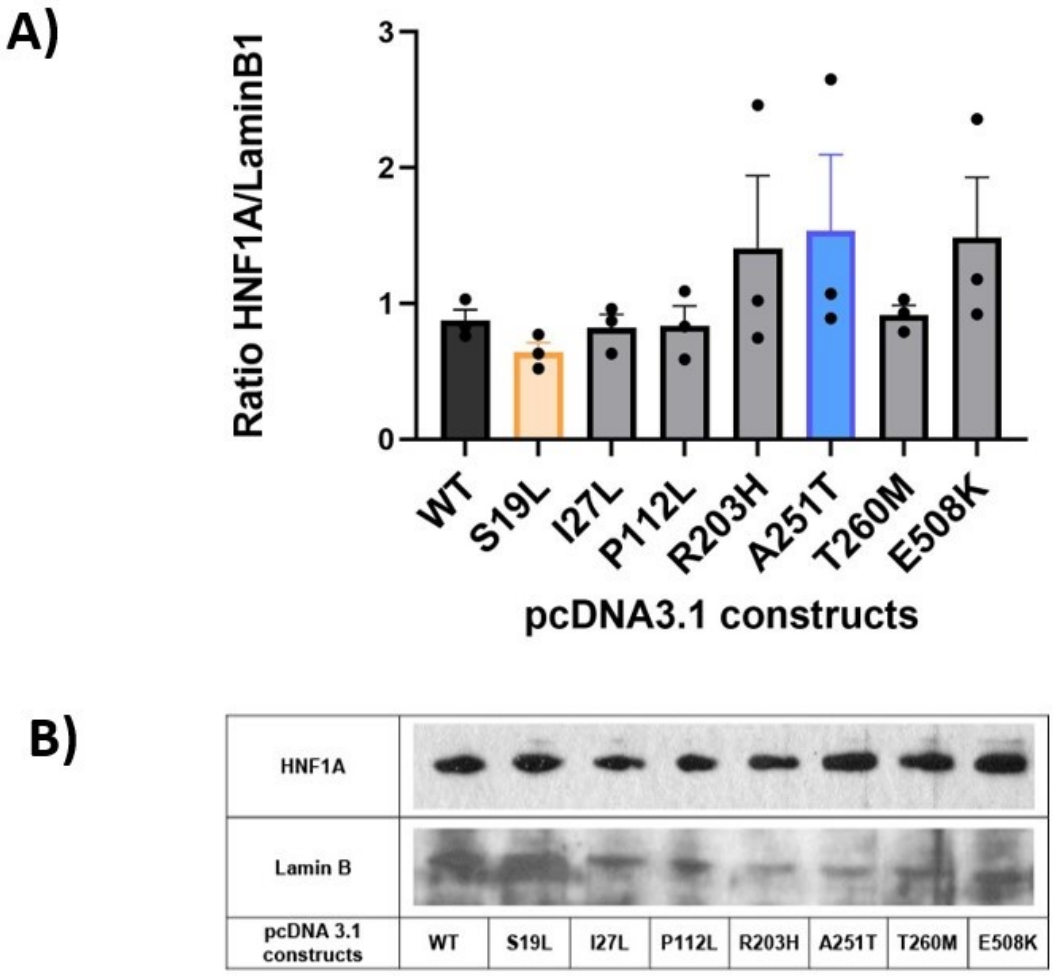

Figure 3.9**: Expression Nuclear extract from DNA-binding assays.**

Panel A shows band fold change as ratio of endogenous nuclear Lamin B expression: orange and blue bars represent the two variants of interests, p.S19L, p.A251T, respectively; grey bars represent positive controls *HNF1A* variant with previous published effects on functional assays (published results summarise and presented in Table 3-5). Western blots were performed on nuclear protein extract from HeLa cells after being transiently transfected (24h), with WT or variant *HNF1A*. Data shown is the mean (SEM) of n=3 biological replicates as ratio of Lamin B1. A two-tailed students t-test was used to compare the mean variant activity to WT. The Panel B shows western blot from one of the biological replicates.

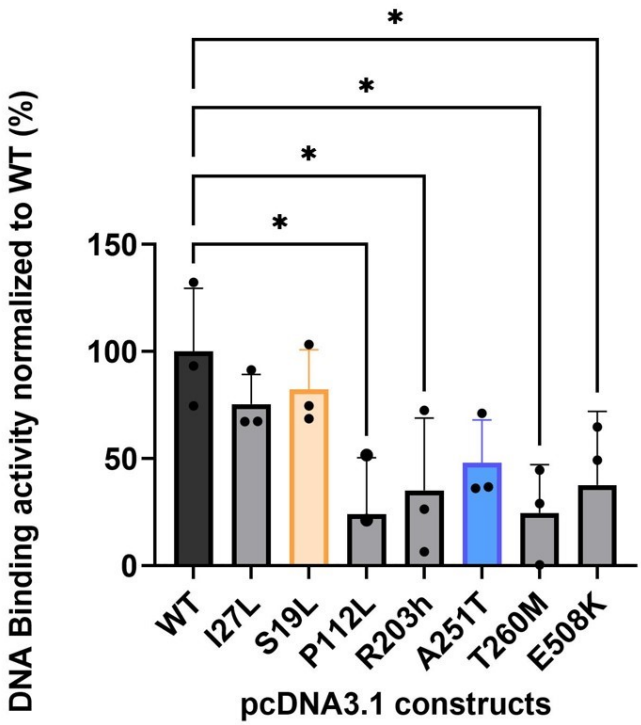

Figure 3.10: **Comparative DNA-Binding Activity of *HNF1A* Variants and Wild-Type.**
Bar graph shows the DNA-protein binding activity normalised to WT HNF1A in HeLa cells using biotin-labelled double-stranded oligo and DNA-Protein Binding Colorimetric Assay Kit (Figure 3.3, DNA-Binding Assay). HeLa cells were transiently transfected (24h), with WT or variant *HNF1A*. Each bar represents the mean of nine readings normalised to WT corrected to the baseline value for empty pcDNA3.1.

3.3.5.4 Subcellular Localisation of *HNF1A* p.S19L and p.A251T Variants

The subcellular localisation of HNF1A protein variant was investigated in transiently transfected INS1 832/3 cells. The plasmids containing *HNF1A* WT and variant sequences were engineered to include a poly-histidine tag, also known as 6-His-Tag, enabling indirect immunofluorescence using a primary antibody against specific 6-His-tag motif. This approach allowed to specifically detect the signal from the tagged HNF1A proteins while cancelling background signal from endogenous proteins, thereby enhancing the accuracy of the image analysis.

To maintain consistency and reproducibility in the subcellular experiments, three biological replicates and three technical replicates for each variant and WT HNF1A protein, with over 30 cells per technical experiment were analysed. The results of subcellular localisation were presented as the ratio of nucleus specific HNF1A tagged protein fluorescence to the total (whole cell) fluorescent signal from HNF1A tagged protein, corrected for baseline value of empty pcDNA3. Typical images illustrating the subcellular distribution were included in the panel B of the Figure 3.11.

The analysis involved the evaluation of the nucleus-to-total cell HNF1A signal ratio (6-His-tagged) for three conditions: wild-type (WT) HNF1A, along with two VUS p.S19L variant and the p.A251T. HNF1A is predominantly localised in the nucleus to regulate target genes. The median ratio of nuclear to total cell HNF1A signal for the WT was 0.8120 (IQR 0.74-0.99; Figure 3.11), indicating strong nuclear localisation, and comparable to WT. In comparison, the *HNF1A* p.S19L variant displayed lower medians of 0.6443 (IQR 0.54-0.70; Figure 3.11), and this difference was found to be statistically significant (Dunn's multiple comparisons test, ****$p < 0.0001$), suggesting that p.S19L reduced nuclear localisation of HNF1A. When comparing WT with the *HNF1A* p.A251T variant, no statistically significant difference was observed, with a ratio of 0.85 (0.66-1.01; ns, Figure 3.11). This suggests that the subcellular localisation of *HNF1A* p.A251T does not significantly differ from that of the WT.

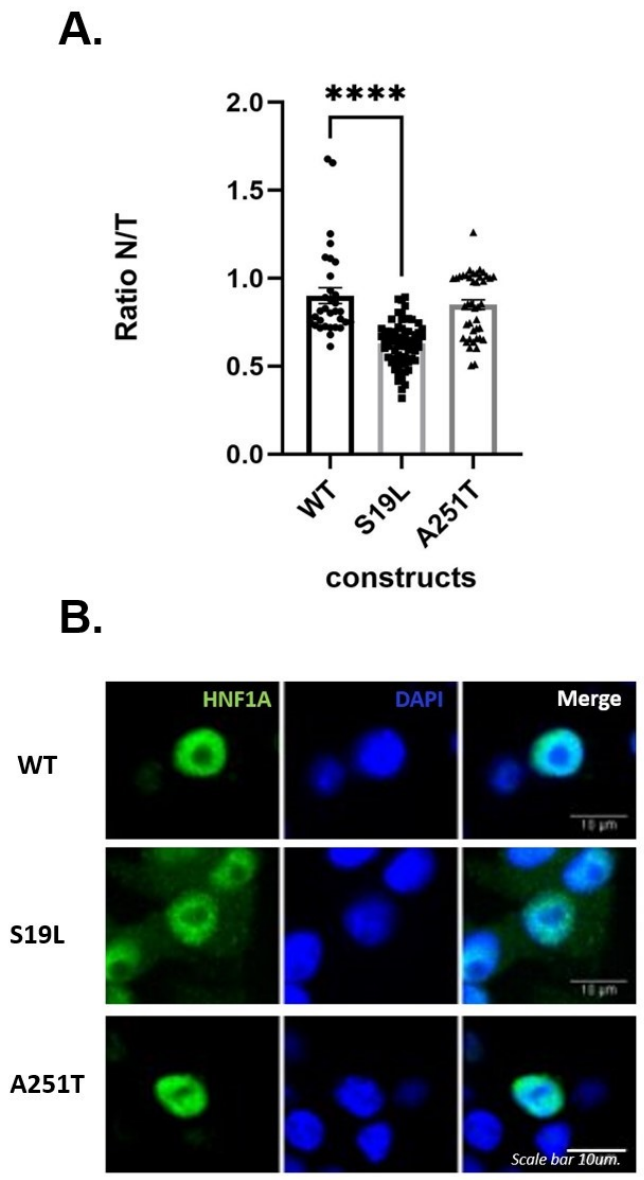

Figure 3.11: **Subcellular Localisation *HNF1A* p.S19L and p.A251T Variants**

Panel A shows the analysis of nuclear localisation of HNF1A protein variants in INS-1 cells. Subcellular localisation in a minimum of n=30 cells was assessed for each *HNF1A* variant and WT. The percentage of cells with nuclear accumulation alone is presented normalised to WT. Panel B: Representative images of in INS-1 cells for the p.A25T and p.S19L variants, and WT nuclear localisation. Cells were transiently transfected for 24h and 6-His-epitope–tagged HNF1A signal were detected by indirect immunofluorescence, Alexa Fluor 488 (green). DNA staining (DAPI) is shown in blue. Three experiments were performed using biological replicates for each variant, WT, using the Eclipse T-I Microscope with a spinning disc confocal system (Nikon), x40, oil immersion.

3.4 Summary of Findings and Discussion

Computational predictions of protein structure (Chimera, Figure 3.11) indicate that the novel *HNF1A* p.S19L variant is unlikely to be functionally silent as the variant destabilises the folded dimeric state of HNF1A, suggesting a potential reduction in transcriptional activity compared to WT HNF1A protein.

Subsequent *in vitro* investigation demonstrated that the novel p.S19L variant adversely affects the transactivation activity of HNF1A in HeLa and INS1 832/3 cells. However, no impact was observed in Endoc-βH3 cells. This implies that the influence of the *HNF1A* variant on transcriptional activity could potentially differ based on the specific cell type employed in the experimental setup, owing to variations in the intrinsic gene expression of *HNF1A* and cell-specific regulatory mechanisms. Notably, HeLa cells exhibited an absence of endogenous *HNF1A* expression, thereby lacking the capacity to counterbalance the diminished transcriptional activity induced by the *HNF1A* p.S19L variant. Using multiple cell types in the experimental design can provide a more comprehensive understanding of the variant's effects and its relevance in different cellular contexts.

Conversely, the HNF1A p.A251T variant displayed a modest impact on the reduction of transcriptional activity when compared to the WT HNF1A. This effect was observed exclusively in HeLa cells, likely due to the same underlying mechanism as described above. The presence of endogenous *HNF1A* expression seem to mitigate the decrease in transcriptional activity.

The results of DNA-binding assays indicate that the *HNF1A* p.A251T variant shows a tendency to diminish DNA-binding activity, albeit without reaching statistical significance and to a lesser extent than observed with established pathogenic variants within the same domain (e.g *HNF1A* p.T260M, Figure 3.7). This effect cannot be attributed to differential HNF1A protein expression, as indicated by Western blot results (Figure 3.9), which demonstrate no discernible difference in HNF1A protein level when compared to WT HNF1A.

The signal of HNF1A p.A251T exhibits subcellular localisation restricted to the nucleus, similar to that of the WT HNF1A protein. On the other hand, the *HNF1A* variant p.S19L leads to compromised nuclear protein localisation compared to WT, resulting in fewer cells showing exclusive nuclear accumulation and increased cytoplasmic HNF1A signal. This observation may suggest a translocation impairment induced by the *HNF1A* p.S19L variant.

These findings provide an overview of the potential impact of p.S19L on HNF1A protein function, indicating reduced transactivation and diminished nuclear localisation compared to the WT. However, this assessment is subject to limitations due to inherent variability among different cell types. Notably, no discernible effect on transcriptional activity was observed in the Endoc-BH3 assay. Likewise, a modest decrease in transactivation activity induced by *HNF1A* p.A251T was observed exclusively in HeLa cells. However, no alterations in transcriptional activity, in comparison to WT, were noted in the Endoc-BH3 or INS1 cells. Therefore, these conflicting outcomes underscore the limitations of employing these techniques to definitively assign pathogenicity.

While these results contribute to enhancing our overall understanding of the protein, their strength is relatively modest. In contrast, numerous MODY-causing mutations, such as p.T260M and p.P112L, significantly impact transactivation, exhibiting less than 20-30% of WT activity, also published in previous studies (Johansson *et al.*, 2017; Najmi *et al.*, 2017).These mutations exhibit a considerably more pronounced effect than the findings of this study.

These findings further hinder the definitive assignment of VUSs pathogenicity in this specific case and offer limited insight into how these effects contribute to MODY progression and phenotypes. A comprehensive understanding of the impact of VUSs in *HNF1A* within the context of MODY necessitates a more relevant *in vitro* cellular modelling. In conjunction with these current results, a comprehensive approach that combines these findings on the functional aspects of the protein, along with additional evaluation of the functional repercussions of these variants on human β-cells *in vitro*,

would significantly enhance our understanding of the intricate mechanisms through which VUS exert their effects.

Statement of Contribution:

The initial *in silico* predictions were conducted by Dr. Shivani Misra, while protein structure prediction for both variants was performed with the help of Dr. Richard B. Sessions (University of Bristol). The clinical presentation data included in this chapter were collected by Dr. Shivani Misra.

A Fiji macro was developed for the purpose of analysing cellular fluorescence microscopy images and determining subcellular localisation of HNF1A. This macro was created by Mr. Stephen Rothery, Senior Technician at the Faculty of Medicine, National Heart and Lung Institute, Imperial College London.

4 Chapter 4: Method and Protocols for Generating Human Pluripotent Stem Cells and Directed Differentiation of B-cell-like cells.

Summary

The third chapter of this thesis assesses the *HNF1A* p.S19L and p.A251T VUSs impact, using a combination of *in silico* prediction and *in vitro* functional assessment through established assays in immortalised cell lines. Computational predictions revealed that the p.S19L variant destabilises the folded dimeric state of the HNF1A homodimer, potentially leading to reduced transcriptional activation, supported by *in vitro* assays demonstrating detrimental effects on transactivation activity and altered subcellular localisation with abnormal HNF1A protein accumulation in the cytoplasm. On the other hand, the *HNF1A* p.A251T variant exhibited a milder impact on HNF1A protein, with a modest reduction in transcriptional activity.

The main limitation underscored in the *HNF1A* p.S19L and p.A251T functional assessment presented in Chapter 3 is centred around the reliance on immortalised cell lines alone. The *in vitro* study performed using immortalised cell lines (e.i. HeLa, INS1) did not replicate the impact of the *HNF1A* variant on human β-cells, responsible for causing the HNF1A-MODY phenotype. Additionally, the mechanism by which the p.A251T variants affect HNF1A transactivation activity remains unclear, which does not appear to have protein function alterations (e.g., in *HNF1A* gene expression or subcellular localisation).

Chapter 4 focuses on developing methodologies to generate human β-cell-like cells from hPSCs to address the limitations presented above. The objective is to provide a more relevant disease context for investigating of *HNF1A* VUSs impact.

4.1 Introduction

4.1.1 Modelling HNF1A-MODY: Human β-Cell-Like Cells

HNF1A-MODY is typically caused by heterozygous loss-of-function mutations. Understanding the functional consequences of these variants is essential to uncover their effects on HNF1A protein function and how they influence the progression of diabetes. Since *HNF1A* is expressed in the endocrine pancreas (Nammo *et al.*, 2002), gaining a comprehensive understanding of the disease phenotype of HNF1A-MODY requires focused investigations on human islets, particularly human β-cells, as they play a central role in the pathogenesis of diabetes.

Obtaining donor islets for individuals with HNF1A-MODY is challenging due to its rarity compared to T1D and T2D. This difficulty is exacerbated when investigating specific genetic variants of unknown significance in *HNF1A*, as donors carrying a specific variant may be limited to a single individual.

The majority of research on HNF1A-MODY has been conducted using rodent models, particularly mice (Pontoglio *et al.*, 1998; Garcia-Gonzalez *et al.*, 2016). However, mice have a significant limitation in their ability to accurately replicate the role of *HNF1A* mutations in the MODY phenotype observed in humans, particularly with regard to β-cell dysfunction (Rees and Alcolado, 2005; Cujba *et al.*, 2022). For instance, mice with heterozygous mutations in *HNF1A* exhibit a normal phenotype (Pontoglio *et al.*, 1998). Only mice with homozygous null mutations display a diabetic metabolic phenotype with a diminished insulin secretion response when exposed to high glucose or arginine (Garcia-Gonzalez *et al.*, 2016). Additionally, rodents models of HNF1A-MODY lack the typical complications seen in patients, particularly renal and kidney complications, including nephropathy, which are commonly observed in individuals with HNF1A-MODY, which can be attributed to the significantly shorter lifespan of mice compared to humans (Isomaa *et al.*, 1998; Poitou *et al.*, 2012).

Generating human β-cell model *in vitro* for HNF1A-MODY study is crucial for uncovering the underlying molecular mechanisms of the disease progression and identifying potential therapeutic targets.

4.1.2 Generation of Genome-Edited Human Embryonic Stem Cell Lines

Given the disparities between rodent and human MODY phenotypes associated with *HNF1A* mutations, it is necessary to establish a human cellular model *in vitro*. Stem cell-derived β-cells carrying specific single nucleotide changes offer a valuable approach for understanding the underlying mechanisms of β-cell dysfunction (Hu *et al.*, 2020). To generate such a human β-cell-like cell model, genome editing techniques such as CRISPR/Cas9 and homologous recombination can be utilised. CRISPR/Cas9 is used to induce targeted DNA break repair via homologous recombination (HR) and non-homologous end joining (NHEJ).

In the context of HR DNA repair, the introduction of a repair template DNA alongside CRISPR/Cas9 and guide RNA enables the precise integration of a specific sequence into the genomic DNA of the targeted cells. This repair template consists of a homologous sequence containing one or more modified nucleotides and has sufficient similarity to the regions surrounding the Cas9 cutting site to be introduced at precise locations via HR repair mechanism. Using this approach, it is possible to modify the genome of hPSCs by incorporating genetic variants of unknown significance identified in the genome of HNF1A-MODY proband (Ding *et al.*, 2013; Hou *et al.*, 2013; Genga, Kearns and Maehr, 2016; Li *et al.*, 2020). hPSCs genetically modified have the ability to be directed differentiated into β-cell-like cells, to study the specific variant impact on human β-cells model *in vitro* (Zhu *et al.*, 2016; Cardenas-Diaz *et al.*, 2019).

The effectiveness of HR has variability across different hPSC lines, depending on factors such as the target site and surrounding DNA sequence. This variability significantly diminishes the efficiency of the technique (Zhu and Huangfu, 2013), and, moreover, may result in editing occurring in off-target regions. (Chen *et al.*, 2015).

Base editing technology has recently emerged as an innovative approach for introducing precise single nucleotide changes in the genome (Komor *et al.*, 2016). Compared to HR, base editing offers several advantages, including a reduced occurrence of off-target modifications and improved efficiency of single nucleotide editing. Base editors consist of chimeric proteins that incorporate a modified version

of the Cas9 enzyme called dead Cas9 (dCas9), along with adenine (A) or cytidine (C) deaminases. These enzymes enable targeted modification of specific nucleotides without the need for double-strand breaks. Adenine base editors facilitate the conversion of A-T base pairs to G-C, while cytosine base editors promote the conversion of C-G base pairs to T-A. This technology opens up new possibilities for precise and efficient genome editing to study precise HNF1A-MODY variant (Eid, Alshareef and Mahfouz, 2018; Hu *et al.*, 2020).

4.1.3 Generation of Patient-Derived iPSC Lines with HNF1A-MODY

An alternative approach to obtain hPSCs carrying the *HNF1A* variant associated with MODY is through the reprogramming of somatic cells. This method involves the conversion of somatic cells obtained from individuals carrying the specific HNF1A-MODY variant into iPSCs. Reprogramming vectors, such as OKSM (Oct4, Klf4, Sox2, and c-Myc), are used to induce the pluripotent state in these cells, allowing them to differentiate into various cell types, including β-cells. This approach offers a valuable tool to study the impact of *HNF1A* variants on β-cell function and HNF1A-MODY disease development (Takahashi *et al.*, 2007). iPSCs are usually generated from fibroblasts but can also be derived from alternative sources such as blood, hair follicles, or even urine (Takahashi *et al.*, 2007; Colman and Dreesen, 2009; Zhou *et al.*, 2011; El Hokayem, Cukier and Dykxhoorn, 2016; Lim *et al.*, 2016). To gain a thorough understanding of the consequences of a *HNF1A* genetic variant in β-cell, CRISPR/Cas9 technology can be employed to correct the genomic variant and revert it back to the “wild-type” *HNF1A* sequence in iPSCs derived from patient-specific cells (Liu *et al.*, 2018). Genome editing techniques, such as base editor or CRISPR/HR, can be applied to induce single nucleotide changes and reverse mutations in iPSCs. These modified iPSCs can then be directed differentiated into β-like cells, enabling the study of specific variants in a genetic context identical to that of the individual carrying the HNF1A-MODY variant (Rezania *et al.*, 2014; Russ *et al.*, 2015; Nair *et al.*, 2019; Veres *et al.*, 2019).

4.1.4 Directed Differentiation of Human Pluripotent Stem Cells into β-Cell-Like Cells

iPSCs and hESCs, genetically modified using previously presented techniques, have the capacity to differentiate into pancreatic β-cell-like cells. By studying the impact of HNF1A-MODY variants in these *in vitro* models of human β-cells, directed differentiation of hPSCs overcome the limitations associated with sourcing primary human islets and gain valuable insights into the phenotypic manifestations of HNF1A-MODY. This knowledge can further contribute to developing more effective therapeutic strategies for individuals affected by early-onset diabetes associated with HNF1A-MODY variants.

4.1.4.1 Differentiation of Human Pluripotent Stem Cells into Definitive Endoderm

The initial stage of differentiation involves the differentiation of hPSCs into definitive endoderm. This process can be achieved by activating the Nodal signalling pathway by adding Activin A (Toivonen, Lundin, *et al.*, 2013; Payne, King and Hay, 2011). Careful regulation of Activin A concentration is crucial to prevent unintended neuronal differentiation, as Activin A has been shown to promote this pathway under certain conditions *in vitro*. Simultaneously, inhibiting PI3K signalling and activating pathways such as the Wingless-related integration site (Wnt) pathway further facilitate the formation of definitive endoderm (McLean *et al.*, 2007; Zhang *et al.*, 2009; Jiang, Wang and Zhang, 2013).

4.1.4.2 Differentiation of Definitive Endoderm into Posterior Foregut and Pancreas Progenitors

Essential regulators of the differentiation process of definitive endoderm into the posterior foregut and then into pancreas progenitor are signalling molecules such as including the fibroblast growth factor (FGF), and retinoic acid (RA) molecules (Zhang *et al.*, 2022). FGF signalling, specifically FGF10, promotes the specification of DE that give rise to the foregut posterior and pancreatic lineages (Bhushan *et al.*, 2001). In conjunction with FGF10, prolonged RA signalling promotes pancreatic progenitor

differentiation from DE (Memon *et al.*, 2018). The keratinocyte growth factor (KGF or FGF7), stimulates ductal cell proliferation and promotes DE differentiation in the posterior foregut by doing so (Uzan *et al.*, 2009; Kunisada *et al.*, 2012).

4.1.4.3 Differentiation of Pancreas Progenitors into Endocrine Progenitor Cells and β-Cell-Like Cells

The activation of the EGFR (epidermal growth factor) signalling pathway, facilitated by the addition of EGF in combination with nicotinamide signalling, inhibits the BMP (bone morphogenetic protein) pathway and promotes the generation of pancreatic progenitor expressing pancreatic islet transcription factors, including the homeodomain protein *NKX6.1* (Nostro *et al.*, 2015).

The differentiation from pancreatic progenitor cells to endocrine precursor cells involves the inhibition of Notch (neurogenic locus Notch) signalling, which allows for the expression of Neurogenin 3 (*NGN3*) (Jensen *et al.*, 2000). Inhibition of Notch signalling, achieved using γ-secretase inhibitors, promotes the differentiation of pancreatic progenitor cells into endocrine progenitors (Murtaugh *et al.*, 2004; Luistro *et al.*, 2009).

Cells expressing *NGN3* initiate the differentiation into endocrine progenitors, and this event occurs downstream of the expression of *NKX6.1* (Zhou *et al.*, 2013). The inhibition of ALK5 (Activin receptor-like kinase 5) signalling pathway, plays a pivotal role in promoting the generation of endocrine cells and eventually INS-positive β-cell-like cells (Lin *et al.*, 2009; Nostro *et al.*, 2011; Chen *et al.*, 2018). In addition, thyroid hormone, specifically Triiodothyronine 3, promotes the β-cell differentiation and its maturation by increasing *MAFA* transcription (Furuya *et al.*, 2013).

4.1.4.4 The Maturation Process of Immature β-Cell Progenitors

In recent years, substantial progress has been achieved in refining culture and directed differentiation protocols for generating pancreatic progenitors, leading to improved efficacy and reproducibility in obtaining β-cell-like cells that closely resemble their native counterparts. However, the maturation process of β-cell progenitors

remains incompletely understood. Key transcription factors involved in β-cell maturation, including *NKX6.1*, *MAF* (v-maf avian musculoaponeurotic fibrosarcoma oncogene), homolog A and B have been identified as critical β-cell progenitors regulators (Nishimura *et al.*, 2006; Al-Khawaga *et al.*, 2018). These factors play crucial roles in orchestrating the developmental program that drives β-cell maturation and acquisition of functional characteristics. Further investigations are still needed to fully understand cell signalling pathway underlying the last stage of β-cell maturation process.

These recent protocols aim to generate a mixture of cells that are predominantly co-expressing *NKX6.1* and *INS* while minimising the presence of other cell types, such as somatostatin-positive cells, glucagon-positive cells, and immature cells co-expressing insulin and glucagon.

Sui, Leibel and Egli, 2018 established a method to increase the production of β-cell-like cells. In 2021, they improved the method by adding aphidicolin (APH) treatment during the final stage of differentiation, which increased the yield of β-cell-like cells expressing *PDX1*, *NKX6.1*, and *MAFA*. In the present work study, protocols developed by Sui, Leibel and Egli, 2018, and an updated protocol by Sui *et al.*, 2021, were utilised to direct differentiate hPSCs with the *HNF1A* p.A1251T variant of interest.

4.1.5 Aim of the Study

Aim: To develop a robust cellular model for studying the functional consequences of *HNF1A* variants in a physiologically relevant context, using:

1) Genome editing to introduce *HNF1A* p.S19L and p.A251T variants in hESCs and use a directed differentiation protocol to obtain β-cell-like cells.

2) iPSCs generation cells probands carrying *HNF1A* p.S19L and p.A251T variants and then directed the differentiation of iPSCs into β-cell-like cells.

4.2 Methods

All materials and equipment details are presented in the Table 6-1, in addition all antibodies primary and secondary, are presented in the Table 6-4.

4.2.1 Collection of Skin Punch Biopsy and Expansion of Fibroblasts

The DIPS study, studying rare diabetes using iPSC, PI: Dr. Shivani Misra, was approved by Westminster Research Ethics Committee (20/LO/1071) to perform skin biopsies from probands carrying the *HNF1A* p.S19L and p. A251T variants.

Using a biopsy punch, 4-mm-diameter epidermal biopsies were obtained. Skin sample were cut into 5-15 smaller sections in a T75 flask and cultured at 37 °C with 5% CO_2 in Dulbecco's Modified Eagle's Medium (DMEM; Thermo Fisher) supplemented with 15% Foetal Bovine Serum (FBS; Thermo Fisher) and Antibiotic-Antimycotic cocktail (Gibco). The culture medium was then replaced every 48 hours. Around day 15, fibroblasts outgrown from the skin biopsies. Fibroblasts were passaged at 70% confluency using Trypsin-Edta solution 1x (Sigma) and seeded at a ratio 1:2 to 1:5 depending on the morphology and density of cells. The primary cells were frozen in a freezing solution containing 90% DMEM medium supplement with 10% FBS and no antibiotics and 10% DMSO.

4.2.2 Generation of Induced Pluripotent Stem Cells Using Plasmids Episomal Vectors

Four days before transfection, fibroblasts were seeded onto a T75 flask so that they would reach between 80-90% confluency on the day of transfection. A minimum of $3x10^6$ fibroblast cells were electroporated (1650V, 10ms, 3 pulses) with 3ug of three 3 reprogramming plasmids containing the episomal factors Oct4, Sox2, Klf4, Lin28, and L-Myc (OSKM): pCXLE-hSK (Addgene), pCXLE-hUL (Addgene) and pCXLE-hOCT3/4-shp53-F (Addgene). Fibroblasts were resuspended in pre-warmed Fibroblast Medium containing DMEM, supplemented with 15% FBS, 10 mM Y-27632 (ROCK inhibitor, Stem Cell Technology), and 4 ng/mL Heat Stable Recombinant

Human bFGF (Thermo Fisher). From days 1 to 15 post-transfection, the media was switched to supplemented N2B27 Medium containing DMEM/High Glucose plus N2 (Thermo Scientific) and B27 without Vitamin A (Thermo Fisher), supplemented with CHALP molecules: 0.5 μM PD0325901 (MEK Inhibitor, Sigma), 3 μM CHIR99021 (GSK3β inhibitor, Sigma), 0.5 μM A-83-01 (TGF-β/Activin/Nodal receptor inhibitor, Reprocell), 10 ng/mL hLIF (STEMCELL Technologies), 10 μM HA-100 (Santa Cruz) and 100 ng/mL bFGF. The N2B27 Medium with CHALP was replaced every 48 hours. On day 15 post-transfection, the supplement N2B27 Medium was replaced with Essential 8 Medium for human stem cell culture (Thermo Fisher) and changed every 24 hours. Between days 15 to 30, hPSC-like colonies start appearing (Figure 4.1). Between days 21 to 40 post-transfection, colonies are of sufficient size to be manually picked and expanded in Vitronectin-coated 24-well plates (Vitronection; STEMCELL Technologies), or alternatively Getrex-coated 24-well plates for 10 passages (Geltrex; Thermo Fisher) (see Figure 4.1).

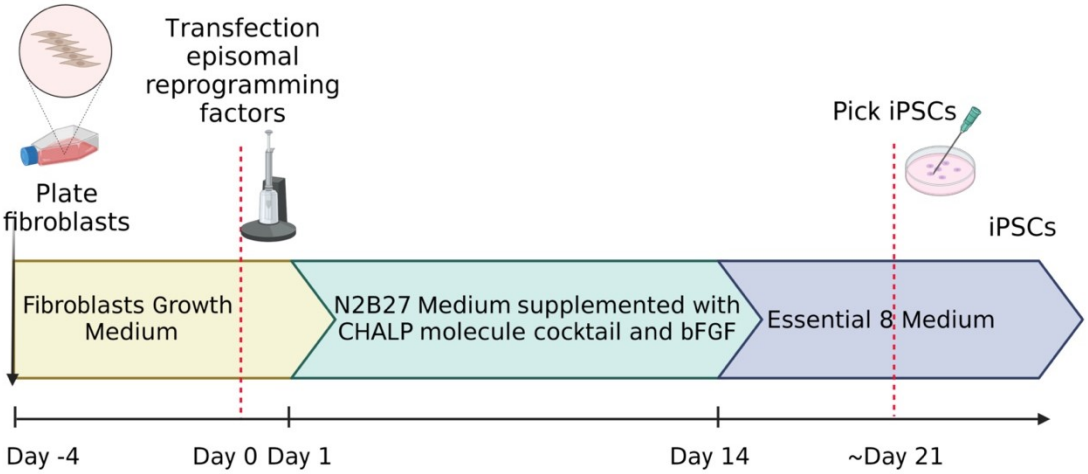

Figure 4.1: **Schematic Representation of the Reprogramming Process Using Episomal Reprogramming Plasmids (Oct4, Klf4, Sox2 and L-Myc)**

Day -4 prior to transfection, fibroblasts are seeded to reach over 80% confluency the day of transfection. Exogenous human reprogramming factors Oct4, Klf4, Sox2 and L-Myc in plasmid vectors are transfected by electroporation into fibroblasts to induce pluripotency. The media was changed from days 1 to 15 post-transfection to N2B27 Medium supplemented with CHALP molecules (including PD0325901, CHIR99021, A-83-, hLIF, HA-100, and bFGF). On day 15 post-transduction, the medium was substituted with Essential 8 human stem cell medium. Around day 21, colonies of iPSCs are large enough to be manually picked and culture separately for further pluripotency and stability characterisation.

4.2.3 Human Pluripotent Stem Cells Culture

hESCs/iPSCs were grown on a 1% Geltrex-coated six-well plate (Thermo Fisher) or vitronectin-coated (STEMCELL Technologies) six-well plate. For optimal cell growth, hPSCs were passaged using 0.5 mM EDTA in dPBS without Ca^{2+} and Mg^{2+} (Thermo Fisher) or TrypLE Express (Thermo Fisher), and seeded at a ratio of 1:10 to 1:50, $2x10^5$ and $1x10^6$ viable cells per well in a six-well plate. After passage, hPSCs were resuspended in human stem cells medium either Essential 8 Medium (E8, Thermo Fisher) or StemFlex (SF, Thermo Fisher) medium containing 1 µL/mL of 10 mM ROCK inhibitor (Ri, Y-27632, STEMCELL Technologies) for 24 hours. The medium was replaced with human stem cells medium (E8/SF) without Ri the following day, and then every other day until the next passage. hPSCs were cultured in an incubator at 37°C and 5% CO_2 humidity. hPSCs were frozen in a solution containing 90% KnockOut Serum Replacement (KSR, Thermo Fisher) and 10% dimethyl sulfoxide (DMSO, Thermo Fisher). For each passage, a minimum of 10^6 cells were frozen.

4.2.4 HEK293 Cells Culture

The HEK293 cells were cultured in DMEM supplemented with 10% FBS in T75 flask. The medium was replaced every 2-3 days. The HEK293 cells were passaged when reaching over 80% confluency using Trypsin-EDTA solution 1x. The HEK293 cells were frozen in a freezing solution containing 90% DMEM medium supplement with 10% FBS and no antibiotics and 10% DMSO.

4.2.5 iPSCs Characterisation

4.2.5.1 Alkaline Phosphatase

Alkaline phosphatase activity was determined using the Alkaline Phosphatase Staining Kit (Abcam). A day prior to performing the Alkaline phosphatase assay, the cells were seeded on a 6-well plate coated with 1% Geltrex (3 wells from each iPS clone to characterise). After 24 hours, the iPSCs were washed 2-3 times with dPBST: 1X dPBS without Ca2+ and Mg2+ (Thermo Fisher) and 0.1% Tween 20 Detergent (Sigma). The cells were fixed for 2 minutes at room temperature with the Fixing

Solution provided with the Alkaline Phosphatase Staining Kit (Abcam). The fixed iPSCs were washed 2-3 times with dPBST. AP Staining Solution from the kit, freshly prepared, was added and incubated for 15 minutes at room temperature in a dark chamber to prevent exposure to light. After the AP Staining, the stained cells were washed 2-3 times with dPBST. Under a light microscope, colonies of red-stained cells were manually counted; the iPSC colonies differentiating remained colourless and were not counted.

4.2.5.2 Immunofluorescence Staining of Pluripotent Marker OCT-4

Fibroblasts, control 1159 and variant A251T iPSCs were fixed with 4% paraformaldehyde (Sigma) for 15 minutes at room temperature, washed with dPBST, 1X dPBS, 0.1% Tween 20 Detergent, and permeabilised with dPBS, 0.1% Triton-X-100 (Sigma), for 10 minutes at room temperature. The nonspecific binding sites were blocked using dPBST, 2% bovine serum albumin (BSA) (Sigma), for 1 hour at room temperature. After blocking, the cells were incubated overnight at 4°C with the primary antibody, Anti-OCT4 antibody (ab19857, Abcam), at 1:500 PBS with 0.1% bovine serum albumin (BSA). Primary, Rabbit species antibodies were detected by Alexafluor-488 (Invitrogen) secondary antibodies at 1:500 dilution with PBS and 0.1% BSA, incubated 2 hours at room temperature. Each slice was mounted with ProLong Diamond Antifade Mounting with DAPI (Invitrogen) and visualised using the Stellaris 8 Confocal Microscope (Leica).

A macro to count iPSCs with fluorescent staining of OCT4 within the nucleus, using a mask generated with DAPI signal restricted to the nucleus, was specifically coded for the purpose of this experiment by Mr. Stephen Rothery, FILM Manager, and the FILM facility of the Faculty of Medicine, Imperial College.

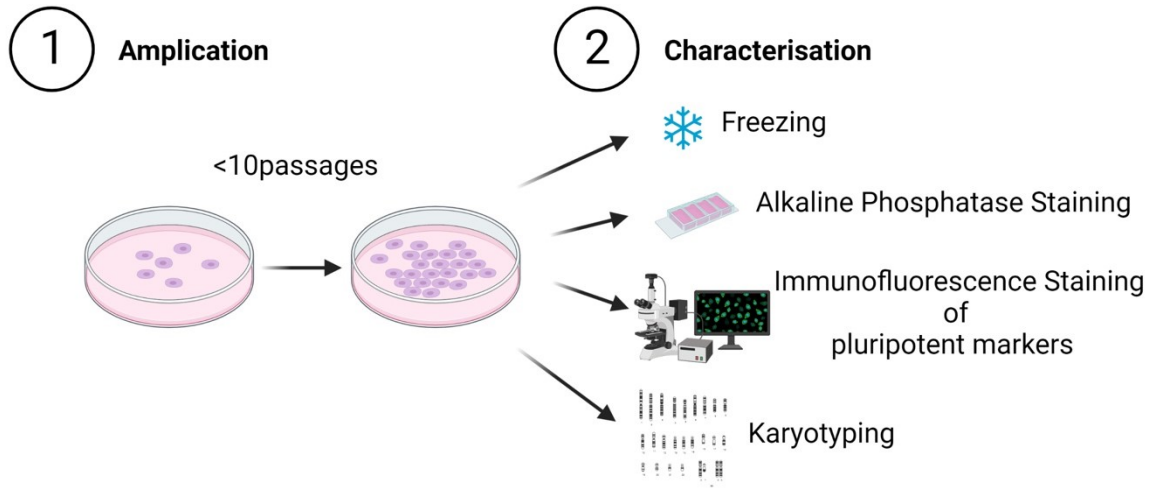

Figure 4.2: **Characterisation of iPSCs.**

Characterising reprogrammed iPSC lines involves multiple steps. 1) iPSCs are passed at least 10 times to ensure the survival of entirely reprogrammed clones, as non-reprogrammed clones are unlikely to survive beyond first passages. In addition, this helps prevent chromosomal abnormalities found in early passage iPSCs (Liu *et al.*, 2020). 2) iPSCs are characterised for pluripotency and chromosomal abnormalities. Each clone is initially frozen as a stock, and freezing and thawing process is assessed several times to determine whether the iPSCs can withstand defrosting and remain viable for culture and future experiments. Alkaline phosphatase activity, which activity is known to be high in hPSCs (Štefková, Procházková and Pacherník, 2015), is measured using a staining assay. In addition, karyotyping is performed to ascertain the induction of pluripotency process did not induce chromosomal aberrations. Lastly, immunofluorescence staining is undertaken to detect the presence of pluripotent markers, e.g. OCT-4, thereby validating the pluripotent nature of the iPSCs. These phases of characterisation provide crucial information regarding the quality, viability, and pluripotency of the iPSC lines, ensuring that only high-quality and entirely reprogrammed clones are utilised in subsequent experiments.

4.2.6 Genome Editing to Introduce *HNF1A* Variant in hPSCs

4.2.6.1 Control Base Editing in HEK293

HEK293 cells were seeded at a density of 10^5 cells per well in a 24-well plate containing DMEM supplemented with 10% FBS and no antibiotics. BE4-max (1 µg) and mCherry-puro-sgRNA-S19L (1 µg) was mixed with Lipofectamine 2000 (Thermo Fisher) at a ratio of 1:3 ratio of (DNA in µg: Lipofectamine 2000 in µl). DNA: Lipofectamine mix was incubated at room temperature for 30 minutes before being added to the respective wells of HEK293 cells; 3 wells were transfected in each of the three experiments (n=9) and incubated for 24 h at 37°C in an incubator containing 5% CO_2. The next day, 2.5 g/mL Puromycin Dihydrochloride (Thermo Fisher) was added to the HEK cells medium for antibiotic selection, and cells were incubated for 72 h. Next, genomic DNA was extracted using the Invitrogen PureLink Genomic DNA Mini Kit (Thermo Fisher) according to the manufacturer's instructions.

Using Q5 High-Fidelity DNA Polymerase, the *HNF1A* exon 1 was amplified in a PCR reaction containing 1X Q5 Reaction Buffer, 200 M dNTPs, 0.5 M Forward and Reverse Primers for each *HNF1A* exon, gDNA (>1000 ng), and 0.02 U/l Q5 High-Fidelity DNA Polymerase. The PCR products were sequenced (Sanger sequencing services, GENEWIZ Azenta) with primers specific to the target region in Exon 1.

4.2.6.2 Base Editing of hPSCs

MEL-1 hESC line with $INS^{GFP/wt}$ were cultured for base editing in Stemflex Medium (following Human Pluripotent Stem Cells). 4 days prior to transfection, hPSCs were seeded at a density of 20,000 cells/cm^2 to reach confluency of over 80% on the day of transfection. StemFlex medium without antibiotics was replaced every day. On the day of transfection, hPSCs medium was washed twice with dPBS without Ca^{2+} and $Mg^{2+}$and hPSCs were dissociated from the 6-well plate using TrypLE Express.

For the electroporation using Neon Transfection system (Thermo Fisher) preparation: the hPSCs were resuspended at a density of $1x10^7$ cells/mL, in a total volume of 100 µL of R buffer provided with Neon Transfection System Kit (Thermo Fisher), along with

3 µg of AncBE4max-P2A-GFP plasmid DNA and 3 µg of mCherry-puro-sgRNA-S19L plasmid DNA. According to the Neon Transfection System Cell Line, hPSCs were electroporated using the following parameters: 2 pulses, a voltage of 1100 V, and a pulse width of 30 ms. The cells were plated in a pre-coated Geltrex 6-well plate, in StemFlex supplemented with a 10 µM of Ri, for 24 hours. For single-cell sorting, the cells were dissociated into single cells using TryPLE and pelleted by centrifugation at 250 × g for 4 minutes at room temperature. Pellet cells were resuspended in 200 µL of sorting buffer 0.5% KSR in dPBS without Ca^{2+} and Mg^{2+} and filtered through a 40 nm cell strainer. The cells were sorted for double positive signals at 488 nm and 561 nm, respectively transient expression of AncBE4max-P2A-GFP plasmid DNA and mCherry-puro-sgRNA-S19L, using a BD FACSAria II SORP flow cytometer. The sorted hPSCs were resuspended in StemFlex supplemented with a 10 µM of Ri, or in RevitaCell Supplement (100X) at a final concentration of 1X to the media, 100 µg/mL Normocin (Invivogen) and plated in a Geltrex-coated 60-mm petri dish (Thermo Fisher). The medium was changed every other day. If hPSC colonies were too small cells, the Ri or alternatively RevitaCell supplement could be refreshed and incubated for an extended period (<24 hours). Approximately 15 days post-electroporation, surviving clones were selected and amplified in triplicate in 96-well plates (one replicate for freezing in KSR 10% DMSO, one for cell culture and expansion through multiple passages, and one for genotyping).

Genomic DNA was extracted using the Invitrogen PureLink Genomic DNA Mini Kit (Thermo Fisher) when the density of cells was high or QuickExtract DNA Extraction Solution (Cambio) according to the manufacturer's instructions. The *HNF1A* target genomic region was subsequently sequenced (Sanger sequencing service, GENEWIZ Azenta) after PCR amplification using Q5 High-Fidelity DNA Polymerase. The process is depicted in Figure 4.3.

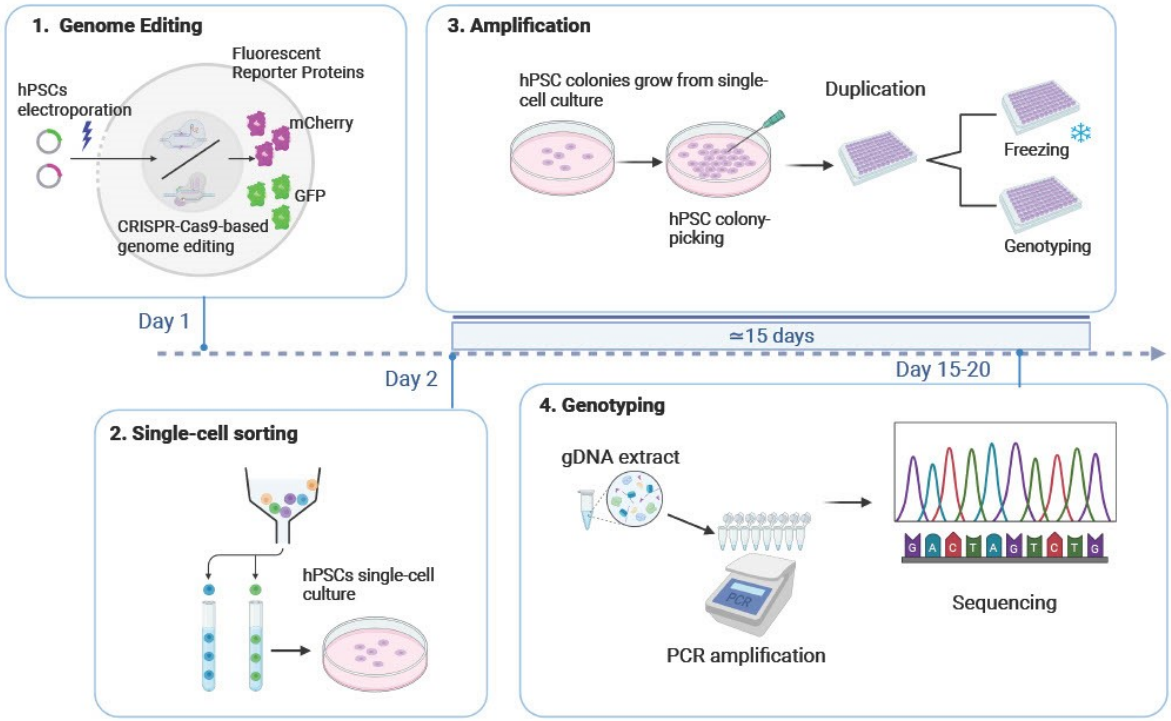

Figure 4.3: **Method of Genome Editing of Human Pluripotent Stem Cells Using Base Editor Technology for the *HNF1A* Variant.**

Panel 1 shows the first step of base editing of the hESC line by electroporation of plasmids containing sgRNA targeting the *HNF1A* p.S19L variant and the base editor (AncBE4-max-GFP), carrying the reporter genes mCherry and GFP respectively. Panel 2 depicts single-cell sorting performed 24 hours post transfection to isolate cells with double positive signals for GFP and mCherry, related to transient expression of both constructs sgRNA targeting the *HNF1A* p.S19L variant and the base editor. Panel 3 show hPSCs single cell growth, and 5 to 10 days after cell sorting, the picking of hPSCs. hPSCs are expanded in duplicate or triplicate wells in a 96-wells plate, depending on the size of the colonies picked, and expanded for freezing and genotyping. Panel 4 shows hPSCs clones genotyping to analyse if genetic variants were successfully introduced, using PCR amplifying specific *HNF1A* exons corresponding to the target sites of the sgRNA/base editor complex. The subsequent PCR product is sequenced and only clones with the desired genetic change is expanded and would undergo directed differentiation.

4.2.6.3 Isolation of hPSC Colonies through Picking

Using a needle (18G x 38mm, VWR), hPSCs colonies were cut into smaller cell clumps, under the laminar flow hood, using EVOS XL Core Imaging System (Thermo Fisher) or alternatively light microscope (Optika). Then, 2-3 small cell clumps were aspirated with a 200 L pipette and plated onto a 1% Geltrex-coated 96-well plate well containing Stemflex supplemented with a ROCK inhibitor. Each clone was seeded in duplicate, or triplicate of a 96-well plate based on the size of the initial colony picked. The cells were placed in an incubator at 37°C and 5% CO_2. The StemFlex medium was replaced daily. The process is depicted in Figure 4.4.

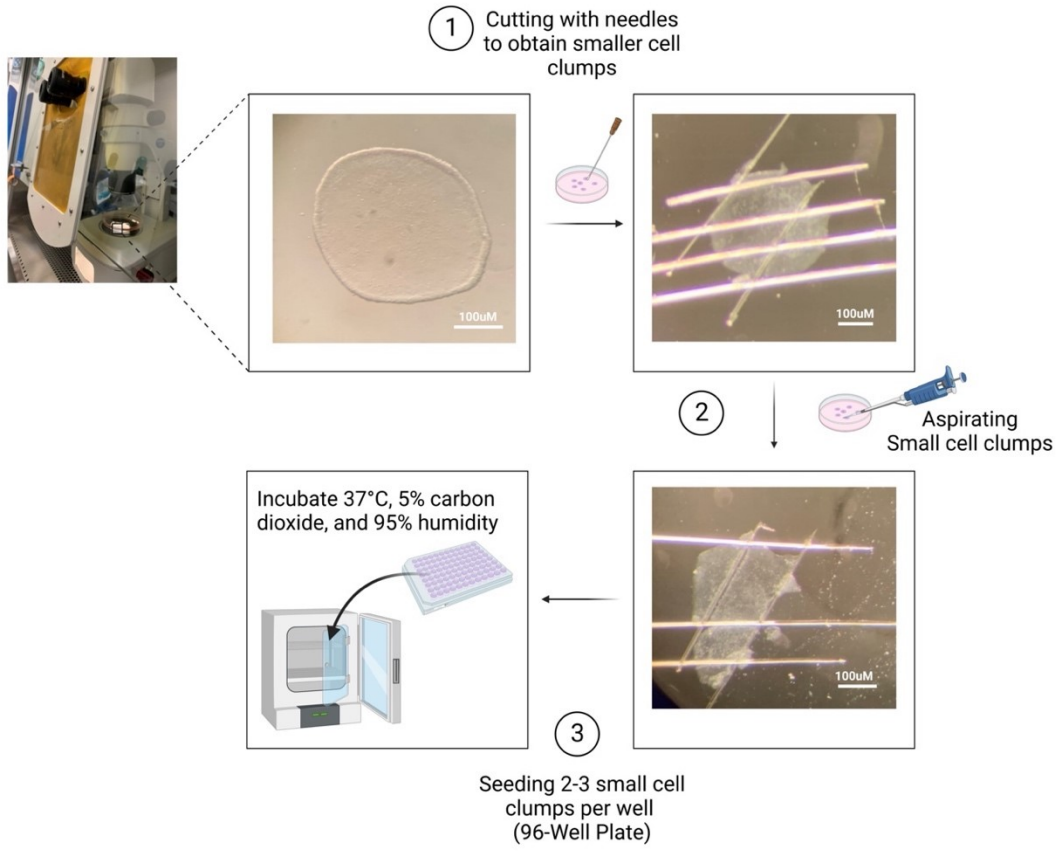

Figure 4.4: **Stepwise Method for hPSC Colony Picking, Isolation, and Expansion.**
1) Colonies of hPSCs were cut into smaller clumps using a needle. 2) 2-3 cell clumps were aspirated and 3) plated onto a 96-well plate with StemFlex supplemented with ROCK inhibitor for 24 hours. The hPSCs were then incubated at 37°C and 5% CO_2, with daily replacement of StemFlex medium.

4.2.6.4 CRISPR/Cas9 Homologous Recombination

The hPSCs cells were seeded 2-4 days prior to nucleofection to allow them to reach approximately 80% confluency on the day of transfection. For each nucleofection, $2x10^6$ cells were cultured in duplicate wells of a Geltrex coated 6-well plate. On the day of nucleofection, solution X (for 100 µl Single Nucleocuvette) from the Cell Line Nucleofector Kit V (Lonza) was prepared according to manufacturer's instructions, by adding the supplement solution and solution 1 provided in a 1:4.5 ratio, together with Cas9-GFP plasmid vector (5 µg), gBlock (2.5 µg), and repair template (2.5 µg). Then, the hPSCs were seeded with TrypLE to dissociate them into single cells and resuspended in StemFlex media supplemented with 10 µM Ri. hPSCs were subsequently centrifuged at 250 × g for 4 minutes at room temperature, washed twice with dPBS without Ca^{2+} and Mg^{2+} and resuspended in the nucleofector solution named "X". The mixture hSPCs/solution "X" was nucleofected using the Nucleofector 4D system (Lonza), program A-023 for hPSCs. After nucleofection, the cells were added dropwise to a well of a 6-well plate that had been pre-coated with 1% Geltrex containing pre-warmed SF, 10 µM Ri medium. The cells were places into an incubator at 37°C and 5% CO_2 for 48 hours. At 48 hours post nucleofection, single-cell sorting was performed on GFP positive cells (transiently expressing Cas9-GFP) using a BD FACSAria II SORP flow cytometer (FILM Facility, Imperial College). The sorted cells were resuspended in SF, 10 µM Ri and plated in a Geltrex-coated 60 mm petri dish.

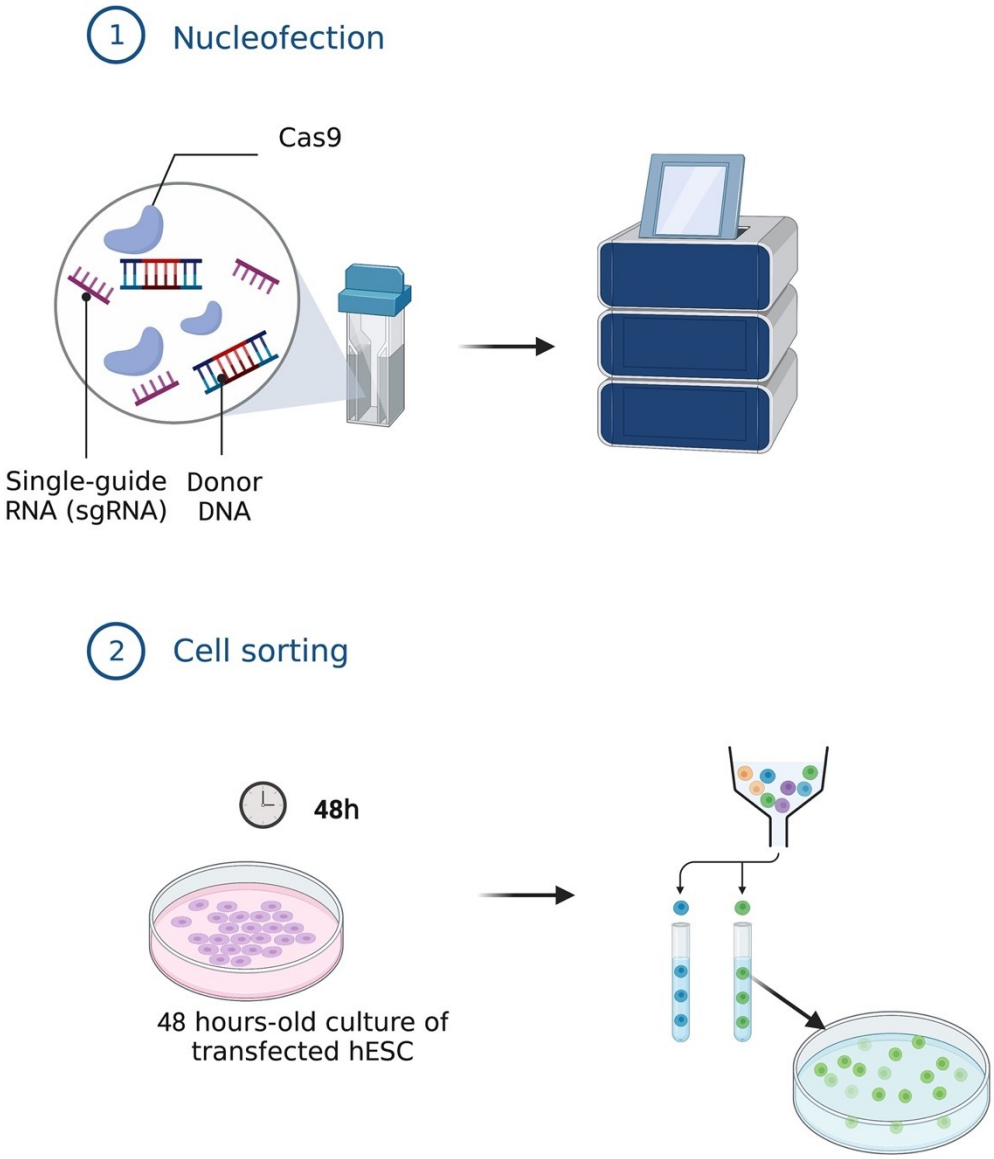

Figure 4.5: **CRISPR/Cas9 Genome Editing of Human Embryonic Stem Cells Using Homologous Recombination.**

On the day of nucleofection, nucleofection solution “X” was prepared containing Cas9-GFP plasmid vector, gBlock (containing single-guide RNA sequence), and donor DNA also known as repair template. The cells were nucleofected using the Nucleofector Lonza system. After nucleofection, hPSCs cells were culture for 48 hours in stem cell media (StemFlex supplemented with Ri). 2) Single-cell sorting was performed on GFP-positive cells (expressing Cas9-GFP), and sorted cells were cultured in Geltrex petri dish until surviving colonies grew enough for picking, amplification, and further analyses.

4.2.7 β-Cell Directed Differentiation

For the directed differentiation toward β-cells, the following hPSCs were cultured: MEL-1 hESC line with $INS^{GFP/wt}$ (Micallef *et al.*, 2012) was utilised to optimise β-cell directed differentiation. iPSCs A251T (4.2.2) carrying p.A251T variant in *HNF1A*, were compared to iPSCs 1159, derived from a healthy donor, and characterised at Columbia University's Stem Cell Core Facility, New York City.

First, iPSCs/hESCs were seeded in StemFlex medium (Thermo Fisher) for 2 hours to reach 100% confluence and form a monolayer of cells (1.8 to 2.1 $x10^6$ cells for a well of a 6-well plate), on a Geltrex-coated 6-well plate (Thermo Fisher). The SF medium was replaced by the definitive endoderm basal medium supplemented with components A and B from definitive endoderm kit (Stem cell Technology) in 1:100 ratio and incubated at 37°C, 5% CO_2 incubator for 24 hours. The medium was then replaced to freshly prepared definitive endoderm basal media supplemented with component B from definitive endoderm kit in a 1:100 for 36 hour and replaced with fresh medium for 24 hours. From days 4 to 6 cell medium was replaced by primitive gut tube stage medium containing: RPMI 1640 plus GlutaMAX (Life Technology) 1% (v/v) penicillin-streptomycin (Thermo Fisher), 1% (v/v) B-27 serum-free supplement (50×) (Life Technology), 50 ng/mL FGF7 (R&D Systems). From days 6 through 8 media was replaced every 48 hours with posterior foregut stage media: DMEM plus GlutaMAX (Thermo Fisher), 1% (v/v) penicillin-streptomycin, 1% (v/v) B-27 serum-free supplement (50×), 0.25 µM KAAD-cyclopamine (Sigma), 2 µM retinoic acid (Reprocell), 0.25 µM LDN193189 (Sigma). From days 8 to 12 medium was replaced every 48 hours with pancreatic progenitor stage medium: DMEM plus GlutaMAX 1% (v/v), penicillin-streptomycin 1% (v/v), B-27 serum-free supplement (50×), 50 ng/mL EGF (R&D Systems), 25 ng/mL FGF7 (Thermo Fisher). At day 12, 3-D cell clusters were prepared by detaching the monolayer cells using TrypLE and resuspended in cluster medium: DMEM plus GlutaMAX, 1% (v/v) penicillin-streptomycin, 1% (v/v) B-27 serum-free supplement (50×), 1 µM RepSox (Sigma), 10 µg/mL heparin (Sigma), 25 ng/mL FGF7, 10 µM Y-27632, Ri. Cells were transferred to aggreWell 400 Microwell culture plates (STEMCELL Technologies) and incubated for 24 hours. On day 13, the clusters of cells were transferred to low-adhesion 6-well plates (Thermo Fisher) and

the medium was changed to pancreatic endocrine progenitor stage medium: RPMI plus GlutaMAX, 1% (v/v) penicillin-streptomycin, 1% (v/v) B-27 serum-free supplement (50×), 1 μM thyroid hormone (T3) (Sigma), 10 μM RepSox (Sigma), 10 μM zinc sulfate (Sigma), 10 μg/mL heparin (Sigma), 100 nM gamma-secretase inhibitor (DBZ) (Sigma), and 10 μM Y-27632, Ri. The medium was changed daily until day 15, by collecting the clusters using P1000 filter tips and pipets, allowing the clusters to settle to the bottom of a 50-mL conical tube under gravity for 5 minutes, and aspirating as much supernatant as possible without disturbing the cell clusters. On day 15, the medium was replaced with pancreatic endocrine progenitor stage medium supplemented with 1 μM aphidicolin, and this medium was replaced with fresh pancreatic endocrine progenitor stage medium supplemented with 1 μM aphidicolin until day 20. From days 20 to day 27, the medium was replaced with pancreatic β-cell stage medium: RPMI plus GlutaMAX, 1% (v/v) penicillin-streptomycin, 1% (v/v) B-27 serum-free supplement (50), 10% (v/v) FBS, 10 μM Ri. Resulting β-cell-like cells were ready for analysis on day 25.

4.2.8 Statistical Analysis

A Shapiro test was used to assess the normality of the data (Shapiro and Wilk, 1965). Mann-Whitney U test (Mann and Whitney, 1947) was employed for two-group comparisons. Statistical analysis was performed using GraphPad Prism 9 software. Statistical significance was considered when p-value were equal to or less than 0.05 (*), 0.01 (**), 0.001 (***), or 0.0001 (****).

4.3 Representative Results Method for Generating B-like Cells

Initial *in vitro* assays of the *HNF1A* variants, p.A251T and p.S19L, revealed functional alterations in the HNF1A protein using immortalised cell lines. However, these lines did not fully replicate β-cell function, and the mechanism by which the p.A251T variant exerts negative impact on transactivation remains unclear. Thus, it was necessary to conduct functional assessment on human insulin-secreting cells to assess the VUS variant impact on β-cell function. The methodology presented below aims to develop a cellular model for studying the functional consequences of *HNF1A* variants in a physiologically relevant context.

4.3.1 Genome Editing in Human Pluripotent Stem Cells

4.3.1.1 CRISPR-Mediated Homologous Recombination: *HNF1A* p.A251T

Several genomes editing method, including base editing with cytosine and adenine base editors or CRISPR technology HR, were investigated to generate hPSCs carrying variants of interest *HNF1A* p.A251T and p.S19L.

The selection of these alternative methodologies was based on the variants´ specific sequence and surrounding context. Due to the requirement for a C-T change in cytosine deaminase-based base editing or an A-T change in adenine deaminase-based base editing, the *HNF1A* p.A251T variant did not meet the criteria for base editing. The chosen technique for the *HNF1A* p.A251T variant was CRISPR/HR.

CRISPR/HR allows for genome editing of up to 20-nucleotide DNA sequence that meets two key conditions: the sequence must be distinct from the rest of the genome and located near a Protospacer Adjacent Motif (PAM) which allow the binding and subsequent cleavage of Cas9 endonuclease. Both the *HNF1A* p.S19L and *HNF1A* p.A251T variants met these requirements, making them suitable for CRISPR/HR editing.

CRISPR/HR genome editing was utilised to introduce single-nucleotide changes targeting the *HNF1A* p.A251T genetic variant, in the MEL-1 ($INS^{GFP/WT}$) hESC line. The hESCs were nucleofected with Cas9-GFP, gBlock, and a repair template. From

the nucleofected cells, a total of 1427 GFP-positive cells were selected for further culture and expansion (Population 3, as shown in the Figure 4.6). However, most of the cells did not survive the sorting process. From the surviving cells, 192 clones were expanded, and seeded onto two separate 96-well plates. After 10 days of expansion, one well from each of the 192 GFP-positive clones sequenced using Sanger sequencing to examine the detect the presence of the *HNF1A* p.A251T variant. The sequencing outcomes did not confirm the presence of the *HNF1A* p.A251T variant in any of the hESCs MEL-1 selected clones. This experiment was repeated three times, and each time the sequencing results consistently failed to identify hESCs carrying the *HNF1A* p.A251T variant. Due to the lack of success with CRISPR/HR genome editing, alternative methods for generating hPSCs carrying the *HNF1A* p.A251T variant were explored. These alternative approaches will be described and presented in detail in the subsequent sections of this chapter.

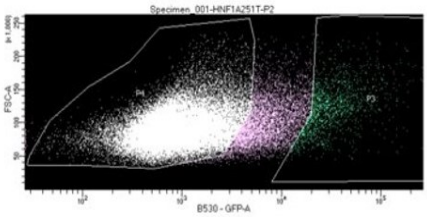

Tube: HNF1A251T

Population	#Events	%Parent	%Total
All Events	100,281	####	100.0
P1	71,888	71.7	71.7
P2	63,605	88.5	63.4
P3	1,427	2.2	1.4
P4	55,256	86.9	55.1

Figure 4.6: **Representative Cell Sorting Plot for Segregated hESCs Expressing Cas9-GFP.**
P1 (Population 1) consisted of non-fluorescent hPSCs, which served as a negative control and were selected based on sorting of control, not transfected, hESCs MEL-1 WT cells. P2 comprised cells that exhibited fluorescence upon excitation at 488 nm, although it is possible that this fluorescence was due to autofluorescence rather than the desired GFP expression. P3 represented the MEL-1 hESC population expressing the GFP reporter for Cas9-GFP. In this population, a total of 1427 “events” corresponding to 1427 GFP-positive cells were sorted.

4.3.1.2 Base Editing Strategy for *HNF1A* p.S19L and Construct Design

Base editors' function by specifically deaminating cytosine or adenine within a narrow activity window of approximately 5 nucleotides surrounding the target site. Therefore, the desired genetic change must be driven by the conversion of a C-G base pair to a T-A base pair (cytosine base editors, Figure 1.5) or by the conversion of an A-T base pair to a G-C base pair (adenine base editors). The second requirement for base editors is that nucleotide changes occurring within their activity window should not induce unintended mutations. In other words, any additional changes near the target site should result in silent mutations, meaning they do not alter the amino acid sequence of the resulting protein. Within the *HNF1A* gene, the p.S19L variant, among the novel variants, has the potential for genetic editing using base editor technology. Specifically, the c.56C>T mutation induced the p. Ser19Leu amino acid change.

The AncBE4max–P2A–GFP base editor was chosen due to its demonstrated high efficiency, making it the most suitable base editor at the commencement of this investigation. This fourth-generation base editor incorporates a DNA glycosylase inhibitor to prevent the repair of uracil, thereby enhancing base editing efficiency. Additionally, it includes an ancestral sequence reconstruction of the deaminase component, resulting in improved protein expression. The presence of a GFP reporter enables the selection of cells expressing the vector based on GFP positivity.

To prevent unintended insertions or deletions at the target site, the activity window DNA sequence of the base editor was analysed and showed that no C-to-T conversions occurring within this targeted sequence surrounding the c.56C>T mutation would lead to the silent mutations (see Figure 4.7).

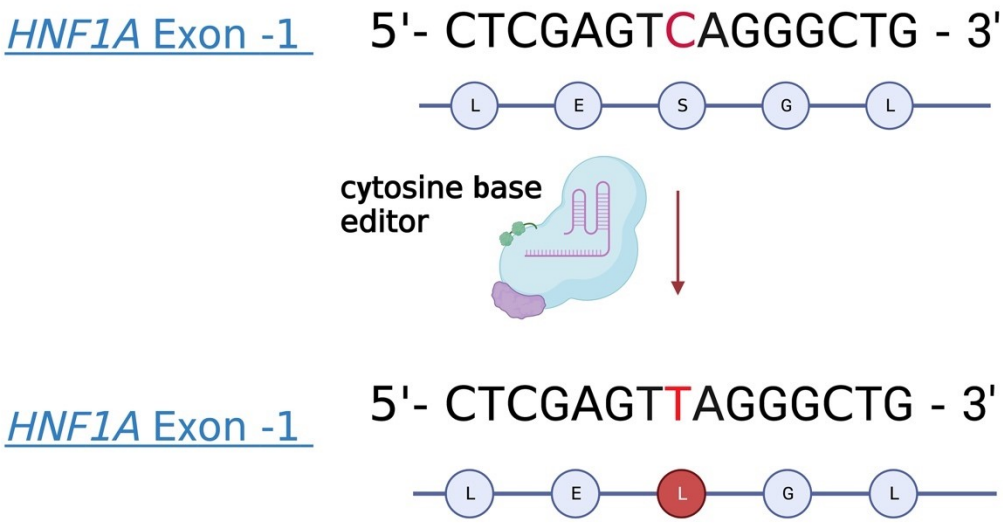

Figure 4.7: **Cytosine Base Editing of the *HNF1A* p.S19L Variant.**
Schematic representation of the sequence of the WT *HNF1A* (on top), in which the amino acid serine is located at position 19 (nucleotide in red). The missense variant c.56C>T, identified as a novel *HNF1A* variant can be generated using the cytosine base editor (AncBE4max–P2A–GFP). The sequence also illustrates the surrounding nucleotides that could be targeted by the base editor. All potential changes in cytosine within this region result in silent mutations, meaning that the alteration would not affect the amino acid sequence and produce the same amino acid (bottom) as in the wild-type sequence.

A gRNA sequence was designed and validated using established guidelines (Schindele, Wolter and Puchta, 2020) to produce accurate base editing at the target locus, c.56C>T, in the *HNF1A* gene. The PAM sequence located 20 nucleotides 5' downstream of the target sequence was considered when selecting the gRNA sequence to assure its specificity to the target region. The BE-analyzer (Hwang and Bae, 2021) was used to evaluate the predicted efficiency of the designed gRNA sequence, confirming its suitability for base editing experiments.

To enable efficient transfection of the gRNA and base editor components, a DNA plasmid construct was generated using a cloning vector service (Vector Builder). The construct was designed to contain essential elements for successful editing, including an ampicillin resistance gene for bacterial amplification, a mCherry: P2A: Puro reporter sequence for selection purposes so the cells expressing the construct would have puromycin resistance and mCherry fluorescence.

The genome editing strategy consisted of a co-transfection approach that involved the use of a base editor vector expressing a GFP reporter, and a guide RNA construct expressing an mCherry reporter. By selectively sorting cells that were positive for both mCherry and GFP, it was possible to identify and isolate cells that were successfully transfected with both the base editor and guide RNA constructs. This approach minimised the need for extensive clonal expansion of hPSCs.

4.3.1.3 Control Base Editing Targeting the *HNF1A* p.S19L Variant in HEK293 Cells

The HEK293 cell line was transfected with a base editing construct to confirm the potential of both constructs to induce the p.A251T variant in *HNF1A*. The objective was then to perform the same method for the MEL1 hESCs only if the sequencing results from HEK293 cell line confirm the presence of the single nucleotide change (*HNF1A* c.56C>T, Figure 4.7). Following puromycin selection, the entire transfected cell population was sequenced to evaluate the efficacy of the constructs in inducing the desired base editing. Figure 4.8 illustrates the chromatogram displaying the sequencing results of the whole-cell transfection. Green corresponds to adenine, red to thymine, black to guanine, and blue to cytosine in the chromatogram's peaks. At the target site, two coloured peaks representing cytosine and thymine are observed (indicated by an arrow in the figure). This indicates the occurrence of a cytosine-to-thymine single nucleotide change, confirming the successful base editing. These results demonstrate the potential of both constructs to induce cytosine-to-thymine alterations in hPSCs.

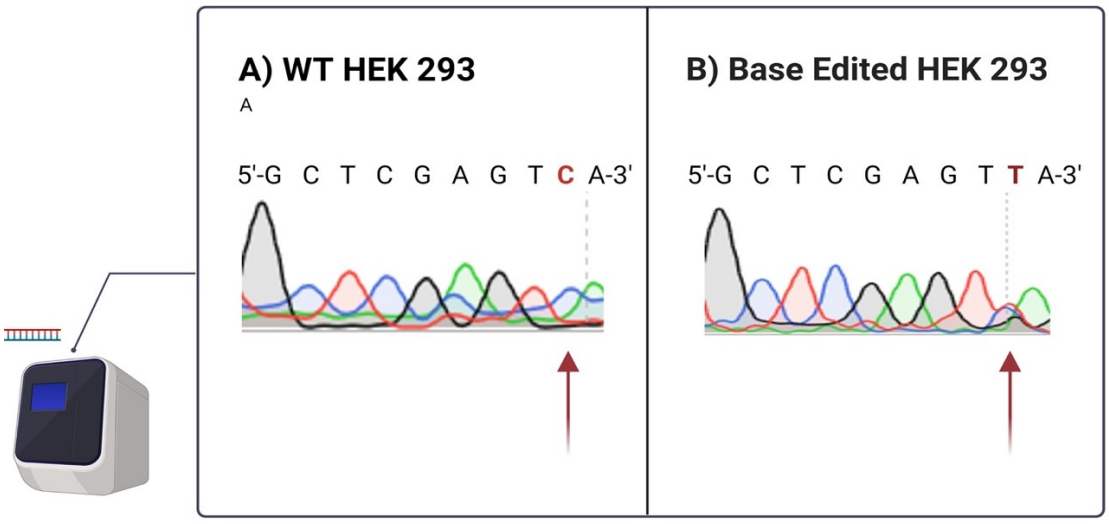

Figure 4.8: **Sanger Sequencing Results Comparing Base-Edited HEK 293 Cells to Wild-Type HEK 293 Cells.**

The chromatogram in the figure displays four colours, with green representing adenine, red representing thymine, black representing guanine, and blue representing cytosine. At the specific site of interest, highlighted by a red arrow, the Sanger sequencing of base edited HEK 293 cells reveals the presence of two-coloured peaks corresponding to cytosine and thymine. This observation indicates a cytosine-to-thymine single nucleotide change within the population of sequenced cells, confirming the successful introduction of the desired genetic alteration.

4.3.1.4 Base Editing in the MEL-1 hESC line

Base editing was performed on the MEL-1 hESC line, as the introduction of the *HNF1A* p.S19L variant would lead to the generation of β-cell-like cells expressing the INS^{GFP} reporter. Electroporation of cells was performed using two constructs: the sgRNA plasmid construct (pRP-mCherry-P2A-Puro-U6-HNF1A-S19L) and the base editor construct (AncBE4max–P2A–GFP). Cells exhibiting both mCherry and GFP signals were cell sorted for further sequencing.

Despite conducting over ten experiments, only a limited number of cells exhibited double-positive signals, representing less than 1,000 events for each cell sorting, and fewer than 10 surviving clones for further sequencing. However, no confirmed *HNF1A* c.56C>T variant was found in clones selected transiently expressing both mCherry and GFP signals, by sequencing analysis of exon 1 of the *HNF1A* target gene.

To address this issue, the protocol was optimised by increasing the initial number of transfected cells to 3 million and modifying the electroporation parameters, including the number of pulses, length of pulses and voltage, in addition to DNA concentration for each construct. However, even with optimisation, only a small number of cells displayed co-positivity, and subsequent sequencing results still did not indicate the presence of the c.56C>T variant. Consequently, an alternative approach utilising iPSCs was explored, as detailed in the following section.

4.3.2 Generation of Induced Pluripotent Stem Cells

4.3.2.1 Skin Punch Biopsy and Primary Cell Culture of Fibroblasts

To generate hPSCs carrying *HNF1A* p.S19L and p.A251T variants, somatic cells were reprogrammed into iPSCs following this method presented in Figure 4.1. Skin samples were collected from two probands with the *HNF1A* p.S19L and p.A251T variants. The skin biopsy contained mostly two cell types, including fibroblasts and keratinocytes. Fibroblasts are preferentially selected among these cell types to be reprogrammed into iPSCs (Takahashi *et al.*, 2007) (see Introduction, Figure 1.4).

Within 3-5 days after skin biopsy, keratinocytes began to proliferate (shown in Figure 4.9). The medium and supplements were adjusted specifically for the growth of fibroblasts (presented in Method 4.2.2), allowing for the selective culture of these cells. Under fibroblast medium conditions, keratinocytes were unable to proliferate as they required different medium with specific growth factors supplementation (e.g. epidermal growth factor) compared to fibroblasts (Rikken, Niehues and van den Bogaard, 2020). Consequently, the proliferation of keratinocytes stopped, leading to cellular senescence over the subsequent weeks. The implementation of the culture-selective fibroblasts medium facilitated the refinement of fibroblast cultures, effectively eliminating the presence of other cell types.

Figure 4.9 illustrates the outgrowth of keratinocytes and fibroblasts from the skin biopsy and their subsequent expansion during the weeks of culture for the skin biopsy obtained from the proband carrying the *HNF1A* p.A251T variant.

Approximately two weeks after culturing the skin biopsy from the proband carrying the *HNF1A* p.A251T variant, fibroblasts outgrew from the skin cut biopsies characterised by their elongate spindle-shape with an oval nucleus (Dick, Miao and Limaiem, 2023) (Figure 4.9). After an additional 10 days, the fibroblasts reached 70% confluence and were subsequently transferred to two T75 flasks for further expansion. A minimum of 5 million fibroblasts were amplified as per the experimental requirements (Method 4.2.2) to initiate the pluripotency induction experiment.

The skin biopsy from the proband with the *HNF1A* p.S19L variant was less successful, as the isolated fibroblasts could not be reprogrammed into iPSCs. The fibroblast cultures did not achieve a cell count of 5 million required for initiating the induction of pluripotency. Moreover, the number of fibroblasts decreased after two passages of culture, indicating a reduction in cell proliferation, and limiting their suitability for further experiments.

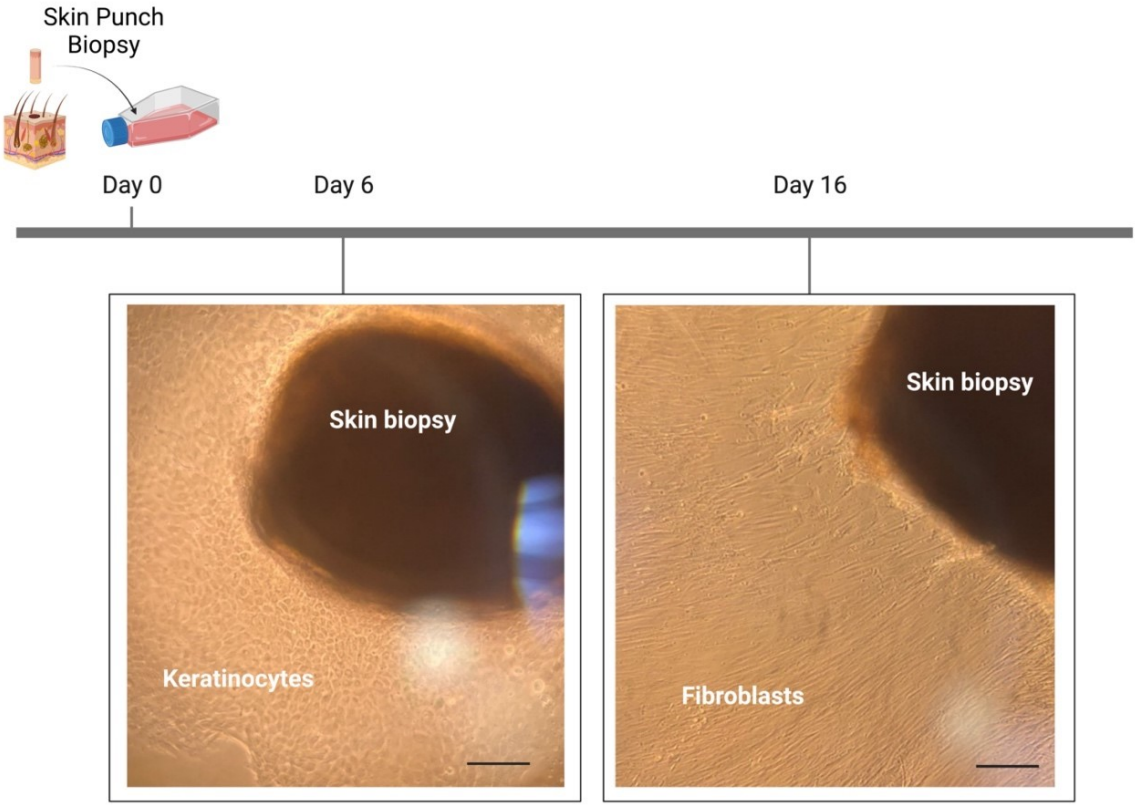

Figure 4.9 : **Primary Culture of Fibroblasts Derived from the Proband Carrying the *HNF1A* p.A251T Variant.**

The figure shows the progressive proliferation of keratinocytes and fibroblasts from a skin biopsy obtained from a proband carrying the *HNF1A* p.A251T variant. On day 6 post biopsy (left panel), keratinocytes exhibited robust outgrowth surrounding the explant, forming multi-layered of polygonal cell characteristic of keratinocytes. On day 16 (right panel), fibroblast cells outgrew from the skin biopsy, displaying the typical elongated morphology and forming bundled structures as they reached confluence. The scale bars in the figure correspond to 200 µm.

4.3.2.2 Reprograming Somatic Cells into iPSCs Harboring the *HNF1A* p.A251T Variant

To generate iPSCs from the HNF1A-MODY proband carrying the p.A251T variant, fibroblasts expanded from proband skin biopsies were transfected with the Oct4, Sox2, Nanog, Lin28, L-Myc, and Klf4 factors (following the Method 4.2.2). Approximately 15-18 days after reprogramming, eight colonies displaying characteristic human stem cell morphology were observed in the culture (white arrow, Figure 4.10). Based on their distinct morphological features, spherical bright refractile border, these stem cell-like colonies were manually picked and isolated from the main culture plate for further characterisation.

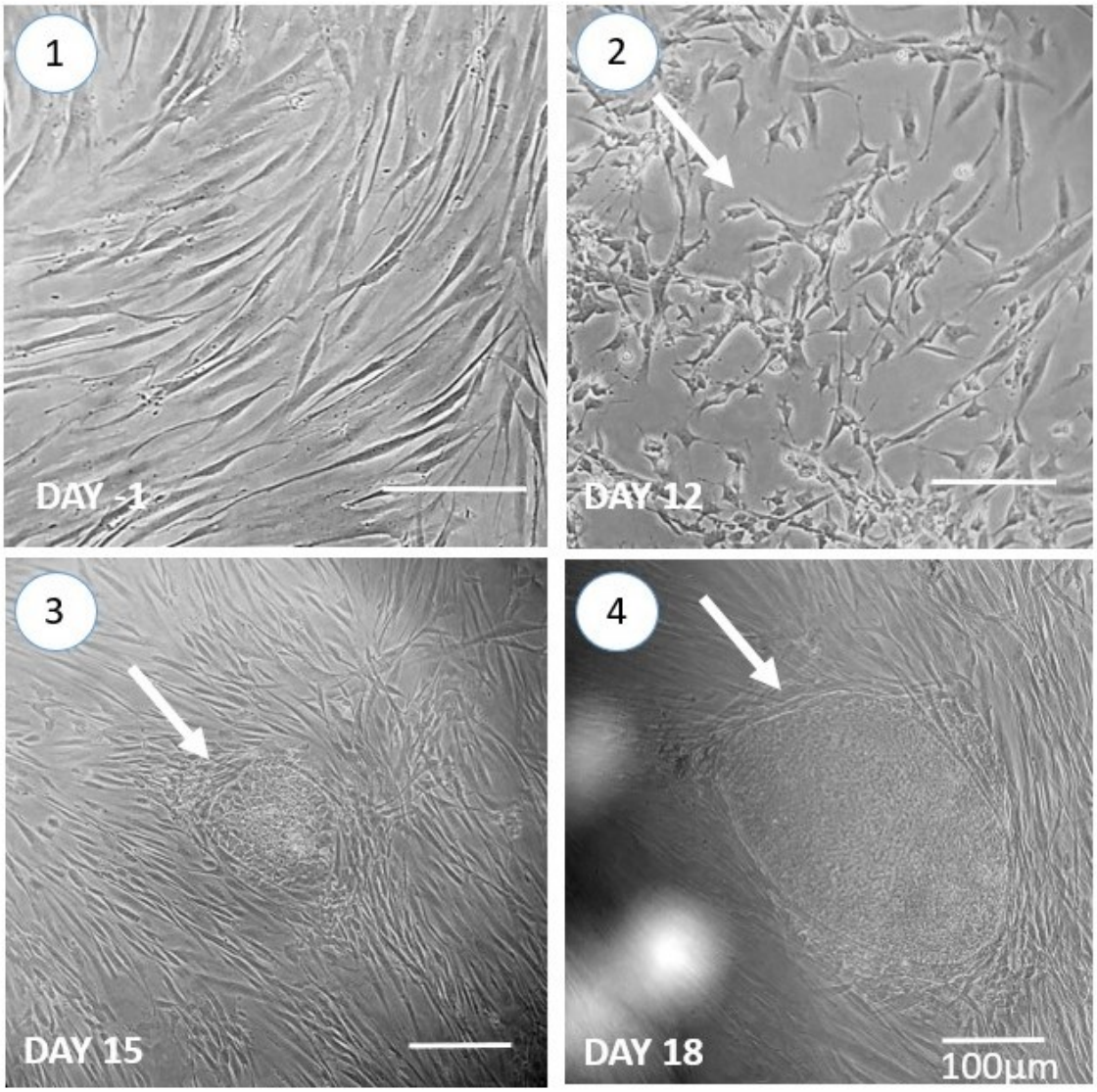

Figure 4.10: **Morphological Changes During the Reprogramming of Induced Pluripotent Stem Cells.**

The figure presents phase contrast images depicting the cell morphology changes observed throughout the reprogramming process of human iPSCs. (1) Day 1: Fibroblasts, typically elongated, spindle-shaped cell, the day prior to transfection of the reprogramming OKSM vectors. (2) Day 12 post-transfection: Morphological changes can be observed in the cells, indicating the ongoing reprogramming process. (3) Day 15: iPSC colonies (white arrow) begin to emerge, although they are small (<100 µm). (4) Day 18: The colonies exhibit a typical hPSCs morphology. The size of the colonies typically ranges between 300-500 µm.

4.3.2.3 Characterisation of iPSCs A251T

After selecting clones morphologically resembling stem cell colonies with spherical bright refractile borders, characterisation of the iPSCs for stability, possible chromosomal abnormalities, and pluripotency was performed.

Early passages of iPSC-like clones often display chromosomal abnormalities and instability, which can lead to their inability to survive beyond a few passages (Warren *et al.*, 2010; DuBose *et al.*, 2022). Additionally, spontaneous differentiation can occur during the first weeks of expansion. Short first experiments involving freezing and thawing were conducted to identify viable clones that could withstand freezing without losing viability. Clones were passaged for at least 10 passages, and only viable clones were selected. Three iPSC clones were selected for further characterisation.

To evaluate pluripotency, alkaline phosphatase (AP) staining was performed. Elevated levels of AP are indicative of pluripotent stem cells (Sharma, Pal and Prasad, 2014). A staining assay for AP activity was used to select iPSC clones with high AP activity after passage 10. In this assay, AP acts on a substrate to produce a red colour when the AP activity is high. Clones in which most of the colony exhibited a strong red stain (Figure 4.11), indicating positive AP activity, were subsequently expanded, and kept for further characterisation. Among the selected iPSC clones, three clones were chosen for subsequent characterisation, specifically evaluating the relative expression of the pluripotent marker OCT-4.

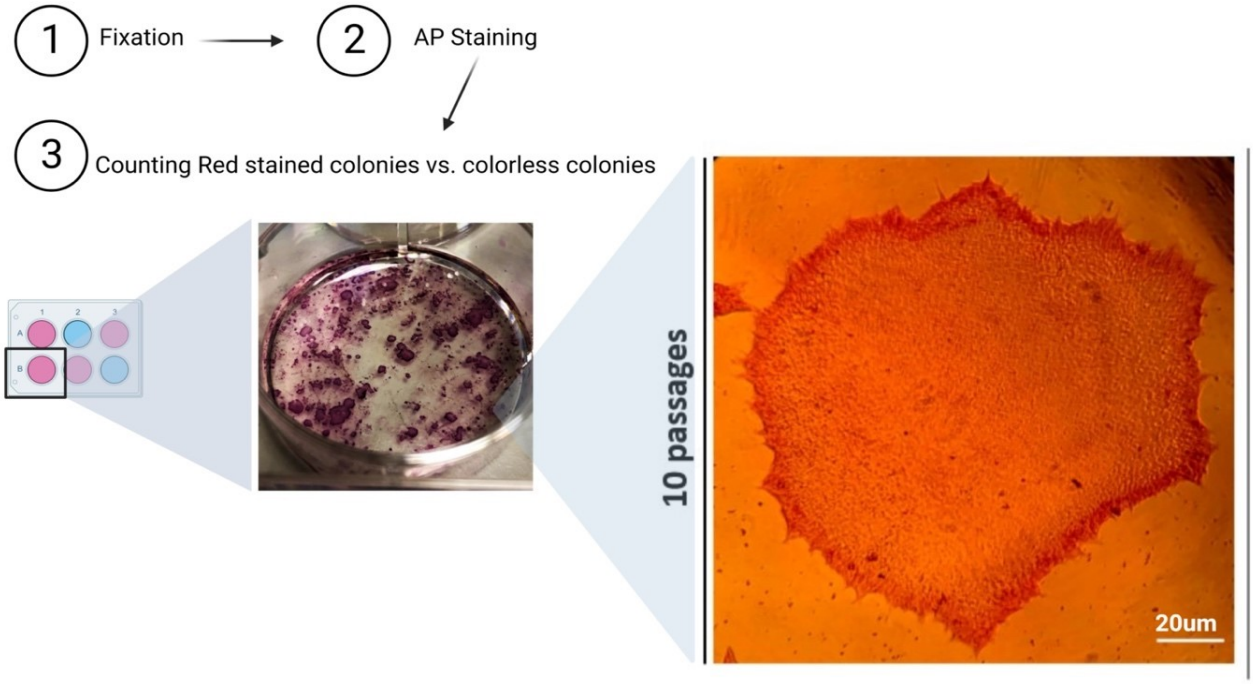

Figure 4.11: **Alkaline Phosphatase Activity of Induced Pluripotent Stem Cell-Like Colonies.**
The figure shows an iPSC-like clone derived from a proband carrying the *HNF1A* p.A251T variant at passage 10. All colonies show a predominantly red staining indicating high AP activity. The image on the right provides a close-up view of one colony, demonstrating its red coloration, which serves as an example of the colonies selected. This specific clone was chosen for further characterisation.

4.3.2.4 Karyotyping Analysis of iPSC-Like Clones Derived from a Proband with the *HNF1A* p.A251T Variant

The karyotyping analysis for this study was conducted by the KaryoStat Service (provided by Thermo Fisher). The results presented in Panel B of Figure 4.12 display the karyotyping outcomes, which were obtained from the analysis performed by the KaryoStat Service.

Two iPSCs-like clones derived from a proband carrying *HNF1A* p.A251T variant were analysed via karyotyping to confirm the stability of its chromosomal composition and the detection of any chromosomal abnormalities, such as structural variations or numerical aberrations. The genome of iPSC-like clones was extracted, and Karyotyping Service (Karyostat, Thermo fisher) perform the karyotyping analysis.

Only one clone had a normal karyotype, with a complete set of 46 chromosomes, including two X chromosomes as the donor is a female (Figure 4.12). No chromosomal abnormalities, such as deletions, duplications, or translocations, were detected (Figure 4.12). The karyotyping analysis conducted on the iPSC clone has provided substantial evidence supporting the preservation of chromosomal integrity and stability. These findings validate the suitability of the iPSC clone for subsequent experiments and investigations.

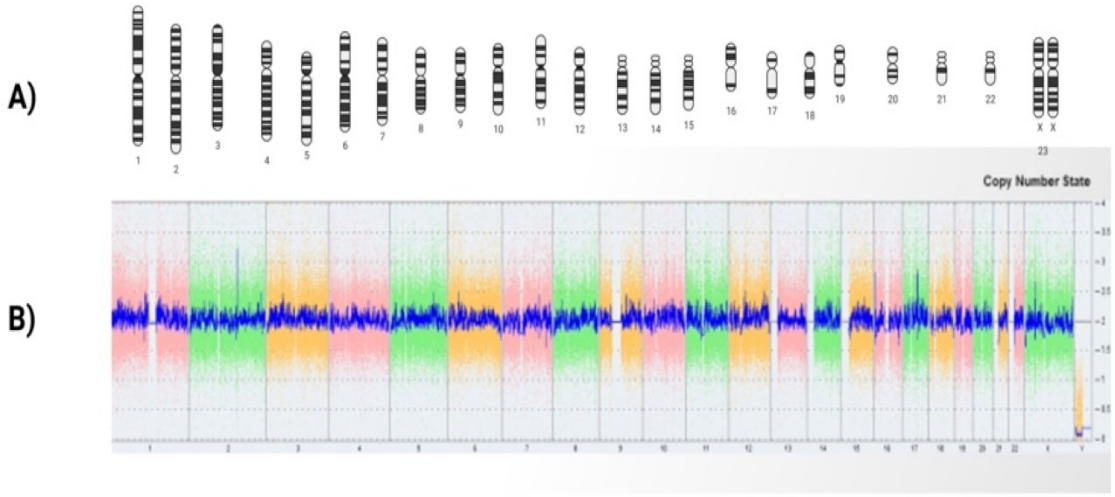

Figure 4.12: **Karyotyping of iPSCs Carrying the *HNF1A* p.A251T Variant**

Panel A: Schematic representation of the iPSCs chromosome results. Panel B: Whole genome view displaying somatic and sex chromosomes with high-level copy number resolution. The smooth signal plot (right y-axis) represents smoothed log2 ratios of probe signal intensities obtained from microarray analysis. A log2 ratio value of 2 corresponds to a normal copy number state (CN = 2). The pink, green, and yellow colours indicate the raw signal intensities of individual chromosome probes, while the blue signal represents the normalised probe signal used to identify copy number aberrations. Notably, no copy number aberrations were detected in this analysis, indicating genomic stability in the iPSCs clone.

4.3.2.5 Assessment of Pluripotency Marker OCT-4 Expression in A251T iPSCs

The third phase of characterising and validating iPSC clones carrying the *HNF1A* p.A251T variant (referred to as iPSCs A251T) involved examining the relative expression of pluripotent markers, with a focus on OCT-4. Immunostaining of OCT-4 was performed on A251T iPSCs and compared to the control iPSC line 1159, derived from anonymous healthy donor, generated, and characterised at the Columbia Stem Cell Initiative, Columbia University in NYC. Additionally, fibroblasts derived from a skin biopsy of a patient carrying the p.A251T *HNF1A* variant were used as a negative control, as fibroblasts do not express pluripotent markers. The iPSCs A251T exhibited a mean OCT-4 expression of 98.75% ± 0.6% (n=15), while the 1159 control iPSCs showed 100% positivity for OCT-4 in all cells. In comparison, the A251T fibroblasts did not express the OCT-4 pluripotent marker. The findings demonstrate that A251T iPSCs express the pluripotent marker OCT-4 in a high proportion of cells within the colony, further validating their pluripotent nature in comparison to the control iPSCs and the A251T fibroblasts.

These characterisations, including morphological evaluation, expansion over 10 passages, cycles of freezing and thawing, AP activity assay, and pluripotency marker immunostaining results, collectively validate the identity of A251T iPSCs as reprogrammed cells.

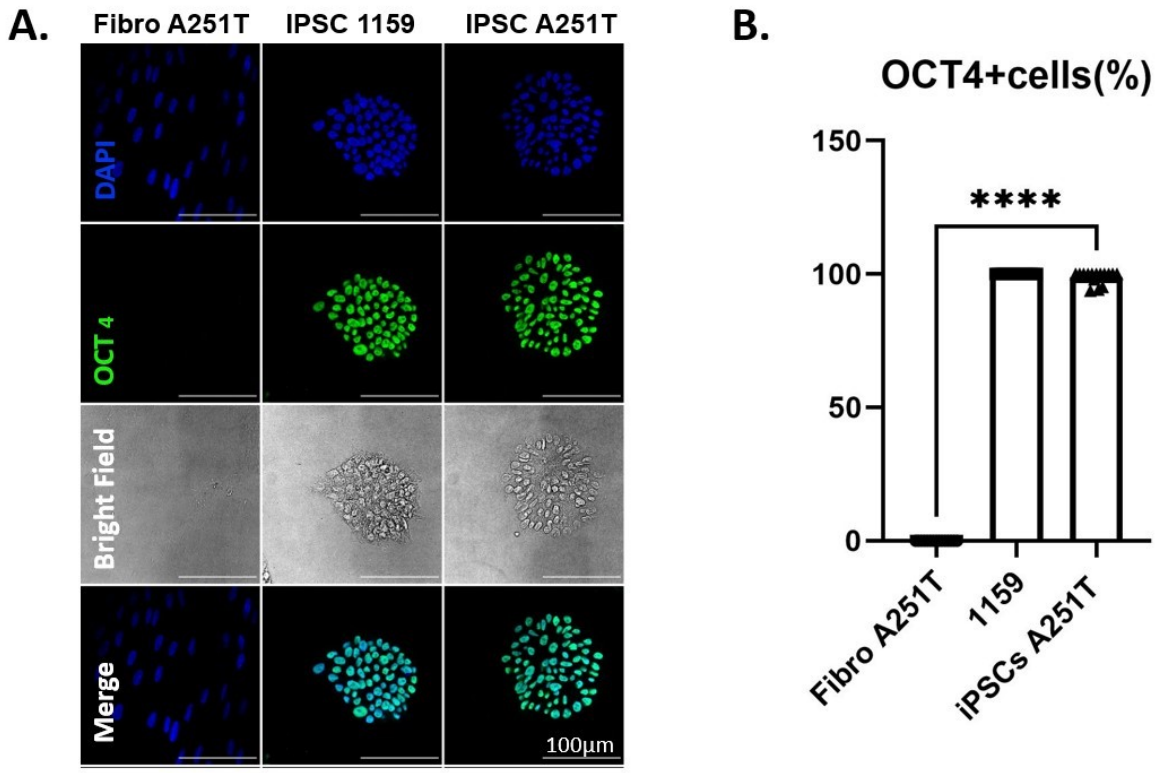

Figure 4.13: **Immunofluorescence Staining of OCT-4 in iPSC Clones and Fibroblasts.**
Panel A: Immunofluorescence images of OCT-4 staining in fibroblast A251T (fibro A251T), iPSC 1159 (control), and iPSC A251T carrying the *HNF1A* p.A251T variant. Nuclei are stained with DAPI (blue), OCT-4 is stained with Alexa 488 (green). Brightfield images depict the morphology of iPSC colonies and fibroblast cells. Merge images show localisation of DAPI and OCT-4 in iPSCs 1159 and iPSCs A251T, indicating nuclear expression of OCT-4 and the pluripotent state of iPSCs A251T. Images were acquired using the STELLARIS 8 Confocal Microscope from Leica, (x40, oil immersion). Scale bar: 100 µm. Panel B: Quantification of OCT-4-positive cells in iPSC clones using a custom-designed macro developed by Dr. Stephen Rothery at the Facility for Imaging, Imperial College. Relative quantification represents the percentage of cells positive for OCT-4, Mann–Whitney U test; p-value **** $P \leq 0.0001$, (n=15).

4.3.3 Directed Differentiation of Pluripotent Stem Cells into β-Cells

Considering the unsuccessful attempt to generate genome-edited hPSC lines containing the targeted base-edited *HNF1A* variants, as well as their corresponding isogenic controls, the strategy was adapted to utilise iPSCs (1159) procured from a healthy donor. These iPSCs were utilised as a control for iPSC line differentiation and subsequent functional assessment.

The MEL-1 hESC line was used to perform optimisation experiments for β-cell differentiations, to establish the procedure for functional analysis of iPSCs carrying the *HNF1A* variant. MEL-1, along with the control iPSCs (1159) and A251T iPSCs, underwent a directed differentiation into β-cell-like cells using the protocol of our collaborator Dr. Egli at the Naomi Berrie Diabetes Center's Stem Cell Initiative (CSCI) (Sui, Leibel and Egli, 2018; Sui *et al.*, 2021). The β-cell differentiations were conducted at the ICTEM Cell Biology and Functional Genomics Laboratory at Imperial College London. As the β-cell differentiation process had not been previously performed in our laboratory, I undertook the task of optimising and establishing the protocol within our laboratory. This was done to maintain consistency and minimise any variations in the experimental procedures initially performed at the CSCI.

The process of β-cell differentiation comprised a sequential progression through six distinct stages, involving the induction of definitive endoderm from hPSCs, followed by the formation of the primitive gut tube, specification of the posterior foregut fate, generation of pancreatic progenitor cells, development of pancreatic endocrine progenitor cells, and ultimately culminating in the generation of pancreatic β-cell-like cells (see details in the Introduction section 1.5) (Sui, Leibel and Egli, 2018). Each stage of directed differentiation of hPSCs towards β-cell-like cells involves the regulation of specific cell signalling pathways at specific time points. Figure 4.14 presents the directed differentiation of hPSCs towards β-cell-like cells for the hPSCs cell lines of this study. The protocol used was a combination of two protocols described by Sui, Egli, et al. (2018 and 2021), with the specific modification of adding aphidicolin treatment at the last stage (6) from day 25-28 to increase the yield of β-cell-like cells (202, 326).

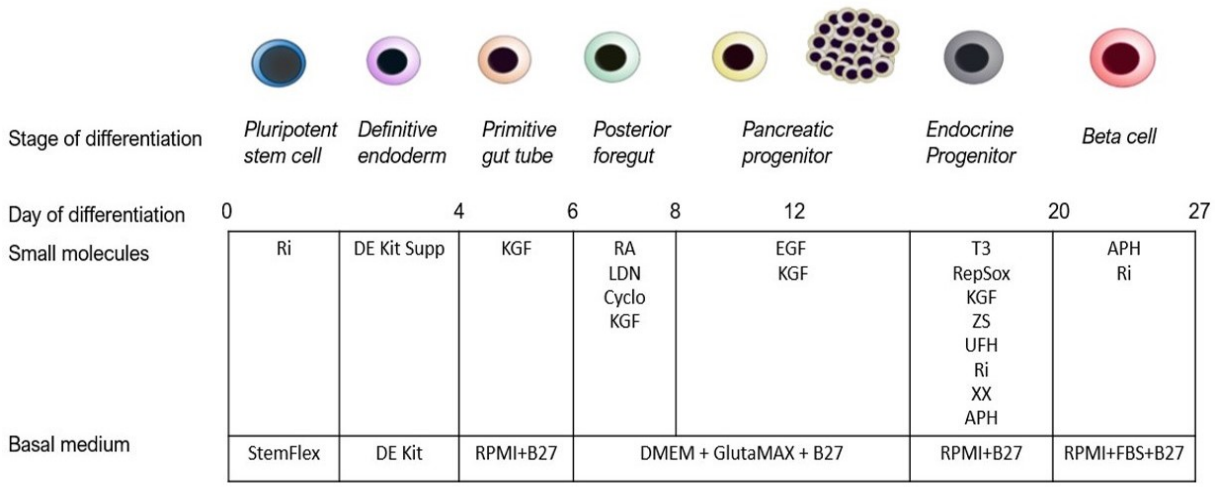

Figure 4.14: **Directed Differentiation of hPSCs towards Pancreatic β-Cells.**
The differentiation process encompasses six stages: definitive endoderm induction, primitive gut tube formation, posterior foregut fate specification, pancreatic progenitor generation, pancreatic endocrine progenitor formation, and ultimately, pancreatic β-cell differentiation. Each stage involves the regulation of specific cell signalling pathways at specific time points. The abbreviations used in the figure include: B27 - B-27 Supplement; Ri - rho-associated protein kinase inhibitor or ROCK inhibitor; T3 - thyroid hormone; KGF - human KGF/FGF-7 protein; RepSox - Activin/Nodal/TGFβ pathway inhibitor that inhibits ALK5; RA - Retinoic acid; ZS - zinc sulfate; UFH - unfractionated heparin; XX - gamma-Secretase Inhibitor XX; APH - aphidicolin; EGF - epidermal growth factor; LDN - BMP Inhibitor III, LDN-212854; Cyclo - Cyclopamine-KAAD.

The directed differentiation process involved a transition from a 2-dimensional 2D cell culture to a 3D culture using specific microwell plates. The formation of 3D clusters is illustrated in Figure 4.15. The figure also shows the morphology of cells at various stages of differentiation, starting from hPSCs culture in a monolayer on the first day of differentiation. By day 12, clusters have formed in the microwells of a six-well plate after cell dissociation at the pancreatic progenitor stage. On day 13, the clusters are transferred to a low-attachment six-well plate and maintained in suspension culture until days 25-28 of differentiation, during which functional assays are performed to assess the maturation and functionality of the pancreatic β-cells.

Stem cell-derived β-cell-like cells obtained from various hPSC lines (hESC MEL1, 1159 iPSC, and A251T iPSC) exhibited morphological similarities to human islets (shown in Figure 4.15). At day 25 of differentiation, β-cell clusters derived from iPSC lines generated from proband A251T appeared smaller in size, upon visual examination, compared to control β-cell clusters derived from MEL-1 hESCs. These morphological differences may be attributed to the inherent characteristics of iPSC lines, as previous studies have reported that iPSCs tend to exhibit less efficient differentiation compared to hESCs (Toivonen, Ojala, *et al.*, 2013; Balboa, Saarimäki-Vire and Otonkoski, 2019). Additionally, the β-like cells derived from 1159 iPSCs appeared slightly larger than those derived from A251T. Figure 4.16 illustrates the MEL-1 hESC line, which expresses an INS $^{GFP/w}$ reporter, displaying green fluorescence indicative of GFP+ cells co-producing insulin.

The morphological assessment conducted via phase contrast microscopy during the entire process of directed differentiation plays a pivotal role in quality control. It enables the confirmation of the accurate morphology expected at each developmental stage (as indicated in Figure 4.15). Additionally, the presence of GFP^+ cells that co-produce insulin observed in the MEL-1 hESC line (as shown in Figure 4.16) further validates the successful generation of insulin-producing cells through the directed differentiation protocol.

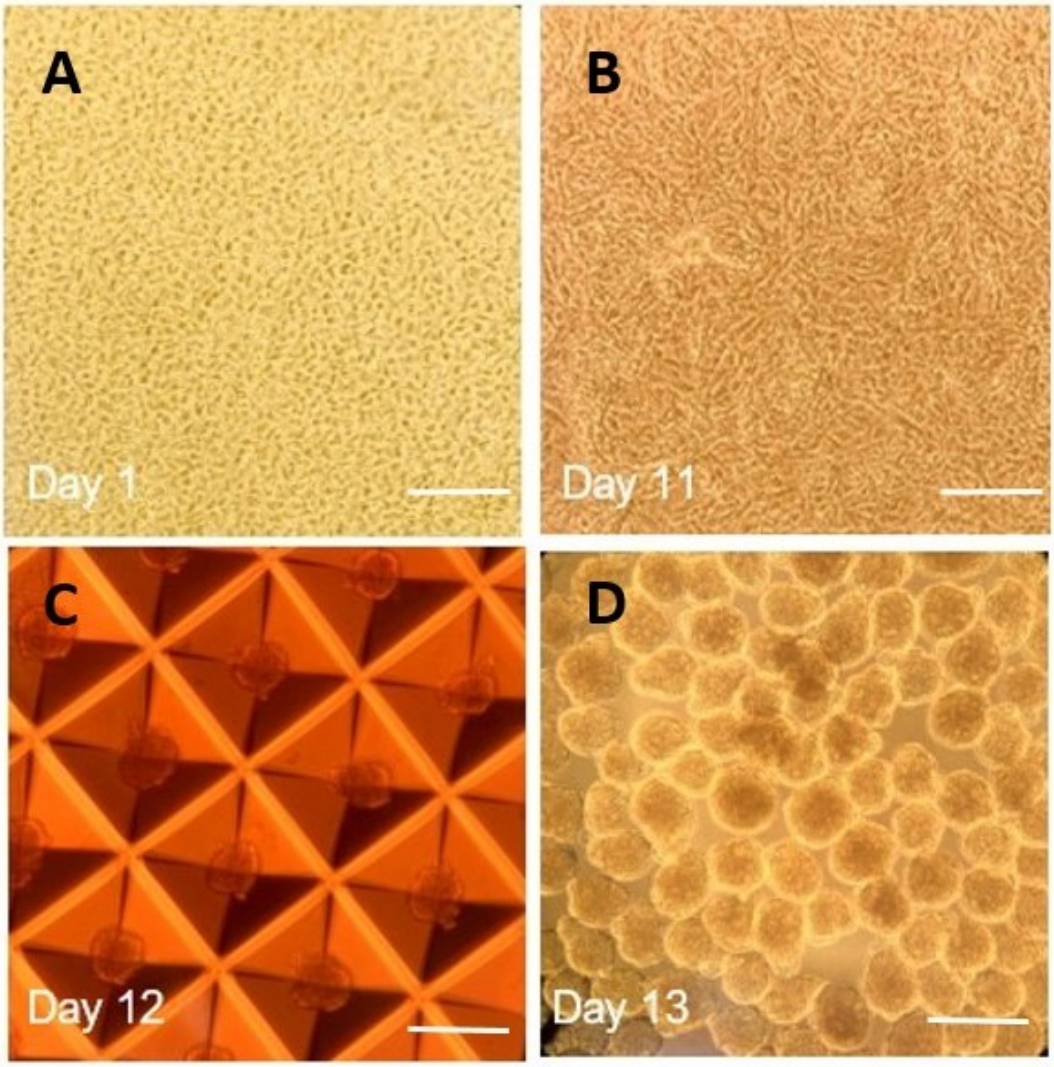

Figure 4.15: **Morphological Progression During hPSC Differentiation into Pancreatic β-Cells**. (A) Image of human pluripotent stem cells on the first day of differentiation, represented by a monolayer of HPSCs. Scale bar: 100 μm. (B) On day 11, cells are at the pancreatic progenitor stage. Scale bar: 100 μm. (C) On day 12, clusters are formed in microwells of a six-well plate following the dissociation of cells at the pancreatic progenitor stage. Scale bar: 200 μm. (D) On day 13, clusters are observed in a low-attachment six-well plate. Scale bar: 200 μm

.

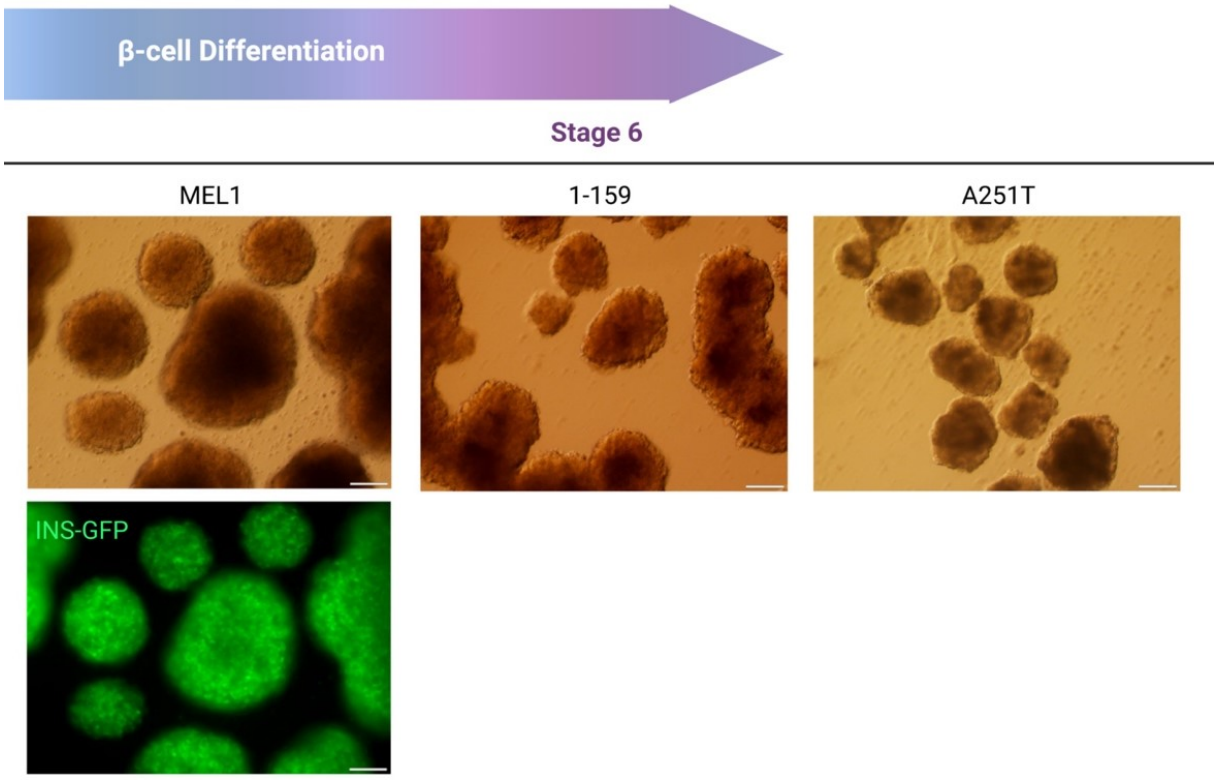

Figure 4.16: **Morphology of Cell Clusters at Stage 6 of Pancreatic Directed Differentiation.** The figure shows selected images captured on day 25 of differentiation, highlighting the morphology of MEL-1 hESCs, control iPSCs 1159, and iPSCs derived from the proband A251T. The cells were cultured in a low-attachment, 6-well plate to facilitate differentiation towards the pancreatic lineage. The scale bar is 100 µm.

4.4 Discussion

HNF1A plays a crucial role in human β-cell function. Previous studies have demonstrated that HNF1A-deficient β-cells exhibit impaired insulin secretion in response to glucose stimulation and defective insulin granule exocytosis (52,53). Therefore, understanding the impact of *HNF1A* variants is essential. However, the use of immortalised cell lines with overexpressing vectors (as in Chapter 3), which do not have the features of human β-cells, prevent a comprehensive understanding of the molecular consequences of the *HNF1A* variants p.S19L and p.A251T.

To overcome the limitations of existing methods, the main objective of this chapter was to present a method for generating human β-cell-models that can be used to investigate the functional impact of the *HNF1A* variants p.S19L and p.A251T on β-cell function. The analysis of the *HNF1A* VUS functional implications in human β-cell-models will be described in detail in Chapter 5.

iPSCs were generated from skin biopsy tissues obtained from probands carrying the *HNF1A* p.A251T variant and subsequently validated for karyotyping, pluripotency marker expression, and high alkaline phosphatase activity. Following this validation, the iPSC lines were subjected to directed differentiation into β-cell-like cells using a protocol described by Sui et al. (Sui, Leibel and Egli, 2018; Sui *et al.*, 2021).

Efforts to generate hESCs for both variants utilising base editing and CRISPR-mediated homologous recombination have proven unsuccessful. Consequently, isogenic control lines with the same genetic background specific to the *HNF1A* variants have not been established in this study.

As an alternative approach, control lines were generated from iPSCs derived from healthy donor (1159). While the generated iPSC control line may not provide the same level of detailed insights into the specific functional consequences of the A251T variant, it serves as a valuable tool for comparative analysis of β-cell function.

This method expands the investigation of the A251T variant beyond the capabilities of *in vitro* functional analysis using immortalised cell lines alone.

Statement of Contribution:

Dr. Dilshad Sachedina, Imperial College London NHS Trust, performed the skin punch biopsies for the probands carrying *HNF1A* p.A251T and p.S19L at the Imperial College Healthcare NHS Trust's Hammersmith facility in London. Her expertise and dedication have been instrumental in advancing the research presented in this chapter. Licence to Attend was obtained to collect the skin biopsies and transport them to the Cell Biology and Functional Genomics laboratory, where all laboratory experiments and cell culture were conducted.

The DIPS study, studying rare diabetes using iPSC, PI: Dr. Shivani Misra, was approved by Westminster Research Ethics Committee (20/LO/1071) to perform skin biopsies from probands carrying the HNF1A p.S19L and p. A251T variants.

Dr. James Elliott assisted with the cell sorting presented in this chapter at the LMS/NIHR Imperial Biomedical Research Centre Flow Cytometry Facility.

Publication Acknowledgment:

1) The sections on β-like cells generation in this chapter's introduction and method are revised from the manuscript title “Optimised protocol for generating functional pancreatic insulin-secreting cells from human pluripotent stem cells.”, id 65530_RE, that I have submitted as the first author to the JOVE Method journal. The manuscript id 65530_RE has been accepted and is currently undergoing final revisions. In addition, the Figure 5.3 will be included in the JOVE Method manuscript 65530_RE, (designed by me using Autodesk SketchBook and Microsoft PowerPoint).

2) The Figure 1.4 included in the introduction was published in “Functional Genomics in Pancreatic β-cells: Recent Advances in Gene Deletion and Genome Editing Technologies for Diabetes Research.” Frontiers in endocrinology, vol. 11 576632., the 8 Oct. 2020, doi:10.3389/fendo.2020.576632, in which I am a co-author alongside Dr. Ming Hu, Prof. Guy Rutter, and Dr. Shivani Misra. The figure was designed by me using Autodesk SketchBook.

5 Chapter 5: Functional Assessment of β-Cell-like Cells Derived from iPSCs Carrying the Variant *HNF1A* p.A251T

Summary

The previous chapter (4) described the approach generating a human β-like cell line derived from iPSCs obtained from a proband carrying the *HNF1A* p.A251T variant. The main objective of the present chapter is to present a functional characterisation of these A251T β-like cells and thus gain insights into the impact of the *HNF1A* p.A251T variant on β-cell function. A series of experiments were conducted to evaluate both β-cell identity and function. This was done by combining immunofluorescence staining for β-cell markers and insulin with the assessment of β-cell function, including glucose stimulated insulin secretion and Ca^{2+} levels in response to high glucose challenges. The findings indicated that the A251T β-like cells displayed reduced insulin secretion, even when exposed to high glucose levels, and exhibited an impaired K_{ATP} channel-mediated membrane depolarisation. Eventually, testing glucose-stimulated insulin secretion after administering the K_{ATP} channel blocker sulfonylurea (glibenclamide) aimed to determine if it could restore reduced insulin secretion as individuals with HNF1A-MODY, are responsive to sulfonylurea treatment, yet it failed to rectify the impaired insulin secretion in A251T β-like cells.

This chapter addresses the limitations of *in vitro* assessments, non-replicability of β-cell and MODY phenotype, and offers insights into the defective impact of the *HNF1A* p.A251T variant.

5.1 Introduction

5.1.1 The Endocrine Pancreas as a Regulator of Glucose Homeostasis: A Focus on β-Cell and Insulin Secretion

This chapter centres on exploring the influence of *HNF1A* variants on β-cell function, a critical player in the regulation of glucose homeostasis through tightly controlled insulin secretion mediated by Ca^{2+} signalling (Klec *et al.*, 2019). The entry of Ca^{2+} governs the initiation of exocytosis for insulin-laden secretory granules. This intricate process is coupled with synchronised oscillations that correspond to changes in the cell membrane's electrical activity (as shown in Figure 1.2) (Grapengiesser, Gylfe and Hellman, 1988; Santos *et al.*, 1991).

As insulin secretion is central to glucose metabolism, understanding its regulation is essential for investigating the impact of *HNF1A* VUSs on β-cell function and identity. This chapter 5 focuses on the functional aspects of pancreatic β-cells insulin secretion and its correlation with Ca^{2+} oscillations. Recent studies have revealed heterogeneity in Ca^{2+} response among β-cells, with specialized "hub" cells acting as pacemakers to coordinate oscillations within the islet (Valdeolmillos *et al.*, 1993; Lei *et al.*, 2018; Chabosseau *et al.*, 2023). Dysregulated Ca^{2+} levels have been implicated in diabetes pathogenesis, affecting pulsatile insulin signals and β-cell function (Goodner, Sweet and Harrison, 1988; O'Rahilly, Turner and Matthews, 1988; Bingley *et al.*, 1992; Jones, Persaud and Howell, 1992; Hellman *et al.*, 1994).

5.1.2 β-Cell Identity: The Role of *NKX6.1* and *PDX1*

To characterise β-like cell models effectively, defining criteria for proper control and context is essential. This includes identifying specific gene expression patterns, such as *PDX1* and *NKX6.1*, which serve as crucial regulators of β-cell identity, maturation, and function (Offield *et al.*, 1996; Sander *et al.*, 2000; Fujimoto and Polonsky, 2009; Schaffer *et al.*, 2013; Taylor, Liu and Sander, 2013; Gao *et al.*, 2014; Petersen *et al.*, 2017). These markers are frequently utilised in *in vitro* differentiation protocols to assess β-cell differentiation efficacy (Memon *et al.*, 2018). *PDX1* and *NKX6.1* play crucial roles in hPSC differentiation into insulin-expressing cells, promoting β-cell

differentiation and decreasing the number multihormonal endocrine cell formation (Clark *et al.*, 1993; Macfarlane *et al.*, 1999; Lavon, Yanuka and Benvenisty, 2006; Kubo *et al.*, 2011; Taylor, Liu and Sander, 2013). In mature β-cells, *NKX6.1* and *PDX1*, along with *NKX2.2* and *NEUROD1*, maintain β-cell identity and regulate insulin synthesis (Tran, Moraes and Hoesli, 2020).

This chapter aims to explore the functional consequences of *HNF1A* VUS in β-like cells, with a focus on insulin secretion and Ca^{2+} signalling. This will provide insights into the impact of these variant on β-cell function and identity and will help to establish robust *in vitro* functional assays using β-cell-like cells derived from iPSCs carrying the variant of interest. These assays will contribute to our understanding of the HNF1A-MODY phenotype.

5.1.3 Aim of the Study

The hypothesis is that the *HNF1A* p.A251T has impacts on HNF1A protein function with consequences for β-cell function, β-cell identity, and insulin secretion.

Aim: To characterise and assess functionally human β-cells directly differentiated from iPSCs derived from p.A251T patient-fibroblasts to investigate the impact of *HNF1A* p.A251T through the implementation of innovative functional assays**.**

5.1.4 Study Design

The present study involved two parts:

1) Optimising of the functional assessment for β-cell-like cells derived from common hESC lines using the MEL1 hESC line, $INS^{GFP/w}$ that expresses a green fluorescent protein (GFP) reporter gene at the *INS* locus. This optimisation process involved refining the techniques and protocols used to evaluate the function of β-cell-like cells and establish a robust study pipeline that enables the comprehensive assessment of β-like cell function in the context of the *HNF1A* variant.

2) Conducting a functional analysis on β-cell-like cells carrying the *HNF1A* p.A251T variant. A comparative functional assessment is made with control β-cell-like cells procured from a healthy donor. The characterisation process is multifaceted and employs well-established methods.

This process encompasses an evaluation of β-cell functionality, specifically using glucose-stimulated insulin secretion assay. In addition to the functional analysis, the study also examined the β-cell identity of *HNF1A* p.A251T variant cells by assessing the expression of β-cell signature genes, such as *NKX6.1* and *PDX1*. The study also evaluated the relative proportion of α-cells and β-cells within islet-like clusters, which can provide insights into the efficiency of differentiation and potential biases towards the α-cell lineage. Finally, the study investigates subsequent Ca^{2+} dynamics triggered by high glucose concentrations.

Figure 5.1 presents the study design and a summary of the methods employed for a comprehensive understanding of the experimental approach.

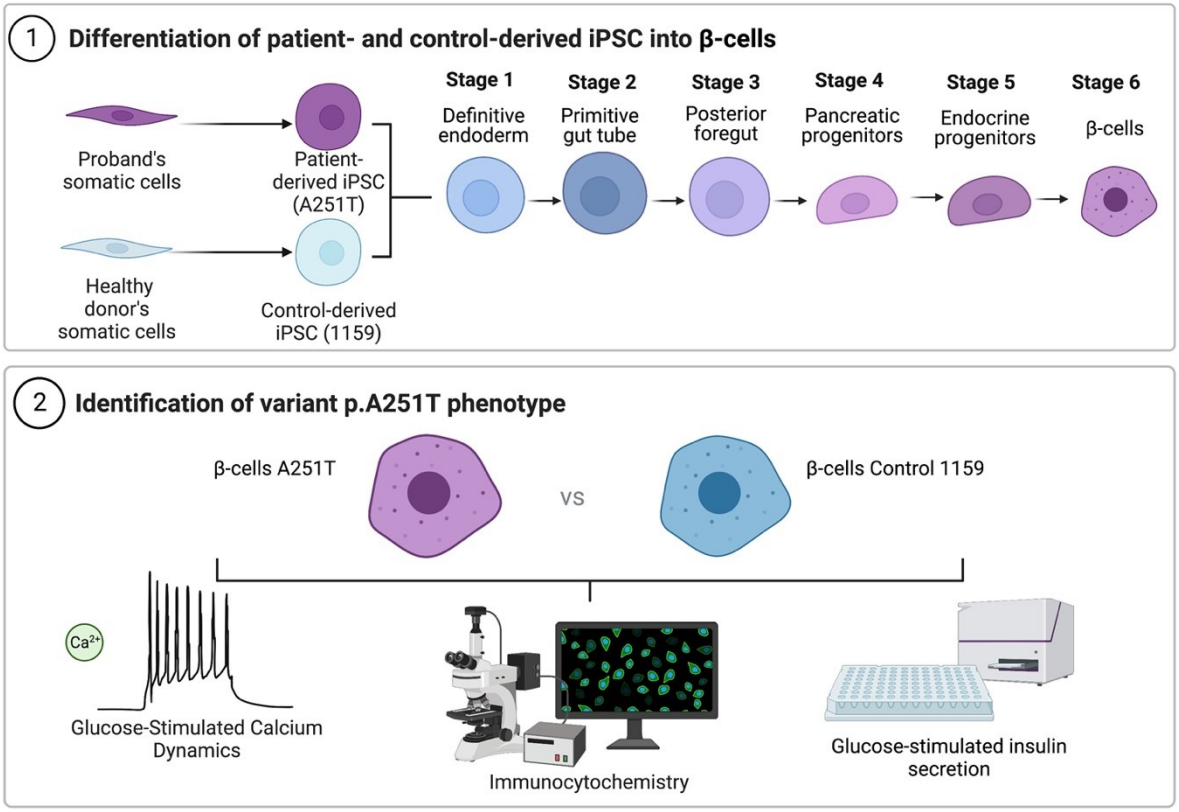

Figure 5.1: **Schematic Representation and Functional Analysis of Control and A251T β-Cell-Like Cells.**

The figure illustrates the functional analysis performed on control cells and β-like cells A251T. The method employed to functionally analyse β-cells derived from proband A251T is compared to β-like cells derived from a healthy donor (1159). The same steps were initially optimised using MEL1, ensuring standardised protocols for all hPSCs studied. The functional analysis consisted first into the directed differentiation of both control cells and patient-derived β-cells following a six-stage process: stage 1) differentiation into definitive endoderm, stage 2) formation of primitive gut tube, stage 3) differentiation into posterior foregut, stage 4) induction of pancreatic progenitors, stage 5) generation of endocrine progenitors, and stage 6) differentiation into β-like cells. Secondly, the characterisation of β-like cells from each cell lines, both control and those derived from iPSCs carrying the A251T variant, was performed. This characterisation included three aspects: 1) assessment of glucose-stimulated Ca^{2+} dynamics (left), 2) immunostaining to identify the presence of β-cell markers (*PDX1* and *NKX6.1*), insulin, and glucagon for different cell types within the islet-like clusters at the final stage of directed differentiation (centre), and 3) measurement of glucose-stimulated insulin secretion (right).

5.2 Methods

The protocol for generating β-cells is described in detail in Chapter 4.

The Table 6-2 provides all the necessary details of the suppliers and catalogue numbers. Additionally, the Table 6-4 summarises the details of the primary and secondary antibodies, including their dilutions and suppliers, catalogue numbers.

5.2.1 Immunofluorescence Staining of Pancreatic β-Cell Clusters Derived from Human Pluripotent Stem Cells

On day 25, during stage 6 of pancreatic β-cell differentiation (Figure 5.1), 5-10 clusters were collected and fixed with 4% paraformaldehyde (PFA) for 15 minutes at room temperature. Following fixation, the clusters were washed with PBS, resuspended in 30% (w/v) sucrose, and incubated overnight at 4°C. The clusters were then embedded in optimal cutting temperature compound (O.C.T.) (Agar Scientific) medium in a cryomold, and rapidly frozen on dry ice before storage at -80°C. Cryosections of 5-µm thickness were prepared from the frozen blocks using a cryostat microtome (Cryostat NX70) and mounted onto microscope SuperFrost Plus Slides (Thermo Fisher) for further analysis (method presented in Figure 5.2). Slides were stored at −80°C and left 10 min at room temperature the day of staining. Each cryosection was circled using a hydrophobic PAP pen (Vector Lab) and rehydrated in PBS for 15 min. PBS was switched to cold methanol for 10 min at −20°C. The slides were washed with PBS and blocked for 1 hour with PBS 2% normal donkey serum (Sigma) at room temperature. After blocking the slides were incubated overnight at 4°C with either Insulin (Dako), Glucagon (Sigma), NKX6.1 (Novus Biologicals) or PDX1 (Abcam) antibodies, diluted 1:50, 1:5000, 1:2000 and 1:1000, respectively, in PBS 2% normal donkey serum. Slides were then incubated with respective secondary Alexa Fluor 488, Alexa Fluor 561, Alexa Fluor 568, Alexa Fluor 647 antibodies for 1 hour at room temperature. The slides were mounted with solution ProLong Diamond Antifade Mounting with DAPI (Invitrogen) and visualised using the Eclipse T-I Microscope with a spinning disc confocal system (Nikon), x40, oil immersion, for clusters derived from MEL-1 hESCs and STELLARIS 8 Inverted Confocal Microscope (Leica), x40, oil immersion, for

clusters derived from iPSCs. The procedure for immunofluorescence staining of the pancreas is depicted in Figure 5.2.

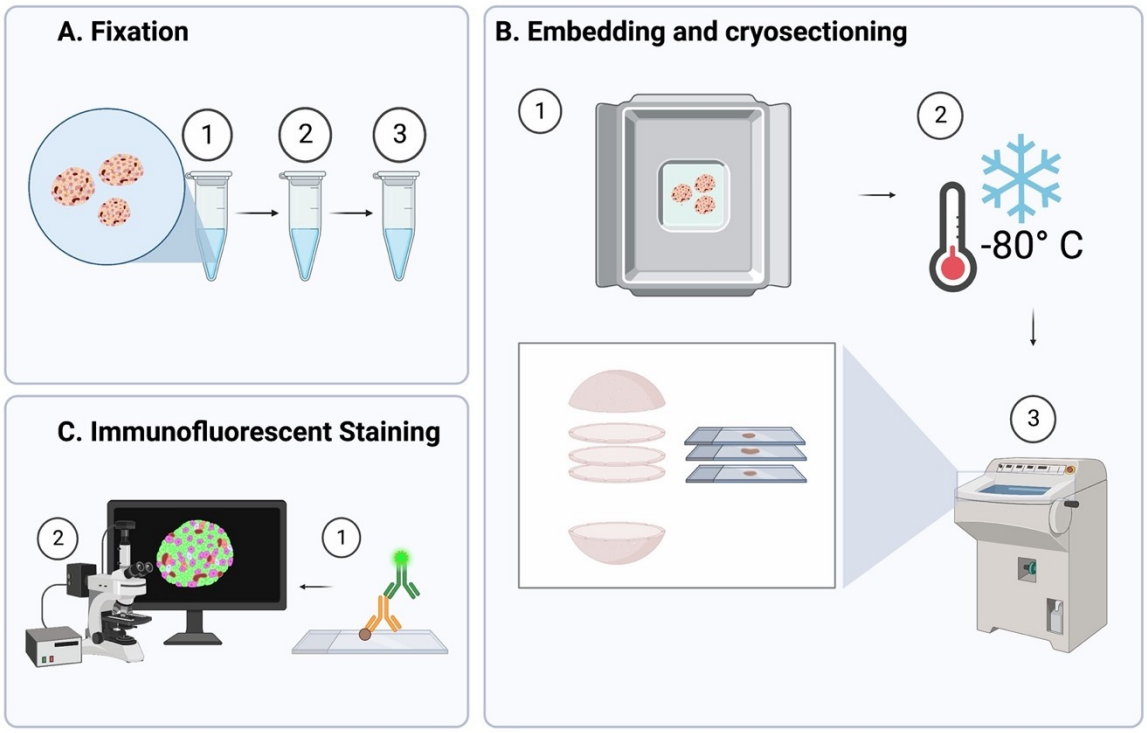

Figure 5.2: **Method for Immunofluorescence Staining of Pancreatic β-Cell Clusters Derived from hPSCs.**

Panel A: Fixation at day 25, with 4% PFA. Panel B: Embedding and cryosection of cryomold containing fixed clusters (islet-like cells). All clusters were transferred into a cryomold mixed with O.C.T. medium. The frozen blocks were then cryosection (5-µm) on microscope slides using a microtome. Panel C: Immunofluorescent staining for Insulin, Glucagon, NKX6.1, and PDX.and mounted with DAPI and visualised using spinning disc confocal system.

5.2.2 Glucose-Stimulated Insulin Secretion

Before each experiment, KREBS solutions (118 mM sodium chloride NaCl, 4.7 mM calcium chloride KCl, 1.2 mM magnesium sulfate MgSO4, 1.2 mM monopotassium phosphate KH2PO4, 2.5 mM calcium chloride CaCl2, and 25 mM sodium bicarbonate NaHCO3, 10 mM HEPES, pH- 7.2) with different glucose concentrations were prepared and warmed at a 37°C water bath. These were: low glucose KREBS solution (3.3mM glucose), high glucose KREBS solution (16.7mM glucose, Sigma), KREBS solution with KCl (3.3mM glucose, 11mM KCl), KREBS solution with exendin-4 (Sigma)(100 nM) in 16.7mM glucose, and KREBS solution with glibenclamide (Sigma)(GBC) (10 μM) in 16.7mM glucose. Around 10-15 clusters at day 25 of similar sizes were collected in a 1.5mL tube and placed in a tube rack, allowing the clusters to settle at the bottom. The clusters were incubated in the low glucose KREBS solution at 37°C for 1 h. After the incubation, 200 μL of supernatant was stored at -80°C for insulin measurement. Following that, 200 μL of low glucose KREBS solution was added to the clusters and they were then further incubated at 37°C for 30 min, after which the supernatants were stored at -80°C for insulin measurements. After removing the supernatant, the clusters were washed with glucose-free KREBS. Subsequently, the clusters were resuspended in ultra-pure water for the total insulin content procedure (refer Quantification of Total Insulin Content in Pancreatic β-). The same procedure was repeated for the high glucose KREBS solution, for each treatment with KCl, Exendin-4 and glibenclamide, incubated for 30 min, and supernatants stored at -80°C for insulin measurement. Insulin measurement was performed using the insulin ultra-sensitive assay kit homogeneous time resolved fluorescence (HTRF, Cisbio), following the manufacturer's instructions. The measurement was conducted using multiwell plate readers (Thermo Fisher).

5.2.3 Quantification of Total Insulin Content in Pancreatic β-Like Cells

At the end of the GSIS experiment, 1:3 (50 μL/tube) of ultrapure water was added to the samples, following 2:3 (150 μL/tube) of acid ethanol solution was added to the tube containing the islets and ultrapure water. The samples were then stored overnight at 4°C for a duration of 12-15 h. The next day, each sample was vortexed to ensure

proper mixing, and sonicated using a sonicator (Fisherbrand S-Series Unheated Ultrasonic Bath) set to 20% power for 10 second to achieve complete lysis of the islet tissue. Next, the samples were centrifuged at 10,000×g for 10 minutes.

To determine the DNA concentration in each sample, a nanodrop spectrophotometer was employed (DNA wavelength of 260 nm, A260 of 1.0 = 50µg/ml). This DNA concentration measurement was used to normalise the insulin measurements obtained from the samples.

5.2.4 Intracellular Ca^{2+} Imaging

Prior to each experiment, KREBS solutions with different glucose concentrations Clusters at day 28 were incubated for 1 h at 37 °C, 5% CO^2 in a (10 µM) working solution of Cal-520 dye (Stratech) prepared in a KREBS low glucose (3.3mM glucose) with 0.02% Pluronic F-127 (Introgen). Ca^{2+} imaging was achieved using a spinning disk confocal microscope ZEISS Axiovert. The signal emitted from Cal 520 (excitation wavelength: 488 nm, emission wavelength: 525 ± 25 nm) was continuously monitored in time-series experiments for a duration of 25 min., comprising 750 frames, at 2 s per frame. The experiment was initiated using a precise timing of 0-120 s under baseline conditions (3.3 mM), 120-1200 s at high glucose (16.7mM) and 1200-1500s during KCl stimulation.

5.2.5 Statistical Analysis

The normality of the data was evaluated using the Shapiro-Wilk test (Shapiro and Wilk, 1965). When comparing two groups, either parametric t-tests or nonparametric Mann-Whitney U tests were used. For comparisons among multiple groups, a two-way analysis of variance (ANOVA) was performed, followed by multiple comparisons test. Statistical significance was considered when p-value were equal to or less than 0.05 (*), 0.01 (**), 0.001 (***), or 0.0001 (****).

5.3 Results Functional Analysis of A251T β-Cells

5.3.1 Optimisation of Functional Assays of β-Cells (MEL1 hESCs)

The functional assessment experiments for β-cells derived from hPSCs were carefully designed to evaluate the efficiency of directed differentiation of β-like cells. I received training for β-cell generation and functional assessment techniques from Dr. Qian Du and Dr. Dieter Egli at the Stem Cell Initiative Laboratory, Columbia University, New York City. This training allowed me to adapt and validate the protocol, ensuring that all necessary steps and functional analyses were rigorously tested and optimised to maintain a robust directed differentiation protocol for all hPSCs studied.

For this study, the $INS^{GFP/w}$ hESC reporter line (MEL1) was utilised (Micallef *et al.*, 2012), as initial data regarding β-cell function from the protocol developed by Sui et al. were collected and published using MEL1 cells. Additionally, the functional assessment of β-cells derived from hPSCs has been extensively performed using MEL1 cells (Russ *et al.*, 2015; Sui, Leibel and Egli, 2018; Nair *et al.*, 2019; Jin and Jiang, 2022; Liang *et al.*, 2023). The MEL1 cell line is particularly advantageous as it expresses a GFP reporter under the control of the insulin promoter allowing for easier visualisation of insulin-producing cells under a fluorescence microscope. This facilitated the optimisation of a scalable protocol for this study on *HNF1A* variant iPSCs, enabling the replication of an identical protocol for all hPSCs studied.

5.3.1.1 **Characterisation of Islet-Like Clusters and β-Cell Identity**

The first step of the study involved assessing the efficiency of insulin-producing cell generation (5.1.4). This was achieved through immunofluorescence staining of insulin, which allowed for the quantification of relative insulin expression and β-cell markers, including *PDX1* and *NKX6.1*. All functional experiments were performed during stage 6 of the β-cell generation protocol, at day 25. All clusters were fixed the same day to ensure a consistent and robust starting point. To optimise the protocol, 5µm cryosections of cell clusters were performed. This technique minimised the presence of multiple cell layers, resulting in a maximum of 3-4 cells in each z-stack. Smaller sections were necessary as β-cells derived from iPSCs form smaller clusters than β-

cells derived from hESC (as shown in Figure 5.2). The refinement of the cutting technique was crucial to obtain satisfactory results for these smaller sections.

The evaluation of directed differentiation efficiency involved immunostaining to check for the presence of β-cells, and subsequent cell counting using a Fiji software macro specifically designed for the purpose of this study (coded by Mr. Stephen Rothery, see statement of contribution at the end of this chapter). Cell counting was performed from nine islets obtained through three separate differentiations. The results demonstrate a high enrichment of insulin-expressing cells within the pancreatic lineage (60.5±15.5%, n=9, Figure 5.3). This indicates the successful directed differentiation of hESCs into β-like cells that specifically express insulin. The results reveal an enrichment of insulin-positive cells consistent with previous studies utilising a similar protocol involving APH treatment in the late stage of differentiation (approximate 60% of insulin-positive cells, n=12, Figure 5.3).

To evaluate the β-cell identity of the differentiated cells, the relative expression of signature genes such as NKX6.1 and PDX1 was examined using immunochemistry. NKX6.1 and PDX1 are crucial for the establishment and maintenance of β-cells (Memon *et al.*, 2018). The analysis revealed that within the clusters, 24.9±6.2% (n=9 clusters) of cells expressed NKX6.1, while 40.2±6.2% (n=9 clusters) of cells expressed the β-cell marker PDX1, providing additional evidence for the presence of differentiated β-like cells within the clusters.

The clusters resulting from the directed differentiation represented a mixed population of cells, including other cell types than β-like cells. 15±1.7% of cells per cluster expressed glucagon (mean of n=9 clusters), suggesting the presence of α-like cells within the clusters.

This composition of α-like cells and β-like cells closely resembles the cell population observed in native human islets of Langerhans, where β-cells constitute approximately 70% of the total cell population and α-cells make up 20-40% (Da Silva Xavier, 2018). These findings emphasise the similarity between the clusters and the native cell

composition of islets, supporting their functional relevance in representing islet-like structures.

5.3.1.2 Characterisation of β-Cell Glucose Responsiveness in Islet-Like Clusters

The glucose responsiveness of MEL1-derived clusters was assessed by monitoring glucose-stimulated insulin secretion (GSIS), in experiments which also included measurements of baseline insulin secretion, high glucose, and KCl-stimulated insulin conditions. The results are presented in the Figure 5.3.

Under high-glucose (16.7 mM) conditions, the MEL1-derived clusters displayed an increase in insulin secretion compared to low-glucose concentrations, although this increase did not achieve statistical significance. Notably, one of the technical replicates displayed a substantial increase in insulin secretion when exposed to high glucose, while the other two replicates demonstrated a less pronounced increase compared to low-glucose conditions, despite consistent conditions and protocols across replicates. Insulin secretion in response to high glucose was approximately 100-fold higher than that observed at low glucose levels. Specifically, the percentage of insulin secretion (normalised to insulin content) was measured at 0.003±0.002% (mean ± SEM, n= 9) under 3.3 mM low glucose and 0.24±0.20% (mean ± SEM, n= 9) at 16.7 mM high glucose.

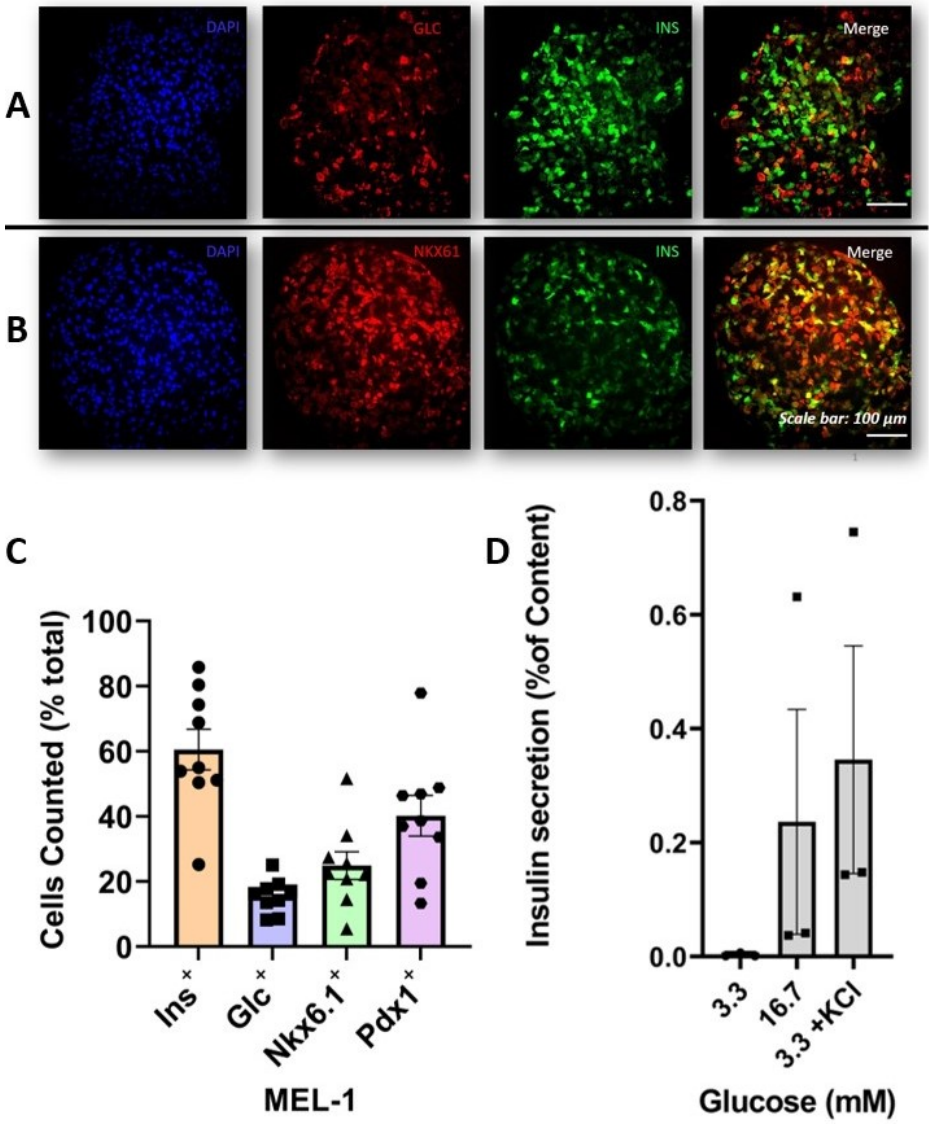

Figure 5.3: **Characterisation of Islet-Like Cluster Cell Types, β-Cell Identity, and Function.** Clusters obtained from differentiated MEL-1 hESC reporter line (Micallef *et al.*, 2012) were evaluated for the presence of insulin-producing cells expressing β-cell maturity markers. Panel A: Immunofluorescence images of the clusters were captured from cryomold sections using spinning disk confocal microscopy (x40, oil immersion), which revealed the predominance of insulin-producing cells (approximately 60%) compared to glucagon-producing cells (approximately 15%) (n=9 clusters). Scale bar: 100 µm. Panel B: Immunofluorescence images showed the predominance of insulin-producing cells co-expressing the pancreatic β-cell markers *NKX6.1*(spinning disk confocal microscopy, x40, oil immersion), (n=9 clusters). Scale bar: 100 µm. Panel C: ImageJ cell counter macro was employed to determine the percentage of insulin-positive, glucagon-positive, and β-cell markers NKX6.1 positive cells, and β-cell markers PDX1 positive cells. Panel D: The GSIS of MEL-1 derived β-cell-like cells was

evaluated, which exhibited an increase of 100-fold in response to high glucose stimulation (16.7mM glucose, n=9, SEM).

5.3.1.3 Optimisation of Functional Experiments on MEL1-Derived β-Cells: Ca^{2+} Imaging

To assess the functional properties of β-cells derived MEL1, Ca^{2+} signalling was quantified at different glucose concentrations. The depolarisation of the β-cell plasma membrane, induced by increasing glucose concentrations, leads to Ca^{2+} influx, which triggers insulin secretion (see Introduction, Figure 1.2)

The objective of these experiments was to optimise the experimental conditions for assessing the function of β-cells derived from iPSCs. The experiment was initiated using a precise timing of 0-120 seconds under baseline conditions (3.3 mM), 120-1200 seconds at high glucose (16.7mM) and 1200-1500 seconds during KCl stimulation. The mean fluorescence intensity was measured for each frame (every 2 seconds) and normalised to the mean fluorescence of 30 timepoints at a glucose concentration of 3.3 mM.

The results are presented in Figure 5.4 where each trace represents one cluster. After a delay of 1-2 min, there was a variable change in cytosolic Ca^{2+} upon high glucose (16.7 mM) stimulation compared to the baseline glucose concentration (3.3 mM). Whilst increases in Ca^{2+} were observed in several clusters, the net change was small, or there was a decrease, in others. However, upon KCl-induced depolarisation of MEL1-derived β-cells, a maximal and consistent 2.5-fold increase in fluorescence intensity relative to the baseline (red dashed line, Figure 5.4) was observed, suggesting the clusters' sensitivity to KCl-induced depolarisation.

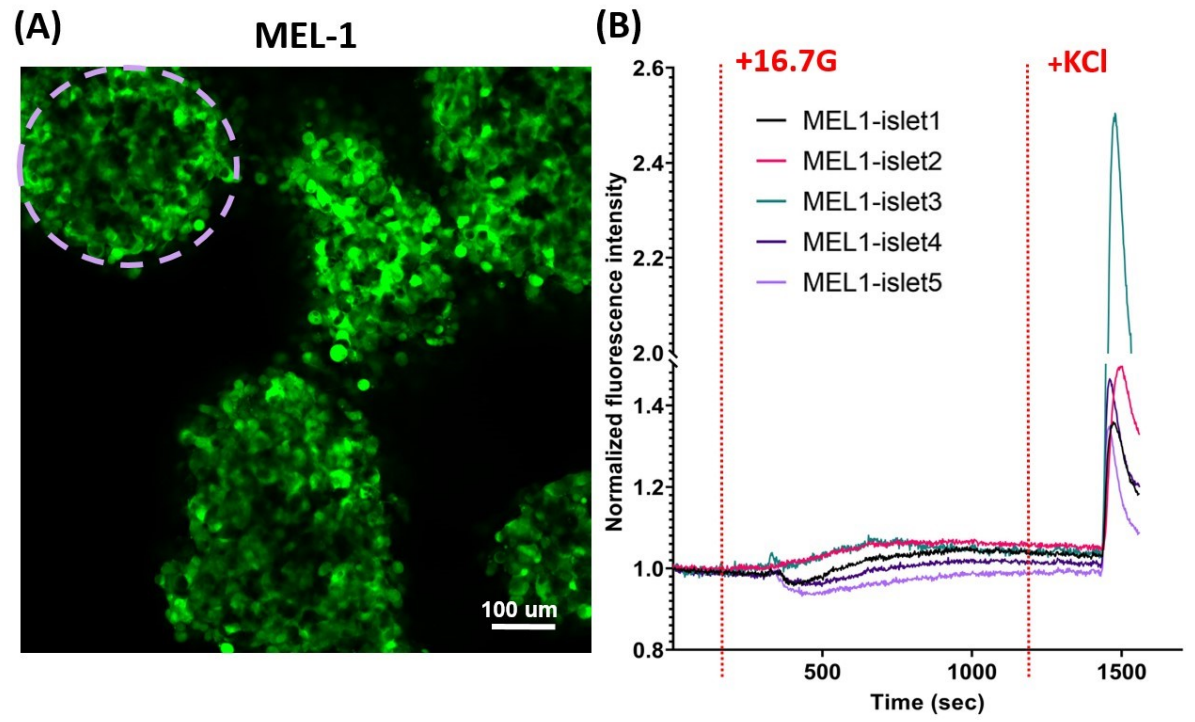

Figure 5.4: **Ca^{2+} imaging Optimisation using MEL-1 hESCs.**

Panel A: Representative image of Ca^{2+} imaging with a screenshot from the optimisation video featuring 5 islets. Ca^{2+} changes relative fluorescent is visualised by the signal of Cal-520 AM, a fluorogenic Ca^{2+}sensitive dye that selectively detects intracellular Ca^{2+} levels. The white dashed circles indicate the regions of interest (ROI) selected for one islet as an example. Mean fluorescence intensity is recorded for each ROI at each time frames (1 frame per 2 seconds). Panel B: Graph illustrating Ca^{2+} imaging. Each trace represents a single cluster. The optimisation was performed using 5 islets and focused on high glucose (16.7 mM) and KCl stimulation. The experiment consisted of 750-time frames. The graph displays the normalised fluorescent intensity relative to the baseline (3.3 mM glucose) from 0 to 120 seconds. The red dashed line indicates the addition of high glucose (16.7 mM) at 120 seconds. The second red dashed line, at 1200 seconds, shows the transition from high glucose to 3.3 mM glucose with KCl stimulation.

5.3.2 Results Functional Analysis of β-Cells Derived from iPSCs A251T

5.3.2.1 Characterisation of β-Cell Clusters A251Tt: β-Cell Identity

After optimising the functional assessment experimental protocol for β-like cells control MEL1, the next step was to study β-cell function in clusters derived from iPSCs carrying the *HNF1A* p.A251T variant.

To confirm the presence of β-cell-like cells within the clusters of cells derived from iPSCs carrying p.A251T variant, the relative expression of β-cell markers including PDX1 and NKX6.1, and INS, was analysed by immunofluorescence staining, at the end of differentiation (stage 6, day 25). The results are presented in Figure 5.5.

The positive cells for each marker PDX1 and NKX6.1 alone and co-positive NKX6.1/INS were counted. Based on the findings obtained from the immunofluorescence analysis, a comparison between the A251T cell clusters and the control group 1159 (Figure 5.5) revealed a marked reduction in the relative expression of insulin within the A251T clusters (31.16 ± 1.2% of total cells/cluster, n = 15) as compared to the control group (42.45 ± 3.60% of total cells/cluster, p = 0.006, n = 15).

The relative expression of the β-cell marker *NKX6.1* exhibited no significant difference between the β-like cells within cell clusters derived from control 1159 iPSCs (mean 24.8 ± 2.2% of total cells/cluster) and A251T iPSCs (mean 21.1 ± 1.6% of total cells/cluster), (p = 0.2, n = 15). Similarly, no statistically significant difference was found in the relative expression of *PDX1* between the control 1159 clusters and the A251T clusters (mean of 40.7 ± 6.2% and 34.7 ± 3.5%, respectively; p = 0.4; n = 9). In addition, there were no statistically significant differences in the percentage of INS+/NKX6.1+ cells between the A251T islet-like clusters (11.5%, IQR 10.8-19.5, n = 9) and the control islet-like clusters (16%, IQR 8.3- 28.0, n = 9), (p > 0.99, Mann-Whitney test).

Although the A251T variants did not exert a significant impact on the expression of the key β-cell transcription factors NKX6.1 and PDX1, nor on the proportion of cells co-

expressing NKX6.1 and insulin, a notable reduction in the relative expression of insulin alone was observed within the A251T clusters. It is plausible that the A251T variant may influence the function or activity of other crucial β-cell transcription factors and regulatory proteins that were not specifically examined in this study. Additionally, it is worth noting that the immunostaining was conducted during the later stages of the differentiation process (day 25), potentially missing changes in PDX1 and NKX6.1 expression occurring earlier in the differentiation process.

5.3.2.2 Identification of Pancreatic Cell Types (α- and β-Like Cells) in A251T Islet-Like Clusters

In the differentiated cell clusters from iPSCs derived from the A251T proband, a heterogeneous mixture of pancreatic endocrine cells was observed, comprising glucagon-secreting cells (α-like cells) and insulin-secreting cells (β-like cells).

The immunofluorescence results comparing the A251T β-cells to the control 1159 β-cells are depicted in Figure 5.6. Three different directed differentiations were performed, with a minimum of three clusters per differentiation (n=9) to 5 for insulin relative expression analysis (n=15), all fixed the same day (day 25, stage 6) of the differentiation protocol.

The analysis revealed a significant difference in relative glucagon expression for the A251T clusters compared to control 1159 clusters. In the late stage of differentiation, the A251T-derived clusters exhibited a significantly greater proportion of glucagon-positive cells per cluster (mean A251T clusters = 19.4% ± 2.2%, n=9) compared to the control 1159 clusters (mean 1159 clusters = 13.6% ± 1.4%, n=9) with a p-value of 0.04.

These findings indicate that the *HNF1A* p.A251T variant significantly influenced the relative expression of glucagon in A251T clusters, potentially indicating a bias in differentiation toward the α-cell (glucagon-secreting cells) lineage during late stage of differentiation.

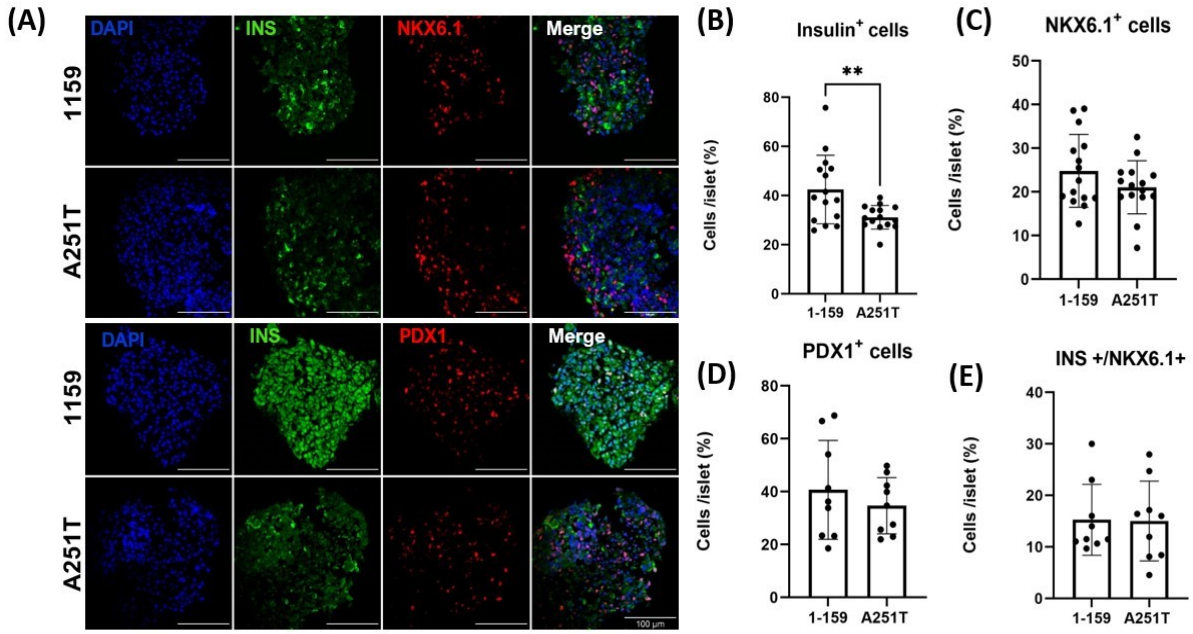

Figure 5.5: **Immunofluorescence Analysis of β-Cells Derived from iPSCs Carrying *HNF1A* p.A251T.**

Panel A: Immunofluorescence images of islet-like clusters from the 1159 control and the A251T. The upper panel A shows representative clusters stained for INS/NKX6.1, while the lower panel in A shows representative clusters stained for INS/PDX1 (confocal microscopy, x40, oil immersion). Scale bar = 100 µm. Red indicates NKX6.1, green indicates insulin, blue indicates DAPI (nuclear stain), and the merge panel shows INS/NKX6.1 immunofluorescence staining (top) and INS/PDX1 (bottom). Panel B: Histogram representing the percentage of cells within the islet-like clusters expressing *INS* (n = 15). Panel C: Percentage of cells within the islet-like clusters expressing *NKX6.1* (n = 15). Panel D: Percentage of cells within the islet-like clusters expressing *PDX1* (n = 9). Panel E: Percentage of cells within the islet-like clusters co-expressing *NKX6.1* and *INS* (n = 9). P-value (**) indicates statistical significance at the 5% level.

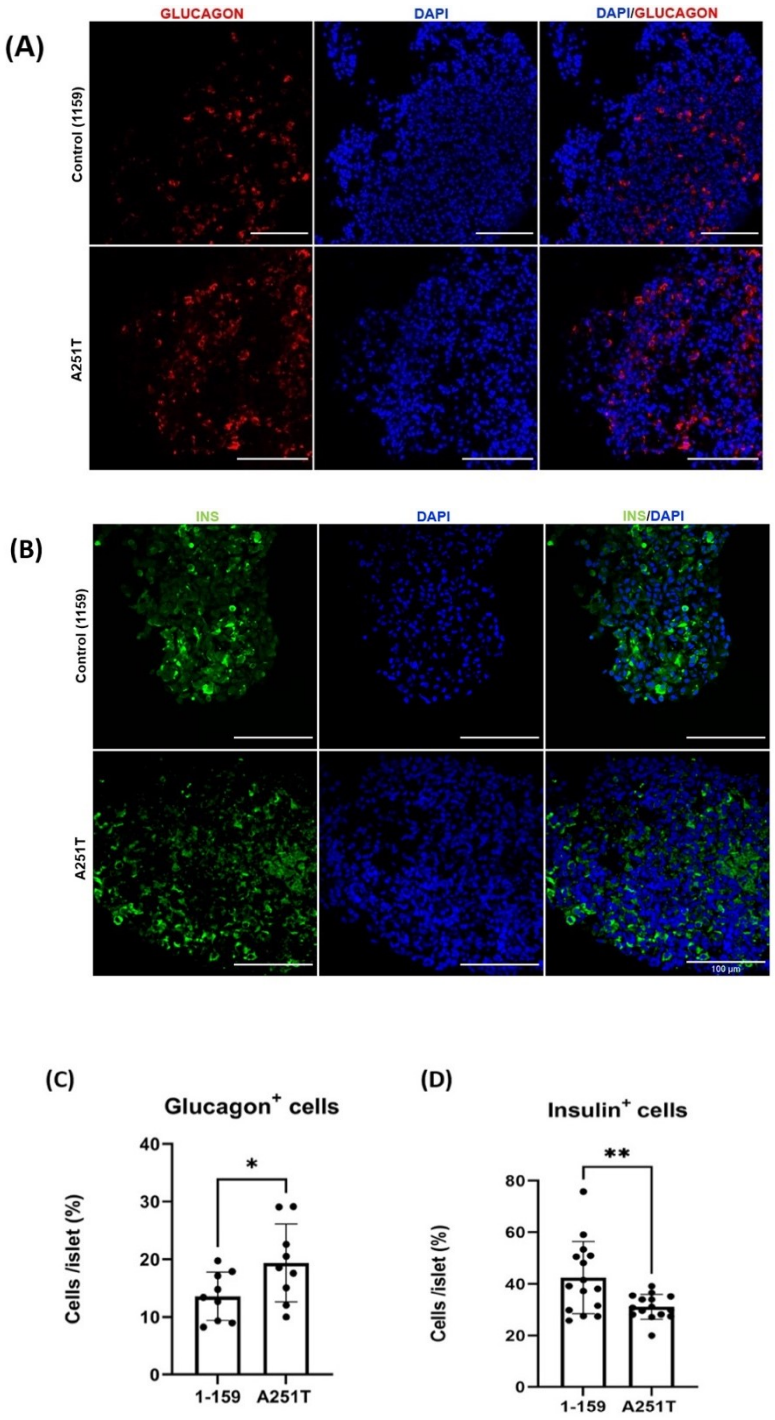

Figure 5.6: **Immunofluorescence Staining Analysis of Islet-like Cluster A251T:** α-cells and β-like cells **composition.**

A: Immunostaining of islet-like cells (stage 6, day 25) showing glucagon ((red) and DNA staining with DAPI (blue). B: Immunostaining showing insulin expression (green) (confocal microscopy, x40, oil immersion); scale bar: 100 µm. C: Histogram representing the percentage of cells within the islet-like

clusters expressing glucagon (n = 9). D: Histogram representing the percentage of cells within the islet-like clusters expressing insulin (n = 15). P-value≤ 0.05 (*) indicates statistical significance.

5.3.2.3 Functional Assessment of Glucose-Stimulated Insulin Secretion in β-Like Cells A251T Variant

GSIS was examined to investigate the differentiated function of β-cells derived from a proband carrying the *HNF1A* p.A251T variant. These results were compared to control β-cells derived from a healthy donor (1159). The experimental conditions for GSIS were optimised using β-cell-like cells derived from hESCs MEL1. The conditions included a baseline glucose concentration of 3.3 mM, high glucose stimulation at 16.7 mM, and the use of KCl as a positive control to stimulate membrane depolarisation (see above, Method section 5.2.2). Additionally, secretagogues such as the GLP-1R agonist exendin-4 (Ex-4) and the sulphonylurea glibenclamide (GLB) were used to evaluate the response of the β-like cells A251T to common treatments. GLB is a sulfonylurea commonly used to treat individuals with young-onset diabetes who carry mutations in *HNF1A* and are sensitive to sulfonylurea therapy. The results are presented in the Figure 5.7.

Insulin secretion was assessed in clusters of cells derived from iPSCs carrying the A251T variant, which included β-like cells and other endocrine cell types such as α-like cells. This evaluation was compared to control 1159 cell clusters under various glucose conditions and in the presence of Ex-4 or GLB. The results showed no significant difference in insulin secretion at baseline glucose concentration (3.3 mM, Figure 5.7) between the A251T variant and control cells. When challenged with a higher glucose concentration (16.7 mM, Figure 5.7), the A251T variant β-like cells exhibited significantly lower insulin secretion compared to the control 1159 cells ($p < 0.001$, n=9). The A251T β-like cells showed insulin secretion of 0.05% (normalised to total insulin content) compared to 0.20% for the control 1159 cells. Similarly, when exposed to high glucose and GLP-1 receptor agonist Exendin-4 (16.7 mM + Ex4, Figure 5.7) and GLB (16.7 mM + GLB, Figure 5.7), the A251T variant cells exhibited lower insulin secretion ($p<0.0001$ n=9; $p=0.001$ n=9, respectively) compared to the control 1159 β-like cells. The A251T variant β-like cells showed insulin secretion of 0.12% compared to 0.31% for the control cells with Ex-4, and 0.21% compared to 0.34% with GLB ($p < 0.001$, n=9). Under the condition of KCl (3.3 mM + KCl, Figure 5.7), which mimics K_{ATP}-mediated membrane depolarisation, the A251T β-like cells

exhibited significantly lower insulin secretion than 1159 control cells (0.31% for the A251T variant β-like cells compared to 0.48% for the 1159 β-like cells, $p = 0.0002$, $n = 9$).

The differentiated endocrine cells within the A251T cluster demonstrated reduced insulin secretion compared to control 1159 cells derived from healthy donors in response to all tested conditions: high glucose, Ex-4, GLP1 and KCl. However, it is essential to consider that the variability in glucose-stimulated insulin secretion among replicates, akin to the optimisation observed with MEL-1, could potentially introduce complexity into the interpretation of results. Furthermore, the genetically heterogeneous background between the control 1159 cells and the A251T cells, involves that the *HNF1A* p.A251T variant alone may not be a contributing factor to the observed reduction in insulin secretion.

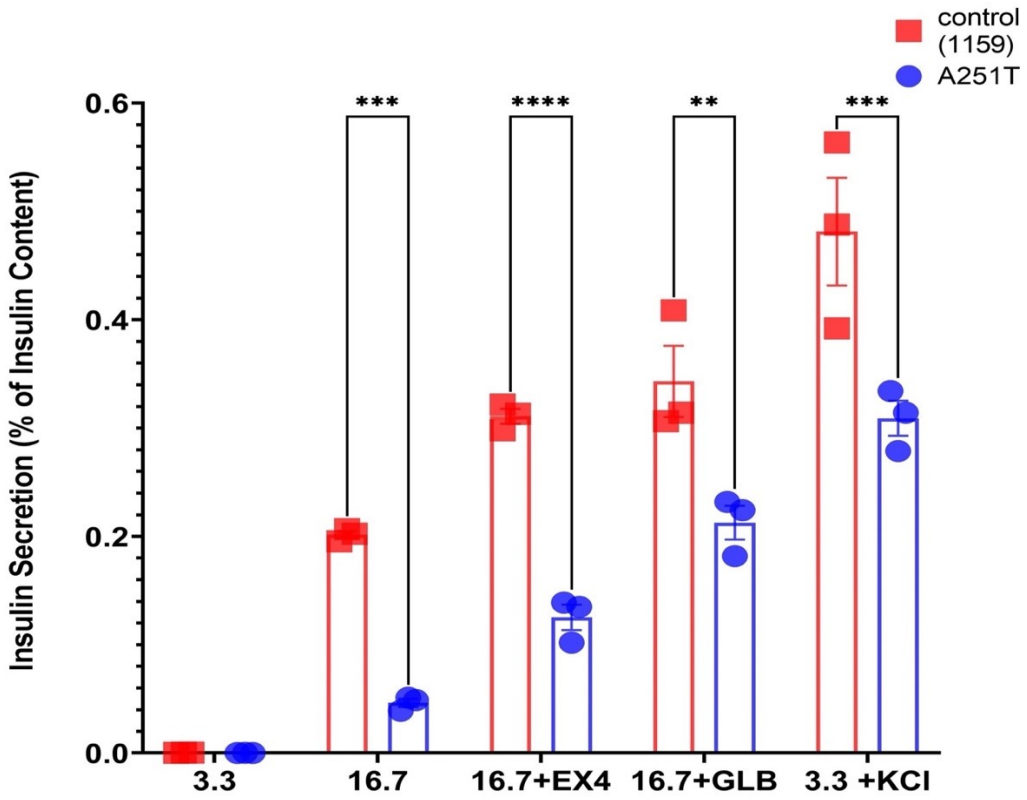

Figure 5.7: **Glucose- and Other Secretagogue-Stimulated Insulin Secretion of A251T β-Like Cells**. The figure illustrates the percentage of insulin secretion, representing the proportion of insulin secreted normalised to the total insulin content. The experimental conditions (y-axis) included: baseline glucose concentration (3.3 mM), high glucose stimulation (16.7 mM), high glucose with Exendin-4 (a GLP-1 receptor agonist) noted as 16.7 + Ex-4, high glucose with Glibenclamide noted as 16.7 + GLB, and low glucose with KCl potassium chloride (a positive control stimulation of insulin secretion mediated by membrane depolarisation) noted as 3.3 + KCl. Insulin quantification was performed using the Insulin Ultra-Sensitive HTFR kit. The Thermo Fisher Varioskan Lux Microplate Reader was used for insulin quantification. Statistical significance was considered when p-value were equal to or less than 0.05 (*), 0.01 (**), 0.001 (***), or 0.0001 (****).

5.3.2.4 Calcium Imaging of A251T β-like Cells

To elucidate the mechanisms underlying the observed diminished insulin secretion in A251T β-like cell clusters, intracellular Ca^{2+} dynamics were investigated in response to increasing glucose levels, specifically, at baseline (3.3 mM) and at high (16.7 mM) glucose (Figure 5.8).

Real-time monitoring of cytosolic Ca^{2+} changes was performed using the intracellular dye Cal520, and the results were compared to the control line 1159 β-like cell clusters derived from iPSCs of healthy donor.

Under high glucose conditions (16.7 mM), 1159 β-like cell clusters exhibited a characteristic oscillatory pattern of increasing intracellular Ca^{2+} levels, resembling a wave-like pattern. In comparison, the A251T β-like cell clusters displayed a tendency towards reduced signal of Ca^{2+} in response to high glucose, although this difference was not statistically significant.

The wave-pattern of Ca^{2+} oscillations characteristic of human native islets in response to high glucose, was found to differ between the A251T and control clusters. In response to high glucose, the 1159 control clusters exhibited a rapid increase in cytosolic calcium levels, followed by a wave-like pattern. In contrast, the A251T clusters exhibited a steady-state rise in cytosolic calcium levels.

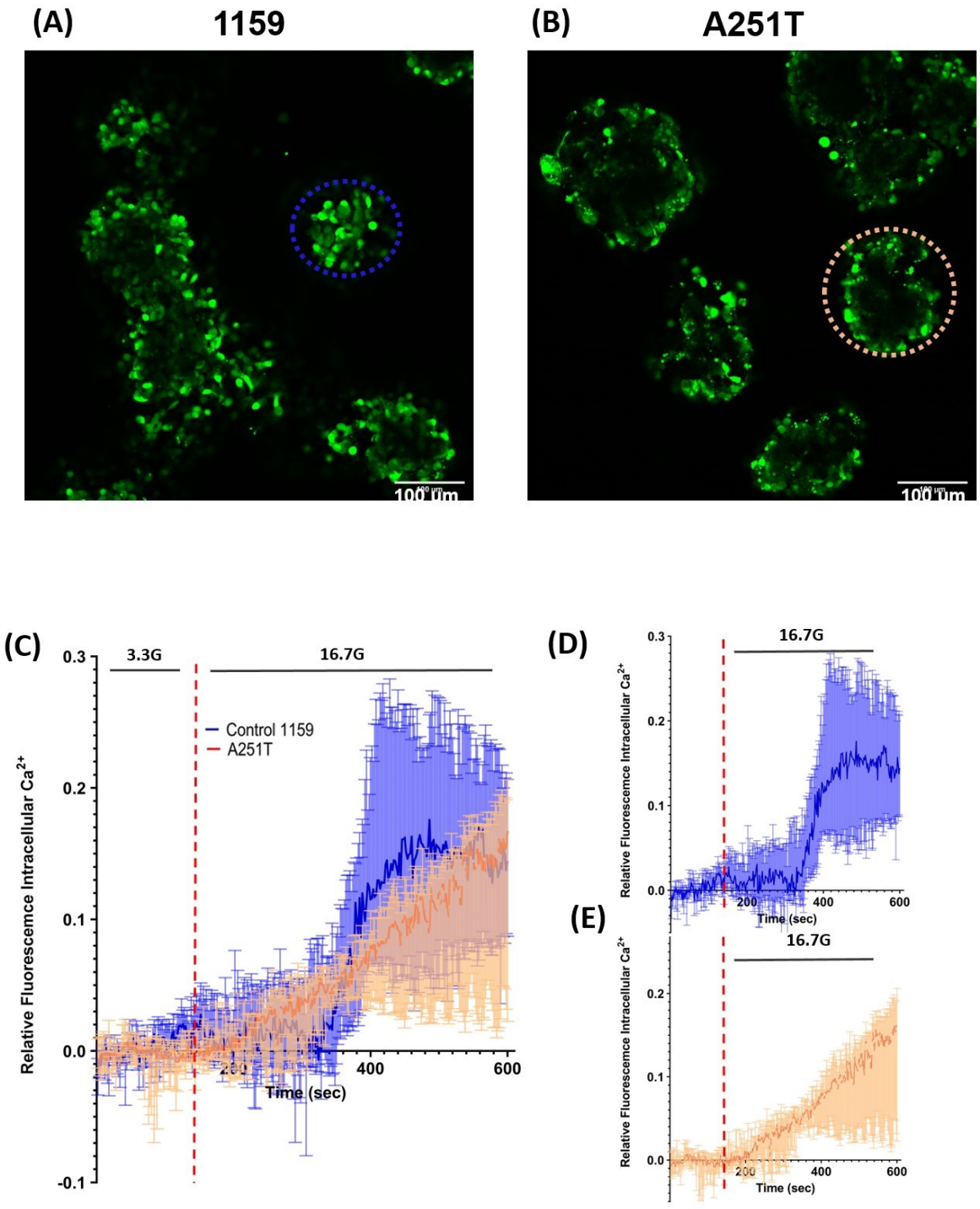
(A)
1159
(B)
A251T
100 μm
100 μm
(C)
3.3G
16.7G
Control 1159
A251T
Relative Fluorescemce Intracellular Ca2+
Time (sec)
(D)
16.7G
Relative Fluorescemce Intracellular Ca2+
Time (sec)
(E)
16.7G
Relative Fluorescemce Intracellular Ca2+
Time (sec)

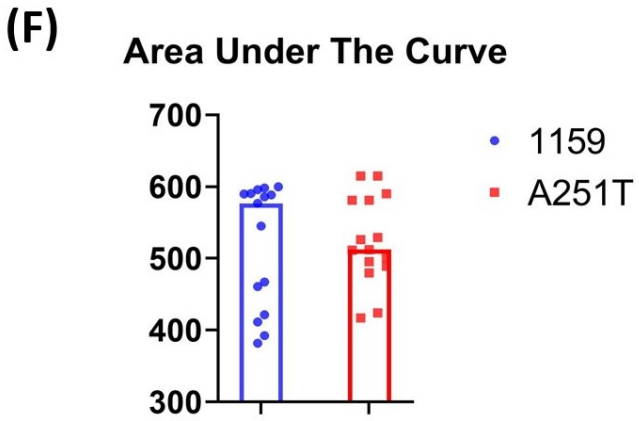

Figure 5.8: **Ca^{2+} Dynamics in Islet-Like Clusters from Control and A251T β-Cell-Like Clusters.** Panel A: Typical screenshot image from the video depicting a selected region of interest (ROI) corresponding to one islet-like cluster (n=1). The blue circle represents one control islet-like cluster refer as 1159. The scale bar represents 100 µm. Panel B: Typical screenshot image for islet-like clusters derived from iPSCs carrying the *HNF1A* p. A251T; scale bar 100 µm, with red circle indicating one A251T cluster. Panel C: Relative fluorescence of Ca^{2+} over time, median (±95 % CI, n=15). Mean intensity (Cla520 reporter, 488nm) was measured in each ROI for each frame (1 frame/2seconds). Red dashed line: addition of 16.7mM glucose at 120 seconds. Panel D; E: Relative fluorescence of Ca^{2+} over time, median (±95 % CI), with addition of 16.7mM glucose for 120 seconds. Panel D: 1159 islet-like clusters; E: A251T (n=15). Panel F: Bar graph of average area under the curve (AUC) of relative fluorescence of Ca^{2+} over time (n=15); red: A251T; blue: control 1159.

5.4 Discussion

This study aimed to develop a human β-cell model derived from iPSCs carrying the recessive *HNF1A* p.A251T genetic variant and investigate its functional characteristics to gain insights into the impact of this variant on β-cell function and the underlying mechanisms contributing to the development of phenotype observed in the proband.

The generation of the β-cell-like cells carrying the *HNF1A* p.A251T variant was described in Chapter 4. In Chapter 5, functional investigations were conducted to assess the effects of the A251T variant on β-cell function. This study aimed to establish an *in vitro* model for evaluating the functional consequences of *HNF1A* VUS on β-cell function, forming a pipeline for investigating the pathogenicity of these variants and unravelling the mechanisms underlying MODY disease.

Given that MODY is typically characterised by an insulin secretion deficiency leading to early-onset diabetes (Bonnefond *et al.*, 2023), this study investigated the insulin-secreting function of β-cells, with particular attention to the role of Ca^{2+} signalling in the response to glucose as previous findings demonstrated a diminished Ca^{2+} response to elevated glucose concentrations in HNF1A-deficient β-cells (González *et al.*, 2022a).

The establishment of the A251T homozygous β-like cell line is a significant achievement as it is the first instance of a homozygous *HNF1A* recessive variant β-like cells. This study sought to contribute to a more comprehensive understanding of MODY and expand the spectrum of genetic variants in *HNF1A.*

5.4.1 Initial Optimisation of MEL1 Outcomes

The protocol for β-cell differentiation was optimised using the MEL1 reporter cell line $INS^{GFP/w}$ as a control (Micallef *et al.*, 2012). The optimisation process was crucial to minimise experimental variability and ensure the generation of reliable and consistent results, especially considering that no prior experience in differentiating and culturing hPSCs existed within the laboratory, except for my own expertise.

All experiments were uniformly conducted at the same stage (day 25 for the GSIS and ICC, and day 28 Ca^{2+} imaging). To enhance reliable and consistent results, three distinct technical replicates were performed, and the control (1159) and variant (A251T) iPSC lines were directed differentiated in parallel. Morphological changes were evaluated at each stage of the differentiation process to ensure the quality of β-cell generation. Notably, the transition from 2D to 3D clustering was examined (as indicated in Figure 4.15). These observations, while not quantifiable, can be attributed to accurate cell differentiation.

By comparing the characteristics of β-like cells derived from hESC MEL1, the current β-like cells generation protocol's efficiency and validity was evaluated. The results from the optimisation phase of this chapter indicated successful generation of β-like cells with approximately 60% expressing insulin, 25% expressing the β-cell marker *NKX6.1*, and 40% expressing the β-cell marker *PDX1*. Additionally, the proportion of glucagon-positive cells in the differentiated cell mixture was consistent with previously published findings, accounting for around 15% of the total cell population (Sui, Leibel and Egli, 2018).

In addition to assessing β-cell identity, β-cell function was investigated by evaluating glucose-stimulated insulin secretion to assess the responsiveness of β-cells derived from hESC MEL1 to high-glucose challenges. The MEL1 cells displayed an approximately 100-fold increase in insulin secretion when exposed to high glucose levels compared to low glucose levels. Nonetheless, the assessment of glucose responsiveness in β-cells derived from hESC MEL1 is hindered by substantial variability across experiments. This variability in glucose responsiveness in distinct experiments can likely be attributed to the differentiation efficiency of hESCs into β-like cells, potentially resulting in varying proportions of mature and functional β-cells in each experiments (Karimova, Gvazava and Vorotelyak, 2022).

To account for potential variation between differentiation experiments, it is advisable to monitor cell markers at various stages of differentiation. This approach enables the detection of key markers indicative of the correct cell lineage, serving as a quality control measure to reveal variations that might not be apparent when solely examining

the late stage of differentiation. Additionally, it is essential to verify the presence of cells distinct from pancreatic cells such as enterochromaffin cells, which are intestinal enteroendocrine cells found in the colon. These enterochromaffin cells may be present in differentiated cell clusters at the late stage of differentiation, as evidenced by the expression of endocrine marker genes such as NEUROD1, LMX1A, and CXCL14 (Veres *et al.*, 2019). The existence of enterochromaffin cells can potentially introduce bias into the results. Therefore, including these quality control experiments in this research is crucial for gaining a comprehensive understanding of whether differentiation efficiency remains consistent across experiments and how it may impact the outcomes of late-stage functional experiments (Veres *et al.*, 2019).

Despite these variations, the obtained results validated the effectiveness of β-cell differentiation and set up the experimental conditions to establish the framework for subsequent experiments investigating the effects of the *HNF1A* p.A251T variant on insulin secretion.

The third functional analysis aimed to study the Ca^{2+} dynamics in response to high glucose and, thus, to understand the mechanisms involved in changes in regulated insulin secretion. The results demonstrated that high glucose influenced the Ca^{2+} signalling in islet-like clusters derived from hESC MEL1, showing small oscillatory wave patterns and high responsiveness to KCl-induced depolarisation. Although the changes in Ca^{2+} levels in response to high glucose challenge were not statistically significant in control MEL1 β-cell-like cells, the effects under glucose stimulation (wave-like oscillation patterns) provided valuable insights into the experimental conditions required for studying the impact of the *HNF1A* VUSs.

After optimising the experimental conditions, the functional assessments were conducted to evaluate the β-cells identity and function of β-cell-like cells derived from iPSCs carrying the *HNF1A* p.A251T variant and compared to β-cells derived from iPSCs of a healthy donor (1159).

5.4.2 Functional Assessment Outcomes of A251T Homozygous β-Like Cells

Immunostaining analysis was performed to examine the relative expression of insulin and β-cell markers (*PDX1* and *NKX6.1*) in β-cell-like cells derived from iPSCs A251T and compared to control β-cell-like cells (1159). The results demonstrated a significant decrease in insulin expression in A251T β-cell-like cells compared to control 1159, but there were no differences between the two groups in the expression of the β-cell markers *PDX1* and *NKX6.1.* These findings suggest that the diminished insulin expression in A251T β-cell-like cells is driven by mechanisms other than altered regulation by *HNF1A* of *PDX1* and *NKX6.1,* which are themselves known regulators of insulin gene expression (Aigha and Abdelalim, 2020; Ebrahim, Shakirova and Dashinimaev, 2022).

During the process of directed differentiation, a mixed population of cells, including both α-like cells and β-like cells, was obtained. The ratio of glucagon-positive cells to insulin-producing cells in the A251T β-cell-like cells revealed that the islet-like clusters A251T had a higher proportion of glucagon-positive cells, suggesting a potential bias towards the α-cell fate during their differentiation. This finding is consistent with previous research indicating that a deficiency in *HNF1A* can lead to an increased bias of late stage of directed differentiation towards the α-cell expressing glucagon (Cardenas-Diaz *et al.*, 2019; González *et al.*, 2022b).

The A251T β-like cells exhibited diminished insulin secretion compared to control β-cells under high glucose conditions, indicating impaired differentiated β-cell function. Intriguingly, the impaired glucose-stimulated insulin secretion observed in A251T β-like cells was not rescued by the administration of two-well defined non-nutrient secretagogues, notably the GLP-1 agonist and the sulfonylurea glibenclamide, even though individuals with HNF1A-MODY carrying the *HNF1A* p.A251T variant benefit from sulfonylurea treatment (Misra *et al.*, 2020).

Furthermore, the insulin secretion in response to KCl-induced membrane depolarisation was also reduced in A251T β-like cells, suggesting additional changes, such as a reduction in the number of morphologically docked granules caused by the

HNF1A p.A251T variant, or a lowering in the number of Ca^{2+} channels. Studies using electron microscopy (Olofsson *et al.*, 2002) or near-field (evanescent wave) microscopy (Pinton *et al.*, 2002) would provide suitable means of exploration the first of these possibilities.

The presented data offer novel insights into the impact of the *HNF1A* variant p.A251T on Ca^{2+} dynamic in β-like cell clusters. The findings of the study demonstrate that this genetic variant exerts an influence on Ca^{2+} dynamics when exposed to elevated glucose concentrations. Specifically, the characteristic wave-like oscillations of Ca^{2+} in response to high glucose levels transform into a continuous elevation in Ca^{2+} levels. This alteration in Ca^{2+} signalling is expected to be linked with the disruption of pulsatile insulin secretion, a hallmark feature of diabetes (Klec *et al.*, 2019). This can potentially contribute to the diminished insulin secretion, which is consistent with previous research linking *HNF1A* deficiency to reduced Ca^{2+} levels in response to high glucose levels (González *et al.*, 2022a).

The response of Ca^{2+} influx to glucose slightly differs in native islets. If we were to directly compare the results of this experiment to native islets from healthy donors, including a control group, we would expect a higher proportion of primary islet cells to respond to elevated glucose levels. This discrepancy is due to recent findings that have shown variations in Ca^{2+} influx between the control differentiation clusters and native islets, with higher responses observed in the native islets, even at basal glucose conditions (Balboa *et al.*, 2022).

Further investigations to fully understand the specific molecular mechanisms through which the *HNF1A* variant p.A251T alters Ca^{2+} signalling in β-cells is required. Exploration of the latter possibility could in future be carried out by monitoring Ca^{2+} changes after depolarisation with KCl in the A251T proband-derived and control cells, or through quantification of the expression levels (mRNA) of the channel subunits. Also of interest would be assessments of the changes in Ca^{2+} at the level of individual cells and of the degree of “connectivity” between cells (Johnston *et al.*, 2016; Lei *et al.*, 2018; Salem *et al.*, 2019; Chabosseau *et al.*, 2023).

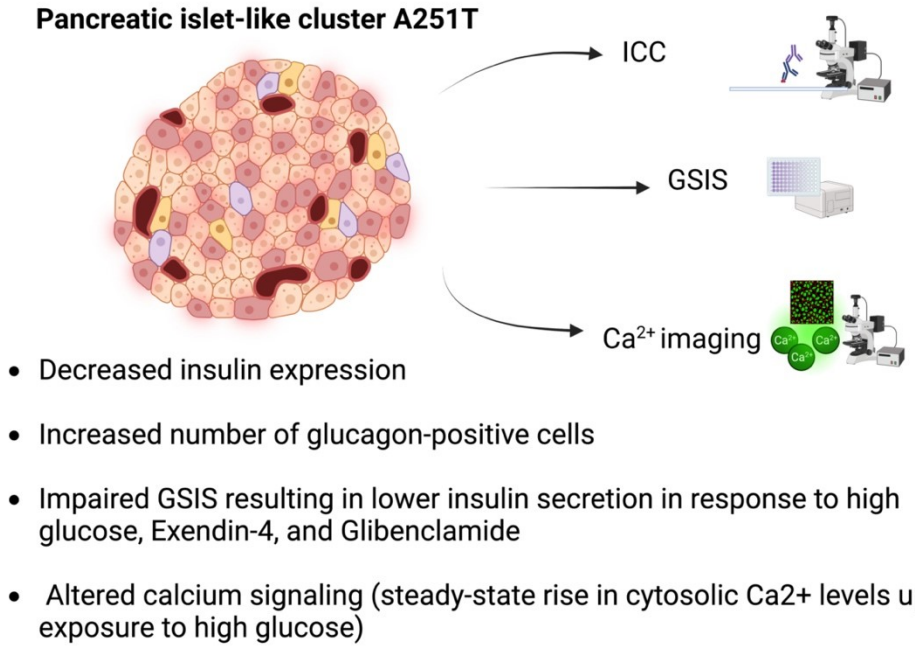

Figure 5.9: **Summary of Phenotypic and Functional Changes in Islet-Like Clusters Derived from iPSCs Carrying the A251T Variant.**

The schematic representation summarises the results of the functional assessment of islet-like clusters derived from iPSCs carrying the *HNF1A* p.A251T variant. The assessment involved key functional analyses: 1) Immunocytochemistry (ICC) staining of insulin and β-cell markers (*PDX1, NKX6.1*) to study β-cell identity, revealing a decrease in the relative expression of insulin; 2) Staining for other cell types present within the islet, specifically α-like cells (glucagon cell staining), demonstrating an increase in glucagon-expressing cells; 3) Glucose-Stimulated Insulin Secretion (GSIS) was performed to evaluate the glucose responsiveness of islets derived from β-cell-like cells. The results demonstrated a decrease in insulin secretion in response to high glucose and secretagogues, including GLP-1 agonists and sulfonylureas; 4) Ca^{2+} imaging to evaluate the Ca^{2+} dynamics in response to high glucose concentration, revealing an altered calcium signalling pattern with a steady-state rise in cytosolic Ca^{2+} levels under high glucose conditions.

5.4.3 Limitations of Methods and Functional Assessment of β-Cells to Understand A251T *HNF1A* Variant Pathogenicity

Functional assessment of β-cell-like cells derived from iPSCs carrying the *HNF1A* p.A251T variant were compared to β-cells derived from iPSCs of a healthy donor (1159). The methodology used in this study has some limitations, which arise from the choice of the control line for the functional assessment. The ideal control for this study would have been an isogenic line, but this was not available due to the unsuccessful generation of a CRISPR-edited A251T hESCs cell line.

As a result, a control iPSCs 1159 derived from a healthy donor was used. While this control line is appropriate for preliminary experiments, it does not allow for definitive assignment of variant *HNF1A* p.A251T pathogenicity. The absence of an isogenic control line makes it difficult to isolate the specific effects of the *HNF1A* p.A251T variant on β-cell function, as inherent genetic variations within the iPSC lines themselves may also contribute to the observed functional differences (Ar, 2017).

Statement of Contribution:

Dr. Pauline Chabosseau, University of Medicine, Department of Medicine, CRCHUM Montreal, conducted the first set of calcium imaging.

Mr. Stephen Rothery, at the FILM facility of Imperial College London, devised a macro using the Fiji software for cell counting purposes. This macro was tailored for the purpose of the experiment of immunofluorescence staining for β-cell markers, insulin, and glucagon.

Publication Acknowledgment:

The methods and results of β-cells derived from MEL-1 hESC line for the two functional assessments including GSIS and immunostaining for insulin, PDX1, NKX6.1, as well as glucagon expression, are revised from manuscript 65530_RE, currently undergoing final revisions before submission to the JOVE journal, for which I am the first author.

6 Chapter 6: Discussion

6.1 Study Context: Uncovering the Pathogenicity of Two *HNF1A* VUSs p.A251T and p.S19L

HNF1A-MODY is typically caused by autosomal dominant mutations in the *HNF1A* gene (McDonald and Ellard, 2013). The identification of MODY-causing mutations is carried out through genome sequencing, either targeting specific MODY genes or analysing the entire genome. When VUS is found within the *HNF1A* gene, it poses a challenge in determining VUS pathogenicity and therefore the carrier's diagnosis. Understanding the pathogenicity of these variants is crucial for implementing targeted treatments as individuals with HNF1A-MODY and HNF4A-MODY show sensitivity to low-dose sulfonylurea therapy, which offers lifestyle improvements compared to insulin injections.

The overall aim of this study was to evaluate the pathogenicity of two *HNF1A* variants, p.A251T and p.S19L, in individuals with early-onset diabetes. To achieve a more precise diagnosis of HNF1A-MODY, a comprehensive method was employed to assess the pathogenicity of the VUS. The investigation followed a stepwise approach, incorporating a multimodal strategy that combined a clinical study, *in vitro* functional analysis of the impact of the VUS on HNF1A protein function, and the examination of the VUS on β-cell function. These findings show promising potential for enhancing diagnostic accuracy for VUS cases. Moreover, this study provided significant insights into the case of *HNF1A* p.A251T variant, representing the first reported case of a hypomorphic *HNF1A* variant inherited in the homozygous state. This novel finding contributes to a better understanding of the distinct effects of heterozygous and homozygous recessive *HNF1A* variants, enriching the knowledge of the genetic basis of HNF1A-MODY.

6.2 Study Outcomes: Uncovering the Pathogenicity of Two *HNF1A* Variants: p.S19L and p.A251T

6.2.1 Study 1: A Cohort Study of the Clinical Characteristics of *HNF1A/HNF4A* VUS

The objective of the clinical study was to investigate if the pathogenicity of *HNF1A* and *HNF4A* VUS could be established solely based on clinical criteria. Three cohorts were examined: the T2D cohort, the HNF1A/HNF4A MODY pathogenic variants cohort, and the cohort of individuals with VUS in the *HNF1A*/*HNF4A* genes. The objective of the study was to compare the clinical characteristics of individuals with *HNF1A* or *HNF4A* VUS and identify specific features that could confidently distinguish between whether the VUS is MODY-causing, benign and of no consequence, or a risk variant for T2D.

The comparison between the T2D and HNF1A/HNF4A-MODY cohorts revealed differences in clinical presentations within each cohort. Individuals with HNF1A/HNF4A-MODY were diagnosed at a younger age and exhibited lower levels of the inflammatory marker hs-CRP compared to the T2D cohort. Additionally, this MODY subgroup displayed lower BMI and waist-to-hip ratio compared to the T2D cohort. In terms of lipid profiles, individuals with HNF1A/HNF4A-MODY had elevated HDL-cholesterol and reduced LDL-cholesterol levels. Employing a multivariable logistic regression approach, significant associations were uncovered between non-insulin dependence, younger age at diagnosis, higher HDL levels, and the likelihood of having HNF1A/HNF4A MODY.

In the evaluation of pathogenicity within the HNF1A/HNF4A-MODY VUS cohort, a thorough analysis of clinical criteria and biomarkers was undertaken, revealing similarities in glycaemic markers (i.e. capillary blood glucose monitoring, HbA1c, etc.), age at diagnosis, and family history across the three cohorts. The common clinical features made it difficult to determine whether the described *HNF1A* or *HNF4A* VUS were benign or pathogenic MODY-associated variants, solely relying on available clinical criteria.

An evaluation of specific clinical features that distinguish between T2D and HNF1A/HNF4A-MODY (identified from the findings Study 2.3.1 and 2.3.3) was undertaken to investigate the feasibility of using these clinical parameters—lipid profiles, insulin independence, BMI, WHR, and hs-CRP—as criteria to potentially classify VUS either as T2D risk factors or as causing MODY. However, it was found that most individuals with VUS did not consistently present criteria that aligned with one specific cohort but rather exhibited a mix of some criteria resembling T2D, while others were closer to the HNF1A/HNF4A-MODY cohort. The overlapping symptoms further complicated the identification of pathogenicity, highlighting the complexity of diagnosing MODY variants.

In summary, this clinical study showed that relying solely on clinical criteria did not lead to confidence in assigning pathogenicity. The study underscored the importance of adopting a multimodal approach beyond clinical criteria to assess pathogenicity of *HNF1A* VUS. By integrating *in silico* and *in vitro* functional assessments alongside clinical data, a more reliable and accurate classification of *HNF1A* VUSs might be achieved.

6.2.2 Study 2: Functional Studies of *HNF1A*, *In Silico* and *In Vitro*

The clinical study's findings were inconclusive in determining confidently the pathogenicity of *HNF1A* and *HNF4A* VUS. To address this limitation, well-established *in vitro* experiments were conducted, involving functional assessments of HNF1A protein overexpressing variant p.S19L and p.A251T. While these experiments successfully predicted the impact of these VUSs on HNF1A protein function, they did not definitively ascertain their pathogenicity.

The functional effects of the *HNF1A* p.S19L and p.A251T variants were initially assessed using *in silico* analysis. Subsequently, *in vitro* assays were performed on various immortalised cell lines to evaluate the transactivation potential, subcellular localisation, DNA binding, and protein expression.

Computational *in silico* predictions of protein structure revealed that the p.S19L variant is likely to destabilise the folded dimeric state of the HNF1A homodimer, potentially

leading to reduced transcriptional activity. *In vitro* experiments confirmed the *in silico* predictions, as the p.S19L variant showed significantly lower transactivation activity compare to WT HNF1A.

On the other hand, the p.A251T variant displayed a more modest reduction of transcriptional activity, which was observed in HeLa cells only, a cell line that lacks endogenous *HNF1A* expression. DNA-binding assays revealed that both the p.S19L and p.A251T variants had non-significant reductions in DNA-binding ability. The subcellular localisation analysis demonstrated that the p.A251T variant exhibited nuclear localisation similar to WT. Conversely, the p.S19L variant displayed compromised nuclear transport compared to WT, with diminished nuclear accumulation and abnormal increase of cytoplasmic localisation of HNF1A protein.

The findings of this study provide valuable insights into the functional implications of the p.S19L and p.A251T variants for HNF1A protein function and shed light on their potential roles in disease pathogenesis. The p.A251T variant has decreased transcriptional activity in only one cell type compared to WT, while exhibiting similar DNA binding affinity and subcellular localisation. The functional assay outcomes reveal a multifaceted impact of the p.A251T variant, yet but they do not provide a precise understanding of how this variant negatively affects the transcriptional function of HNF1A.

The study reveals that the functional effects of *HNF1A* VUSs vary depending on the specific cellular context and the cell type used. Notably, there were significant differences in transactivation activity for both p.S19L and p.A251T variants between Endoc-BH3 and HeLa cell lines, and HeLa cells. These variations limit the suitability of this method for confidently determining pathogenicity and underscore the need for additional investigations to achieve a comprehensive understanding of the overall impact exerted by these variants.

These results provide limited clarity on the pathogenicity of *HNF1A* VUS and establish a basis for the following section, which introduces innovative methods to better comprehend the pathways through which this variant exerts its effects.

6.2.3 Study 3: Functional Assay of A251T β-Like Cells

The initial *in vitro* functional assays (described in Chapter 3) have inherent limitations. Therefore, it appeared essential to supplement the *in vitro* study with functional investigations in relevant cellular models to gain a comprehensive understanding of the impact of VUS on disease pathogenesis.

Specifically, the functional assessment did not yield conclusive evidence to definitively attribute pathogenicity to the *HNF1A* p.A251T variant. It revealed a modest impairment in transactivation, unrelated to DNA binding or subcellular localisation of the HNF1A protein. These findings underscore a multifaceted impact of the p.A251T variant that warrants further investigation.

This subsequent study aimed to generate a human pluripotent stem cell line carrying the *HNF1A* variant p.A251T, to gain further insights into its functional impact. This process involved generating iPSCs from skin biopsies of individuals with the *HNF1A* p.A251T variant, followed by thorough validation to ensure pluripotency. The iPSCs were then directed differentiate into β-like cells.

For the optimisation of functional assessments in β-like cells, the MEL1 hESC line was used, featuring an INS-GFP reporter to facilitate the process monitoring. The β-cell directed differentiation successfully yielded β-like cells with a high proportion expressing insulin (over 50%), and essential β-cell signature genes *PDX1* and *NKX6.1*. The MEL1 β-cell-like cells did not exhibited glucose responsiveness in response to high glucose challenge.

Following this, the evaluation of Ca^{2+} dynamics in MEL1 islet-like clusters revealed changes in cytosolic Ca2+ levels upon exposure to elevated glucose concentration and KCl, accompanied by the characteristic oscillatory pattern of Ca^{2+} in response to glucose stimulation. This preliminary functional experiment established the experimental conditions utilised for the subsequent analysis of β-like cells carrying the *HNF1A* p.A251T variant.

After the successful optimisation of experimental parameters in islet-like clusters derived from MEL1 hESCs, functional assessments were performed on β-cell-like cells carrying the *HNF1A* p.A251T variant.

β-like cells carrying the *HNF1A* p.A251T variant exhibited a significant decrease in insulin relative expression compared to control islet-like clusters derived from iPSCs from healthy donors. β-like cells A251T show impaired GSIS with reduced insulin secretion in response to high glucose and KCl-induced depolarisation, indicating potential defects in β-cell insulin secretion function associated with the *HNF1A* p.A251T variant. The impaired glucose-stimulated insulin secretion in A251T β-like cells was not rescued by secretagogues like Exendin-4 or sulfonylurea, in contrast to the observed benefits of sulfonylurea treatment in individuals with HNF1A-MODY carrying the *HNF1A* p.A251T variant.

The study investigated the underlying mechanism of this defect and found that in A251T β-like cells, the Ca^{2+} dynamics in response to elevated glucose oscillation pattern was abnormal. Specifically, a constant rise pattern of Ca^{2+} entry into the cytosol was observed, indicating the absence of oscillation with “wave”-like typical pattern. The altered Ca^{2+} signalling response suggests a potential mechanism for the reduced insulin secretion observed in response to high glucose.

Within the context of *HNF1A* variants, it is plausible that specific variants may exert an impact on insulin expression and Ca^{2+} dynamics, even in the absence of direct alterations to DNA-binding capability, subcellular localisation, or overall protein expression. This phenomenon could be attributed to the intricate network of molecular interactions occurring within the β-cell environment, where HNF1A acts as a modulator of signalling cascades. The modest reduction in transactivation activity, as evidenced by functional assessments, could potentially trigger subtle changes in the expression of critical genes and pathways involved in insulin synthesis and signalling, as well as Ca2+ signalling. Consequently, the overall insulin expression and Ca^{2+} dynamics within β-cells could undergo significant modifications through indirect mechanisms prompted by *HNF1A* p. A251T variants.

The A251T variant appears to hinder the relative expression of the insulin gene in β-cells, potentially contributing to the development of early-onset diabetes observed in the proband carrying this variant. A more in-depth investigation is warranted to better understand the precise genes that could be affected by the diminished transcriptional activity.

6.2.4 Contributions of a Study on *HNF1A* VUS

The present study focused specifically on exploring the functional consequences of two variants, p.S19L and p.A251T, in the *HNF1A* gene. By conducting comprehensive, *in silico* and *in vitro* characterisations, the research aimed to gain insights into these variants´ pathogenicity and their potential contributions to disease development. The study successfully elucidated the functional effects of the p.S19L and p.A251T variants on HNF1A using various cell lines.

The computational predictions aligned with *in vitro* findings, supporting the hypothesis that both VUSs impact HNF1A function and contribute to MODY pathogenesis. The β-like model provided valuable insights into the mechanism underlying defect in insulin secretion and its contribution to MODY disease progression for the p.A251T variant. Regarding the p.S19L variant, additional *in vitro* experiments are necessary to confidently ascertain its VUS pathogenicity, given that a β-cell-like model for p.S19L was not generated in this study. Further investigations will play a crucial role in assigning the pathogenicity of this variant.

6.3 Comparison of Study Findings with Existing Research

6.3.1 Pathophysiology of Insulin Secretion Defects

One of this study´s main findings pertain to the mechanism of pathophysiology observed in human stem cell-derived β-cells carrying the *HNF1A* p.A251T variant. The study's findings on insulin secretion defects are consistent with previous research on HNF1A-MODY, which is characterised by reduced insulin secretion before the onset of diabetes in affected individuals (Byrne *et al.*, 1996, p. 12).

These results are consistent with observations of *HNF1A* deficiency in various functional investigations both *in vitro* and *ex vivo*. For instance, similar observations were made in *ex vivo* islets from Hnf1a-null mice and MIN6 cells expressing a dominant negative mutant of *HNF1A* p.291fsinsC, which also showed impaired insulin secretion responses (Pontoglio *et al.*, 1998; Tanizawa *et al.*, 1999). Similarly, investigations in *ex vivo* islets human islets from an individual carrying the *HNF1A* p.T260M variant revealed reduced insulin secretion under glucose challenge (Haliyur *et al.*, 2019). HNF1A-deficient β-cells, in addition to β-cells derived from iPSCs carrying the MODY-causing heterozygous mutation HNF1A (p.H126D), exhibit a substantial reduction in insulin secretion, affecting both basal and glucose-stimulated insulin secretion, and this outcome can be attributed to alterations in glucose metabolism (Cardenas-Diaz *et al.*, 2019; Low *et al.*, 2021; González *et al.*, 2022b).

In conclusion, our results provide evidence supporting the impact of the *HNF1A* p.A251T variant on insulin secretion in β-like cells and confirm that it is pathogenic. These collective data underscore the critical role of *HNF1A* in regulating insulin secretion.

6.3.2 Mechanisms Underlying the Defect of Insulin Secretion

The study revealed that the *HNF1A* p.A251T variant had an impact on Ca^{2+} dynamics under high glucose conditions, which could be a potential mechanism contributing to impaired insulin secretion. The alterations in Ca^{2+} signalling was characterised by a potential loss of the typical wave-like response upon high glucose stimulation. Instead, there was a steady-state rise in cytosolic Ca^{2+} levels. This loss of wave-like oscillations might be associated with the early progression of diabetes, leading to a reduction in pulsatile insulin secretion and decreased glucose responsiveness of β-cells over time (O'Rahilly, Turner and Matthews, 1988; Bingley *et al.*, 1992).

A previous study using islets from mice with *HNF1A* deficiency have reported a reduced Ca^{2+} cytosolic levels in response to high glucose (Uchizono *et al.*, 2009). Similar results were found with β-like cells derived from hESC-derived *HNF1A* KO β-like cells with significant reduction in Ca^{2+} cytosolic levels compared to *HNF1A* WT β-

like cells (González *et al.*, 2022a). In the latter study, single-cell RNA sequencing of *HNF1A* KO β-like cells revealed a reduction in intracellular Ca^{2+} signalling gene expression (*CACNA1A, S100A6, and TMEM37*) and in a gene associated with calcium-mediated insulin secretion (*KCNH6*) (González *et al.*, 2022a).

The data presented here suggest that *HNF1A* plays a critical role in regulating Ca^{2+} signalling in β-cells. Although the homozygous *HNF1A* p.A251T variant did not exhibit a significant reduction in Ca^{2+} influx as observed in *HNF1A* KO β-like cells, the change in pattern of Ca^{2+} influx a sufficient alteration to alter Ca^{2+} dynamic of β-cells and subsequently insulin secretion. The difference in apparent Ca^{2+} changes between *HNF1A* KO β-like cells and homozygous *HNF1A* A251T β-cells suggests that the latter may have specific molecular mechanisms induce by the *HNF1A* p.A251T specific genetic variant. The complexity of these genetic and regulatory factors may contribute to the variability and transcriptional and genome expression patterns of *HNF1A* A251T β-cells need to be further investigate.

In contrast to prior literature on *HNF1A* deficiency, a recent study has revealed distinct mechanisms underlying the development of MODY. This research provides evidence that the β-cell functional defect observed in patients with HNF1A-MODY may originate from hypersecretion of insulin associated with increased Ca^{2+} signalling, which diverges from the previously proposed mechanism linking reduced insulin secretion to diminished Ca^{2+} signalling. The observed increase in Ca^{2+} influx in β-cells derived from iPSCs of individuals with HNF1A-MODY, carrying the MODY-causing mutation *HNF1A* p.R272C, is attributed to enhanced membrane depolarisation in response to glucose stimulation (Hermann *et al.*, 2023). This mechanism has been found in rare instances of HNF1A MODY-causing mutations associated with congenital hyperinsulinism (Stanescu *et al.*, 2012). A more comprehensive investigation into the mechanisms underlying HNF1A-MODY is essential for understanding whether these findings are due to a specific mutation or whether they can be extended to other cellular models of *HNF1A* deficiency.

6.3.3 Alpha Cell Differentiation Bias

This study revealed another mechanism associated with the homozygous *HNF1A* p.A251T mutation, which involves a higher proportion of glucagon-positive cells in the islet-like clusters. This increase in glucagon-positive produce by directed differentiation has been previously described and suggests a potential bias towards the α-cell fate during the during directed differentiation of these cells (Cardenas-Diaz *et al.*, 2019; González *et al.*, 2021). The mechanism underlying the increase in α-cells in islet-like clusters derived from hPSCs carrying *HNF1A* mutations has been predicted to be a transcriptional bias favouring the α-cell fate by the up-regulation of glucagon gene expression (Cardenas-Diaz *et al.*, 2019; González *et al.*, 2021). In addition, islet-like clusters derived from hESC-derived *HNF1A* KO cells revealed a decrease in the insulin-positive population. This decrease was accompanied by a downregulation of insulin gene expression (González *et al.*, 2021), as previously shown (Wang *et al.*, 2000; Cardenas-Diaz *et al.*, 2019).

The functional investigation of A251T β-cell-like cells suggests that *HNF1A* plays a role in regulating the relative expression of insulin. These findings underscore the altered function of A251T β-cell-like cells and its influence on the balance between α- and β-cells in islet like clusters suggesting a bias towards the α-cell fate during directed differentiation.

6.4 Limitations of the Study and Their Implications for Future Research

6.5 Clinical study

In the clinical investigation, a potential limitation arises from the relatively small number of individuals in the VUS cohort, which consisted of only six cases. This limited sample size may hinder the ability to establish predictive clinical characteristics and criteria for diagnosing HNF1A-MODY.

The limited sample size of this study, consisting of only 15 cases of MODY HNF1A/HNF4A and 6 cases of VUS, has implications for the statistical power and

precision of the results. This limitation restricts the extent to which the clinical findings can contribute to research on the potential of clinical features to attribute VUS pathogenicity. Consequently, the clinical study was unable to comprehensively assess metrics such as sensitivity and specificity, which are essential for evaluating the diagnostic performance of genetic variants within a clinical context.

To overcome this limitation, larger cohorts of individuals with VUS should be studied. However, this introduces an additional limitation, as the identification of VUS relies on genetic sequencing, which is conducted when clinical criteria for suspected MODY prompt sequencing of the individual. Nonetheless, the pool of individuals selected for genetic sequencing remains restricted, underscoring the need for enhanced diversity in variant databases. Moreover, the financial aspect of DNA sequencing must be considered, recognising that not all clinical studies have access to sequencing technologies.

These limitations underscore the need for a comprehensive and robust approach to studying VUS. Integrating multimodal study, including clinical information and *in vitro* functional assays, to understand the effects of novel variants and VUSs on gene function and disease pathogenesis. Moreover, efforts to increase the size and diversity of cohorts and implement cost-effective sequencing strategies are crucial in advancing our knowledge of HNF1A-MODY VUSs.

6.5.1.1 Immortalised Cell Lines: A Functional assessment Tool with Limitations

The main limitation of using immortalised cell types such as HeLa and INS1 for studying the impact of *HNF1A* VUS is that these cell lines may not represent accurately the cellular physiological environment needed to understand the functional impact of the VUS. Immortalised cell lines are derived from cancer cells or immortalised *in vitro* cells, and they often lack the cell-specific functions and regulatory mechanisms that are present in primary cells.

In the context of HNF1A-MODY, *HNF1A* plays a critical role in regulating gene expression in pancreatic β-cells, the use of immortalised cell lines derived from Rat insulinoma (INS1) (Asfari *et al.*, 1992) and cervical cancer (HeLa) (Culliton, 1974) may

not replicate the complex regulatory network and physiological functions of *HNF1A*. Consequently, these cell lines may not accurately mimic the impact of VUS in a normal cellular context(Pan *et al.*, 2009).

All functional assessments conducted utilised overexpressed variant constructs which do not reflect accurately the physiological levels of the *HNF1A* variant protein. This difference can potentially result in non-physiological effects and interactions within the cell, leading to a misinterpretation of the variant's true functional impact on HNF1A protein function. *In vivo*, the expression of proteins is tightly regulated through various mechanisms (e.g., transcriptional control and post-transcriptional modifications) which are not reflected in the *in vitro* overexpressed variant functional assessments (Prelich, 2012; Moriya, 2015). Additionally, overexpression of mutant proteins lead to cellular stress or toxicity, which further complicate the interpretation of functional assessment results (Prelich, 2012; Moriya, 2015).

In summary, functional assessment of the impact of the *HNF1A* p.A251T variant in immortalised cell lines have not been solely considered when determining its pathogenicity. The complemented *in vitro* investigation of β-cell-like cells allows one to assign pathogenicity of the variant more accurately.

As for the *HNF1A* p.S19L variant, its pathogenicity remains unclear *in vitr*o, and the inability to generate β-cell-like cells prevents an accurate assignment of its pathogenicity. Further research is needed to fully understand the implications of the *HNF1A* p.S19L variant by generating a β-cell-like cell model that expresses the variant, and ideally isogenic control.

6.5.1.2 hPSC isogenic line as control for *HNF1A* p.A251T functional assessment

The absence of isogenic cell lines in the *HNF1A* p.A251T genetic impact study presents a significant issue, as it hinders the precise assessment of the variant's effects alone. The β-cell-like cells derived from a healthy donor, used as a control, are not genetically identical to the ones carrying the *HNF1A* p.A251T variant. This limitation is essential because without isogenic lines, comparing the effects of the specific variant can be confounded by genetic heterogeneity.

As a result, observed cellular differences in the β-cell-like cells, when compared to the control derived from a healthy donor (1159), could potentially be attributed to the *HNF1A* p.A251T genetic variant or other background genetic variations across all functional assessments.

Despite the existing limitations, the comparison between control derived from healthy donor and *HNF1A* p.A251T cells revealed significant differences, demonstrating the potential impact of the genetic variant. However, generating isogenic cell lines for this study is crucial as it will create a controlled experimental setting, allowing for a more accurate assessment of the specific effects of *HNF1A* p.A251T.

6.5.1.3 β-Cell-Like Cell Functional Impact of *HNF1A* p.A251T *In Vitro*

The direct differentiation of hPSCs into β-cell-like cells approach has certain limitations. Despite significant progress in optimising differentiation protocols to increase the proportion of mature insulin-secreting cells, the resulting β-like cells often exhibit varying degrees of maturity, functionality, and heterogeneity in their phenotype (Shahjalal *et al.*, 2018; Balboa *et al.*, 2022; Karimova, Gvazava and Vorotelyak, 2022).

This heterogeneity can complicate the interpretation of experimental results and hinder the establishment of consistent and reproducible research. Moreover, the derived β-like cells may not fully recapitulate the functional characteristics of mature pancreatic β-cells *in vivo.*

While these cells may express some β-cell markers and exhibit glucose responsiveness, they might not possess the same level of complexity and functionality as primary β-cell. Variations in insulin secretion capacity, calcium dynamics, and other critical cellular processes can limit the reliability and translatability of findings obtained from these cell models (Shahjalal *et al.*, 2018; Balboa *et al.*, 2022; Karimova, Gvazava and Vorotelyak, 2022).

Another limitation is that the differentiation process itself can be time-consuming and costly. It requires extensive optimisation and validation to generate a functional and homogenous β-cell population.

The limitations inherent in the β-cell-like cell approach imply that cells carrying the *HNF1A* p.A251T variant may not precisely replicate the functional effects associated with the variant. For instance, the observed bias towards α-cells might, to some extent, stem from heterogeneity in β-cell generation during the process of directed differentiation.

Despite the mentioned limitations, the outcomes of the functional assessments conducted on A251T β-cell-like cells revealed minimal variability among technical replicates and exhibited statistically significant effects. This provides greater confidence in associating the impact of the *HNF1A* p.A251T variant with the observed effects on β-cell-like cell function.

6.5.1.4 The Study's Contributions to assigning VUS pathogenicity: A Summary

This thesis highlights the value of a multimodal approach to investigate the pathogenicity of *HNF1A* VUS, combining clinical, *in silic*o predictions, *in vitro* functional assays in established immortalised cell lines, and *in vitro* β-cell-like cell assessments to understand the mechanisms underlying MODY phenotypes.

By integrating combined clinical data and functional assessment this study provides crucial insights into the impact of the two VUS sequenced in individuals with young onset diabetes *HNF1A* p.S19L, and p.A251T. This comprehensive approach enhances the accuracy of variant classification for *HNF1A* VUS cases.

While *in silico* predictions and clinical characteristics offer initial insights, they may not be sufficient for definitive variant pathogenicity assignment. Incorporating functional assessments in human β-cell-like cells provides a more robust understanding of the *HNF1A* p.S19L, and p.A251T variant's effects.

This study successfully elucidated the impact of a VUS *HNF1A* p.A251T variant associated with MODY. The findings from functional assessment of human β-cell-like cells derived from A251T iPSCs provided valuable insights into the variant's effects, revealing impaired insulin expression and secretion, as well as altered glucose-induced Ca^{2+} signalling. This human β-cell model thus bridges the gap between rodent models and clinical presentation in HNF1A-MODY, offering a relevant platform for studying HNF1A-MODY phenotype.

Overall, this study underscores the significance of human β-cell models in understanding the pathogenicity of VUS *HNF1A* variants and contributes significantly to our knowledge of MODY genetics. The study's comprehensive methods aim to enhance the management of HNF1A-MODY by addressing challenges in accurate diagnosis and therapeutic strategies, thus optimising patient care for affected individuals.

References

Adzhubei, I.A. *et al.* (2010) 'A method and server for predicting damaging missense mutations', *Nature Methods*, 7(4), pp. 248–249. Available at: https://doi.org/10.1038/nmeth0410-248.

Aguayo-Mazzucato, C. *et al.* (2013) 'Thyroid hormone promotes postnatal rat pancreatic β-cell development and glucose-responsive insulin secretion through MAFA', *Diabetes*, 62(5), pp. 1569–1580. Available at: https://doi.org/10.2337/db12-0849.

Aguayo-Mazzucato, C. and Bonner-Weir, S. (2010) 'Stem cell therapy for type 1 diabetes mellitus', *Nature Reviews Endocrinology*, 6(3), pp. 139–148. Available at: https://doi.org/10.1038/nrendo.2009.274.

Aguilar-Bryan, L. and Bryan, J. (2008) 'Neonatal diabetes mellitus', *Endocrine Reviews*, 29(3), pp. 265–291. Available at: https://doi.org/10.1210/er.2007-0029.

Aigha, I.I. and Abdelalim, E.M. (2020) 'NKX6.1 transcription factor: a crucial regulator of pancreatic β cell development, identity, and proliferation', *Stem Cell Research & Therapy*, 11(1), p. 459. Available at: https://doi.org/10.1186/s13287-020-01977-0.

Al-Attar, S. *et al.* (2011) 'Clustered regularly interspaced short palindromic repeats (CRISPRs): the hallmark of an ingenious antiviral defense mechanism in prokaryotes', *Biological Chemistry*, 392(4), pp. 277–289. Available at: https://doi.org/10.1515/BC.2011.042.

Alfa, R.W. *et al.* (2015) 'Suppression of Insulin Production and Secretion by a Decretin Hormone', *Cell metabolism*, 21(2), pp. 323–333. Available at: https://doi.org/10.1016/j.cmet.2015.01.006.

Ali, O. (2013) 'Genetics of type 2 diabetes', *World Journal of Diabetes*, 4(4), pp. 114–123. Available at: https://doi.org/10.4239/wjd.v4.i4.114.

Al-Khawaga, S. *et al.* (2018) 'Pathways governing development of stem cell-derived pancreatic β cells: lessons from embryogenesis', *Biological Reviews*, 93(1), pp. 364–389. Available at: https://doi.org/10.1111/brv.12349.

Althari, S. *et al.* (2020) 'Unsupervised Clustering of Missense Variants in HNF1A Using Multidimensional Functional Data Aids Clinical Interpretation', *American Journal of Human Genetics*, 107(4), pp. 670–682. Available at: https://doi.org/10.1016/j.ajhg.2020.08.016.

Althari, S. and Gloyn, A.L. (2015) 'When is it MODY? Challenges in the Interpretation of Sequence Variants in MODY Genes', *The Review of Diabetic Studies : RDS*, 12(3–4), pp. 330–348. Available at: https://doi.org/10.1900/RDS.2015.12.330.

Aly, R.M. (2020) ‘Current state of stem cell-based therapies: an overview’, *Stem Cell Investigation*, 7, p. 8. Available at: https://doi.org/10.21037/sci-2020-001.

American Diabetes Association (2009) ‘Diagnosis and Classification of Diabetes Mellitus’, *Diabetes Care*, 32(Supplement_1), pp. S62–S67. Available at: https://doi.org/10.2337/dc09-S062.

American Diabetes Association (2011) ‘Diagnosis and classification of diabetes mellitus’, *Diabetes Care*, 34 Suppl 1(Suppl 1), pp. S62-69. Available at: https://doi.org/10.2337/dc11-S062.

American Diabetes Association (2020) ‘2. Classification and Diagnosis of Diabetes: Standards of Medical Care in Diabetes—2021’, *Diabetes Care*, 44(Supplement_1), pp. S15–S33. Available at: https://doi.org/10.2337/dc21-S002.

Anık, A. *et al.* (2015) ‘Maturity-onset diabetes of the young (MODY): an update’, *Journal of pediatric endocrinology & metabolism: JPEM*, 28(3–4), pp. 251–263. Available at: https://doi.org/10.1515/jpem-2014-0384.

Anzalone, A.V. *et al.* (2019) ‘Search-and-replace genome editing without double-strand breaks or donor DNA’, *Nature*, 576(7785), pp. 149–157. Available at: https://doi.org/10.1038/s41586-019-1711-4.

Ar, B. (2017) ‘Editing the genome of hiPSC with CRISPR/Cas9: disease models’, *Mammalian genome : official journal of the International Mammalian Genome Society*, 28(7–8). Available at: https://doi.org/10.1007/s00335-017-9684-9.

Arnes, L. *et al.* (2012) ‘Ghrelin Expression in the Mouse Pancreas Defines a Unique Multipotent Progenitor Population’, *PLoS ONE*, 7(12), p. e52026. Available at: https://doi.org/10.1371/journal.pone.0052026.

Asfari, M. *et al.* (1992) ‘Establishment of 2-mercaptoethanol-dependent differentiated insulin-secreting cell lines’, *Endocrinology*, 130(1), pp. 167–178. Available at: https://doi.org/10.1210/endo.130.1.1370150.

Atkinson, M.A., Eisenbarth, G.S. and Michels, A.W. (2014) ‘Type 1 diabetes’, *The Lancet*, 383(9911), pp. 69–82. Available at: https://doi.org/10.1016/S0140-6736(13)60591-7.

Babiss, L.E. *et al.* (1987) ‘Factors that interact with the rat albumin promoter are present both in hepatocytes and other cell types’, *Genes & Development*, 1(3), pp. 256–267. Available at: https://doi.org/10.1101/gad.1.3.256.

Bakhti, M., Böttcher, A. and Lickert, H. (2019) ‘Modelling the endocrine pancreas in health and disease’, *Nature Reviews Endocrinology*, 15(3), pp. 155–171. Available at: https://doi.org/10.1038/s41574-018-0132-z.

Balboa, D. *et al.* (2022) ‘Functional, metabolic and transcriptional maturation of human pancreatic islets derived from stem cells’, *Nature Biotechnology*, 40(7), pp. 1042–1055. Available at: https://doi.org/10.1038/s41587-022-01219-z.

Balboa, D., Saarimäki-Vire, J. and Otonkoski, T. (2019) ‘Concise Review: Human Pluripotent Stem Cells for the Modeling of Pancreatic β-Cell Pathology’, *Stem Cells (Dayton, Ohio)*, 37(1), pp. 33–41. Available at: https://doi.org/10.1002/stem.2913.

Bastidas-Ponce, A. *et al.* (2017) ‘Cellular and molecular mechanisms coordinating pancreas development’, *Development (Cambridge, England)*, 144(16), pp. 2873–2888. Available at: https://doi.org/10.1242/dev.140756.

Baumhueter, S. *et al.* (1990) ‘HNF-1 shares three sequence motifs with the POU domain proteins and is identical to LF-B1 and APF’, *Genes & Development*, 4(3), pp. 372–379. Available at: https://doi.org/10.1101/gad.4.3.372.

Bellanné-Chantelot, C. *et al.* (2004) ‘Clinical spectrum associated with hepatocyte nuclear factor-1beta mutations’, *Annals of Internal Medicine*, 140(7), pp. 510–517. Available at: https://doi.org/10.7326/0003-4819-140-7-200404060-00009.

Bellanné-Chantelot, C. *et al.* (2008) ‘The type and the position of HNF1A mutation modulate age at diagnosis of diabetes in patients with maturity-onset diabetes of the young (MODY)-3’, *Diabetes*, 57(2), pp. 503–508. Available at: https://doi.org/10.2337/db07-0859.

Benazra, M. *et al.* (2015) ‘A human beta cell line with drug inducible excision of immortalizing transgenes’, *Molecular Metabolism*, 4(12), pp. 916–925. Available at: https://doi.org/10.1016/j.molmet.2015.09.008.

Berget, C., Messer, L.H. and Forlenza, G.P. (2019) ‘A Clinical Overview of Insulin Pump Therapy for the Management of Diabetes: Past, Present, and Future of Intensive Therapy’, *Diabetes Spectrum : A Publication of the American Diabetes Association*, 32(3), pp. 194–204. Available at: https://doi.org/10.2337/ds18-0091.

Bhushan, A. *et al.* (2001) ‘Fgf10 is essential for maintaining the proliferative capacity of epithelial progenitor cells during early pancreatic organogenesis’, *Development (Cambridge, England)*, 128(24), pp. 5109–5117. Available at: https://doi.org/10.1242/dev.128.24.5109.

Bingley, P.J. *et al.* (1992) ‘Loss of regular oscillatory insulin secretion in islet cell antibody positive non-diabetic subjects’, *Diabetologia*, 35(1), pp. 32–38. Available at: https://doi.org/10.1007/BF00400849.

Bjørkhaug, L. *et al.* (2003) ‘Hepatocyte nuclear factor-1 alpha gene mutations and diabetes in Norway’, *The Journal of Clinical Endocrinology and Metabolism*, 88(2), pp. 920–931. Available at: https://doi.org/10.1210/jc.2002-020945.

Blanchi, B. *et al.* (2023) ‘EndoC-βH5 cells are storable and ready-to-use human pancreatic beta cells with physiological insulin secretion’, *Molecular Metabolism*, 76, p. 101772. Available at: https://doi.org/10.1016/j.molmet.2023.101772.

Bluestone, J.A., Buckner, J.H. and Herold, K.C. (2021) ‘Immunotherapy: Building a bridge to a cure for type 1 diabetes’, *Science (New York, N.Y.)*, 373(6554), pp. 510–516. Available at: https://doi.org/10.1126/science.abh1654.

Boj, S.F. *et al.* (2001) ‘A transcription factor regulatory circuit in differentiated pancreatic cells’, *Proceedings of the National Academy of Sciences of the United States of America*, 98(25), pp. 14481–14486. Available at: https://doi.org/10.1073/pnas.241349398.

Bonnefond, A. *et al.* (2012) ‘Whole-exome sequencing and high throughput genotyping identified KCNJ11 as the thirteenth MODY gene’, *PloS One*, 7(6), p. e37423. Available at: https://doi.org/10.1371/journal.pone.0037423.

Bonnefond, A. *et al.* (2023) ‘Monogenic diabetes’, *Nature Reviews. Disease Primers*, 9(1), p. 12. Available at: https://doi.org/10.1038/s41572-023-00421-w.

Bonner, C. *et al.* (2015) ‘Inhibition of the glucose transporter SGLT2 with dapagliflozin in pancreatic alpha cells triggers glucagon secretion’, *Nature Medicine*, 21(5), pp. 512–517. Available at: https://doi.org/10.1038/nm.3828.

Bowman, P. *et al.* (2012) ‘Heterozygous ABCC8 mutations are a cause of MODY’, *Diabetologia*, 55(1), pp. 123–127. Available at: https://doi.org/10.1007/s00125-011-2319-x.

Braverman-Gross, C. and Benvenisty, N. (2021) ‘Modeling Maturity Onset Diabetes of the Young in Pluripotent Stem Cells: Challenges and Achievements’, *Frontiers in Endocrinology*, 12, p. 622940. Available at: https://doi.org/10.3389/fendo.2021.622940.

Brissova, M. *et al.* (2006) ‘Pancreatic islet production of vascular endothelial growth factor--a is essential for islet vascularization, revascularization, and function’, *Diabetes*, 55(11), pp. 2974–2985. Available at: https://doi.org/10.2337/db06-0690.

Buchanan, T.A. and Xiang, A.H. (2005) ‘Gestational diabetes mellitus’, *The Journal of Clinical Investigation*, 115(3), pp. 485–491. Available at: https://doi.org/10.1172/JCI24531.

Buganim, Y., Faddah, D.A. and Jaenisch, R. (2013) ‘Mechanisms and models of somatic cell reprogramming’, *Nature reviews. Genetics*, 14(6), pp. 427–439. Available at: https://doi.org/10.1038/nrg3473.

Buteau, J. *et al.* (1999) ‘Glucagon-like peptide-1 promotes DNA synthesis, activates phosphatidylinositol 3-kinase and increases transcription factor pancreatic and duodenal homeobox gene 1 (PDX-1) DNA binding activity in beta (INS-1)-cells’,

Diabetologia, 42(7), pp. 856–864. Available at: https://doi.org/10.1007/s001250051238.

Byrne, M.M. *et al.* (1996) 'Altered insulin secretory responses to glucose in diabetic and nondiabetic subjects with mutations in the diabetes susceptibility gene MODY3 on chromosome 12', *Diabetes*, 45(11), pp. 1503–1510. Available at: https://doi.org/10.2337/diab.45.11.1503.

Cabrera, O. *et al.* (2006) 'The unique cytoarchitecture of human pancreatic islets has implications for islet cell function', *Proceedings of the National Academy of Sciences of the United States of America*, 103(7), pp. 2334–2339. Available at: https://doi.org/10.1073/pnas.0510790103.

Cardenas-Diaz, F.L. *et al.* (2019) 'Modeling Monogenic Diabetes using Human ESCs Reveals Developmental and Metabolic Deficiencies Caused by Mutations in HNF1A', *Cell Stem Cell*, 25(2), pp. 273-289.e5. Available at: https://doi.org/10.1016/j.stem.2019.07.007.

Cauchi, S. and Froguel, P. (2008) 'TCF7L2 genetic defect and type 2 diabetes', *Current Diabetes Reports*, 8(2), pp. 149–155. Available at: https://doi.org/10.1007/s11892-008-0026-x.

Chabosseau, P. *et al.* (2023) 'Molecular phenotyping of single pancreatic islet leader beta cells by "Flash-Seq"', *Life Sciences*, 316, p. 121436. Available at: https://doi.org/10.1016/j.lfs.2023.121436.

Chakera, A.J. *et al.* (2015) 'Recognition and Management of Individuals With Hyperglycemia Because of a Heterozygous Glucokinase Mutation', *Diabetes Care*, 38(7), pp. 1383–1392. Available at: https://doi.org/10.2337/dc14-2769.

Chang, H.H.Y. *et al.* (2017) 'Non-homologous DNA end joining and alternative pathways to double-strand break repair', *Nature Reviews. Molecular Cell Biology*, 18(8), pp. 495–506. Available at: https://doi.org/10.1038/nrm.2017.48.

Chapman, N.M. *et al.* (2012) 'The microbiology of human hygiene and its impact on type 1 diabetes', *Islets*, 4(4), pp. 253–261. Available at: https://doi.org/10.4161/isl.21570.

Chen, C. *et al.* (2018) 'The Roles of Thyroid and Thyroid Hormone in Pancreas: Physiology and Pathology', *International Journal of Endocrinology*, 2018, p. 2861034. Available at: https://doi.org/10.1155/2018/2861034.

Chen, Y. *et al.* (2015) 'Engineering Human Stem Cell Lines with Inducible Gene Knockout using CRISPR/Cas9', *Cell Stem Cell*, 17(2), pp. 233–244. Available at: https://doi.org/10.1016/j.stem.2015.06.001.

Chhabra, K.H. *et al.* (2013) 'Pancreatic angiotensin-converting enzyme 2 improves glycemia in angiotensin II-infused mice', *American Journal of Physiology.*

Endocrinology and Metabolism, 304(8), pp. E874-884. Available at: https://doi.org/10.1152/ajpendo.00490.2012.

Chi, Y.-I. *et al.* (2002) 'Diabetes mutations delineate an atypical POU domain in HNF-1alpha', *Molecular Cell*, 10(5), pp. 1129–1137. Available at: https://doi.org/10.1016/s1097-2765(02)00704-9.

Chi, Y.-I. (2005) 'Homeodomain revisited: a lesson from disease-causing mutations', *Human Genetics*, 116(6), pp. 433–444. Available at: https://doi.org/10.1007/s00439-004-1252-1.

Chiu, K.C. *et al.* (2000) 'The I27L Amino Acid Polymorphism of Hepatic Nuclear Factor-1α Is Associated with Insulin Resistance1', *The Journal of Clinical Endocrinology & Metabolism*, 85(6), pp. 2178–2183. Available at: https://doi.org/10.1210/jcem.85.6.6618.

Chong, Z.X., Yeap, S.K. and Ho, W.Y. (2021) 'Transfection types, methods and strategies: a technical review', *PeerJ*, 9, p. e11165. Available at: https://doi.org/10.7717/peerj.11165.

Clark, A.R. *et al.* (1993) 'Human insulin gene enhancer-binding proteins in pancreatic alpha and beta cell lines', *FEBS letters*, 329(1–2), pp. 139–143. Available at: https://doi.org/10.1016/0014-5793(93)80210-l.

Colclough, K. *et al.* (2013) 'Mutations in the genes encoding the transcription factors hepatocyte nuclear factor 1 alpha and 4 alpha in maturity-onset diabetes of the young and hyperinsulinemic hypoglycemia', *Human Mutation*, 34(5), pp. 669–685. Available at: https://doi.org/10.1002/humu.22279.

Colclough, K. *et al.* (2014) 'Clinical utility gene card for: Maturity-onset diabetes of the young', *European Journal of Human Genetics*, 22(9). Available at: https://doi.org/10.1038/ejhg.2014.14.

Colman, A. and Dreesen, O. (2009) 'Pluripotent stem cells and disease modeling', *Cell Stem Cell*, 5(3), pp. 244–247. Available at: https://doi.org/10.1016/j.stem.2009.08.010.

Cook, D.L. *et al.* (1988) 'ATP-Sensitive K+ Channels in Pancreatic β-Cells: Spare-Channel Hypothesis', *Diabetes*, 37(5), pp. 495–498. Available at: https://doi.org/10.2337/diab.37.5.495.

Cook, J.T. *et al.* (1993) 'Hyperglycaemic progression in subjects with impaired glucose tolerance: association with decline in beta cell function', *Diabetic Medicine: A Journal of the British Diabetic Association*, 10(4), pp. 321–326. Available at: https://doi.org/10.1111/j.1464-5491.1993.tb00072.x.

Cooper, D.N., Stenson, P.D. and Chuzhanova, N.A. (2006) 'The Human Gene Mutation Database (HGMD) and its exploitation in the study of mutational mechanisms', *Current Protocols in Bioinformatics*, Chapter 1, p. Unit 1.13. Available at: https://doi.org/10.1002/0471250953.bi0113s12.

Coune, C. and Paquot, N. (2022) '[Residual insulin secretion and management of type 1 diabetes: Interest of new C-peptide assays]', *Revue Medicale Suisse*, 18(792), pp. 1556–1559. Available at: https://doi.org/10.53738/REVMED.2022.18.792.1556.

Cujba, A.-M. *et al.* (2022) 'An HNF1α truncation associated with maturity-onset diabetes of the young impairs pancreatic progenitor differentiation by antagonizing HNF1β function', *Cell Reports*, 38(9), p. 110425. Available at: https://doi.org/10.1016/j.celrep.2022.110425.

Culliton, B.J. (1974) 'HeLa Cells: Contaminating Cultures around the World', *Science (New York, N.Y.)*, 184(4141), pp. 1058–1059. Available at: https://doi.org/10.1126/science.184.4141.1058.

Da Silva Xavier, G. (2018) 'The Cells of the Islets of Langerhans', *Journal of Clinical Medicine*, 7(3), p. 54. Available at: https://doi.org/10.3390/jcm7030054.

D'Amour, K.A. *et al.* (2006) 'Production of pancreatic hormone–expressing endocrine cells from human embryonic stem cells', *Nature Biotechnology*, 24(11), pp. 1392–1401. Available at: https://doi.org/10.1038/nbt1259.

D'Angelo, A. *et al.* (2010) 'Hepatocyte nuclear factor 1alpha and beta control terminal differentiation and cell fate commitment in the gut epithelium', *Development (Cambridge, England)*, 137(9), pp. 1573–1582. Available at: https://doi.org/10.1242/dev.044420.

Davis, J.C. *et al.* (2020) 'Glucose Response by Stem Cell-Derived β Cells In Vitro Is Inhibited by a Bottleneck in Glycolysis', *Cell reports*, 31(6), p. 107623. Available at: https://doi.org/10.1016/j.celrep.2020.107623.

Davis, T.M. *et al.* (2017) 'The prevalence of monogenic diabetes in Australia: the Fremantle Diabetes Study Phase II', *The Medical Journal of Australia*, 207(8), pp. 344–347. Available at: https://doi.org/10.5694/mja16.01201.

Davis, T.M. *et al.* (2019) 'Updated prevalence of monogenic diabetes in Australia: Fremantle Diabetes Study Phase 2', *The Medical Journal of Australia*, 211(4), pp. 189-189.e1. Available at: https://doi.org/10.5694/mja2.50290.

DeFronzo, R.A. *et al.* (2015) 'Type 2 diabetes mellitus', *Nature Reviews. Disease Primers*, 1, p. 15019. Available at: https://doi.org/10.1038/nrdp.2015.19.

Del Prato, S. and Pulizzi, N. (2006) 'The place of sulfonylureas in the therapy for type 2 diabetes mellitus', *Metabolism: Clinical and Experimental*, 55(5 Suppl 1), pp. S20-27. Available at: https://doi.org/10.1016/j.metabol.2006.02.003.

Delvecchio, M., Pastore, C. and Giordano, P. (2020) 'Treatment Options for MODY Patients: A Systematic Review of Literature', *Diabetes Therapy*, 11(8), pp. 1667–1685. Available at: https://doi.org/10.1007/s13300-020-00864-4.

Diane, A. *et al.* (2022) ‘β-cell mitochondria in diabetes mellitus: a missing puzzle piece in the generation of hPSC-derived pancreatic β-cells?’, *Journal of Translational Medicine*, 20(1), p. 163. Available at: https://doi.org/10.1186/s12967-022-03327-5.

Dick, M.K., Miao, J.H. and Limaiem, F. (2023) ‘Histology, Fibroblast’, in *StatPearls*. Treasure Island (FL): StatPearls Publishing. Available at: http://www.ncbi.nlm.nih.gov/books/NBK541065/ (Accessed: 11 August 2023).

Ding, Q. *et al.* (2013) ‘Enhanced efficiency of human pluripotent stem cell genome editing through replacing TALENs with CRISPRs’, *Cell Stem Cell*, 12(4), pp. 393–394. Available at: https://doi.org/10.1016/j.stem.2013.03.006.

Dolenšek, J., Rupnik, M.S. and Stožer, A. (2015) ‘Structural similarities and differences between the human and the mouse pancreas’, *Islets*, 7(1), p. e1024405. Available at: https://doi.org/10.1080/19382014.2015.1024405.

Doudna, J.A. and Charpentier, E. (2014) ‘Genome editing. The new frontier of genome engineering with CRISPR-Cas9’, *Science (New York, N.Y.)*, 346(6213), p. 1258096. Available at: https://doi.org/10.1126/science.1258096.

DuBose, C.O. *et al.* (2022) ‘Dynamic Features of Chromosomal Instability during Culture of Induced Pluripotent Stem Cells’, *Genes*, 13(7), p. 1157. Available at: https://doi.org/10.3390/genes13071157.

Dukes, I.D. *et al.* (1998) ‘Defective pancreatic beta-cell glycolytic signaling in hepatocyte nuclear factor-1alpha-deficient mice’, *The Journal of Biological Chemistry*, 273(38), pp. 24457–24464. Available at: https://doi.org/10.1074/jbc.273.38.24457.

Ebrahim, N., Shakirova, K. and Dashinimaev, E. (2022) ‘PDX1 is the cornerstone of pancreatic β-cell functions and identity’, *Frontiers in Molecular Biosciences*, 9. Available at: https://www.frontiersin.org/articles/10.3389/fmolb.2022.1091757 (Accessed: 18 July 2023).

Edghill, E.L. *et al.* (2008) ‘Insulin mutation screening in 1,044 patients with diabetes: mutations in the INS gene are a common cause of neonatal diabetes but a rare cause of diabetes diagnosed in childhood or adulthood’, *Diabetes*, 57(4), pp. 1034–1042. Available at: https://doi.org/10.2337/db07-1405.

Eeckhoute, J., Formstecher, P. and Laine, B. (2004) ‘Hepatocyte Nuclear Factor 4α enhances the Hepatocyte Nuclear Factor 1α-mediated activation of transcription’, *Nucleic Acids Research*, 32(8), pp. 2586–2593. Available at: https://doi.org/10.1093/nar/gkh581.

Ehrhardt, J.D. and Gomez, F. (2023) ‘Embryology, Pancreas’, in *StatPearls*. Treasure Island (FL): StatPearls Publishing. Available at: http://www.ncbi.nlm.nih.gov/books/NBK545243/ (Accessed: 31 July 2023).

Eid, A., Alshareef, S. and Mahfouz, M.M. (2018) ‘CRISPR base editors: genome editing without double-stranded breaks’, *The Biochemical Journal*, 475(11), pp. 1955–1964. Available at: https://doi.org/10.1042/BCJ20170793.

El Hokayem, J., Cukier, H.N. and Dykxhoorn, D.M. (2016) ‘Blood Derived Induced Pluripotent Stem Cells (iPSCs): Benefits, Challenges and the Road Ahead’, *Journal of Alzheimer’s disease & Parkinsonism*, 6(5), p. 275. Available at: https://doi.org/10.4172/2161-0460.1000275.

Ellard, S. *et al.* (2008) ‘Best practice guidelines for the molecular genetic diagnosis of maturity-onset diabetes of the young’, *Diabetologia*, 51(4), pp. 546–553. Available at: https://doi.org/10.1007/s00125-008-0942-y.

Ellard, S. and Colclough, K. (2006) ‘Mutations in the genes encoding the transcription factors hepatocyte nuclear factor 1 alpha (HNF1A) and 4 alpha (HNF4A) in maturity-onset diabetes of the young’, *Human Mutation*, 27(9), pp. 854–869. Available at: https://doi.org/10.1002/humu.20357.

Elleri, D., Dunger, D.B. and Hovorka, R. (2011) ‘Closed-loop insulin delivery for treatment of type 1 diabetes’, *BMC Medicine*, 9(1), p. 120. Available at: https://doi.org/10.1186/1741-7015-9-120.

ElSayed, N.A., Aleppo, G., Aroda, V.R., Bannuru, R.R., Brown, F.M., Bruemmer, D., Collins, B.S., Hilliard, M.E., Isaacs, D., Johnson, E.L., Kahan, S., Khunti, K., Leon, J., Lyons, S.K., Perry, M.L., Prahalad, P., Pratley, R.E., Seley, J.J., Stanton, R.C. and Gabbay, R.A. (2023) ‘2. Classification and Diagnosis of Diabetes: Standards of Care in Diabetes—2023’, *Diabetes Care*, 46(Suppl 1), pp. S19–S40. Available at: https://doi.org/10.2337/dc23-S002.

ElSayed, N.A., Aleppo, G., Aroda, V.R., Bannuru, R.R., Brown, F.M., Bruemmer, D., Collins, B.S., Hilliard, M.E., Isaacs, D., Johnson, E.L., Kahan, S., Khunti, K., Leon, J., Lyons, S.K., Perry, M.L., Prahalad, P., Pratley, R.E., Seley, J.J., Stanton, R.C., Gabbay, R.A., *et al.* (2023) ‘2. Classification and Diagnosis of Diabetes: Standards of Care in Diabetes-2023’, *Diabetes Care*, 46(Suppl 1), pp. S19–S40. Available at: https://doi.org/10.2337/dc23-S002.

Fajans, S.S. and Bell, G.I. (2011) ‘MODY: history, genetics, pathophysiology, and clinical decision making’, *Diabetes Care*, 34(8), pp. 1878–1884. Available at: https://doi.org/10.2337/dc11-0035.

Fajans, S.S., Bell, G.I. and Polonsky, K.S. (2001) ‘Molecular mechanisms and clinical pathophysiology of maturity-onset diabetes of the young’, *The New England Journal of Medicine*, 345(13), pp. 971–980. Available at: https://doi.org/10.1056/NEJMra002168.

Fareed, F.M.A. *et al.* (2021) ‘HNF1A-MODY Mutations in Nuclear Localization Signal Impair HNF1A-Import Receptor KPNA6 Interactions’, *The Protein Journal*, 40(4), pp. 512–521. Available at: https://doi.org/10.1007/s10930-020-09959-0.

Fazeli Farsani, S. *et al.* (2017) 'Incidence and prevalence of diabetic ketoacidosis (DKA) among adults with type 1 diabetes mellitus (T1D): a systematic literature review', *BMJ open*, 7(7), p. e016587. Available at: https://doi.org/10.1136/bmjopen-2017-016587.

Fendler, W. *et al.* (2011) 'HDL cholesterol as a diagnostic tool for clinical differentiation of GCK-MODY from HNF1A-MODY and type 1 diabetes in children and young adults', *Clinical Endocrinology*, 75(3), pp. 321–327. Available at: https://doi.org/10.1111/j.1365-2265.2011.04052.x.

Fernandez-Zapico, M.E. *et al.* (2009) 'MODY7 gene, KLF11, is a novel p300-dependent regulator of Pdx-1 (MODY4) transcription in pancreatic islet beta cells', *The Journal of Biological Chemistry*, 284(52), pp. 36482–36490. Available at: https://doi.org/10.1074/jbc.M109.028852.

Flannick, J. *et al.* (2013) 'Assessing the phenotypic effects in the general population of rare variants in genes for a dominant mendelian form of diabetes', *Nature genetics*, 45(11), pp. 1380–1385. Available at: https://doi.org/10.1038/ng.2794.

Fletcher, B., Gulanick, M. and Lamendola, C. (2002) 'Risk factors for type 2 diabetes mellitus', *The Journal of Cardiovascular Nursing*, 16(2), pp. 17–23. Available at: https://doi.org/10.1097/00005082-200201000-00003.

Fridlyand, L.E., Tamarina, N. and Philipson, L.H. (2010) 'Bursting and calcium oscillations in pancreatic beta-cells: specific pacemakers for specific mechanisms', *American Journal of Physiology. Endocrinology and Metabolism*, 299(4), pp. E517-532. Available at: https://doi.org/10.1152/ajpendo.00177.2010.

Fritzler, M.J. *et al.* (2018) 'The Utilization of Autoantibodies in Approaches to Precision Health', *Frontiers in Immunology*, 9, p. 2682. Available at: https://doi.org/10.3389/fimmu.2018.02682.

Froguel, P. *et al.* (1992) 'Close linkage of glucokinase locus on chromosome 7p to early-onset non-insulin-dependent diabetes mellitus', *Nature*, 356(6365), pp. 162–164. Available at: https://doi.org/10.1038/356162a0.

Froguel, P. *et al.* (1993) 'Familial hyperglycemia due to mutations in glucokinase. Definition of a subtype of diabetes mellitus', *The New England Journal of Medicine*, 328(10), pp. 697–702. Available at: https://doi.org/10.1056/NEJM199303113281005.

Fu, J. *et al.* (2019) 'Using Clinical Indices to Distinguish MODY2 (GCK Mutation) and MODY3 (HNF1A Mutation) from Type 1 Diabetes in a Young Chinese Population', *Diabetes Therapy: Research, Treatment and Education of Diabetes and Related Disorders*, 10(4), pp. 1381–1390. Available at: https://doi.org/10.1007/s13300-019-0647-x.

Fuchsberger, C. *et al.* (2016) 'The genetic architecture of type 2 diabetes', *Nature*, 536(7614), pp. 41–47. Available at: https://doi.org/10.1038/nature18642.

Fujimoto, K. and Polonsky, K.S. (2009) 'Pdx1 and other factors that regulate pancreatic beta-cell survival', *Diabetes, Obesity & Metabolism*, 11 Suppl 4(Suppl 4), pp. 30–37. Available at: https://doi.org/10.1111/j.1463-1326.2009.01121.x.

Furuya, F. *et al.* (2013) 'Ligand-bound Thyroid Hormone Receptor Contributes to Reprogramming of Pancreatic Acinar Cells into Insulin-producing Cells', *The Journal of Biological Chemistry*, 288(22), pp. 16155–16166. Available at: https://doi.org/10.1074/jbc.M112.438192.

Galán, M. *et al.* (2011) 'Differential effects of HNF-1α mutations associated with familial young-onset diabetes on target gene regulation', *Molecular Medicine (Cambridge, Mass.)*, 17(3–4), pp. 256–265. Available at: https://doi.org/10.2119/molmed.2010.00097.

Gao, T. *et al.* (2014) 'Pdx1 maintains β cell identity and function by repressing an α cell program', *Cell Metabolism*, 19(2), pp. 259–271. Available at: https://doi.org/10.1016/j.cmet.2013.12.002.

Garcia, F.A. de O., de Andrade, E.S. and Palmero, E.I. (2022) 'Insights on variant analysis in silico tools for pathogenicity prediction', *Frontiers in Genetics*, 13, p. 1010327. Available at: https://doi.org/10.3389/fgene.2022.1010327.

Garcia-Gonzalez, M.A. *et al.* (2016) 'A suppressor locus for MODY3-diabetes', *Scientific Reports*, 6, p. 33087. Available at: https://doi.org/10.1038/srep33087.

Gardner, D.S. and Tai, E.S. (2012) 'Clinical features and treatment of maturity onset diabetes of the young (MODY)', *Diabetes, Metabolic Syndrome and Obesity: Targets and Therapy*, 5, pp. 101–108. Available at: https://doi.org/10.2147/DMSO.S23353.

Gaudelli, N.M. *et al.* (2017) 'Programmable base editing of A•T to G•C in genomic DNA without DNA cleavage', *Nature*, 551(7681), pp. 464–471. Available at: https://doi.org/10.1038/nature24644.

Gaulton, K.J., Ferreira, T., Lee, Y., Raimondo, A., Mägi, R., Hreidarsson, A.B., *et al.* (2015) 'Genetic fine mapping and genomic annotation defines causal mechanisms at type 2 diabetes susceptibility loci.', *Nature genetics*, 47(12), pp. 1415–1425. Available at: https://doi.org/10.1038/ng.3437.

Gaulton, K.J., Ferreira, T., Lee, Y., Raimondo, A., Mägi, R., DIAbetes Genetics Replication And Meta-analysis (DIAGRAM) Consortium, *et al.* (2015) 'Genetic fine mapping and genomic annotation defines causal mechanisms at type 2 diabetes susceptibility loci', *Nature Genetics*, 47(12), pp. 1415–1425. Available at: https://doi.org/10.1038/ng.3437.

Geer, L.Y. *et al.* (2010) 'The NCBI BioSystems database', *Nucleic Acids Research*, 38(Database issue), pp. D492-496. Available at: https://doi.org/10.1093/nar/gkp858.

Genga, R.M., Kearns, N.A. and Maehr, R. (2016) ‘Controlling transcription in human pluripotent stem cells using CRISPR-effectors’, *Methods (San Diego, Calif.)*, 101, pp. 36–42. Available at: https://doi.org/10.1016/j.ymeth.2015.10.014.

Glucksmann, M.A. *et al.* (1997) ‘Novel Mutations and a Mutational Hotspot in the M0DY3 Gene’, *Diabetes*, 46(6), pp. 1081–1086. Available at: https://doi.org/10.2337/diab.46.6.1081.

González, B.J. *et al.* (2021) ‘Human stem cell model of *HNF1A* deficiency shows uncoupled insulin to C-peptide secretion with accumulation of abnormal insulin granules’. Available at: https://doi.org/10.1101/2021.01.26.428260.

González, B.J. *et al.* (2022a) ‘Reduced calcium levels and accumulation of abnormal insulin granules in stem cell models of HNF1A deficiency’, *Communications Biology*, 5, p. 779. Available at: https://doi.org/10.1038/s42003-022-03696-z.

González, B.J. *et al.* (2022b) ‘Reduced calcium levels and accumulation of abnormal insulin granules in stem cell models of HNF1A deficiency’, *Communications Biology*, 5(1), p. 779. Available at: https://doi.org/10.1038/s42003-022-03696-z.

Goodner, C.J., Sweet, I.R. and Harrison, H.C. (1988) ‘Rapid reduction and return of surface insulin receptors after exposure to brief pulses of insulin in perifused rat hepatocytes’, *Diabetes*, 37(10), pp. 1316–1323. Available at: https://doi.org/10.2337/diab.37.10.1316.

Grapengiesser, E., Gylfe, E. and Hellman, B. (1988) ‘Glucose-induced oscillations of cytoplasmic Ca2+ in the pancreatic beta-cell’, *Biochemical and Biophysical Research Communications*, 151(3), pp. 1299–1304. Available at: https://doi.org/10.1016/s0006-291x(88)80503-5.

Grapin-Botton, A. (2005) ‘Ductal cells of the pancreas’, *The International Journal of Biochemistry & Cell Biology*, 37(3), pp. 504–510. Available at: https://doi.org/10.1016/j.biocel.2004.07.010.

Gregory, G.A. *et al.* (2022) ‘Global incidence, prevalence, and mortality of type 1 diabetes in 2021 with projection to 2040: a modelling study’, *The Lancet. Diabetes & Endocrinology*, 10(10), pp. 741–760. Available at: https://doi.org/10.1016/S2213-8587(22)00218-2.

Guo, T. *et al.* (2018) ‘Harnessing accurate non-homologous end joining for efficient precise deletion in CRISPR/Cas9-mediated genome editing’, *Genome Biology*, 19(1), p. 170. Available at: https://doi.org/10.1186/s13059-018-1518-x.

Haliyur, R. *et al.* (2019) ‘Human islets expressing HNF1A variant have defective β cell transcriptional regulatory networks’, *The Journal of Clinical Investigation*, 129(1), pp. 246–251. Available at: https://doi.org/10.1172/JCI121994.

Harries, L.W. *et al.* (2006) ‘Isomers of the TCF1 gene encoding hepatocyte nuclear factor-1 alpha show differential expression in the pancreas and define the relationship

between mutation position and clinical phenotype in monogenic diabetes', *Human Molecular Genetics*, 15(14), pp. 2216–2224. Available at: https://doi.org/10.1093/hmg/ddl147.

Harries, L.W., Brown, J.E. and Gloyn, A.L. (2009) 'Species-specific differences in the expression of the HNF1A, HNF1B and HNF4A genes', *PloS One*, 4(11), p. e7855. Available at: https://doi.org/10.1371/journal.pone.0007855.

Hasegawa, K. *et al.* (2010) 'Comparison of Reprogramming Efficiency Between Transduction of Reprogramming Factors, Cell–Cell Fusion, and Cytoplast Fusion', *Stem Cells*, 28(8), pp. 1338–1348. Available at: https://doi.org/10.1002/stem.466.

Hattersley, A.T. *et al.* (2018) 'ISPAD Clinical Practice Consensus Guidelines 2018: The diagnosis and management of monogenic diabetes in children and adolescents', *Pediatric Diabetes*, 19 Suppl 27, pp. 47–63. Available at: https://doi.org/10.1111/pedi.12772.

Hattersley, A.T. and Patel, K.A. (2017) 'Precision diabetes: learning from monogenic diabetes', *Diabetologia*, 60(5), pp. 769–777. Available at: https://doi.org/10.1007/s00125-017-4226-2.

Haurwitz, R.E. *et al.* (2010) 'Sequence- and structure-specific RNA processing by a CRISPR endonuclease', *Science (New York, N.Y.)*, 329(5997), pp. 1355–1358. Available at: https://doi.org/10.1126/science.1192272.

Hebrok, M. (2003) 'Hedgehog signaling in pancreas development', *Mechanisms of Development*, 120(1), pp. 45–57. Available at: https://doi.org/10.1016/s0925-4773(02)00331-3.

Hegele, R.A. *et al.* (1999) 'Genome-wide scanning for type 2 diabetes susceptibility in Canadian Oji-Cree, using 190 microsatellite markers', *Journal of Human Genetics*, 44(1), pp. 10–14. Available at: https://doi.org/10.1007/s100380050097.

Heimberg, H. *et al.* (1995) 'Differences in glucose transporter gene expression between rat pancreatic alpha- and beta-cells are correlated to differences in glucose transport but not in glucose utilization', *The Journal of Biological Chemistry*, 270(15), pp. 8971–8975. Available at: https://doi.org/10.1074/jbc.270.15.8971.

Hellman, B. *et al.* (1994) 'Glucose induces oscillatory Ca2+ signalling and insulin release in human pancreatic beta cells', *Diabetologia*, 37 Suppl 2, pp. S11-20. Available at: https://doi.org/10.1007/BF00400821.

Henry, B.M. *et al.* (2019) 'Development of the human pancreas and its vasculature - An integrated review covering anatomical, embryological, histological, and molecular aspects', *Annals of Anatomy = Anatomischer Anzeiger: Official Organ of the Anatomische Gesellschaft*, 221, pp. 115–124. Available at: https://doi.org/10.1016/j.aanat.2018.09.008.

Hermann, F.M. *et al.* (2023) ‘An insulin hypersecretion phenotype precedes pancreatic beta cell failure in MODY3 patient-specific cells’, *Cell Stem Cell*, 30(1), pp. 38–51.

Hilderink, J. *et al.* (2015) ‘Controlled aggregation of primary human pancreatic islet cells leads to glucose-responsive pseudoislets comparable to native islets’, *Journal of Cellular and Molecular Medicine*, 19(8), pp. 1836–1846. Available at: https://doi.org/10.1111/jcmm.12555.

Holmkvist, J. *et al.* (2006) ‘Common variants in HNF-1 alpha and risk of type 2 diabetes’, *Diabetologia*, 49(12), pp. 2882–2891. Available at: https://doi.org/10.1007/s00125-006-0450-x.

Holt, R.I.G. *et al.* (2021) ‘The management of type 1 diabetes in adults. A consensus report by the American Diabetes Association (ADA) and the European Association for the Study of Diabetes (EASD)’, *Diabetologia*, 64(12), pp. 2609–2652. Available at: https://doi.org/10.1007/s00125-021-05568-3.

Horikawa, Y. *et al.* (1997) ‘Mutation in hepatocyte nuclear factor-1 beta gene (TCF2) associated with MODY’, *Nature Genetics*, 17(4), pp. 384–385. Available at: https://doi.org/10.1038/ng1297-384.

Hou, Z. *et al.* (2013) ‘Efficient genome engineering in human pluripotent stem cells using Cas9 from Neisseria meningitidis’, *Proceedings of the National Academy of Sciences of the United States of America*, 110(39), pp. 15644–15649. Available at: https://doi.org/10.1073/pnas.1313587110.

Hu, M. *et al.* (2020) ‘Functional Genomics in Pancreatic β Cells: Recent Advances in Gene Deletion and Genome Editing Technologies for Diabetes Research’, *Frontiers in Endocrinology*, 11. Available at: https://www.frontiersin.org/articles/10.3389/fendo.2020.576632 (Accessed: 3 July 2023).

Hua, Q.X. *et al.* (2000) ‘Diabetes-associated mutations in a beta-cell transcription factor destabilize an antiparallel “mini-zipper” in a dimerization interface’, *Proceedings of the National Academy of Sciences of the United States of America*, 97(5), pp. 1999–2004. Available at: https://doi.org/10.1073/pnas.97.5.1999.

Hwang, G.-H. and Bae, S. (2021) ‘Web-Based Base Editing Toolkits: BE-Designer and BE-Analyzer’, *Methods in Molecular Biology (Clifton, N.J.)*, 2189, pp. 81–88. Available at: https://doi.org/10.1007/978-1-0716-0822-7_7.

Iafusco, D. *et al.* (2012) ‘Minimal incidence of neonatal/infancy onset diabetes in Italy is 1:90,000 live births’, *Acta Diabetologica*, 49(5), pp. 405–408. Available at: https://doi.org/10.1007/s00592-011-0331-8.

Irwin, N. and Flatt, P.R. (2013) ‘Enteroendocrine hormone mimetics for the treatment of obesity and diabetes’, *Current Opinion in Pharmacology*, 13(6), pp. 989–995. Available at: https://doi.org/10.1016/j.coph.2013.09.009.

Isomaa, B. *et al.* (1998) ‘Chronic diabetic complications in patients with MODY3 diabetes’, *Diabetologia*, 41(4), pp. 467–473. Available at: https://doi.org/10.1007/s001250050931.

Jang, H.-K. and Kim, B.-S. (2010) ‘Modulation of Stem Cell Differentiation with Biomaterials’, *International Journal of Stem Cells*, 3(2), pp. 80–84.

Jang, K.M. (2020) ‘Maturity-onset diabetes of the young: update and perspectives on diagnosis and treatment’, *Yeungnam University Journal of Medicine*, 37(1), pp. 13–21. Available at: https://doi.org/10.12701/yujm.2019.00409.

Jennings, R.E. *et al.* (2013) ‘Development of the human pancreas from foregut to endocrine commitment’, *Diabetes*, 62(10), pp. 3514–3522. Available at: https://doi.org/10.2337/db12-1479.

Jensen, J. *et al.* (2000) ‘Independent development of pancreatic alpha- and beta-cells from neurogenin3-expressing precursors: a role for the notch pathway in repression of premature differentiation’, *Diabetes*, 49(2), pp. 163–176. Available at: https://doi.org/10.2337/diabetes.49.2.163.

Jiang, J. *et al.* (2007) ‘Generation of insulin-producing islet-like clusters from human embryonic stem cells’, *Stem Cells (Dayton, Ohio)*, 25(8), pp. 1940–1953. Available at: https://doi.org/10.1634/stemcells.2006-0761.

Jiang, W., Wang, J. and Zhang, Y. (2013) ‘Histone H3K27me3 demethylases KDM6A and KDM6B modulate definitive endoderm differentiation from human ESCs by regulating WNT signaling pathway’, *Cell Research*, 23(1), pp. 122–130. Available at: https://doi.org/10.1038/cr.2012.119.

Jin, W. and Jiang, W. (2022) ‘Stepwise differentiation of functional pancreatic β cells from human pluripotent stem cells’, *Cell Regeneration*, 11, p. 24. Available at: https://doi.org/10.1186/s13619-022-00125-8.

Johannesson, M. *et al.* (2009) ‘FGF4 and Retinoic Acid Direct Differentiation of hESCs into PDX1-Expressing Foregut Endoderm in a Time- and Concentration-Dependent Manner’, *PLoS ONE*, 4(3), p. e4794. Available at: https://doi.org/10.1371/journal.pone.0004794.

Johansson, B.B. *et al.* (2011) ‘Diabetes and Pancreatic Exocrine Dysfunction Due to Mutations in the Carboxyl Ester Lipase Gene-Maturity Onset Diabetes of the Young (CEL-MODY)’, *The Journal of Biological Chemistry*, 286(40), pp. 34593–34605. Available at: https://doi.org/10.1074/jbc.M111.222679.

Johansson, B.B. *et al.* (2017) ‘Targeted next-generation sequencing reveals MODY in up to 6.5% of antibody-negative diabetes cases listed in the Norwegian Childhood Diabetes Registry’, *Diabetologia*, 60(4), pp. 625–635. Available at: https://doi.org/10.1007/s00125-016-4167-1.

Johnston, N.R. *et al.* (2016) ‘Beta Cell Hubs Dictate Pancreatic Islet Responses to Glucose’, *Cell Metabolism*, 24(3), pp. 389–401. Available at: https://doi.org/10.1016/j.cmet.2016.06.020.

Jones, P.M., Persaud, S.J. and Howell, S.L. (1992) ‘Ca2(+)-induced insulin secretion from electrically permeabilized islets. Loss of the Ca2(+)-induced secretory response is accompanied by loss of Ca2(+)-induced protein phosphorylation’, *The Biochemical Journal*, 285 (Pt 3)(Pt 3), pp. 973–978. Available at: https://doi.org/10.1042/bj2850973.

Juszczak, A. *et al.* (2016) ‘When to consider a diagnosis of MODY at the presentation of diabetes: aetiology matters for correct management’, *The British Journal of General Practice*, 66(647), pp. e457–e459. Available at: https://doi.org/10.3399/bjgp16X685537.

Juszczak, A. *et al.* (2018) ‘Plasma Fucosylated Glycans and C-Reactive Protein as Biomarkers of HNF1A-MODY in Young Adult–Onset Nonautoimmune Diabetes’, *Diabetes Care*, 42(1), pp. 17–26. Available at: https://doi.org/10.2337/dc18-0422.

Kahn, S.E. *et al.* (2009) ‘The beta cell lesion in type 2 diabetes: there has to be a primary functional abnormality’, *Diabetologia*, 52(6), pp. 1003–1012. Available at: https://doi.org/10.1007/s00125-009-1321-z.

Kahn, S.E., Cooper, M.E. and Del Prato, S. (2014) ‘Pathophysiology and treatment of type 2 diabetes: perspectives on the past, present, and future’, *Lancet (London, England)*, 383(9922), pp. 1068–1083. Available at: https://doi.org/10.1016/S0140-6736(13)62154-6.

Karimova, M.V., Gvazava, I.G. and Vorotelyak, E.A. (2022) ‘Overcoming the Limitations of Stem Cell-Derived Beta Cells’, *Biomolecules*, 12(6), p. 810. Available at: https://doi.org/10.3390/biom12060810.

Katsarou, A. *et al.* (2017) ‘Type 1 diabetes mellitus’, *Nature Reviews Disease Primers*, 3(1), pp. 1–17. Available at: https://doi.org/10.1038/nrdp.2017.16.

Kavvoura, F.K. and Owen, K.R. (2012) ‘Maturity onset diabetes of the young: clinical characteristics, diagnosis and management’, *Pediatric endocrinology reviews: PER*, 10(2), pp. 234–242.

Kim, S.K. and MacDonald, R.J. (2002) ‘Signaling and transcriptional control of pancreatic organogenesis’, *Current Opinion in Genetics & Development*, 12(5), pp. 540–547. Available at: https://doi.org/10.1016/s0959-437x(02)00338-6.

Kircher, M. *et al.* (2014) ‘A general framework for estimating the relative pathogenicity of human genetic variants’, *Nature Genetics*, 46(3), pp. 310–315. Available at: https://doi.org/10.1038/ng.2892.

Klec, C. *et al.* (2019) ‘Calcium Signaling in ß-cell Physiology and Pathology: A Revisit’, *International Journal of Molecular Sciences*, 20(24), p. 6110. Available at: https://doi.org/10.3390/ijms20246110.

Kleinberger, J.W. *et al.* (2018) ‘Monogenic Diabetes in Overweight and Obese Youth Diagnosed with Type 2 Diabetes: The TODAY Clinical Trial’, *Genetics in medicine : official journal of the American College of Medical Genetics*, 20(6), pp. 583–590. Available at: https://doi.org/10.1038/gim.2017.150.

Kleinberger, J.W. and Pollin, T.I. (2015) ‘Undiagnosed MODY: Time for Action’, *Current diabetes reports*, 15(12), p. 110. Available at: https://doi.org/10.1007/s11892-015-0681-7.

Kolios, G. and Moodley, Y. (2013) ‘Introduction to Stem Cells and Regenerative Medicine’, *Respiration*, 85(1), pp. 3–10. Available at: https://doi.org/10.1159/000345615.

Komor, A.C. *et al.* (2016) ‘Programmable editing of a target base in genomic DNA without double-stranded DNA cleavage’, *Nature*, 533(7603), pp. 420–424. Available at: https://doi.org/10.1038/nature17946.

Krischer, J.P. *et al.* (2015) ‘The 6 year incidence of diabetes-associated autoantibodies in genetically at-risk children: the TEDDY study’, *Diabetologia*, 58(5), p. 980. Available at: https://doi.org/10.1007/s00125-015-3514-y.

Kristinsson, S.Y. *et al.* (2001) ‘MODY in Iceland is associated with mutations in HNF-1alpha and a novel mutation in NeuroD1’, *Diabetologia*, 44(11), pp. 2098–2103. Available at: https://doi.org/10.1007/s001250100016.

Kritis, A.A. *et al.* (1993) ‘An indirect negative autoregulatory mechanism involved in hepatocyte nuclear factor-1 gene expression’, *Nucleic Acids Research*, 21(25), pp. 5882–5889. Available at: https://doi.org/10.1093/nar/21.25.5882.

Kroon, E. *et al.* (2008) ‘Pancreatic endoderm derived from human embryonic stem cells generates glucose-responsive insulin-secreting cells in vivo’, *Nature Biotechnology*, 26(4), pp. 443–452. Available at: https://doi.org/10.1038/nbt1393.

Kubo, A. *et al.* (2011) ‘Pdx1 and Ngn3 overexpression enhances pancreatic differentiation of mouse ES cell-derived endoderm population’, *PloS One*, 6(9), p. e24058. Available at: https://doi.org/10.1371/journal.pone.0024058.

Kuhtreiber, W.M. *et al.* (2015) ‘Low levels of C-peptide have clinical significance for established Type 1 diabetes’, *Diabetic Medicine: A Journal of the British Diabetic Association*, 32(10), pp. 1346–1353. Available at: https://doi.org/10.1111/dme.12850.

Kumar, A. *et al.* (2023) ‘Prevalence of diabetes in India: A review of IDF Diabetes Atlas 10th edition’, *Current Diabetes Reviews* [Preprint]. Available at: https://doi.org/10.2174/1573399819666230413094200.

Kunisada, Y. *et al.* (2012) ‘Small molecules induce efficient differentiation into insulin-producing cells from human induced pluripotent stem cells’, *Stem Cell Research*, 8(2), pp. 274–284. Available at: https://doi.org/10.1016/j.scr.2011.10.002.

Kuo, C.J. *et al.* (1992) ‘A transcriptional hierarchy involved in mammalian cell-type specification’, *Nature*, 355(6359), pp. 457–461. Available at: https://doi.org/10.1038/355457a0.

Läll, K. *et al.* (2017) ‘Personalized risk prediction for type 2 diabetes: the potential of genetic risk scores’, *Genetics in Medicine: Official Journal of the American College of Medical Genetics*, 19(3), pp. 322–329. Available at: https://doi.org/10.1038/gim.2016.103.

Larsen, H.L. and Grapin-Botton, A. (2017) ‘The molecular and morphogenetic basis of pancreas organogenesis’, *Seminars in Cell & Developmental Biology*, 66, pp. 51–68. Available at: https://doi.org/10.1016/j.semcdb.2017.01.005.

Lau, H.H. *et al.* (2018) ‘The molecular functions of hepatocyte nuclear factors - In and beyond the liver’, *Journal of Hepatology*, 68(5), pp. 1033–1048. Available at: https://doi.org/10.1016/j.jhep.2017.11.026.

Lavon, N., Yanuka, O. and Benvenisty, N. (2006) ‘The effect of overexpression of Pdx1 and Foxa2 on the differentiation of human embryonic stem cells into pancreatic cells’, *Stem Cells (Dayton, Ohio)*, 24(8), pp. 1923–1930. Available at: https://doi.org/10.1634/stemcells.2005-0397.

Leete, P. *et al.* (2018) ‘The Effect of Age on the Progression and Severity of Type 1 Diabetes: Potential Effects on Disease Mechanisms’, *Current Diabetes Reports*, 18(11), p. 115. Available at: https://doi.org/10.1007/s11892-018-1083-4.

Lei, C.-L. *et al.* (2018) ‘Beta-cell hubs maintain Ca2+ oscillations in human and mouse islet simulations’, *Islets*, 10(4), pp. 151–167. Available at: https://doi.org/10.1080/19382014.2018.1493316.

Lemelman, M.B., Letourneau, L. and Greeley, S.A.W. (2018) ‘Neonatal Diabetes Mellitus: An Update on Diagnosis and Management’, *Clinics in perinatology*, 45(1), pp. 41–59. Available at: https://doi.org/10.1016/j.clp.2017.10.006.

Li, H. *et al.* (2020) ‘Applications of genome editing technology in the targeted therapy of human diseases: mechanisms, advances and prospects’, *Signal Transduction and Targeted Therapy*, 5, p. 1. Available at: https://doi.org/10.1038/s41392-019-0089-y.

Li, X.-Y., Zhai, W.-J. and Teng, C.-B. (2015) ‘Notch Signaling in Pancreatic Development’, *International Journal of Molecular Sciences*, 17(1), p. 48. Available at: https://doi.org/10.3390/ijms17010048.

Liang, S. *et al.* (2023) ‘Differentiation of stem cell-derived pancreatic progenitors into insulin-secreting islet clusters in a multiwell-based static 3D culture system’, *Cell*

Reports Methods, 3(5), p. 100466. Available at: https://doi.org/10.1016/j.crmeth.2023.100466.

Lim, S.J. *et al.* (2016) 'Induced pluripotent stem cells from human hair follicle keratinocytes as a potential source for in vitro hair follicle cloning', *PeerJ*, 4, p. e2695. Available at: https://doi.org/10.7717/peerj.2695.

Lin, H.-M. *et al.* (2009) 'Transforming growth factor-beta/Smad3 signaling regulates insulin gene transcription and pancreatic islet beta-cell function', *The Journal of Biological Chemistry*, 284(18), pp. 12246–12257. Available at: https://doi.org/10.1074/jbc.M805379200.

Ling, C. and Rönn, T. (2019) 'Epigenetics in Human Obesity and Type 2 Diabetes', *Cell Metabolism*, 29(5), pp. 1028–1044. Available at: https://doi.org/10.1016/j.cmet.2019.03.009.

Liu, C. *et al.* (2018) 'Modeling human diseases with induced pluripotent stem cells: from 2D to 3D and beyond', *Development (Cambridge, England)*, 145(5), p. dev156166. Available at: https://doi.org/10.1242/dev.156166.

Liu, L. *et al.* (2012) 'Comparison of Next-Generation Sequencing Systems', *Journal of Biomedicine and Biotechnology*. Edited by P.J. Oefner, 2012, p. 251364. Available at: https://doi.org/10.1155/2012/251364.

Liu, L. *et al.* (2013) 'Mutations in KCNJ11 are associated with the development of autosomal dominant, early-onset type 2 diabetes', *Diabetologia*, 56(12), pp. 2609–2618. Available at: https://doi.org/10.1007/s00125-013-3031-9.

Liu, X. *et al.* (2020) 'Chromosomal aberration arises during somatic reprogramming to pluripotent stem cells', *Cell Division*, 15, p. 12. Available at: https://doi.org/10.1186/s13008-020-00068-z.

Locke, J.M. *et al.* (2018) 'The common HNF1A variant I27L is a modifier of age at diabetes diagnosis in HNF1A-MODY individuals', *Diabetes*, 67(9), pp. 1903–1907. Available at: https://doi.org/10.2337/db18-0133.

Low, B.S.J. *et al.* (2021) 'Decreased GLUT2 and glucose uptake contribute to insulin secretion defects in MODY3/HNF1A hiPSC-derived mutant β cells', *Nature Communications*, 12(1), p. 3133. Available at: https://doi.org/10.1038/s41467-021-22843-4.

Lucey, B.P., Nelson-Rees, W.A. and Hutchins, G.M. (2009) 'Henrietta Lacks, HeLa Cells, and Cell Culture Contamination', *Archives of Pathology & Laboratory Medicine*, 133(9), pp. 1463–1467. Available at: https://doi.org/10.5858/133.9.1463.

Luistro, L. *et al.* (2009) 'Preclinical profile of a potent gamma-secretase inhibitor targeting notch signaling with in vivo efficacy and pharmacodynamic properties', *Cancer Research*, 69(19), pp. 7672–7680. Available at: https://doi.org/10.1158/0008-5472.CAN-09-1843.

Ma, Y. *et al.* (2020) ‘New clinical screening strategy to distinguish HNF1A variant-induced diabetes from young early-onset type 2 diabetes in a Chinese population’, *BMJ open diabetes research & care*, 8(1), p. e000745. Available at: https://doi.org/10.1136/bmjdrc-2019-000745.

Macfarlane, W.M. *et al.* (1999) ‘Glucose stimulates translocation of the homeodomain transcription factor PDX1 from the cytoplasm to the nucleus in pancreatic beta-cells’, *The Journal of Biological Chemistry*, 274(2), pp. 1011–1016. Available at: https://doi.org/10.1074/jbc.274.2.1011.

Maechler, P., Carobbio, S. and Rubi, B. (2006) ‘In beta-cells, mitochondria integrate and generate metabolic signals controlling insulin secretion’, *The International Journal of Biochemistry & Cell Biology*, 38(5–6), pp. 696–709. Available at: https://doi.org/10.1016/j.biocel.2005.12.006.

Magliano, D.J. *et al.* (2020) ‘Young-onset type 2 diabetes mellitus - implications for morbidity and mortality’, *Nature Reviews. Endocrinology*, 16(6), pp. 321–331. Available at: https://doi.org/10.1038/s41574-020-0334-z.

Malik, N. and Rao, M.S. (2013) ‘A Review of the Methods for Human iPSC Derivation’, *Methods in molecular biology (Clifton, N.J.)*, 997, pp. 23–33. Available at: https://doi.org/10.1007/978-1-62703-348-0_3.

Mann, H.B. and Whitney, D.R. (1947) ‘On a Test of Whether one of Two Random Variables is Stochastically Larger than the Other’, *The Annals of Mathematical Statistics*, 18(1), pp. 50–60. Available at: https://doi.org/10.1214/aoms/1177730491.

Martagón, A.J. *et al.* (2018) ‘Mexican Carriers of the HNF1A p.E508K Variant Do Not Experience an Enhanced Response to Sulfonylureas’, *Diabetes Care*, 41(8), pp. 1726–1731. Available at: https://doi.org/10.2337/dc18-0384.

Martin, G.R. (1981) ‘Isolation of a pluripotent cell line from early mouse embryos cultured in medium conditioned by teratocarcinoma stem cells.’, *Proceedings of the National Academy of Sciences*, 78(12), pp. 7634–7638. Available at: https://doi.org/10.1073/pnas.78.12.7634.

McCall, A.L. and Farhy, L.S. (2013) ‘Treating type 1 diabetes: from strategies for insulin delivery to dual hormonal control’, *Minerva endocrinologica*, 38(2), pp. 145–163.

McDaniel, S., Komor, A. and Goren, A. (2022) ‘The use of base editing technology to characterize single nucleotide variants’, *Computational and Structural Biotechnology Journal*, 20, pp. 1670–1680. Available at: https://doi.org/10.1016/j.csbj.2022.03.031.

McDonald, T. J. *et al.* (2011) ‘Islet autoantibodies can discriminate maturity-onset diabetes of the young (MODY) from Type 1 diabetes’, *Diabetic Medicine: A Journal of the British Diabetic Association*, 28(9), pp. 1028–1033. Available at: https://doi.org/10.1111/j.1464-5491.2011.03287.x.

McDonald, Tim J. *et al.* (2011) ‘Response to Comment on: McDonald et al. High-Sensitivity CRP Discriminates HNF1A-MODY From Other Subtypes of Diabetes. Diabetes Care 2011;34:1860–1862’, *Diabetes Care*, 34(12), p. e187. Available at: https://doi.org/10.2337/dc11-1766.

McDonald, T.J. *et al.* (2012) ‘Lipoprotein composition in HNF1A-MODY: differentiating between HNF1A-MODY and type 2 diabetes’, *Clinica Chimica Acta; International Journal of Clinical Chemistry*, 413(9–10), pp. 927–932. Available at: https://doi.org/10.1016/j.cca.2012.02.005.

McDonald, T.J. and Ellard, S. (2013) ‘Maturity onset diabetes of the young: identification and diagnosis’, *Annals of Clinical Biochemistry*, 50(Pt 5), pp. 403–415. Available at: https://doi.org/10.1177/0004563213483458.

McLean, A.B. *et al.* (2007) ‘Activin a efficiently specifies definitive endoderm from human embryonic stem cells only when phosphatidylinositol 3-kinase signaling is suppressed’, *Stem Cells (Dayton, Ohio)*, 25(1), pp. 29–38. Available at: https://doi.org/10.1634/stemcells.2006-0219.

Meier, J.J. (2012) ‘GLP-1 receptor agonists for individualized treatment of type 2 diabetes mellitus’, *Nature Reviews Endocrinology*, 8(12), pp. 728–742. Available at: https://doi.org/10.1038/nrendo.2012.140.

Memon, B. *et al.* (2018) ‘Enhanced differentiation of human pluripotent stem cells into pancreatic progenitors co-expressing PDX1 and NKX6.1’, *Stem Cell Research & Therapy*, 9(1), p. 15. Available at: https://doi.org/10.1186/s13287-017-0759-z.

Meur, G. *et al.* (2010) ‘Insulin gene mutations resulting in early-onset diabetes: marked differences in clinical presentation, metabolic status, and pathogenic effect through endoplasmic reticulum retention’, *Diabetes*, 59(3), pp. 653–661. Available at: https://doi.org/10.2337/db09-1091.

Micallef, S.J. *et al.* (2012) ‘INS(GFP/w) human embryonic stem cells facilitate isolation of in vitro derived insulin-producing cells’, *Diabetologia*, 55(3), pp. 694–706. Available at: https://doi.org/10.1007/s00125-011-2379-y.

Milbury, C.A., Li, J. and Makrigiorgos, G.M. (2009) ‘PCR-Based Methods for the Enrichment of Minority Alleles and Mutations’, *Clinical chemistry*, 55(4), pp. 632–640. Available at: https://doi.org/10.1373/clinchem.2008.113035.

Misra, S. *et al.* (2020) ‘Homozygous Hypomorphic HNF1A Alleles Are a Novel Cause of Young-Onset Diabetes and Result in Sulfonylurea-Sensitive Diabetes’, *Diabetes Care*, 43(4), pp. 909–912. Available at: https://doi.org/10.2337/dc19-1843.

Molven, A. *et al.* (2008) ‘Mutations in the Insulin Gene Can Cause MODY and Autoantibody-Negative Type 1 Diabetes’, *Diabetes*, 57(4), pp. 1131–1135. Available at: https://doi.org/10.2337/db07-1467.

Moosaie, F. *et al.* (2021) 'Waist-To-Height Ratio Is a More Accurate Tool for Predicting Hypertension Than Waist-To-Hip Circumference and BMI in Patients With Type 2 Diabetes: A Prospective Study', *Frontiers in Public Health*, 9. Available at: https://www.frontiersin.org/articles/10.3389/fpubh.2021.726288 (Accessed: 13 August 2023).

Moreno-Estrada, A. *et al.* (2014) 'The Genetics of Mexico Recapitulates Native American Substructure and Affects Biomedical Traits', *Science (New York, N.Y.)*, 344(6189), pp. 1280–1285. Available at: https://doi.org/10.1126/science.1251688.

Moriya, H. (2015) 'Quantitative nature of overexpression experiments', *Molecular Biology of the Cell*, 26(22), pp. 3932–3939. Available at: https://doi.org/10.1091/mbc.E15-07-0512.

von Mühlendahl, K.E. and Herkenhoff, H. (1995) 'Long-term course of neonatal diabetes', *The New England Journal of Medicine*, 333(11), pp. 704–708. Available at: https://doi.org/10.1056/NEJM199509143331105.

Murphy, R., Ellard, S. and Hattersley, A.T. (2008) 'Clinical implications of a molecular genetic classification of monogenic beta-cell diabetes', *Nature Clinical Practice. Endocrinology & Metabolism*, 4(4), pp. 200–213. Available at: https://doi.org/10.1038/ncpendmet0778.

Murtaugh, L. *et al.* (2004) 'Notch signaling controls multiple steps of pancreatic differentiation', *Proceedings of the National Academy of Sciences of the United States of America*, 100, pp. 14920–5. Available at: https://doi.org/10.1073/pnas.2436557100.

Nair, G.G. *et al.* (2019) 'Recapitulating endocrine cell clustering in culture promotes maturation of human stem-cell-derived β cells', *Nature Cell Biology*, 21(2), pp. 263–274. Available at: https://doi.org/10.1038/s41556-018-0271-4.

Najmi, L.A. *et al.* (2017) 'Functional Investigations of HNF1A Identify Rare Variants as Risk Factors for Type 2 Diabetes in the General Population', *Diabetes*, 66(2), pp. 335–346. Available at: https://doi.org/10.2337/db16-0460.

Nammo, T. *et al.* (2002) 'Expression profile of MODY3/HNF-1alpha protein in the developing mouse pancreas', *Diabetologia*, 45(8), pp. 1142–1153. Available at: https://doi.org/10.1007/s00125-002-0892-8.

Nauck, M.A. *et al.* (2021) 'GLP-1 receptor agonists in the treatment of type 2 diabetes - state-of-the-art', *Molecular Metabolism*, 46, p. 101102. Available at: https://doi.org/10.1016/j.molmet.2020.101102.

Naylor, R., Knight Johnson, A. and del Gaudio, D. (1993) 'Maturity-Onset Diabetes of the Young Overview', in M.P. Adam et al. (eds) *GeneReviews®*. Seattle (WA): University of Washington, Seattle. Available at: http://www.ncbi.nlm.nih.gov/books/NBK500456/ (Accessed: 2 June 2023).

Naylor, R.N. *et al.* (2011) 'Genetics and pathophysiology of neonatal diabetes mellitus', *Journal of Diabetes Investigation*, 2(3), pp. 158–169. Available at: https://doi.org/10.1111/j.2040-1124.2011.00106.x.

Naylor, R.N. *et al.* (2014) 'Cost-Effectiveness of MODY Genetic Testing: Translating Genomic Advances Into Practical Health Applications', *Diabetes Care*, 37(1), pp. 202–209. Available at: https://doi.org/10.2337/dc13-0410.

Nejentsev, S. *et al.* (2007) 'Localization of type 1 diabetes susceptibility to the MHC class I genes HLA-B and HLA-A', *Nature*, 450(7171), pp. 887–892. Available at: https://doi.org/10.1038/nature06406.

Neve, B. *et al.* (2005) 'Role of transcription factor KLF11 and its diabetes-associated gene variants in pancreatic beta cell function', *Proceedings of the National Academy of Sciences of the United States of America*, 102(13), pp. 4807–4812. Available at: https://doi.org/10.1073/pnas.0409177102.

Ng, P.C. and Henikoff, S. (2003) 'SIFT: Predicting amino acid changes that affect protein function', *Nucleic Acids Research*, 31(13), pp. 3812–3814. Available at: https://doi.org/10.1093/nar/gkg509.

Nir, T., Melton, D.A. and Dor, Y. (2007) 'Recovery from diabetes in mice by beta cell regeneration', *The Journal of Clinical Investigation*, 117(9), pp. 2553–2561. Available at: https://doi.org/10.1172/JCI32959.

Nishimura, W. *et al.* (2006) 'A switch from MafB to MafA expression accompanies differentiation to pancreatic beta-cells', *Developmental Biology*, 293(2), pp. 526–539. Available at: https://doi.org/10.1016/j.ydbio.2006.02.028.

Nkonge, K.M., Nkonge, D.K. and Nkonge, T.N. (2020) 'The epidemiology, molecular pathogenesis, diagnosis, and treatment of maturity-onset diabetes of the young (MODY)', *Clinical Diabetes and Endocrinology*, 6, p. 20. Available at: https://doi.org/10.1186/s40842-020-00112-5.

Noble, J.A. and Valdes, A.M. (2011) 'Genetics of the HLA region in the prediction of type 1 diabetes', *Current Diabetes Reports*, 11(6), pp. 533–542. Available at: https://doi.org/10.1007/s11892-011-0223-x.

Nostro, M.C. *et al.* (2011) 'Stage-specific signaling through TGFβ family members and WNT regulates patterning and pancreatic specification of human pluripotent stem cells', *Development (Cambridge, England)*, 138(5), pp. 861–871. Available at: https://doi.org/10.1242/dev.055236.

Nostro, M.C. *et al.* (2015) 'Efficient generation of NKX6-1+ pancreatic progenitors from multiple human pluripotent stem cell lines', *Stem Cell Reports*, 4(4), pp. 591–604. Available at: https://doi.org/10.1016/j.stemcr.2015.02.017.

Nunemaker, C.S. *et al.* (2006) 'Glucose modulates [Ca2+]i oscillations in pancreatic islets via ionic and glycolytic mechanisms', *Biophysical Journal*, 91(6), pp. 2082–2096. Available at: https://doi.org/10.1529/biophysj.106.087296.

Odom, D.T. *et al.* (2004) 'Control of pancreas and liver gene expression by HNF transcription factors', *Science (New York, N.Y.)*, 303(5662), pp. 1378–1381. Available at: https://doi.org/10.1126/science.1089769.

Offield, M.F. *et al.* (1996) 'PDX-1 is required for pancreatic outgrowth and differentiation of the rostral duodenum', *Development (Cambridge, England)*, 122(3), pp. 983–995. Available at: https://doi.org/10.1242/dev.122.3.983.

Olofsson, C.S. *et al.* (2002) 'Fast insulin secretion reflects exocytosis of docked granules in mouse pancreatic B-cells', *Pflugers Archiv: European Journal of Physiology*, 444(1–2), pp. 43–51. Available at: https://doi.org/10.1007/s00424-002-0781-5.

O'Rahilly, S., Turner, R.C. and Matthews, D.R. (1988) 'Impaired pulsatile secretion of insulin in relatives of patients with non-insulin-dependent diabetes', *The New England Journal of Medicine*, 318(19), pp. 1225–1230. Available at: https://doi.org/10.1056/NEJM198805123181902.

P, S. *et al.* (2017) 'Determining the role of missense mutations in the POU domain of HNF1A that reduce the DNA-binding affinity: A computational approach', *PloS One*, 12(4), p. e0174953. Available at: https://doi.org/10.1371/journal.pone.0174953.

Pagliuca, F.W. *et al.* (2014) 'Generation of functional human pancreatic β cells in vitro', *Cell*, 159(2), pp. 428–439. Available at: https://doi.org/10.1016/j.cell.2014.09.040.

Pan, C. *et al.* (2009) 'Comparative Proteomic Phenotyping of Cell Lines and Primary Cells to Assess Preservation of Cell Type-specific Functions', *Molecular & Cellular Proteomics : MCP*, 8(3), pp. 443–450. Available at: https://doi.org/10.1074/mcp.M800258-MCP200.

Pan, F.C. and Brissova, M. (2014) 'Pancreas development in humans', *Current opinion in endocrinology, diabetes, and obesity*, 21(2), pp. 77–82. Available at: https://doi.org/10.1097/MED.0000000000000047.

Pareek, C.S., Smoczynski, R. and Tretyn, A. (2011) 'Sequencing technologies and genome sequencing', *Journal of Applied Genetics*, 52(4), pp. 413–435. Available at: https://doi.org/10.1007/s13353-011-0057-x.

Pauklin, S. and Vallier, L. (2015) 'Activin/Nodal signalling in stem cells', *Development*, 142(4), pp. 607–619. Available at: https://doi.org/10.1242/dev.091769.

Pavić, T. *et al.* (2018) 'Maturity onset diabetes of the young due to HNF1A variants in Croatia', *Biochemia Medica*, 28(2), p. 020703. Available at: https://doi.org/10.11613/BM.2018.020703.

Payne, C., King, J. and Hay, D. (2011) ‘The role of activin/nodal and Wnt signaling in endoderm formation’, *Vitamins and Hormones*, 85, pp. 207–216. Available at: https://doi.org/10.1016/B978-0-12-385961-7.00010-X.

Pearson, E.R. *et al.* (2000) ‘Sensitivity to sulphonylureas in patients with hepatocyte nuclear factor-1alpha gene mutations: evidence for pharmacogenetics in diabetes’, *Diabetic Medicine: A Journal of the British Diabetic Association*, 17(7), pp. 543–545. Available at: https://doi.org/10.1046/j.1464-5491.2000.00305.x.

Pearson, E.R. *et al.* (2003) ‘Genetic cause of hyperglycaemia and response to treatment in diabetes’, *Lancet (London, England)*, 362(9392), pp. 1275–1281. Available at: https://doi.org/10.1016/S0140-6736(03)14571-0.

Pearson, E.R. *et al.* (2006) ‘Switching from insulin to oral sulfonylureas in patients with diabetes due to Kir6.2 mutations’, *The New England Journal of Medicine*, 355(5), pp. 467–477. Available at: https://doi.org/10.1056/NEJMoa061759.

Pedersen, K.B. *et al.* (2013) ‘The transcription factor HNF1α induces expression of angiotensin-converting enzyme 2 (ACE2) in pancreatic islets from evolutionarily conserved promoter motifs’, *Biochimica et biophysica acta*, 1829(11), p. 10.1016/j.bbagrm.2013.09.007. Available at: https://doi.org/10.1016/j.bbagrm.2013.09.007.

Peixoto-Barbosa, R., Reis, A.F. and Giuffrida, F.M.A. (2020) ‘Update on clinical screening of maturity-onset diabetes of the young (MODY)’, *Diabetology & Metabolic Syndrome*, 12, p. 50. Available at: https://doi.org/10.1186/s13098-020-00557-9.

Petersen, M. *et al.* (2017) ‘Single-Cell Gene Expression Analysis of a Human ESC Model of Pancreatic Endocrine Development Reveals Different Paths to β-Cell Differentiation’, *Stem Cell Reports*, 9. Available at: https://doi.org/10.1016/j.stemcr.2017.08.009.

Petersmann, A. *et al.* (2019) ‘Definition, Classification and Diagnosis of Diabetes Mellitus’, *Experimental and Clinical Endocrinology & Diabetes: Official Journal, German Society of Endocrinology [and] German Diabetes Association*, 127(S 01), pp. S1–S7. Available at: https://doi.org/10.1055/a-1018-9078.

Pihoker, C. *et al.* (2013) ‘Prevalence, Characteristics and Clinical Diagnosis of Maturity Onset Diabetes of the Young Due to Mutations in HNF1A, HNF4A, and Glucokinase: Results From the SEARCH for Diabetes in Youth’, *The Journal of Clinical Endocrinology and Metabolism*, 98(10), pp. 4055–4062. Available at: https://doi.org/10.1210/jc.2013-1279.

Pinton, P. *et al.* (2002) ‘Dynamics of glucose-induced membrane recruitment of protein kinase C beta II in living pancreatic islet beta-cells’, *The Journal of Biological Chemistry*, 277(40), pp. 37702–37710. Available at: https://doi.org/10.1074/jbc.M204478200.

Poitou, C. *et al.* (2012) ‘Maturity onset diabetes of the young: clinical characteristics and outcome after kidney and pancreas transplantation in MODY3 and RCAD patients: a single center experience’, *Transplant International: Official Journal of the European Society for Organ Transplantation*, 25(5), pp. 564–572. Available at: https://doi.org/10.1111/j.1432-2277.2012.01458.x.

Polak, M. and Cavé, H. (2007) ‘Neonatal diabetes mellitus: a disease linked to multiple mechanisms’, *Orphanet Journal of Rare Diseases*, 2, p. 12. Available at: https://doi.org/10.1186/1750-1172-2-12.

Pontoglio, M. *et al.* (1998) ‘Defective insulin secretion in hepatocyte nuclear factor 1alpha-deficient mice’, *The Journal of Clinical Investigation*, 101(10), pp. 2215–2222. Available at: https://doi.org/10.1172/JCI2548.

Pontoglio, M. *et al.* (2000) ‘HNF1alpha controls renal glucose reabsorption in mouse and man’, *EMBO reports*, 1(4), pp. 359–365. Available at: https://doi.org/10.1093/embo-reports/kvd071.

Poulsen, P. *et al.* (1999) ‘Heritability of type II (non-insulin-dependent) diabetes mellitus and abnormal glucose tolerance--a population-based twin study’, *Diabetologia*, 42(2), pp. 139–145. Available at: https://doi.org/10.1007/s001250051131.

Prelich, G. (2012) ‘Gene Overexpression: Uses, Mechanisms, and Interpretation’, *Genetics*, 190(3), pp. 841–854. Available at: https://doi.org/10.1534/genetics.111.136911.

Prudente, S. *et al.* (2015) ‘Loss-of-Function Mutations in APPL1 in Familial Diabetes Mellitus’, *American Journal of Human Genetics*, 97(1), pp. 177–185. Available at: https://doi.org/10.1016/j.ajhg.2015.05.011.

Raeder, H. *et al.* (2006) ‘Mutations in the CEL VNTR cause a syndrome of diabetes and pancreatic exocrine dysfunction’, *Nature Genetics*, 38(1), pp. 54–62. Available at: https://doi.org/10.1038/ng1708.

Rawshani, Aidin, Rawshani, Araz and Gudbjörnsdottir, S. (2017) ‘Mortality and Cardiovascular Disease in Type 1 and Type 2 Diabetes’, *The New England Journal of Medicine*, 377(3), pp. 300–301. Available at: https://doi.org/10.1056/NEJMc1706292.

Rees, D.A. and Alcolado, J.C. (2005) ‘Animal models of diabetes mellitus’, *Diabetic Medicine*, 22(4), pp. 359–370. Available at: https://doi.org/10.1111/j.1464-5491.2005.01499.x.

Rezania, A. *et al.* (2012) ‘Maturation of human embryonic stem cell-derived pancreatic progenitors into functional islets capable of treating pre-existing diabetes in mice’, *Diabetes*, 61(8), pp. 2016–2029. Available at: https://doi.org/10.2337/db11-1711.

Rezania, A. *et al.* (2014) ‘Reversal of diabetes with insulin-producing cells derived in vitro from human pluripotent stem cells’, *Nature Biotechnology*, 32(11), pp. 1121–1133. Available at: https://doi.org/10.1038/nbt.3033.

Richards, S. *et al.* (2015) ‘Standards and guidelines for the interpretation of sequence variants: a joint consensus recommendation of the American College of Medical Genetics and Genomics and the Association for Molecular Pathology’, *Genetics in Medicine: Official Journal of the American College of Medical Genetics*, 17(5), pp. 405–424. Available at: https://doi.org/10.1038/gim.2015.30.

Richter, B. *et al.* (2008) ‘Dipeptidyl peptidase-4 (DPP-4) inhibitors for type 2 diabetes mellitus’, *Cochrane Database of Systematic Reviews* [Preprint], (2). Available at: https://doi.org/10.1002/14651858.CD006739.pub2.

Riedel, M.J. *et al.* (2012) ‘Immunohistochemical characterisation of cells co-producing insulin and glucagon in the developing human pancreas’, *Diabetologia*, 55(2), pp. 372–381. Available at: https://doi.org/10.1007/s00125-011-2344-9.

Riggs, E.R. *et al.* (2020) ‘Technical standards for the interpretation and reporting of constitutional copy-number variants: a joint consensus recommendation of the American College of Medical Genetics and Genomics (ACMG) and the Clinical Genome Resource (ClinGen)’, *Genetics in Medicine: Official Journal of the American College of Medical Genetics*, 22(2), pp. 245–257. Available at: https://doi.org/10.1038/s41436-019-0686-8.

Rikken, G., Niehues, H. and van den Bogaard, E.H. (2020) ‘Organotypic 3D Skin Models: Human Epidermal Equivalent Cultures from Primary Keratinocytes and Immortalized Keratinocyte Cell Lines’, *Methods in Molecular Biology (Clifton, N.J.)*, 2154, pp. 45–61. Available at: https://doi.org/10.1007/978-1-0716-0648-3_5.

Rorsman, P. and Renström, E. (2003) ‘Insulin granule dynamics in pancreatic beta cells’, *Diabetologia*, 46(8), pp. 1029–1045. Available at: https://doi.org/10.1007/s00125-003-1153-1.

Rose, R.B. *et al.* (2000) ‘Structural basis of dimerization, coactivator recognition and MODY3 mutations in HNF-1alpha’, *Nature Structural Biology*, 7(9), pp. 744–748. Available at: https://doi.org/10.1038/78966.

Rose, R.B. *et al.* (2004) ‘Biochemical and structural basis for partially redundant enzymatic and transcriptional functions of DCoH and DCoH2’, *Biochemistry*, 43(23), pp. 7345–7355. Available at: https://doi.org/10.1021/bi049620t.

Rosenstock, J. *et al.* (2012) ‘Effects of Dapagliflozin, an SGLT2 Inhibitor, on HbA1c, Body Weight, and Hypoglycemia Risk in Patients With Type 2 Diabetes Inadequately Controlled on Pioglitazone Monotherapy’, *Diabetes Care*, 35(7), pp. 1473–1478. Available at: https://doi.org/10.2337/dc11-1693.

Rother, K.I. and Harlan, D.M. (2004) ‘Challenges facing islet transplantation for the treatment of type 1 diabetes mellitus’, *Journal of Clinical Investigation*, 114(7), pp. 877–883. Available at: https://doi.org/10.1172/JCI200423235.

Rowe, R.G. and Daley, G.Q. (2019) ‘Induced pluripotent stem cells in disease modelling and drug discovery’, *Nature reviews. Genetics*, 20(7), pp. 377–388. Available at: https://doi.org/10.1038/s41576-019-0100-z.

Russ, H.A. *et al.* (2015) ‘Controlled induction of human pancreatic progenitors produces functional beta-like cells in vitro’, *The EMBO Journal*, 34(13), pp. 1759–1772. Available at: https://doi.org/10.15252/embj.201591058.

Russell-Jones, D. and Khan, R. (2007) ‘Insulin-associated weight gain in diabetes – causes, effects and coping strategies’, *Diabetes, Obesity and Metabolism*, 9(6), pp. 799–812. Available at: https://doi.org/10.1111/j.1463-1326.2006.00686.x.

Ryffel, G.U. (2001) ‘Mutations in the human genes encoding the transcription factors of the hepatocyte nuclear factor (HNF)1 and HNF4 families: functional and pathological consequences’, *Journal of Molecular Endocrinology*, 27(1), pp. 11–29. Available at: https://doi.org/10.1677/jme.0.0270011.

Saeedi, P. *et al.* (2019) ‘Global and regional diabetes prevalence estimates for 2019 and projections for 2030 and 2045: Results from the International Diabetes Federation Diabetes Atlas, 9th edition’, *Diabetes Research and Clinical Practice*, 157, p. 107843. Available at: https://doi.org/10.1016/j.diabres.2019.107843.

Salem, V. *et al.* (2019) ‘Leader β-cells coordinate Ca2+ dynamics across pancreatic islets in vivo’, *Nature Metabolism*, 1(6), pp. 615–629. Available at: https://doi.org/10.1038/s42255-019-0075-2.

Sander, M. *et al.* (2000) ‘Homeobox gene Nkx6.1 lies downstream of Nkx2.2 in the major pathway of beta-cell formation in the pancreas’, *Development (Cambridge, England)*, 127(24), pp. 5533–5540. Available at: https://doi.org/10.1242/dev.127.24.5533.

Santos, R.M. *et al.* (1991) ‘Widespread synchronous [Ca2+]i oscillations due to bursting electrical activity in single pancreatic islets’, *Pflugers Archiv: European Journal of Physiology*, 418(4), pp. 417–422. Available at: https://doi.org/10.1007/BF00550880.

Schaffer, A.E. *et al.* (2013) ‘Nkx6.1 controls a gene regulatory network required for establishing and maintaining pancreatic Beta cell identity’, *PLoS genetics*, 9(1), p. e1003274. Available at: https://doi.org/10.1371/journal.pgen.1003274.

Schindele, P., Wolter, F. and Puchta, H. (2020) ‘CRISPR Guide RNA Design Guidelines for Efficient Genome Editing’, *Methods in Molecular Biology (Clifton, N.J.)*, 2166, pp. 331–342. Available at: https://doi.org/10.1007/978-1-0716-0712-1_19.

Schwarz, J.M. *et al.* (2014) ‘MutationTaster2: mutation prediction for the deep-sequencing age’, *Nature Methods*, 11(4), pp. 361–362. Available at: https://doi.org/10.1038/nmeth.2890.

Schymkowitz, J. *et al.* (2005) ‘The FoldX web server: an online force field’, *Nucleic Acids Research*, 33(Web Server issue), pp. W382-388. Available at: https://doi.org/10.1093/nar/gki387.

Shahjalal, H.Md. *et al.* (2018) ‘Generation of pancreatic β cells for treatment of diabetes: advances and challenges’, *Stem Cell Research & Therapy*, 9(1), p. 355. Available at: https://doi.org/10.1186/s13287-018-1099-3.

Shapiro, A.M. *et al.* (2000) ‘Islet transplantation in seven patients with type 1 diabetes mellitus using a glucocorticoid-free immunosuppressive regimen’, *The New England Journal of Medicine*, 343(4), pp. 230–238. Available at: https://doi.org/10.1056/NEJM200007273430401.

Shapiro, A.M.J., Pokrywczynska, M. and Ricordi, C. (2017) ‘Clinical pancreatic islet transplantation’, *Nature Reviews. Endocrinology*, 13(5), pp. 268–277. Available at: https://doi.org/10.1038/nrendo.2016.178.

Shapiro, S.S. and Wilk, M.B. (1965) ‘An Analysis of Variance Test for Normality (Complete Samples)’, *Biometrika*, 52(3/4), pp. 591–611. Available at: https://doi.org/10.2307/2333709.

Sharma, A. *et al.* (2020) ‘Multi-Lineage Human iPSC-Derived Platforms for Disease Modeling and Drug Discovery’, *Cell stem cell*, 26(3), pp. 309–329. Available at: https://doi.org/10.1016/j.stem.2020.02.011.

Sharma, U., Pal, D. and Prasad, R. (2014) ‘Alkaline Phosphatase: An Overview’, *Indian Journal of Clinical Biochemistry*, 29(3), pp. 269–278. Available at: https://doi.org/10.1007/s12291-013-0408-y.

Shepherd, M. *et al.* (2009) ‘A genetic diagnosis of HNF1A diabetes alters treatment and improves glycaemic control in the majority of insulin-treated patients’, *Diabetic Medicine: A Journal of the British Diabetic Association*, 26(4), pp. 437–441. Available at: https://doi.org/10.1111/j.1464-5491.2009.02690.x.

Sherwood, R.I., Chen, T.-Y.A. and Melton, D.A. (2009) ‘Transcriptional dynamics of endodermal organ formation’, *Developmental Dynamics: An Official Publication of the American Association of Anatomists*, 238(1), pp. 29–42. Available at: https://doi.org/10.1002/dvdy.21810.

Shi, T.-T. *et al.* (2018) ‘Angiotensin-converting enzyme 2 regulates mitochondrial function in pancreatic β-cells’, *Biochemical and Biophysical Research Communications*, 495(1), pp. 860–866. Available at: https://doi.org/10.1016/j.bbrc.2017.11.055.

Shields, B.M. *et al.* (2010) ‘Maturity-onset diabetes of the young (MODY): how many cases are we missing?’, *Diabetologia*, 53(12), pp. 2504–2508. Available at: https://doi.org/10.1007/s00125-010-1799-4.

Shields, B.M. *et al.* (2012) ‘The development and validation of a clinical prediction model to determine the probability of MODY in patients with young-onset diabetes’, *Diabetologia*, 55(5), pp. 1265–1272. Available at: https://doi.org/10.1007/s00125-011-2418-8.

Shields, J.D. *et al.* (2010) ‘Induction of lymphoidlike stroma and immune escape by tumors that express the chemokine CCL21’, *Science (New York, N.Y.)*, 328(5979), pp. 749–752. Available at: https://doi.org/10.1126/science.1185837.

Shih, D.Q. *et al.* (2001) ‘Hepatocyte nuclear factor-1alpha is an essential regulator of bile acid and plasma cholesterol metabolism’, *Nature Genetics*, 27(4), pp. 375–382. Available at: https://doi.org/10.1038/86871.

Shih, H.P., Wang, A. and Sander, M. (2013) ‘Pancreas organogenesis: from lineage determination to morphogenesis’, *Annual Review of Cell and Developmental Biology*, 29, pp. 81–105. Available at: https://doi.org/10.1146/annurev-cellbio-101512-122405.

Shu, Y. *et al.* (2007) ‘Effect of genetic variation in the organic cation transporter 1 (OCT1) on metformin action’, *The Journal of Clinical Investigation*, 117(5), pp. 1422–1431. Available at: https://doi.org/10.1172/JCI30558.

Simaite, D. *et al.* (2014) ‘Recessive mutations in PCBD1 cause a new type of early-onset diabetes’, *Diabetes*, 63(10), pp. 3557–3564. Available at: https://doi.org/10.2337/db13-1784.

Slatko, B.E., Gardner, A.F. and Ausubel, F.M. (2018) ‘Overview of Next-Generation Sequencing Technologies’, *Current Protocols in Molecular Biology*, 122(1), p. e59. Available at: https://doi.org/10.1002/cpmb.59.

Sola, D. *et al.* (2015) ‘Sulfonylureas and their use in clinical practice’, *Archives of Medical Science : AMS*, 11(4), pp. 840–848. Available at: https://doi.org/10.5114/aoms.2015.53304.

Srivastava, S. and Goren, H.J. (2003) ‘Insulin Constitutively Secreted by β-Cells Is Necessary for Glucose-Stimulated Insulin Secretion’, *Diabetes*, 52(8), pp. 2049–2056. Available at: https://doi.org/10.2337/diabetes.52.8.2049.

Staffers, D.A. *et al.* (1997) ‘Early-onset type-ll diabetes mellitus (MODY4) linked to IPF1’, *Nature Genetics*, 17(2), pp. 138–139. Available at: https://doi.org/10.1038/ng1097-138.

Stanescu, D.E. *et al.* (2012) ‘Novel Presentations of Congenital Hyperinsulinism due to Mutations in the MODY genes: HNF1A and HNF4A’, *The Journal of Clinical Endocrinology and Metabolism*, 97(10), pp. E2026–E2030. Available at: https://doi.org/10.1210/jc.2012-1356.

Štefková, K., Procházková, J. and Pacherník, J. (2015) ‘Alkaline Phosphatase in Stem Cells’, *Stem Cells International*, 2015, p. e628368. Available at: https://doi.org/10.1155/2015/628368.

Stoffers, D.A. *et al.* (1997) ‘Early-onset type-II diabetes mellitus (MODY4) linked to IPF1’, *Nature Genetics*, 17(2), pp. 138–139. Available at: https://doi.org/10.1038/ng1097-138.

Stride, A. *et al.* (2002) ‘The genetic abnormality in the beta cell determines the response to an oral glucose load’, *Diabetologia*, 45(3), pp. 427–435. Available at: https://doi.org/10.1007/s00125-001-0770-9.

Stuppia, L. *et al.* (2012) ‘Use of the MLPA assay in the molecular diagnosis of gene copy number alterations in human genetic diseases’, *International Journal of Molecular Sciences*, 13(3), pp. 3245–3276. Available at: https://doi.org/10.3390/ijms13033245.

Sui, L. *et al.* (2021) ‘Reduced replication fork speed promotes pancreatic endocrine differentiation and controls graft size’, *JCI insight*, 6(5), p. 141553. Available at: https://doi.org/10.1172/jci.insight.141553.

Sui, L., Leibel, R.L. and Egli, D. (2018) ‘Pancreatic Beta Cell Differentiation From Human Pluripotent Stem Cells’, *Current Protocols in Human Genetics*, 99(1). Available at: https://doi.org/10.1002/cphg.68.

Suissa, Y. *et al.* (2013) ‘Gastrin: a distinct fate of neurogenin3 positive progenitor cells in the embryonic pancreas’, *PloS One*, 8(8), p. e70397. Available at: https://doi.org/10.1371/journal.pone.0070397.

Sung, P. and Klein, H. (2006) ‘Mechanism of homologous recombination: mediators and helicases take on regulatory functions’, *Nature Reviews. Molecular Cell Biology*, 7(10), pp. 739–750. Available at: https://doi.org/10.1038/nrm2008.

Szpirer, J. *et al.* (1994) ‘Localization of the gene for DNA polymerase epsilon (POLE) to human chromosome 12q24.3 and rat chromosome 12 by somatic cell hybrid panels and fluorescence in situ hybridization’, *Genomics*, 20(2), pp. 223–226. Available at: https://doi.org/10.1006/geno.1994.1156.

Takahashi, K. *et al.* (2007) ‘Induction of pluripotent stem cells from adult human fibroblasts by defined factors’, *Cell*, 131(5), pp. 861–872. Available at: https://doi.org/10.1016/j.cell.2007.11.019.

Takahashi, K. and Yamanaka, S. (2006) ‘Induction of pluripotent stem cells from mouse embryonic and adult fibroblast cultures by defined factors’, *Cell*, 126(4), pp. 663–676. Available at: https://doi.org/10.1016/j.cell.2006.07.024.

Takahashi, K. and Yamanaka, S. (2016) ‘A decade of transcription factor-mediated reprogramming to pluripotency’, *Nature Reviews. Molecular Cell Biology*, 17(3), pp. 183–193. Available at: https://doi.org/10.1038/nrm.2016.8.

Tanizawa, Y. *et al.* (1999) ‘Overexpression of dominant negative mutant hepatocyte nuclear factor (HNF)-1alpha inhibits arginine-induced insulin secretion in MIN6 cells’, *Diabetologia*, 42(7), pp. 887–891. Available at: https://doi.org/10.1007/s001250051242.

Tavtigian, S.V. *et al.* (2006) ‘Comprehensive statistical study of 452 BRCA1 missense substitutions with classification of eight recurrent substitutions as neutral’, *Journal of Medical Genetics*, 43(4), pp. 295–305. Available at: https://doi.org/10.1136/jmg.2005.033878.

Taylor, B.L., Liu, F.-F. and Sander, M. (2013) ‘Nkx6.1 is essential for maintaining the functional state of pancreatic beta cells’, *Cell Reports*, 4(6), pp. 1262–1275. Available at: https://doi.org/10.1016/j.celrep.2013.08.010.

Taylor, G.S. *et al.* (2022) ‘Type 1 Diabetes Patients With Different Residual Beta-Cell Function but Similar Age, HBA1c, and Cardiorespiratory Fitness Have Differing Exercise-Induced Angiogenic Cell Mobilisation’, *Frontiers in Endocrinology*, 13, p. 797438. Available at: https://doi.org/10.3389/fendo.2022.797438.

Thanabalasingham, G. *et al.* (2012) ‘Systematic assessment of etiology in adults with a clinical diagnosis of young-onset type 2 diabetes is a successful strategy for identifying maturity-onset diabetes of the young’, *Diabetes Care*, 35(6), pp. 1206–1212. Available at: https://doi.org/10.2337/dc11-1243.

Thanabalasingham, G. and Owen, K.R. (2011) ‘Diagnosis and management of maturity onset diabetes of the young (MODY)’, *BMJ (Clinical research ed.)*, 343, p. d6044. Available at: https://doi.org/10.1136/bmj.d6044.

Thompson, P.J. *et al.* (2023) ‘Islet autoimmunity in human type 1 diabetes: initiation and progression from the perspective of the beta cell’, *Diabetologia* [Preprint]. Available at: https://doi.org/10.1007/s00125-023-05970-z.

Thomson, J.A. *et al.* (1998) ‘Embryonic Stem Cell Lines Derived from Human Blastocysts’, *Science*, 282(5391), pp. 1145–1147. Available at: https://doi.org/10.1126/science.282.5391.1145.

Todd, J.A. *et al.* (2007) ‘Robust associations of four new chromosome regions from genome-wide analyses of type 1 diabetes’, *Nature Genetics*, 39(7), pp. 857–864. Available at: https://doi.org/10.1038/ng2068.

Toivonen, S., Lundin, K., *et al.* (2013) ‘Activin A and Wnt-dependent specification of human definitive endoderm cells’, *Experimental Cell Research*, 319(17), pp. 2535–2544. Available at: https://doi.org/10.1016/j.yexcr.2013.07.007.

Toivonen, S., Ojala, M., *et al.* (2013) ‘Comparative Analysis of Targeted Differentiation of Human Induced Pluripotent Stem Cells (hiPSCs) and Human Embryonic Stem Cells Reveals Variability Associated With Incomplete Transgene Silencing in Retrovirally Derived hiPSC Lines’, *Stem Cells Translational Medicine*, 2(2), pp. 83–93. Available at: https://doi.org/10.5966/sctm.2012-0047.

Tosur, M. and Philipson, L.H. (2022) ‘Precision diabetes: Lessons learned from maturity-onset diabetes of the young (MODY)’, *Journal of Diabetes Investigation*, 13(9), pp. 1465–1471. Available at: https://doi.org/10.1111/jdi.13860.

Tran, R., Moraes, C. and Hoesli, C.A. (2020) ‘Controlled clustering enhances PDX1 and NKX6.1 expression in pancreatic endoderm cells derived from pluripotent stem cells’, *Scientific Reports*, 10(1), p. 1190. Available at: https://doi.org/10.1038/s41598-020-57787-0.

Tumer, G., Simpson, B. and Roberts, T.K. (2023) ‘Genetics, Human Major Histocompatibility Complex (MHC)’, in *StatPearls*. Treasure Island (FL): StatPearls Publishing. Available at: http://www.ncbi.nlm.nih.gov/books/NBK538218/ (Accessed: 28 July 2023).

Uchizono, Y. *et al.* (2009) ‘Role of HNF-1α in regulating the expression of genes involved in cellular growth and proliferation in pancreatic beta-cells’, *Diabetes research and clinical practice*, 84(1), pp. 19–26. Available at: https://doi.org/10.1016/j.diabres.2008.12.014.

Ulinski, T. *et al.* (2006) ‘Renal phenotypes related to hepatocyte nuclear factor-1beta (TCF2) mutations in a pediatric cohort’, *Journal of the American Society of Nephrology: JASN*, 17(2), pp. 497–503. Available at: https://doi.org/10.1681/ASN.2005101040.

Urakami, T. (2019) ‘Maturity-onset diabetes of the young (MODY): current perspectives on diagnosis and treatment’, *Diabetes, Metabolic Syndrome and Obesity: Targets and Therapy*, 12, pp. 1047–1056. Available at: https://doi.org/10.2147/DMSO.S179793.

Uzan, B. *et al.* (2009) ‘Mechanisms of KGF Mediated Signaling in Pancreatic Duct Cell Proliferation and Differentiation’, *PLoS ONE*, 4(3), p. e4734. Available at: https://doi.org/10.1371/journal.pone.0004734.

Valdeolmillos, M. *et al.* (1993) ‘Fluorescence digital image analysis of glucose-induced [Ca2+]i oscillations in mouse pancreatic islets of Langerhans’, *Diabetes*, 42(8), pp. 1210–1214. Available at: https://doi.org/10.2337/diab.42.8.1210.

Valkovicova, T. *et al.* (2019a) ‘Novel insights into genetics and clinics of the HNF1A-MODY’, *Endocrine Regulations*, 53(2), pp. 110–134. Available at: https://doi.org/10.2478/enr-2019-0013.

Valkovicova, T. *et al.* (2019b) ‘Novel insights into genetics and clinics of the HNF1A-MODY’, *Endocrine Regulations*, 53(2), pp. 110–134. Available at: https://doi.org/10.2478/enr-2019-0013.

Velazco-Cruz, L. *et al.* (2019) ‘Acquisition of Dynamic Function in Human Stem Cell-Derived β Cells’, *Stem Cell Reports*, 12(2), pp. 351–365. Available at: https://doi.org/10.1016/j.stemcr.2018.12.012.

Veres, A. *et al.* (2019) ‘Charting cellular identity during human in vitro β-cell differentiation’, *Nature*, 569(7756), pp. 368–373. Available at: https://doi.org/10.1038/s41586-019-1168-5.

Vethe, H. *et al.* (2017) ‘Probing the missing mature β-cell proteomic landscape in differentiating patient iPSC-derived cells’, *Scientific Reports*, 7, p. 4780. Available at: https://doi.org/10.1038/s41598-017-04979-w.

Viollet, B. *et al.* (2012) ‘Cellular and molecular mechanisms of metformin: an overview’, *Clinical Science (London, England : 1979)*, 122(6), pp. 253–270. Available at: https://doi.org/10.1042/CS20110386.

Wallis, Y. *et al.* (2013) ‘Practice Guidelines for the Evaluation of Pathogenicity and the Reporting of Sequence Variants in Clinical Molecular Genetics .’, in. Available at: https://www.semanticscholar.org/paper/Practice-Guidelines-for-the-Evaluation-of-and-the-.-Wallis-Payne/bfe742afc1c056f7ee9de3273d8dfec921dec19e (Accessed: 23 July 2023).

Wang, H. *et al.* (2000) ‘Molecular targets of a human HNF1 alpha mutation responsible for pancreatic beta-cell dysfunction’, *The EMBO journal*, 19(16), pp. 4257–4264. Available at: https://doi.org/10.1093/emboj/19.16.4257.

Wang, Z. *et al.* (2015) ‘Activin A can induce definitive endoderm differentiation from human parthenogenetic embryonic stem cells’, *Biotechnology Letters*, 37(8), pp. 1711–1717. Available at: https://doi.org/10.1007/s10529-015-1829-x.

Warren, L. *et al.* (2010) ‘Highly efficient reprogramming to pluripotency and directed differentiation of human cells using synthetic modified mRNA’, *Cell stem cell*, 7(5), pp. 618–630. Available at: https://doi.org/10.1016/j.stem.2010.08.012.

Wenzlau, J.M. and Hutton, J.C. (2013) ‘Novel Diabetes Autoantibodies and Prediction of Type 1 Diabetes’, *Current Diabetes Reports*, 13(5), pp. 608–615. Available at: https://doi.org/10.1007/s11892-013-0405-9.

Wiedenheft, B., Sternberg, S.H. and Doudna, J.A. (2012) ‘RNA-guided genetic silencing systems in bacteria and archaea’, *Nature*, 482(7385), pp. 331–338. Available at: https://doi.org/10.1038/nature10886.

Wright, N.M. *et al.* (1993) ‘Permanent neonatal diabetes mellitus and pancreatic exocrine insufficiency resulting from congenital pancreatic agenesis’, *American Journal of Diseases of Children (1960)*, 147(6), pp. 607–609. Available at: https://doi.org/10.1001/archpedi.1993.02160300013005.

Xue, A. *et al.* (2018) ‘Genome-wide association analyses identify 143 risk variants and putative regulatory mechanisms for type 2 diabetes’, *Nature Communications*, 9, p. 2941. Available at: https://doi.org/10.1038/s41467-018-04951-w.

Yoo, J. *et al.* (2014) ‘Cell reprogramming into the pluripotent state using graphene based substrates’, *Biomaterials*, 35(29), pp. 8321–8329. Available at: https://doi.org/10.1016/j.biomaterials.2014.05.096.

Yu, L., Zhao, Z. and Steck, A.K. (2017) ‘T1D Autoantibodies: Room for Improvement?’, *Current opinion in endocrinology, diabetes, and obesity*, 24(4), pp. 285–291. Available at: https://doi.org/10.1097/MED.0000000000000348.

Yu, Y. *et al.* (2019) ‘HNF1A/CASC2 regulates pancreatic cancer cell proliferation through PTEN/Akt signaling’, *Journal of Cellular Biochemistry*, 120(3), pp. 2816–2827. Available at: https://doi.org/10.1002/jcb.26395.

Zhang, D. *et al.* (2009) ‘Highly efficient differentiation of human ES cells and iPS cells into mature pancreatic insulin-producing cells’, *Cell Research*, 19(4), pp. 429–438. Available at: https://doi.org/10.1038/cr.2009.28.

Zhang, S. *et al.* (2022) ‘Retinoic acid and FGF10 promote the differentiation of pluripotent stem cells into salivary gland placodes’, *Stem Cell Research & Therapy*, 13(1), p. 368. Available at: https://doi.org/10.1186/s13287-022-03033-5.

Zhou, T. *et al.* (2011) ‘Generation of Induced Pluripotent Stem Cells from Urine’, *Journal of the American Society of Nephrology : JASN*, 22(7), pp. 1221–1228. Available at: https://doi.org/10.1681/ASN.2011010106.

Zhou, Y. *et al.* (2013) ‘Genetic Modification of Primate Amniotic Fluid-derived Stem Cells Produces Pancreatic Progenitor Cells in vitro’, *Cells, tissues, organs*, 197(4), pp. 269–282. Available at: https://doi.org/10.1159/000345816.

Zhu, Z. *et al.* (2016) ‘Genome Editing of Lineage Determinants in Human Pluripotent Stem Cells Reveals Mechanisms of Pancreatic Development and Diabetes’, *Cell Stem Cell*, 18(6), pp. 755–768. Available at: https://doi.org/10.1016/j.stem.2016.03.015.

Zhu, Z. and Huangfu, D. (2013) ‘Human pluripotent stem cells: an emerging model in developmental biology’, *Development (Cambridge, England)*, 140(4), pp. 705–717. Available at: https://doi.org/10.1242/dev.086165.

Zorn, A.M. and Wells, J.M. (2007) ‘Molecular basis of vertebrate endoderm development’, *International Review of Cytology*, 259, pp. 49–111. Available at: https://doi.org/10.1016/S0074-7696(06)59002-3.

Appendix

Table 6-1: Table of Materials In Vitro Functional Assessment.

This table lists the materials and equipment required for conducting in vitro functional assessments, including transactivation assays, DNA-binding assays, subcellular localisation studies, western blot analyses, iPSCs reprogramming, and cell culture. It includes details about the material, suppliers, and catalogue numbers.

	Detail	Supplier	Catalogue Number
Site-Directed Mutagenesis	Q5 Hot Start High-Fidelity 2X	New England Biolabs	E0552S
	NEB 10-beta Competent E. coli (High Efficiency)	New England Biolabs	C3019HVIAL
Plasmid DNA purification	QIAprep Spin Miniprep Kit	Qiagen	27104
Transactivation Activity Assay	Dual-Luciferase Reporter Assay System	Promega	E1910
Nuclear extraction	Nuclear extraction kit	Abcam	ab113474
DNA-Binding	DNA-Protein Binding Assay Kit	Abcam	ab117139
Immunostaining Subcellular localisation	ProLong DAPI	Invitrogen	P36962
Western Blot	Tris-HCl	Alfa Aesar	A11379-0B
	SDS	Thermofisher	28312
	2-Mercaptoethanol	Sigma	M3148
	Glycerol	Sigma	G5516-1L
	Bromophenol blue	Scientific Laboratory	114391-5G
	Tris base	Sigma	T6066-1KG
	Glycine	Sigma	G8898-1KG
	Methanol	VWR	20847.32
	BSA	Sigma	A3803-100G
HeLa/Primary Fibroblast Culture	T-75 cell culture flasks	Sarstedt	83.3911.002
	T-25 flasks	Sarstedt	83.3910
	DMEM (High Glucose, L-Glutamine)	ThermoFisher	11965092
	1% penicillin-streptomycin	ThermoFisher	15140122

	Fetal Bovine Serum	Sigma	F7524
INS-1 832/13 Cell Culture	RPMI-1640 medium	ThermoFisher	11875093
	L-glutamine	Sigma	G7513-100ML
	Sodium pyruvate	ThermoFisher	11360070
	HEPES	Sigma	H3375-500G
	β-mercaptoethanol	Sigma	M3148-100ML
	Trypsin-EDTA	ThermoFisher	15400054
Endoc-BH3 Cell Culture	Accutase Cell dissociation	Sigma	A6964-100ML
	ECM Gel	Sigma	E1270-5ML
	D-(+)-Glucose	Sigma	G8270
	Bovine Serum Albumin Fraction V	Sigma	10775835001
	Nicotinamide	Sigma	N3376
	Human Transferrin	Sigma	T8158-100MG
	Sodium Selenite	Sigma	S5261-10G
	Corning bottle-top vacuum filter	SLS	430770-12EA
Fibroblasts Reprogramming	DMEM/F12	Sigma	D6421
	Neurobasal	ThermoFisher	21103049
	B27 supplement	ThermoFisher	17504044
	N2 supplement	ThermoFisher	17502-048
	L-Glutamine	ThermoFisher	25030024
	PD0325901	Sigma	PZ0162
	CHIR99021	Sigma	SML1046
	A-83-01	Reprocell	04-0014
	hLIF	STEMCELL Technologies	78055
	HA-100	STEMCELL Technologies	72482
	bFGF	Santa Cruz	sc-74412
	Antibiotic-Antimycotic cocktail	Gibco	15240062
Transfection	Lipofectamine 2000	ThermoFisher	11668019
	Puromycin Dihydrochloride	Thermo Fisher	A1113803

iPSCs Characterisation	Alkaline Phosphatase Staining Kit	Abcam	ab284936
Stem cell culture matrix	Geltrex LDEV-Free Reduced Growth Factor Basement	ThermoFisher	A1413302
	DMEM/F-12	ThermoFisher	10565-018
Stem cell culture media	StemFlex Medium	ThermoFisher	A3349401
	Calcium/Magnesium free D-PBS	ThermoFisher	14190144
	6-well Cell culture plate	ThermoFisher	165218
	Y-27632	STEMCELL Technologies	72302
Dissociation Solution	TrypL Express Enzyme (1X)	ThermoFisher	12604013
Equipment	Tube Luminometer, Berthold		
	Nanodrop 2000 spectrophotometer, ThermoFisher		
	Veriti 96-Well Fast Thermal Cycler PCR cycler, ThermoFisher		
	Incubator CO2 incubator (37 °C, 5% CO2)		
	Microplate Reader, BMG reader		
	Eclipse T-I Microscope with spinning disc confocal system, Nikon		
	Confocal Microscope, Stellaris 8 Confocal Microscope, Leica		

Table 6-2: Materials for Human Stem Cell-Derived β-Cell Differentiation.

This table summarises essential ingredients, including details, suppliers, catalog numbers, compositions with comprehensive instructions, final concentrations/dilutions, required for the successful directed differentiation of human stem cells into β-cells.

		Details	Supplier	Catalogue Number	Composition
Washing Medium 1		RPMI 1640 Medium, GlutaMAX Supplement	Thermo Fisher Scientific	61870036	RPMI 1640 plus GlutaMAX 1% PS.
		Penicillin-Streptomycin (PS)	Thermo Fisher Scientific,	15070-063	
Washing Medium 2		DMEM plus GlutaMAX	Thermo Fisher Scientific	10566016	DMEM plus GlutaMAX 1% PS.
Stages	Days	Detail	Supplier	Catalog Number	Composition, with instructions
	Day 1	Basal medium for the Days 0 to 4: STEMdiff Endoderm Differentiation Kit	STEMCELL Technologies	05110	Dilute both Supplements MR and CJ 1:100 into cold STEMdiff Endoderm Basal Medium.
Definitive Endoderm stage 1 Medium	Days 2.5 to 4				Dilute Supplement CJ 1:100 into cold (2-8°C) STEMdiff Endoderm Basal Medium.
Primitive Gut Tube, stage 2 Medium	Day 4	B-27 Supplement (50X), serum free	Thermo Fisher Scientific	17504044	RPMI 1640 plus GlutaMAX 1% PS, 1% B-27 serum-free supplement (50×), 50 ng/ml Human FGF-7 (KGF) Recombinant Protein.
		Human FGF-7 (KGF) Recombinant Protein	Thermo Fisher Scientific	PHG0094	
Posterior Foregut, Stage 3 Medium	Days 6 to 8	Cyclopamine-KAAD	Calbiochem	239804	DMEM plus GlutaMAX 1% PS 1%, 1% B-27 serum-free supplement (50×), 0.25 µM Cyclopamine-KAAD, 2µM Stemolecule All-Trans Retinoic Acid, 0.25 µM LDN193189,
		Stemolecule All-Trans Retinoic Acid	Reprocell	04-0021	
		LDN193189	Sigma-Aldrich	SML0559-5MG	

					50 ng/ml Human FGF-7 Recombinant Protein.
Pancreatic progenitor, Stage 4 Medium	Days 8 to 12	Recombinant Human EGF Protein	R&D Systems	236-EG-200	DMEM plus GlutaMAX 1% PS, 1% B-27 serum-free supplement (50×), 50 ng/ml Recombinant Human EGF Protein, 25 ng/ml Human FGF-7 Recombinant Protein.
Cluster Medium	Day 12	RepSox (Hydrochloride)	STEMCELL Technologies	72394	DMEM plus GlutaMAX 1% PS, 1% B-27 serum-free supplement (50×), 1 µM RepSox, 25 ng/ml Human FGF-7 Recombinant Protein, 10 µM Y-27632.
		Microwell culture plates: AggreWell 400 6-well plate	STEMCELL Technologies	34425	
Pancreatic Endocrine Progenitor, Stage 5 Medium	Day 13	Gamma-Secretase Inhibitor XX	Thermo Fisher Scientific	J64904	RPMI plus GlutaMAX 1% PS, 1% B-27 serum-free supplement (50×), 1 µM thyroid hormone (T3), 10 µM RepSox, 10 µM zinc sulfate, 10 µg/ml heparin, 100 nM gamma-secretase inhibitor gamma-Secretase Inhibitor XX, 10 µM Y-27632.
		Thyroid Tormone 3 (T3)	Sigma-Aldrich	T6397	
		Zinc Sulfate	Sigma-Aldrich	Z4750)	
		Heparin	Sigma-Aldrich	H3149	
		Ultra-Low Adherent Plate for Suspension Culture	Thermo Fisher Scientific	38071	
Pancreatic Endocrine Progenitor, Stage 5 Medium	Days 15 to 19	Aphidicolin	Sigma-Aldrich	A4487	Add to Stage 5 Medium 1 µM Aphidicolin.

Pancreatic β-cell, Stage 6 Medium	Days 20 to 27	Fetal Bovine Serum	Thermo Fisher Scientific	10270098	RPMI 1640 plus GlutaMAX 1% PS, 1% B-27 serum-free supplement (50×), 10% Fetal Bovine Serum 10 µM Y-27632, 1 µM Aphidicolin.

Table 6-3: Table of Materials for Functional Assessment of Clusters-Derived β Cells.

This table provides a list of the materials needed for the functional assessment of clusters-derived β cells. It includes details such as supplier information, catalogue numbers, for each material.

	Detail	Supplier	Catalogue Number
Immunostaining	PBS Tablets,	Thermo Fisher Scientific	7647-14-5
	TWEEN 20, viscous liquid	Sigma	P2287-500ML
	Bovine Serum Albumin, fatty acid free	Sigma	A3803-100G
	Epredi SuperFrost Plus Adhesion slides	Thermo Fisher Scientific	10149870
	ImmEdge Hydrophobic Barrier PAP Pen	Vector Laboratories	H-4000
	Cryomold Intermediate 15 x 15 x 5mm	Agar Scientific	AGG4582
	Rectangular cover glasses, 22×50 mm	VWR	631-0137
	OCT Compound 118 mL	Agar Scientific	AGR1180
	Shandon Immu-mount	ThermoFisher	9990402
	1.5 mL TubeOne Microcentrifuge Tube	Starlabs	S1615-5500
Glucose-stimulated insulin secretion	Calcium chloride dihydrate	Sigma	C3306
	Disodium hydrogen phosphate, anhydrous	Sigma	94046-100ML-
	Magnesium chloride hexahydrate	Sigma	M9272-500G
	Potassium chloride	Sigma	7447-40-7
	Sodium bicarbonate	Sigma	S6014-500G
	Sodium chloride	Sigma	S3014-5KG
	Sodium dihydrogen phosphate anhydrous	Sigma	7558-80-7
	HEPES buffer	Sigma	H3375-500G
	D-(+)-Glucose,BioXtra, ≥99.5% (GC)	Sigma	G7528-1KG

	UltraPure DNase	ThermoFisher	10977015
	Hydrogen chloride	Sigma-h	295426
	Ethanol	VWR	20821.330

Table 6-4: List Primary and Secondary Antibody.

List Antibody	Species	Dilution	Company	Catalogue number
Primary Antibody				
Anti-PDX1	Mouse	1:1000	Abcam	ab84987
Anti-NKX6.1	Rabbit	1:1000	Novus Biologicals	NBP1-49672SS
Anti-Glucagon	Mouse	1:1000	Sigma	G2654-100UL
Anti-Insulin	Guinea pig	1:100	Dako	A0564
Anti 6x-His Tag	Mouse	1:1000	ThermoFisher	MA1-21315
Anti HNF1A	Mouse	1:1000	(Santa Cruz)	sc-393925
Anti-OCT4	Rabbit	1:100	Abcam	ab19857
Secondary Antibody				
List Secondary Antibody		Dilution	Company	Catalog number
Goat anti-Mouse,Alexa Fluor 633		1:1000	Thermo Fisher	A-21052
Goat Anti-Guinea pig, Alexa Fluor 647		1:1000	Abcam	ab150187
Goat Anti-Guinea pig, Alexa Fluor 555		1:1000	Thermo Fisher	A-21435
Goat anti-Rabbit, Alexa Fluor 568		1:1000	Thermo Fisher	A-11011
Anti-Mouse Horseradish Peroxidase		1:1000	GE Healthcare	NXA931-1ML